REGULATION OF ARTERIAL GAP JUNCTIONS BY MECHANICAL FACTORS: AN *EX VIVO* STUDY

by

Yong He

B.S. Mechanical Engineering, Chongqing University, China, 1993

M.S. Biomedical Engineering, Florida International University, 2002

Submitted to the Graduate Faculty of

Swanson School of Engineering in partial fulfillment

of the requirements for the degree of

Doctor of Philosophy

University of Pittsburgh

2008

UNIVERSITY OF PITTSBURGH

SWANSON SCHOOL OF ENGINEERING

This dissertation was presented

by

Yong He

It was defended on

February 1, 2008

and approved by

Harvey S. Borovetz, PhD, Professor, Departments of Bioengineering and Surgery

David A. Vorp, PhD, Associate Professor, Departments of Surgery and Bioengineering

James H-C. Wang, PhD, Associate Professor, Departments of Orthopoedic Surgery, Bioengineering, Mechanical Engineering, and Physical Medicine & Rehabilitation

Kirk P. Conrad, MD, Professor, Departments of Physiology & Functional Genomics and Obstetrics & Gynecology, University of Florida

Sandra A. Murray, PhD, Professor, Department of Cell Biology & Physiology

Sanjeev G. Shroff, PhD, Professor, Departments of Bioengineering and Medicine
Dissertation Director

REGULATION OF ARTERIAL GAP JUNCTIONS BY MECHANICAL FACTORS: AN *EX VIVO* STUDY

Yong He, PhD

University of Pittsburgh, 2008

Introduction: Vascular cells communicate through gap junctions, which are formed by connexin (Cx) proteins. Cx43 is expressed in both endothelial and smooth muscle cells. Studies have demonstrated alterations in gap junctions with atherosclerosis and hypertension, diseases that involve changes in mechanical forces. However, regulation of arterial gap junctions by mechanical forces has not been well understood. **Methods:** In the present study, *ex vivo* perfusion culture of rabbit thoracic aortas was used to investigate the regulation of Cx43 by pressure magnitude and pulsatility. After culturing for 6 or 24 h, the Cx43 protein and mRNA levels were detected by Western blot and real-time PCR, respectively. The Src inhibitor PP1 or NADPH oxidase inhibitor apocynin was added to the culture medium to study the molecular mechanisms in some experiments. **Results: (1)** An increase in the steady pressure level (from 80 to 150 mmHg) significantly increased both mRNA and protein levels of Cx43 at 6 h, which were blocked by PP1. High steady pressure also upregulated Cx43 mRNA at 24 h, although the Cx43 protein levels were similar. This pattern of steady pressure-induced regulation of Cx43 was not altered by the presence of pressure pulsatility or flow levels. **(2)** Cyclic stretch, elicited by pulsatile perfusion (mean: 80 mmHg, pulse: 30 mmHg, 192 cycles/min), decreased Cx43 protein for both 6 and 24 h, compared with steady stretch controls (mean: 80 mmHg, pulse: 0 mmHg). Concomitantly, levels of active and total Src were reduced by cyclic stretch at 24 h. PP1 in steady perfusion culture or apocynin in pulsatile perfusion culture eliminated the observed differences in Cx43 protein between cyclic and steady stretch. In addition, apocynin elevated

active and total Src in aortas under cyclic stretch at 24 h. The ratio of active to total Src was not significantly altered in any case. **Conclusions:** Both pressure magnitude and pulsatility regulate Cx43 expression. High pressure upregulates Cx43 mRNA and is time-independent. High pressure upregulates Cx43 protein and is time-dependent. Cyclic stretch downregulates Cx43 protein and is time-independent. Src and NADPH oxidase may be involved in the signaling pathway.

TABLE OF CONTENTS

ACKNOWLEDGEMENTS XIV

1.0 INTRODUCTION AND SPECIFIC AIMS 1

1.1 INTRODUCTION 1

1.2 SPECIFIC AIMS 4

2.0 BACKGROUND 7

2.1 MECHANOTRANSDUCTION OF VASCULAR ENDOTHELIAL CELLS 7

2.1.1 Mechanotransduction of flow by vascular endothelial cells 7

2.1.2 Mechanotransduction of pressure/stretch by vascular endothelial cells 11

2.2 MECHANOTRANSDUCTION OF VASCULAR SMOOTH MUSCLE CELLS 13

2.2.1 Mechanotransduction of flow by vascular smooth muscle cells 13

2.2.2 Mechanotransduction of pressure/stretch by vascular smooth muscle cells 14

2.3 GAP JUNCTIONS AND CONNEXINS 21

2.3.1 Introduction 21

2.3.2 The life cycle of gap junctions 21

2.3.2.1 Connexin genes 22

2.3.2.2 Connexin biosynthesis 22

2.3.2.3 Connexin assembly into connexons 23

2.3.2.4 Connexon traffic to the plasma membrane 25

2.3.2.5 Docking of connexons into double-membrane spanning gap junction channels 25

2.3.2.6 Gap junction removal and degradation 26

2.3.3 Phosphorylation of connexins 28

2.3.4 Gating of gap junction channels and hemichannels 31

2.3.5 Connexin-interacting molecules 32

2.3.6 Roles of connexins independent of intercellular junctions 35

2.3.7 Gap junction studies using transgenic animal models 36

2.3.8 Gap junction regulation by exogenous chemicals 38

2.3.9 Gap junction regulation by mechanical factors 43

2.4 OVERALL SUMMARY OF BACKGROUND 46

3.0 MATERIALS AND METHODS 47

3.1 ISOLATION OF RABBIT DESCENDING THORACIC AORTAS 47

3.2 PERFUSION ORGAN CULTURE OF AORTAS AND EXPERIMENTAL PROTOCOL 48

3.3 PROTEIN EXTRACTION, ELECTROPHORESIS AND WESTERN BLOT 54

3.4 QUANTITATIVE MESSENGER RNA ANALYSIS 59

3.5 IMMUNOHISTOCHEMISTRY AND CONFOCAL MICROSCOPY 64

3.6 STATISTICAL ANALYSIS 65

4.0 RESULTS 66

4.1 CONNEXIN EXPRESSION IN RABBIT DESCENDING THORACIC AORTAS 66

4.2 REGULATION OF GAP JUNCTIONS BY THE MEAN PRESSURE LEVEL 70

4.2.1 Regulation of gap junction expression by the steady pressure level 70

4.2.2 Effects of pressure pulsatility on the mean pressure level-induced regulation of gap junction expression 79

4.2.3 Potential mechanisms underlying regulation of Cx43 by the steady pressure level 81

4.3 REGULATION OF GAP JUNCTIONS BY CYCLIC STRETCH INDUCED BY PULSATILE PRESSURE 93

4.3.1 Regulation of gap junction expression by pulsatile pressure 93

4.3.2 Regulation of Cx43 expression by long-term pulsatile pressure with a higher mean pressure – cyclic stretch regulates Cx43 expression 97

4.3.3 Potential mechanisms underlying the regulation of Cx43 by cyclic stretch ... 99

4.4 OTHER CONTROL EXPERIMENTS 119

5.0 DISCUSSION 124

5.1 SUMMARY AND DISCUSSION OF RESULTS 124

5.1.1 Effects of mean pressure level on arterial gap junctions 125

5.1.2 Effects of pulsatile pressure on arterial gap junctions 127

5.1.3 Possible role of Src in mediating the regulation of arterial Cx43 expression by pressure 128

5.1.4 Possible role of reactive oxygen species in mediating the regulation of Cx43 expression by pressure 131

5.1.5 Interactions between Src and reactive oxygen species 132

5.1.6 Different regulatory patterns of Cx43 expression by the mean pressure level and cyclic stretch 133

5.1.7 Dissociation of the Cx43 protein level from the mRNA level 134

5.1.8 Cx43 phosphorylation 134

5.1.9 Regulation of Cx40 and Cx37 by pressure 135

5.1.10 Effects of flow on pressure-induced regulation of arterial gap junctions 136

5.2 CLINICAL IMPLICATIONS 137

5.3 ADVANTAGES OF METHODOLOGY 138

5.4 DISADVANTAGES OF METHODOLOGY 139

5.5 RECOMMENDATIONS FOR FUTURE WORK 141

6.0 CONCLUSIONS..... 143

APPENDIX A…… 145

APPENDIX B…… 152

APPENDIX C…… 163

BIBLIOGRAPHY..... 168

LIST OF FIGURES

Figure 2-1 Human Cx43 amino acid sequence, topology, and some interacting molecules. 24

Figure 3-1 Schematic of the perfusion organ culture system. 50

Figure 3-2 TUNEL apoptosis detection of aortic sections..... 51

Figure 3-3 Vasocontraction test of cultured DTA. 52

Figure 3-4 Coomassie blue staining of a transferred gel to test protein transfer efficiency. 57

Figure 3-5 The Cx43 bands are specific to the Cx43 antibody..... 58

Figure 3-6 Saturation test of Cx43 bands. 59

Figure 3-7 Integrity test of total RNA extracted from rabbit aortas. 60

Figure 3-8 One example of the PCR amplification plot of Cx43 (right) and GAPDH (left) genes..... 64

Figure 4-1 Cx43 is expressed in endothelial cells of rabbit descending thoracic aortas. 67

Figure 4-2 Cx40 is expressed in endothelial cells of rabbit descending thoracic aortas. 67

Figure 4-3 Cx37 is expressed in endothelial cells of rabbit descending thoracic aortas. 68

Figure 4-4 Cx43 is expressed in smooth muscle cells of rabbit descending thoracic aortas. 68

Figure 4-5 Cx40 is not expressed in smooth muscle cells of rabbit descending thoracic aortas.. 69

Figure 4-6 Cx37 is not expressed in smooth muscle cells of rabbit descending thoracic aortas.. 69

Figure 4-7 Rabbit left ventricle staining of Cx43. 70

Figure 4-8 The Cx43 antibody (71-0700) can detect a few bands of the Cx43 protein because of phosphorylation. 71

Figure 4-9 Short-term (6 h) regulation of Cx43 expression by steady pressure. 72

Figure 4-10 Short-term (6 h) regulation of Cx43 phosphorylation by steady pressure. 73

Figure 4-11 Short-term (6 h) regulation of Cx40 mRNA expression by steady pressure. 74

Figure 4-12 Long-term (24 h) regulation of Cx43 expression by steady pressure. 75

Figure 4-13 Long-term (24 h) regulation of Cx43 phosphorylation by steady pressure. 76

Figure 4-14 Long-term (24h) regulation of Cx40 mRNA expression by steady pressure..... 77

Figure 4-15 Long-term (24 h) regulation of the Cx43 protein level by steady pressure at high flow (300 ml/min). 78

Figure 4-16 The Cx43 protein level is increased from 6 to 24 h under low steady pressure. 78

Figure 4-17 The Cx43 protein level is increased from 6 to 24 h under high steady pressure. 79

Figure 4-18 Long-term (24 h) regulation of Cx43 expression by mean pressure in the presence of pressure pulsatility. 80

Figure 4-19 Long-term (24 h) regulation of Cx43 phosphorylation by mean pressure in the presence of pressure pulsatility. 81

Figure 4-20 Short-term (6 h) regulation of Src by steady pressure. 82

Figure 4-21 Long-term (24 h) regulation of Src by steady pressure..... 83

Figure 4-22 Long-term (24 h) regulation of Src by mean pressure in the presence of pressure pulsatility..... 84

Figure 4-23 Src may mediate short-term (6 h) regulation of Cx43 expression by steady pressure. 85

Figure 4-24 Src may mediate short-term (6 h) regulation of Cx43 phosphorylation by steady pressure. 86

Figure 4-25 Short-term (6 h) regulation of the p27 protein level by steady pressure..... 87

Figure 4-26 Short-term (6 h) Src inhibition using PP1 in the media of high pressure cultures does not affect regulation of the p27 protein level by steady pressure. 88

Figure 4-27 Long-term (24 h) regulation of the p27 protein level by steady pressure. 89

Figure 4-28 Long-term (24 h) regulation of the p27 protein level by mean pressure in the presence of pressure pulsatility. 89

Figure 4-29 Short-term (6 h) regulation of the beta-catenin protein level by steady pressure. 90

Figure 4-30 Long-term (24 h) regulation of the CD31 protein level by steady pressure. 91

Figure 4-31 Long-term (24 h) regulation of Akt by mean pressure in the presence of pressure pulsatility..... 92

Figure 4-32 Short-term (6 h) regulation of Cx43 expression by pulsatile pressure..... 94

Figure 4-33 Short-term (6 h) regulation of Cx43 phosphorylation by pulsatile pressure..... 95

Figure 4-34 Long-term (24 h) regulation of Cx43 expression by pulsatile pressure..... 96

Figure 4-35 Long-term (24 h) regulation of Cx43 phosphorylation by pulsatile pressure..... 97

Figure 4-36 Long-term (24 h) regulation of Cx43 expression by pulsatile pressure under a higher mean pressure (150 mmHg)..... 98

Figure 4-37 Long-term (24 h) regulation of Cx43 phosphorylation by pulsatile pressure under a higher mean pressure (150 mmHg)..... 99

Figure 4-38 Short-term (6 h) regulation of Src by pulsatile pressure. 100

Figure 4-39 Long-term (24 h) regulation of Src by pulsatile pressure. 101

Figure 4-40 Long-term (24 h) regulation of Src by pulsatile pressure under a higher mean pressure (150 mmHg). 102

Figure 4-41 Src may regulate downregulation of the Cx43 protein level by cyclic stretch. 103

Figure 4-42 Long-term (24 h) regulation of Cx43 phosphorylation by cyclic stretch after inhibition of Src in aortas cultured under steady pressure. 104

Figure 4-43 Superoxide measurement using L-012 in aortic rings..... 106

Figure 4-44 Reactive oxygen species may mediate regulation of Cx43 by long-term (24 h) cyclic stretch. 107

Figure 4-45 Reactive oxygen species may mediate regulation of Cx43 phosphorylation by long-term (24 h) cyclic stretch. 108

Figure 4-46 Apocynin increases the Cx43 protein level in relaxed aortas at 6 h. 109

Figure 4-47 Short-term (6 h) regulation of the p27 protein level by cyclic stretch. 110

Figure 4-48 Long-term (24 h) regulation of the p27 protein level by cyclic stretch. 110

Figure 4-49 Inhibition of Src in aortas under steady stretch for 24 h does not alter the relative level of p27 protein. 111

Figure 4-50 Short-term (6 h) regulation of the beta-catenin protein level by cyclic stretch. 112

Figure 4-51 Long-term (24 h) regulation of the beta-catenin protein level by cyclic stretch..... 112

Figure 4-52 Inhibition of Src in aortas under steady stretch for 24 h does not alter the relative level of beta-catenin protein..... 113

Figure 4-53 Short-term (6 h) regulation of Akt by cyclic stretch. 114

Figure 4-54 Long-term (24 h) regulation of Akt by cyclic stretch. 115

Figure 4-55 Long-term regulation of Akt by pulsatile pressure with a higher mean pressure (150 mmHg). 116

Figure 4-56 Src may regulate Akt activation by long-term (24 h) steady stretch..... 117

Figure 4-57 Inhibition of reactive oxygen species using apocynin does not alter the long-term (24 h) regulation pattern of Akt by cyclic stretch. 118

Figure 4-58 The Cx43 protein level is increased after 6 h under low steady pressure (80 mmHg) compared with fresh aortas (Fr). 120

Figure 4-59 The Cx43protein level is increased after 6 h under cyclic stretch compared with the fresh aorta (Fre)..... 120

Figure 4-60 The protein levels of Cx43 and p27 are increased in aortas cultured in a relaxed state for up to 7 days (7D) as compared with fresh aortas. One typical example of three independent experiments is shown. 121

Figure 4-61 The Src levels in aortas cultured in a relaxed state for up to seven days. 122

Figure 4-62 The Akt levels in aortas cultured in a relaxed state for up to seven days. 123

Figure A-1 Cut-end loading of Lucifer Yellow into aortas for 5 (left) or 10 (right) minutes….147

Figure A-2 FRAP of HUVECs cultured on a coverslip……...149

Figure A-3 Two setups of FRAP on aortas……..150

Figure A-4 FRAP of rabbit aortas……150

Figure B-1 Diagram of the simulink model for pulsatile pressure and flow control……...154

Figure B-2 Mathematical simulation when both pulsatile pumps are not working…….155

Figure B-3 Mathematical simulation when only the upstream pulsatile pump is working…….155

Figure B-4 Mathematical simulation when only the downstream pulsatile pump is working…156

Figure B-5 Mathematical simulation when both pulsatile pumps are working……...156

Figure B-6 Schematic of the pulsatile perfusion system…….....158

Figure B-7 One example of the step response…….159

Figure B-8 The command and actual flow rates generated using the DMC control……...160

Figure B-9 Mathematical simulation of the effects of changing the compliance of the downstream tubing when only the upstream pulsatile pump is working. …….162

Figure C-1 The stabilzer. 163

Figure C-2 The three dimentional view of a vascular stabilizer showing the clamp bar and slider…….……...164

Figure C-3 The isometric and front views of the clamp bar……....165

Figure C-4 The top and left views of the clamp bar……..……...166

Figure C-5 The slider……..…167

ACKNOWLEDGEMENTS

I would like to express my heartfelt appreciation to all of you who have helped and supported me in many different ways during the development of this dissertation. My advisor, Dr. Sanjeev Shroff, has been very supportive and always available whenever I have questions. I also appreciate his patience and encouragement. My committee members, Drs. Harvey Borovetz, David Vorp, James Wang, Sandra Murray, and Kirk Conrad, guided me through this project. Dr. Partha Roy and Dr. Hai Lin, professors in our department, also helped me even though they were not on my committee. I thank Dr. Catherine Baty in the Center of Biological Imaging for helping me explore different approaches to measuring the function of gap junctions. I greatly appreciate Dr. Gerard Apodaca's generosity; he allowed me to use numerous rabbit aortas from his protocol during the initial development stage.

I greatly appreciate help from members of the Shroff laboratory, my fellow graduate students, and several undergraduate students – Caroline, Lauren, Steve, Jon, Dan, Nick, Ted, Katie, and Michael. Steve and Jon, whose desks were close to mine, were my free English teachers as well. Several members of the Vorp Laboratory (Dr. Alejandro Nieponice, Mo, Tim, and Scott) helped me develop the *ex vivo* system used in my experiments. I thank Li and Zhijie from the Roy laboratory for their technical assistance and valuable discussions.

Finally, I owe my wife too much in the last few years. I really appreciate her support, understanding, and patience.

1.0 INTRODUCTION AND SPECIFIC AIMS

1.1 INTRODUCTION

Cardiovascular diseases are the leading causes of morbidity and mortality in developed countries, which accounted for 36.3% of all deaths in the United States of America in 2004.[1] Atherosclerosis is a type of chronic and localized arterial lesion that produces thickening, hardening and restructuring of the arterial wall. Atherosclerosis can induce arterial stenosis, particularly coronary arterial stenosis. Coronary arterial stenosis reduces myocardial blood supply and may lead to ischemia, cardiac insufficiency and myocardial infarction. Atherosclerosis also causes stroke, and gangrene of the extremities.

Atherosclerosis was thought to be a chronic inflammatory disease although the pathogenesis of atherosclerosis is still not completely understood.[2, 3] Atherosclerosis is the result of a complex interaction between blood elements, disturbed flow, and vessel wall abnormality, in particular, endothelial dysfunction. Risk factors of atherosclerosis include a high blood lipid level, diabetes mellitus, hypertension, smoking, family history, genetic predisposition, etc. These risk factors may increase oxidative stress in vascular cells.[1] Although these common risk factors are systemic in nature, atherosclerosis affects some specific vascular sites.[2] Atherosclerosis occurs most in regions with geometric changes, such as curvature, branching and bifurcation. There has been positive correlation between plaque location and low oscillating wall shear stress

in the human carotid bifurcation.[3] This correlation stimulated great interests in studying into the effects of flow on vascular endothelial cells (ECs).[4-6] Vascular smooth muscle cells (VSMCs) maintain the structural integrity of blood vessels. VSMCs also play important roles in atherosclerosis.[10, 11] Arterial cells in hypertension and vein grafts used for coronary bypass surgery are subjected to elevated forces. The process of adapting to the new mechanical milieu, remodeling, may contribute to the complications of hypertension and graft failure. Altered mechanical conditions may play roles in restenosis after stenting as well.[7]

Mammalian cells can exchange small molecules with a molecular weight up to 1000 Daltons (Da) through gap junctions, which are formed by connexin (Cx) molecules.[8] Connexins are named by the predicted molecular weight in kiloDalton (kDa). Gap junctions coordinate vascular cells.[9] In arteries, Cx37, Cx40 and Cx43 may be expressed in ECs, while Cx37, Cx40, Cx43 and Cx45 may be expressed in VSMCs.[9] However, these connexin isotypes are not uniformly expressed in the vasculature. In general, ECs predominantly express Cx40 and Cx37, while arterial SMCs predominantly express Cx43.

In vivo studies have shown that some diseases (e.g., atherosclerosis, hypertension) are associated with altered connexin expression. It is not clear, however, whether these changes in connexin expression contribute to the genesis and/or maintenance of the disease process. In addition, *in vivo* studies have not provided a unified picture of the link between the disease process (or the attendant changes in mechanical milieu) and connexin expression. For example, transgenic mice with reduced Cx43 expression had fewer atherosclerotic lesions following the administration of high-fat diet.[10] In contrast, transgenic mice with smooth muscle cell-specific knockout of Cx43 had thicker neointima following vascular injury.[11] Similarly, vascular connexin expression was variably altered in hypertensive rats, depending on the hypertension

model.[19, 20] Taken together, the *in vivo* studies indicate that regulation of vascular connexin expression is multifactorial and therefore, it is difficult to tease out the effects of mechanical milieu alone from these data.

In vitro cell culture studies have been conducted as well to investigate regulation of vascular gap junctions by mechanical factors. These mechanical factors, specifically flow (shear stress) and pressure /wall stress/stretch, regulate gap junctions. For example, unidirectional and bidirectional (oscillatory) shear stress modulate the Cx43 protein level in ECs.[12] Shear stress spatial gradients also upregulates Cx43 expression in aortic ECs.[13] Cyclic circumferential stretch, but not pressure, increased Cx43 protein in ECs.[12] Twenty percent static stretch of cultured VSMCs increased Cx43 messenger ribonucleic acid (mRNA) and protein.[14] Although these *in vitro* cell culture studies have provided useful information, the results can be questioned for at least two reasons: (1) lack of the native three-dimensional architecture with appropriate combination of multiple vascular wall components (ECs, VSMCs, extracellular matrix proteins), and (2) changes in EC and VSMC phenotypes in *in vitro* cell culture. Therefore, the effects of mechanical factors on vascular gap junctions observed in *in vitro* studies may not reflect the case *in vivo*.

We utilized the approach of *ex vivo* culture of intact arteries to study regulation of gap junctions by mechanical factors in order to avoid some of the above-mentioned problems related to *in vivo* animal and *in vitro* cell culture studies. Specifically, *ex vivo* culture of arteries enabled us to maintain the native vascular architecture and composition and rigorously control the mechanical milieu of interest. In the present study, we primarily examined the link between pressure (both steady and pulsatile) and vascular connexin expression (both mRNA and protein).

1.2 SPECIFIC AIMS

The overall hypothesis is that arterial gap junctions are regulated by mechanical factors. This hypothesis was investigated through the following two specific hypotheses and corresponding aims.

Hypothesis 1: Arterial gap junctions are regulated by the mean pressure level.

Specific Aim 1a: To characterize regulation of Cx43 expression (both gene and protein) by the steady pressure level.

Specific Aim 1b: To examine whether pressure pulsatility affects the regulation of Cx43 expression (both gene and protein) by the mean pressure level.

Specific Aim 1c: To begin investigation of potential mechanisms underlying the steady pressure level-induced regulation of Cx43 expression.

Ex vivo culture of rabbit descending thoracic aortas (DTA) was carried out under high (150 mmHg) or low (80 mmHg) steady pressure to characterize regulation of Cx43 expression (Specific Aim 1a). Two culture durations (6 and 24 h) were explored to investigate the dynamics of this regulation. To examine the effects of pressure pulsatility on the regulation of Cx43 by the steady pressure level (Specific Aim 1b), the same experiments were repeated with the addition of a fixed level of pulsatile pressure (30 mmHg) to both high and low mean pressures. Finally, potential mechanisms underlying the steady pressure-induced regulation of Cx43 expression (Specific Aim

1c) were studied by investigating aspects of cell phenotype changes and certain signaling molecules (e.g., p27, Src, beta-catenin).

Hypothesis 2: Arterial gap junctions are regulated by cyclic stretch induced by pulsatile pressure.

Specific Aim 2a: To characterize regulation of Cx43 expression (both gene and protein) by pulsatile pressure.

Specific Aim 2b: To examine whether the pulsatile pressure-induced regulation of Cx43 expression (both gene and protein) is primarily mediated by cyclic stretch.

Specific Aim 2c: To begin investigation of potential mechanisms underlying the regulation of Cx43 expression by cyclic stretch.

To characterize regulation of Cx43 expression, *ex vivo* culture of DTAs were carried out under two conditions with the same mean pressure (80 mmHg): zero pulse pressure (i.e., steady condition) and 30 mmHg pulse pressure (Specific Aim 2a). This level of pulse pressure induced significant cyclic stretch of cultured aortas. Two culture durations (6 and 24 h) were explored to investigate the dynamics of this regulation. To examine whether cyclic stretch was the primary mediator of the pulsatile pressure-induced regulation of Cx43 expression (Specific Aim 2b), the same experiments were repeated with aortas cultured under a higher mean pressure level (150 mmHg); at this level of mean pressure pulsatile pressure did not induce significant cyclic stretch of the aorta.[15] Finally, potential mechanisms underlying the pulsatile pressure-induced regulation of Cx43 expression (Specific Aim 2c) were studied by investigating aspects

of cell phenotype changes and certain signaling molecules (e.g., p27, Src, reactive oxygen species, Akt).

2.0 BACKGROUND

Because of the prominent roles of mechanical forces in vascular physiology and pathology, effects of forces on vascular cells and transduction of forces into biochemical signals by vascular cells will be briefly reviewed.

2.1 MECHANOTRANSDUCTION OF VASCULAR ENDOTHELIAL CELLS

Being the inner layer of blood vessels, ECs are subject to viscous wall shear stress because of flowing blood. Blood pressure is applied to ECs directly as well. ECs are cyclically stretched due to the intermittent pumping of the heart. Vascular ECs are a transducer and integrator of both humoral and mechanical conditions. ECs actively synthesize and secrete many substances to maintain the homeostasis of the vasculature. The effects of flow, pressure and stretch (strain) on ECs will be reviewed.

2.1.1 Mechanotransduction of flow by vascular endothelial cells

Blood flow is very complex.[16] Blood flow is laminar in straight parts of large and medium-caliber arteries. However, disturbed flow occurs in regions with changing geometries, such as curvature, branching, and bifurcation. Doppler ultrasound and magnetic resonance imaging have

been used to measure blood flow in large arteries. To date, the patterns of disturbed flow are hard to be characterized. Generally, the disturbed flow has low mean wall shear stress with large amplitude and reverses flow direction during some portion of the period (oscillatory flow).

Flow regulates gene expression of ECs, and this regulation depends on flow patterns.[21-23] Laminar flow induces genes that are protective to vascular cells. In contrast, disturbed flow activates genes that may induce dysfunction of ECs. For example, the expression of the monocyte chemotactic protein-1 (MCP-1) is increased by disturbed flow.

The mechanisms of flow transduction by ECs are not completely known even though some mechanosensors of flow in ECs have been revealed. The cell membrane and some membrane proteins have the preference as mechanosensors. These proteins include receptor tyrosine kiases,[17] integrins,[18] G protein-coupled receptors and G proteins,[19] intercellular junctional proteins,[20] and ion channels.[28] The membrane glycocalyx may also be the sensor.[21]

Flow regulates shape and orientation of ECs. ECs align in the direction of blood flow in the straight part of arteries,[22] which depends on a mechanosensory complex comprised of platelet endothelial cell adhesion molecule-1 (PECAM-1), vascular endothelial cell cadherin (VE-cadherin) and vascular endothelial growth factor receptor 2 (VEGFR2).[20] In contrast, ECs have little orientation at branching sites where the flow patterns are disturbed. ECs subjected to oscillatory flow have a polygonal morphology similar to that of static controls.[23]

Under a chronic change in flow, blood vessels undergo structural remodeling via endothelium-dependent mechanisms.[24] Endothelial caveolin-1 and caveolae are required for this remodeling.[25] The ATP-gated P2X4 ion channels[26] and the p47phox-dependent NADPH Oxidases[27] are also necessary. Furthermore, caveolae participate in β1 integrin-mediated mechanotransduction of shear stress.[28]

One major achievement of vascular biology in the last two decades is the discovery that ECs secrete the vasorelaxant nitric oxide (NO). NO is a free radical gas diffusing rapidly from ECs to adjacent cells. Its vasodilation function is through activating soluble guanylate cyclase, which generates cGMP, and ultimately leading to activations of a variety of downstream effectors. NO plays a pivotal role in vascular biology and pathobiology. NO is the most potent vasodilator secreted in the vasculature. It also inhibits lipid oxidation, platelet aggregation and leukocyte adhesion to ECs and suppresses VSMC proliferation and migration. NO regulates the balance between cell proliferation and cell death because it is either proapoptotic or antiapoptotic. NO is generated through the enzyme nitric oxide synthase (NOS). ECs express endothelial nitric oxide synthase (eNOS, or NOS3). ECs may also express the neuronal (nNOS) and inducible isoforms (iNOS) of this enzyme.

NOS is a multi-domain enzyme consisting of an N-terminal oxygenase domain with binding sites for heme, L-arginine, and tetrahydrobiopterin, and a reductase domain bound by FMN, FAD, NADPH, and calmodulin. Two identical subunits form one functional eNOS complex. eNOS is myristoylated and palmitoylated.

Shear stress regulates the gene expression level of eNOS both *in vivo*[29] and *in vitro*,[30] even though eNOS is constitutively expressed in ECs. Bovine aortic ECs had more eNOS mRNA after exposure to 3 h of steady laminar flow. Laminar flow increased eNOS mRNA level through two mechanisms: a transient increase in eNOS transcription followed by a prolonged stabilization of eNOS mRNA molecules.[31] The initial activation of transcription was via c-Src/Ras/Raf/ ERK1/2. The long-term stabilization of eNOS mRNA was also through c-Src, but was independent of Ras and ERK. The effect of flow on eNOS mRNA stability was further found to be related to 3' polyadenylation of the eNOS mRNA.[32] Laminar flow increased

expression of eNOS transcripts with longer poly(A) tails, which extended the half life of eNOS mRNA from 6 h in static cells to 18 h in sheared cells.

Flow increases NO production by regulating eNOS activation. Flow-dependent phosphorylation of bovine eNOS-Ser^{1179} was mediated by a PKA and/or AMP-activated protein kinase-dependent mechanism, and increased the eNOS activity.[33, 34] PECAM-1, VEGFR2, the Scaffolding protein Gab1, the tyrosine phosphatase SHP2, and the receptor tyrosine kinase Tie2 were mechanotransducers that lead to the activation of eNOS in response to flow.[42-45] Another mechanism of the flow-induced activation of eNOS was through recruiting heat-shock protein 90 (Hsp 90) to eNOS.[35]

One of the exciting findings recently is the discovery that the zinc finger-containing transcription factor, lung Kruppel-like factor (KLF2) has crucial roles in regulating vascular structure and function.[36-38] Human umbilical vein endothelial cells (HUVECs) exposed to sustained laminar flow had increased expression of KLF2, which was mediated by nucleolin.[50, 51] However, disturbed flow decreased KLF2 expression both *in vivo* and *in vitro*.[39] KLF2 was involved in the laminar flow-induced increase in eNOS transcription,[36] beneficial effects of statins,[40] endothelial thrombotic function,[41] inhibition of protease-activated receptor-1 expression,[42] and TGF-β signaling.[43] It was further found that KLF2 acted as a central transcriptional switch point between the quiescent and activated states of adult ECs.

Proteins that are specifically activated by disturbed flow may be play roles in atherosclerosis. In an effort to identify the PKC isoforms that were expressed at regions with disturbed flow *in vivo*, PKCzeta was found to be more active among a few PKC isoforms expressed in ECs at regions with disturbed flow.[44] Oscillatory flow activated NADPH oxidase to

generate more superoxide[45] through upregulating the bone morphogenic protein 4 (BMP-4).[46] In contrast, laminar flow inhibited BMP-4 via PKA.[47]

2.1.2 Mechanotransduction of pressure/stretch by vascular endothelial cells

It should be pointed out that although I use pressure/stretch here, pressure and stretch are not the same. ECs are subjected to pressure/stretch as well. Depending on the pulsatility of the pressure and the rigidity of the substrate used to culture ECs, ECs may be compressed by the applied pressure or be stretched as well. Pressure/stretch regulates structure and function of ECs. Some molecular mechanisms have been identified.

Pressure may promote or inhibit EC growth depending on the level, pulsatility and duration of the applied pressure. Low sustained hydrostatic pressure up to the level of physiologic pressure *in vivo* increased proliferation of bovine pulmonary artery ECs (BPAECs) cultured on rigid substrates via basic fibroblast growth factor (bFGF),[48] and of HUVECs by activating αV integrins.[49] However, a higher static pressure (>80 mmHg) caused degeneration of ECs.[50] By contrast, pulsatile pressure (140/100 mmHg) inhibited apoptosis.[51]

Sustained static pressure may induce cytoskeleton remodeling and changes in morphology of ECs.[48] However, this effect was not observed using a pulsatile pressure.[51]

Pressure may affect the synthetic activity of ECs. High static pressure increased the release of endothelin-1 (ET-1),[52] prostacyclin,[53] and interleukin-6 (IL-6) in ECs.[54]

Pulsatile pressure mediates the endothelial barrier function.[55] The change in permeability of HUVECs induced by pulsatile pressure depends on the pressure level. Exposure of HUVECs to a high pulsatile pressure (140/100 versus 60/20 mmHg at 1 Hz) reduced significantly the transendothelial permeability to albumin. Furthermore, this effect occurred concomitantly with

the redistribution of the intracellular tight junction protein zona occludens-1 (ZO-1) and remodeling of actin stress fibers.

Cyclic stretch changes the cytoskeleton organization and orientation of ECs. Arterial ECs *in vivo* align along the flow direction, which is coincidentally perpendicular to the cyclic stretch direction. Although the alignment of ECs with the flow direction does not require cyclic stretch,[56] circumferential stretch may increase the sensitivity of ECs to shear stress.[57] ECs cultured *in vitro* also aligned perpendicular to the uniaxial stretching direction via the kinase Rho[58] and focal adhesion kinase (FAK).[59] Concomitantly, c-jun N-terminal kinase (JNK) was activated.[60] However, equibiaxial cyclic stretch did not reorientate ECs,[60] although both uniaxial and biaxial stretches increased the amount of actin stress fibers.[60] The actin stress fibers of ECs in intact arteries can realign toward the circumferential direction if the arteries are stretched axially and there is no flow.[73]

The regulation of the gene expression of HUVECs by pulsatile pressure was studied using microarray techniques.[61] Pulsatile pressure modulated the expression of 14 genes which encoded some mechanosensitive proteins for homeostasis (tissue plasminogen activator), cell adhesion (integrin α2), and signaling (Rho B, cytosolic phospholipase A2). Vascular endothelial growth factor (VEGF)-C and TGF-β2 were found to be pulsatile pressure-sensitive as well.

Cyclic stretch may increase the expression of some marker proteins of VSMCs in ECs.[62] The mRNA levels of SM22-α, α-smooth muscle actin (α-SMA), caldesmon-1, smooth muscle myosin heavy chain (SMMHC), and calponin-1 were increased in cyclically stretched HUVECs as compared with static controls. On the other hand, the mRNA levels of two EC-specific markers, von Willebrand factor (vWF) and VEGFR2, were downregulated. Furthermore, the protein levels of SM22-α and α-SMA were also increased. Surprisingly, cyclic stretch also

significantly increased network formations on Matrigel (frequently used to measure the endothelial angiogenesis capability) by ECs,[63] although cyclic stretch seemed to transdifferentiate ECs to VSMCs. [62]

Stretch activates a number of proteins in ECs. Activation of eNOS by cyclic stretch was bi-phasic and mediated by two distinct pathways.[64] Cyclic stretch enhanced Akt-dependent antiapoptosis capability in ECs.[65] The superoxide production by NADPH oxidase was increased in cyclically stretched ECs.[66]

2.2 MECHANOTRANSDUCTION OF VASCULAR SMOOTH MUSCLE CELLS

VSMCs are not directly exposed to a significant level of flow in healthy blood vessels. However, when there are injuries and denudation of ECs, VSMCs may directly experience fluid shear. VSMCs can also be exposed to fluid shear because of an interstitial flow induced by the transmural pressure differential.[67] A few studies have demonstrated the effects of flow on VSMCs.

2.2.1 Mechanotransduction of flow by vascular smooth muscle cells

There was a rise in cytosolic Ca^{2+} ion concentration in VSMCs responding to an increase in flow.[68] VSMCs contracted when the shear stress was larger than the threshold value (11 dyne/cm^2).[69] This response was dependent on the Rho-kinase pathway. The transient receptor potential ion channel protein M7 (TRPM7) was accumulated rapidly to the plasma membrane upon flow.[70] Interestingly, ECs showed a low level of TRPM7-like current, which was not

increased by flow. Flow also increased NO production by nNOS in VSMCs.[71] The increased level of NO reduced activation of matrix metalloproteinase (MMP)-2, resulting in a significant flow-induced inhibition of VSMC migration.[72]

Flow may induce endothelial transdifferentiation from VSMCs.[73] Flow increased the mRNA levels of EC markers such as PECAM-1, vWF, and VE-cadherin, accompanied by the decreased mRNA levels of VSMC markers (α-SMA, calponin-1, SMMHC, and transgelin). Protein levels of PECAM-1 and vWF were also significantly increased by flow.

2.2.2 Mechanotransduction of pressure/stretch by vascular smooth muscle cells

The main mechanical factors applied to VSMCs are pressure and the accompanied stretch/strain. These factors mediate the structure and function of VSMCs, which have been extensively investigated.

Pressure/stretch regulates differentiation and phenotypes of VSMCs. In healthy adult arteries, VSMCs are at a fully differentiated, contractile phenotype with a very small rate of proliferation. However, a synthetic phenotype may be induced by vascular injuries, excessive stimulation of growth factors, and pressure/stretch. A certain level of pressure/stretch is required to maintain a differentiated, contractile phenotype of VSMCs. The protein levels of high-molecular-weight caldesmon and filamin, two molecular markers of contractile VSMCs, were maintained in rabbit aortas perfused under an intraluminal pressure of 80 mmHg for 3 days.[74] However, the rates of synthesis of several proteins (α-SMA, calponin, SM22α, tropomyosin, and desmin) in unstretched veins were significantly lower than those in stretched veins. This process was mediated through actin polymerization.[75] VSMCs that were stretched equibiaxially exhibited an increase in the expression of VSMC differentiation markers, and this process was mediated by

Notch/Cp-binding factor 1 (CBF-1)/recombination signal sequence-binding protein-Jκ (RBP-Jκ) signaling.[76]

Pressure/stretch regulates proliferation and apoptosis of VSMCs. Human aortic smooth muscle cells cultured at 160 mmHg atmospheric pressure had a nearly four fold increase in cell proliferation compared to controls. However, static pressure may also reduce proliferation if the pressure is too high (200 mmHg).[77] Vein grafts and cyclically stretched SMCs underwent apoptosis.[78] The signaling pathways leading to apoptosis include p38 mitogen-activated protein kinase (p38 MAPK),[78] β1 integrin/Rac/p53,[79] Ras/Rac/p38 MAPK/NF-κB/IL6,[80] Notch receptor,[94] and hedgehog.[81]

Pressure/stretch mediates a number of pathways involved in many processes of VSMCs, which will be reviewed individually. These include FAK, mitogen-activated protein kinase (MAPK) cascade, NF-κB pathway, MMPs, and NADPH oxidase.

FAK. Focal adhesions are sites where cells connect with extracellular matirx (ECM).[82] A number of signaling and structural proteins are concentrated at focal adhesions. Therefore, focal adhesions can integrate environmental stimuli and mediate the two-way crosstalk between ECM and cells. Focal adhesions are reorganized under stimulation of vascular cells by mechanical factors. Integrin proteins are one of the key sensors of force/deformation at focal adhesions. Integrins are activated and clusterred by mechanical forces. FAK is one of the non-receptor type tyrosine kinases and its activities are regulated through phosphorylation. FAK is activated following integrin activation. Tyrosine phosphorylation of FAK was increased by stretch in rabbit pulmonary arteries.[97] Phosphorylation of specific amino acids in FAK was also studied using *ex vivo* culture of rabbit descending thoracic aortas.[83] Tyrosine phosphorylation of FAK was significantly increased by high steady pressure (150 mmHg) as compared with the 80 mmHg

controls. Inhibition of Src (with the inhibitor PP2) and integrin (using RGD peptide) dampened total FAK phosphorylation in vessels cultured at 150 mmHg. In contrast, cyclic stretch generated by pulsatile perfusion did not induce significant FAK phosphorylation relative to non-pulsatile controls with the same mean pressure at 80 mmHg.

MAPK. The MAPK cascade includes three different pathways which are activated by various stimuli and initiate distinct cellular responses. One is mediated by ERK1/2, whose activation leads to the activity of some regulatory proteins in the cytoplasm and nuclei. The other two are JNK and p38. All these three pathways can be activated by mechanical forces to regulate gene expression, protein synthesis and function. ERK1/2 and JNK were activated in cyclically stretched VSMCs[84] and in rat arteries by acute hypertension.[85] High steady pressure (150 mmHg) and 10% cyclic stretch also activated ERK1/2 as compared with normal steady pressure (80 mmHg) using an *ex vivo* method.[86, 87] However, the mechanisms of activating ERK by high steady pressure and pulsatility differ. Integrin and Src kinase-mediated FAK activations were involved in high steady pressure-induced activation of ERK,[83] while reactive oxygen species (ROS) mediated the latter.[87] Cyclic stretch also activated p38.[87]

NF-κB. NF-*κ*B is a transcription factor, and is found in all cell types. NF-*κ*B belongs to the category of "rapid-acting" transcription factors, because it is present in cells in an inactive state and does not require new protein synthesis to be activated. Inactive NF-*κ*B is sequestered in the cytoplasm by the inhibitor protein, I*κ*B, which is phosphorylated and degraded upon activation of the NF-*κ*B pathway. Released NF-*κ*B is translocated into the nucleus where it transcribes a large range of genes implicated in inflammation, but also genes related to apoptosis repression and survial.

Mechanical factors can activate NF-κB. Cyclic stretch activated NF-κB in human coronary SMCs *in vitro* through stimulating superoxide production.[88] In contrast, NF-κB was not activated by pulsatile perfusion of intact arteries.[83] Higher steady pressure was more effective to activate NF-κB in arteries, which was important to cell survival under increased stress.[89] Blocking nuclear translocation of NF-κB increased apoptotic cells induced by high steady pressure. However, activation of NF-κB was not sufficient to prevent apoptosis in veins used for coronary bypass which underwent arterial perfusion conditions.[80] ROS induced by high intraluminal pressure activated NF-κB.[90] Transforming growth factor alpha (TGF-α) was needed for stretch-induced activation of NF-κB and consequent vascular remodeling.[90]

MMP. MMPs, a family of endoproteinases which have at least 25 members, require the ion zinc in their active sites. The activity of MMPs is suppressed by one of four endogenous tissue inhibitors of MMPs (TIMPs). MMPs are classified into collagenases, gelatinases, stromelysins, membrane type, and other MMPs according to their substrate specificity, sequence similarity, and structure.[91] MMPs have overlapping activities against a variety of ECM, and non-ECM components, such as growth factor binding proteins or latent growth factors. Therefore, MMPs are involved in many processes, such as proliferation, apoptosis, differentiation, and migration of cells in tissues. MMPs regulate modeling and remodeling in response to altered hemodynamic conditions and injuries in cardiovascular system.

Mechanical forces regulate MMPs of VSMCs. The gelatinases, MMP-2 and MMP-9, were mostly studied among vascular MMPs. The nature of the applied strain may mediate MMP-2 and MMP-9 differently. Static strain increased the gene expression and protein levels of MMP-2 and MMP-9 in human saphenous vein SMCs *in vitro*, while cyclic strain did the opposite.[92] These effects, however, were not observed in another study.[93] Cyclic stretch induced more

mRNA and proenzyme of MMP-2 in aortic SMCs via ROS generated by NADPH oxidase. In intact veins, arterial conditions reduced the latent MMP-2 and MMP-9 levels compared to matched veins. This reduction was caused by increased degradation because the synthesis of MMP-2 and MMP-9 was actually increased in arterial condtions.[94] Contrary to this *ex vivo* study, arterialization of canine jugular veins *in vivo* upregulated MMP-9, MMP-2 and MT1-MMP accompanied by TIMP-2 downregulation.[95] Longitudinal stretch of veins increased the level of pro-MMP-9, active MMP-2, and integrin αv, which is the receptor of active MMP-2.[96] Integrin αvβ3 binds to the C-terminus of MMP-2 and this binding is stable in the presence of the detergent sodium dodecyl sulfate (SDS).[97] Arterial MMP-2 and MMP-9 may be regulated differently by pressure.[98] Porcine coronary arteries subjected to normal transmural pressure (100 mmHg) had significantly more active MMP-2 relative to those under high pressure (200 mmHg) and zero-pressure controls for 2 days, regardless of the flow condition.[98] However, arteries subjected to high pressure had more MMP-9 than arteries maintained at normal pressure and zero-pressure controls, also regardless of the flow level. In contrast, mouse carotid arteries maintained at low pressure (10 mmHg) had a stronger MMP-2 activity as compared to arteries at normal pressure (80 mmHg) for 3 days.[99] Under high pressure (150 mmHg), both MMP-2 and MMP-9 activities were induced. Further, high pressure induced MMP-9 contributed to the increased distensibility. Similarly, MMP-9 was important for arterial geometric remodeling and SMC migration.[100] In DOCA-salt hypertensive rats, MMP-2 expression and activity in aortas were increased.[101] Cyclic bending for 4 h down-regulated MMP-1 gene expression in porcine femoral arteries.[102] To date, differential regulation of MMPs in intact blood vessels by cyclic and steady stretch has not been reported.

To have a more complete view of MMP regulation by mechanical forces, the effects of stretch on MMPs in ECs are discussed here.[103] Equibiaxial cyclic strain (0-10% strain, 60 cycles/min) stimulated the MMP-2 gene expression and activity through the G protein Gβγ, receptor tyrosine kinase, Shc, p38- and ERK-dependent pathway in bovine aortic ECs.[104] In addition to MMP-2, MMP-14 was also upregulated at both gene expression and protein levels by cyclic stretch through JNK and tumor necrosis factor-α (TNF-α) in HUVECs.[105] Static stretch also increased the mRNA and protein levels of MMP-2 in skeletal muscle microvascular ECs through JNK, while ERK and ROS did not regulate MMP-2.[106] Cyclic stretch increased the mRNA level of MT1-MMP in rat microvascular EC through the transcription factor Egr-1.[107]

NADPH oxidase. ROS are oxygen-derived small molecules, including superoxide, hydroxyl, peroxyl, ozone, singlet oxygen, and hydrogen peroxide. ROS interact with a variety of molecules, such as proteins, lipids, carbohydrates, and nucleic acids. Therefore, ROS may be important signaling molecules regulating the functions of the interacting molecules. ROS have been implicated in atherosclerosis, hypertension, responses to vascular injuries, and other vascular diseases. The physiological generation of ROS can be either the byproduct of some biological reactions in mitochondria, peroxisomes, and cytochrome *P*-450, or the specific product of uncoupled NOS, xanthine oxidase, cyclo-oxygenase, and NADPH oxidase, which is also called the NOX enzyme.[108] The NADPH oxidase enzyme is a complex of five components: $p40^{phox}$ (*phox* for *ph*agocyte *ox*idase), $p47^{phox}$, $p67^{phox}$, $p22^{phox}$ and NOX, which is the catalytic subunit. The catalytic subunit of the phagocyte NADPH oxidase, commonly referred to as $gp91^{phox}$, is called NOX2. Six homologs of NOX2 have been discovered: NOX1, NOX3, NOX4, NOX5, DUOX1, and DUOX2. They catalyze the production of superoxide by the one-electron reduction of oxygen molecules using NADPH as the electron donor. Three of these five

components, p40^{phox}, p47^{phox} and p67^{phox}, form a complex in the cytosol in resting cells. The other two components are located in the membranes. When the resting cell is stimulated, p47^{phox} is phosphorylated and the cytosolic complex is transferred to the membrane, where it associates with the other two to form the active oxidase. Superoxide can be dismutated by superoxide dismutase (SOD) to hydrogen peroxide, which is then decomposed to water and oxygen by the enzyme catalase.

NADPH oxidases are the major source of superoxide. NOX enzymes are expressed in the vascular wall. NOX4 is the predominant isoform in ECs, NOX1 and NOX4 in SMCs, NOX4 in adventitial fibroblasts, and NOX2 in macrophages. ECs also express NOX2 and NOX5. NOX2 is expressed in SMCs as well.

Mechanical forces activate NADPH oxidase. Cyclic stretch of mouse aortic SMCs caused rapid p47^{phox} membrane translocation and an increase in NOX-1 mRNA.[93] However, the effects of cyclic stretch on superoxide production in human aortic ECs are controversial. Human aortic ECs produced more[66] or less[109] superoxide under cyclic stretch. Further, this response to cyclic stretch may depend on the type of ECs. HUVECs generated more superoxide under cyclic stretch.[109] Static stretch of bovine coronary arteries with denuded endothelium also translocated p47^{phox} to the plasma membrane.[110] High steady pressure increased the phosphorylation of the p47^{phox} via PKC, which led to more superoxide production.[111] Pulsatile perfusion increased the superoxide level compared to the aortas under steady pressure with the same mean value.[87] Oscillatory flow with zero mean shear stress upregulated the mRNA levels of NOX2 and NOX4 in bovine aortic ECs, accompanied by an increase in the superoxide production rate.[45] The increase in the diameter of a mouse carotid artery induced by elevated flow depended on p47^{phox}, but not on NOX2.[27] Cyclic stretch also upregulated the gene expression of p22^{phox}, p47^{phox},

p67^{phox}, NOX1 and NOX4 in mouse embryonic stem cells, and promoted the differentiation of embryonic stem cells towards cardiovascular cells.[112]

2.3 GAP JUNCTIONS AND CONNEXINS

2.3.1 Introduction

Intercellular gap junctions provide direct communication between neighboring cells.[8] Mammalian cells use gap junctions as a fundamental mechanism to behave as a team. Many small molecules can pass through gap junction channels by passive diffusion, such as ions, metabolites, cyclic adenosine monophosphate (cAMP), and cyclic guanosine monophosphate (cGMP). Interestingly, short interfering RNA (siRNA) can also be transported through the Cx43 gap junctions, which may coordinate gene expressions.[113] However, transfer of siRNA was not non-selective. siRNA molecules could not pass through the Cx32/26 gap junction channels. The current knowledge of gap junctions will be reviewed.

2.3.2 The life cycle of gap junctions

Gap junctions are very dynamic structures. The half-life of connexins may be just about 1~5 h both *in vivo*[135, 136] and *in vitro*,[114, 115] which is much shorter than those of most cell membrane proteins. The life cycle of gap junctions is tightly controlled.[116] Therefore, it is necessary to review the current knowledge about all stages of the life cycle of gap junctions in order to understand and study the regulation of gap junctions by chemical and mechanical factors.

2.3.2.1 Connexin genes

Connexin genes are ubiquitously expressed in mammals. Each animal may have multiple types of connexin genes. For example, twenty connexin genes have be identified in mice, while there are 21 in the human genome.[117] The connexin gene structure was found to be simple initially. There are only two or three exons for Cx43,[118] Cx40,[142, 143] and Cx37.[144] The protein coding region is in one exon, which also contains 5'-nontranslated-region (NTR) and 3'-NTR. Other exons are part of the 5'-NTR upstream to the 5'-NTR contained in the coding exon. However, four more exons have been recently found in the 5'-NTR of the mouse Cx43 gene; and nine different Cx43 mRNA species are generated by differential promoter usage and alternative splicing mechanisms.[119] The rat Cx45 gene also has four exons, which are transcribed to four transcripts.[120]The different transcripts are translated at varying efficiencies.[119] And this may be one way of regulating gap junctions. Although mice, rats and humans have a similar organization of the Cx43 gene to, more studies are needed to determine if the human Cx43 gene also has so many exons.

2.3.2.2 Connexin biosynthesis

Connexin mRNA is translated into connexin proteins in ribosomes attached to the endoplasmic reticulum (ER) membrane, the same as other transmembrane proteins. The connexin molecule is a four-transmembrane spanning protein with two extracellular loops and one intracellular loop (Figure 2.1). Both N- and C-termini are intracellular. Among different types of connexins, the two extracellular loops are structurally conserved; however, high variation exists for the cytoplasmic regions (the N-terminus, the intracellular loop, and the C-terminus), which may contribute to the connexin-specific properties. Connexins can be classified into subgroups (α, β or γ) according to their extent of sequence identity and length of the

cytoplasmic loop.[121] The newly synthesized polypeptides are inserted into the ER membrane cotranslationally.[122]

2.3.2.3 Connexin assembly into connexons

One half of a gap junction channel is called a connexon. Unlike most multimeric transmembrane complexes oligomerizing in ER, connexins oligomerize in the place related to the Golgi apparatus. However, the exact place of connexin molecule oligomerization into connexons might be connexin-isoform specific. Cx43 is assembled in the *trans*-Golgi network after exiting from ER,[150-152] while Cx32 is assembled in the ER/*cis*-Golgi network.[124] The minimal motif to prevent ER oligomerization of Cx43 consists of the complete third transmembrane domain and the second extracellular loop.[125]

Different types of connexins can assemble into hetero-oligomeric connexons. For example, Cx43 hetero-oligomerizes with Cx40,[126] or Cx37.[127] Furthermore, these gap junction channels display many unitary conductances different from homomeric/homotypic Cx43 or Cx40 channels.[126] However, hetero-oligomerization is selective. All reported hetero-oligomeric connexons are composed of two members of the same subgroup. For instance, Cx43, an α-type, did not oligomerize with Cx32,[128] or Cx26,[129] a β-type. The specificity of hetero-oligomerization may be based on intrinsic signals that are specific to each connexin subtype.[130]

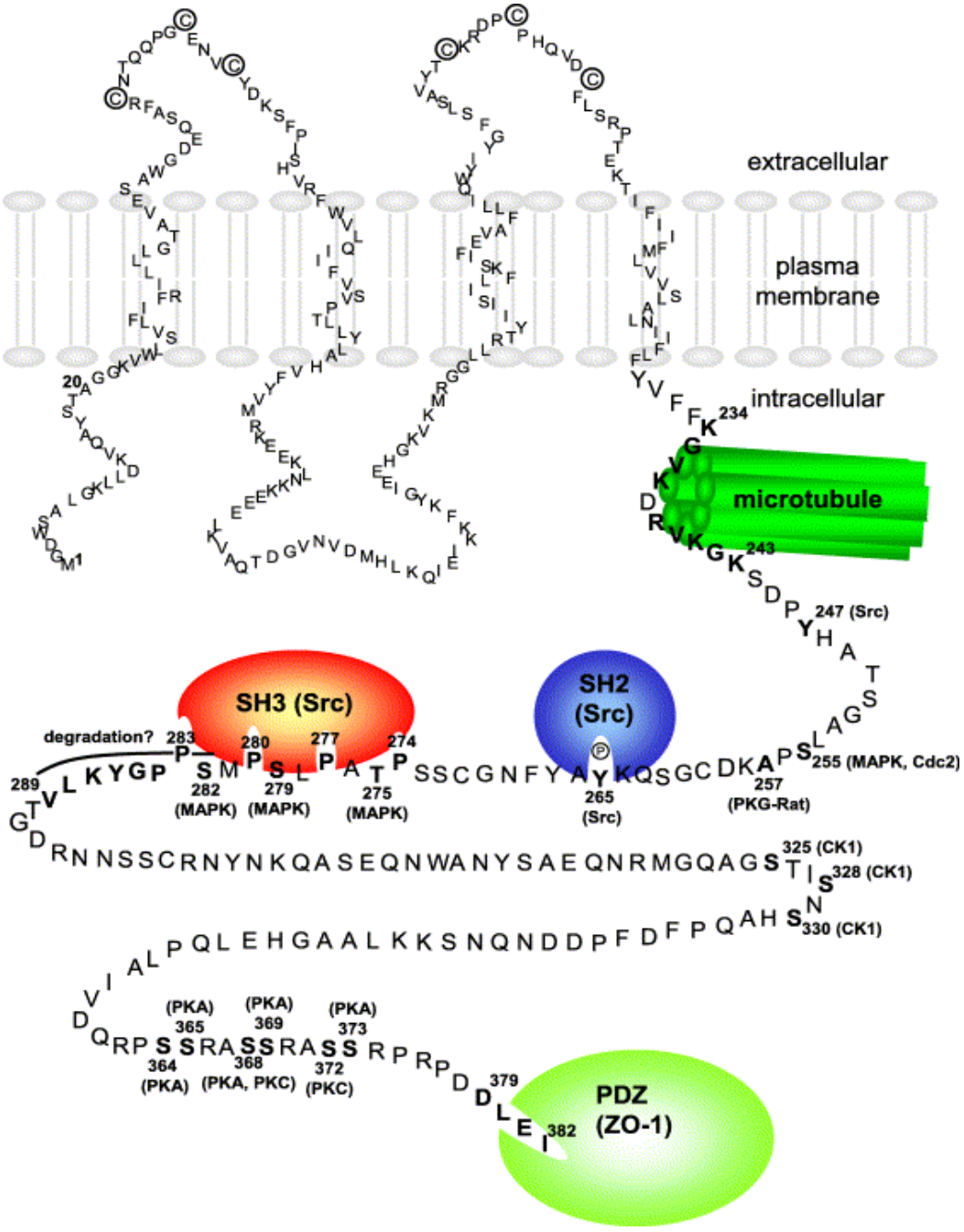

Figure 2-1 Human Cx43 amino acid sequence, topology, and some interacting molecules.

Cited from Giepmans.[123]

2.3.2.4 Connexon traffic to the plasma membrane

Connexons with green fluorescent protein (GFP) tags were delivered in vesicular carriers traveling along microtubules from the Golgi to the plasma membrane in all directions.[131] These connexon-containing vesicles moved along curvilinear tracks to follow microtubules which extended to the plasma membrane. The vesicles of Cx43 were predominantly in 100- to 150-nanometer.[132] This delivery route follows the general intracellular transport pathway for secretory vesicles.[133] However, Cx26 connexons might follow an unidentified alternative pathway that is independent of microtubules.[155, 156] Intact microfilaments were also required for both Cx43 and Cx26 connexon traffic.[134] Cx43 was transported to the plasma membrane in its non-phosphorylated form (Cx43NP).[135] The second extracellular region of Cx43 was required to localize to the plasma membrane.[136] Cx43 proteins with the point mutations F199L, R202E, and E205R in the second extracellular region were localized in the cytoplasm only when expressed in HeLa cells, which do not have Cx43 normally.

2.3.2.5 Docking of connexons into double-membrane spanning gap junction channels

Connexons are predominantly inserted into the nonjunctional plasma membrane instead of gap junctional plaques directly.[131] Connexons can diffuse laterally in the plasma membrane.[134] Therefore, newly synthesized connexons were found to be accumulated to the outer margins of channel clusters using CX43-GFP and fluorescence recovery after photobleaching (FRAP)[131] or recombinant Cx43 proteins and pulse-chase labeling.[132] This process might not be completely random, however. The delivery of Cx43 from a lipid raft domain to gap junctional plaques was mediated by the tight junction protein zona occludens-1(ZO-1) in osteoblastic cells.[137] Docking of connexons was affected by calcium-dependent cell adhesion molecules, such as E-cadherin,[138] and N-cadherin.[139] Adherens junctions, maintaining the structural integrity of cell-cell contacts,

were thought to act as foci for the gap junction formation.[140] The formation of the gap junction intercellular channels required a 30° rotation between connexons for proper docking.[141] Protrusions on one connexon fitted into the valleys of the apposed connexon under this degree of rotation. There are six conserved cysteines in the extracellular loops of each connexin molecule. The disulfides formed between apposing connexons are essential for the docking of connexons. An engineered Cys-less version of Cx43 prevented the formation of functional channels even though connexons had similar permeability to carboxyfluorescein as wild-type Cx43.[142]

Different connexons can form heterotypic intercellular channels.[143] Functional gap junction intercellular channels can be formed by Cx43 with Cx40,[174-176] Cx37,[127] or Cx45;[144] by Cx40 with Cx45,[128] or Cx37.[145] Heterogeneous channels display different gating activities, channel conductance and selectivity compared with homogeneous channels.[143] Gap junction channels aggregate to from plaques. Individual plaques may have multiple subtypes of connexin molecules.[146] Three different connexins of aortic ECs are organized within the same gap-junctional plaques. Some gap junctional plaques are relatively immobile,[147] while others are highly mobile within the plasma membrane, fusing together or segregating into smaller parts.[176]

2.3.2.6 Gap junction removal and degradation

The regulation of gap junction internalization and degradation has not been fully understood. Generally, junctional plaques need to be internalized first before they can be degraded intracellularly. Plaques are removed into one of the apposing cells as annular gap junctions.[148-150] Internalization of a gap junctional plaque occurs in the center of the plaque.[132] Clathrin may play a role in this process. Electron microscopy revealed association of clathrin coats with gap junctions.[151] Inhibition of clathrin-medicated endocytosis blocked EGF-induced Cx43 internalization.[152] A tyrosine-based sorting signal of Cx43, known to be involved in the

intracellular trafficking of many membrane proteins, affected the gap junction turnover.[153] The Cx43-Y286A mutation extended the Cx43 half-life from 2 to 6 h.

Gap junctional plaques are degraded in lysosomes. This degradation is proteasome-dependent in some cell types.[154] Studies have shown more convincing evidence of connexin degradation in lysosomes.[171, 177, 178] Evidence of direct degradation of junctional plaques by proteasomes is still absent although inhibition of proteasomes revealed the involvement of proteasomes in the degradation process.[185, 188, 190, 191] Only Cx43 and Cx32 have been studied for the role of proteasomes so far. It is known that ubiquitination regulates membrane protein degradation,[155] however, the requirement of ubiquitination for Cx43 junctional plaque degradation has not been established. Polyubiquitin modification of proteins is required for proteasome degradation of proteins.[155] Although cell culture studies demonstrated ubiquitination of Cx43,[180, 186, 187] Cx43 was ubiquitinated in the form of multiple monoubiquitinations at lysine residues, instead of polyubiquitin.[156] Monoubiquitination of Cx43 may be related to internalization and degradation of gap junctional plaques.[156] It is not known whether Cx43 is also ubiquitinated *in vivo*. Although the E3 ubiquitin protein ligase Nedd4 was found to bind to Cx43 recently, ubiquitination of Cx43 was not studied.[157] Colocalization of Cx43 and Nedd4 was found in the plasma membrane and cytoplasm. However, attenuation of Nedd4 using siRNA did not significantly increase the total protein level of Cx43 detected by Western blot. Therefore, it is possible that proteasomes play indirect roles in junctional connexin degradation by affecting the level of monoubiquitin ligation, internalization and trafficking of Cx43.[189, 190]

Connexins are phosphor-proteins except Cx26. The short half-life of Cx26 suggests that phosphorylation of connexins is not absolutely required for rapid gap junction degradation.[158] However, phosphorylation of some connexin subtypes may facilitate the regulation of connexin

degradation.[159] Phosphorylation of Cx43 was thought to be required for Cx43 ubiquitination.[156] Although the E3 ubiquitin protein ligase Nedd4 has not been shown to ubiquitinate Cx43, the binding of the three WW domains of Nedd4 to Cx43 depended on the phosphorylation status of Cx43.[157] The WW1 and WW2 domains interacted with the non-phosphorylated form of Cx43 predominantly, while WW3 bound phosphorylated and non-phosphorylated forms of Cx43 equally.

2.3.3 Phosphorylation of connexins

Phosphorylation is a common posttranslational modification of proteins. Phosphorylation has been implicated in the life cycle of connexins, including trafficking, assembly, disassembly and degradation.[160] Many connexins (Cx31,[161] Cx32,[162] Cx37,[163] Cx40,[200] Cx43,[164] Cx45,[165] Cx46,[166] Cx50,[167] and Cx56[168]) have been reported to be phosphorylated except Cx26.[169] Phosphorylation was studied by a shift in electrophoretic mobility or direct incorporation of ^{32}P. Phosphorylated sites were identified by site-directed mutation of target amino acids. The C-terminal region of connexins is the primary phosphorylated domain. Phosphorylation of the N-terminus has not been reported. Since Cx43 is widely expressed in tissues and cell lines, Cx43 phosphorylation has been studied the most (Figure 2.1).

Cx43 can be phosphorylated on serines and tyrosines. The following residues have been found to be phosphorylatable: Y247,[170] S255,[209, 210] S262,[204, 205] Y265,[198-200] S279,[208] S282,[210] S325,[171] S330,[171] S364,[205-207] S365,[172] S368,[173-175] S369,[172] S372,[176] and S373.[172] Multiple kinases are involved (Figure 2.1). Phosphorylation of S364, S365, S368, S369 and S373 was probably cAMP dependent,[172, 177] although PKA has not been established as the kinase for these sites. Agents elevating intracellular cAMP level enhanced gap junctional intercellular

communication (GJIC) and connexin expression,[178] as well as the assembly of new gap junctions.[179] PKA, Epac and Rap1 were in the cAMP enhanced GJIC signaling pathway.[180] S364 is of particular interest. The S364P mutation was associated with visceroatrial heterotaxia.[181] The S364P mutation also disrupted the pH gating of Cx43,[182] and affected left-right patterning.[183] PKC could phosphorylate S368[173] and S372.[216] PKCγ was identified as the specific isoform to phosphorylate S368.[184] PKCε also phosphorylated Cx43 although the specific sites were not explored.[185] Phosphorylation of S368 by PKC induced a conformational change of Cx43 and decreased junctional permeability.[186] S262 was phosphorylated by PKC[187]or p34cdc2.[188] S255, S279 and S282 were phosphorylated by MAPK (ERK1/2, specifically) following EGF treatment.[208, 226] Therefore, one amino acid of connexins can be phosphorylated by multiple protein kinases, and one protein kinase can phosphorylate many residues. Casein kinase 1 (CK1δ) phosphorylated S325, S328 and S330 *in vitro.*[171] Phosphorylation of these sites might facilitate assembly of gap junctions.[171] Cx49 was also phosphorylated by CK1 with decreased dye transfer in lens cells.[189] CK2 phosphorylated S363 of chicken Cx45.6, which reduced the stability of Cx45.6, the homologue of human Cx50.[190] S255 of Cx43 was also phosphorylated in a p34cdc2-dependent manner.[209, 234] Phosphorylation of this site might be related to cell cycle progression.[188] Y247 and Y265 could be phosphorylated by the non-receptor tyrosine kinase Src, which resulted in reduced GJIC.[203, 206, 207] The reduced GJIC might result from reduced channel open probability and possibly altered selectivity.[191] Y265 is critical for docking of the SH2 domain of v-Src to Cx43. The efficient channel closure by v-Src required the phosphorylation of Y247.[170] Lipopolysaccharide (LPS) stimulated protein tyrosine kinase-dependent phosphorylation of cultured rat microvascular ECs.[192] However, the phosphorylated sites and tyrosine kinases involved were not identified.

Dephosphorylation of connexins was less studied. The protein phosphatases that have been studied are PP1, PP2A, PP2B, and receptor protein tyrosine phosphatase mu (RPTPμ). PP1 dephosphorylated Cx43 in rat cells.[231, 232] PP2A dephosphorylated Cx43 of rat cells treated by 18 β-glycyrrhetinic acid,[193] mitotic human vascular ECs,[194] cultured ventricular myocytes of newborn rats,[238] and fibroblasts.[195] PP2A was also found to colocalize with Cx43 of left ventricles in an arrhythmogenic rabbit model of non-ischemic heart failure.[235] PP2B dephosphorylated Cx43 of hypoxic astrocytes.[231] Transgenic mice with cardiac-specific expression of an active form of PP2B had less expression and phosphorylation of Cx43.[196] Cx43 was redistributed from intercalated disk regions to the long axis of the plasma membrane. Endogenous RPTPμ co-immunoprecipitated with Cx43 through the first catalytic domain of RPTPμ.[197] Some protein tyrosine phosphatases might counteract the channel-closure effect of Src phosphorylation.

Detection of phosphorylation events by electrophoretic mobility shift may not reveal the specific phosphorylated sites.[175] More thorough studies are needed to identify the phosphorylated sites, the kinases and phosphatases involved, the temporal and spatial characteristics, and the physiological importance of phosphorylation of connexins under different conditions. The mass spectrometry analysis of protein phosphorylation is emerging as a powerful tool to study all cellular processes.[198, 199] However, some technical difficulties need to be conquered before its routine use. Fortunately, more phosphorylation site-specific antibodies are available, which may detect phosphorylation events *in situ* as well for some antibodies. The antibodies of Cx43 that have been used are for S255,[200] S262,[187] S279/282,[236, 237] and S368.[175] Antibodies for S255, S262, Y265, S279/282, and S368 of Cx43 are commercially available currently.

2.3.4 Gating of gap junction channels and hemichannels

The permeability of gap junction channels may be regulated by Ca^{2+}, pH, transmembrane voltage, phosphorylation and other factors.[243-246] A rise in intracellular calcium concentration correlated with intercellular electrical uncoupling.[201] Furthermore, the uncoupling occurred at the junction where the local calcium concentration was increased because of the injection of Ca^{2+} into the cells. Carbon dioxide-induced acidification reduced channel permeability.[202] Calmodulin (CaM) might be the soluble intermediate to mediate Ca^{2+} and pH gating of gap junction channels. Evidence for this CaM effect was accumulated through a CaM inhibitor,[203] mutation of CaM,[204] colocalization of CaM with connexins,[257, 258] and binding of connexins to CaM.[205] The CaM inhibitor, calmidazolium, inhibited electrical uncoupling induced by an increase in acidity after exposure to 100% CO_2.[203] GJIC shows transjunctional voltage-dependent sensitivity.[206] The charged N-terminal amino acids of both Cx43 (Cx43D12, K13) and Cx40 (Cx40E12, E13) are essential to the voltage-dependent gating property.[129] Intracellular acidification was accompanied by internalization of Cx43 and increased binding of c-Src to Cx43 in astrocytes.[261]

One half of a gap junction channel is called a hemichannel. Hemichannels can also be opened under low extracellular Ca^{2+} concentration,[207] or metabolic stresses.[255] Calcium induced a reversible change in the diameter of the extracellular pore of Cx43 hemichannels that were inserted into the reconstituted lipid bilayer.[208] Opened hemichannels can release ATP,[209, 210] glutamate,[211] and NAD^+.[212] In addition, hemichannels played a role in calcium wave propagation,[213] cell volume regulation,[270] and transduction of cell survival signals.[271]

2.3.5 Connexin-interacting molecules

It is important to know the connexin-interacting molecules in order to understand the regulation of connexins and gap junctions. Some proteins have been found to associate with connexins (Figure 2-1).[123] The kinases and phosphatases interacting with connexins have been discussed before (Section 2.3.3).

Binding of Cx43 with ZO-1 has been established[272-274] and quantified.[275] The C-terminus of Cx43 (Cx43CT) interacted with the second PDZ domain of ZO-1.[214] The PDZ-2 domain of ZO-1 affected the last 19 residues of Cx43CT.[215] ZO-1 localized mostly to the periphery of Cx43 gap junctional plaques.[216] c-Src regulated the interaction between Cx43 and ZO-1 in both astrocytes[217] and cardiac myocytes.[218] Phosphorylation of Y265 of Cx43 and binding of c-Src to Cx43 reduced the binding of ZO-1 to Cx43.[218] However, the function of ZO-1 in regulating Cx43 is still controversial. Induction of gap junction endocytosis increased association of Cx43 with ZO-1, which suggested a role of ZO-1 in gap junction turnover.[219, 220] However, the wild type and mutant Cx43 which could not bind to ZO-1 had similar turnover rates.[246] The mutant Cx43 was translocated to the plasma membrane and formed functional GJIC. Therefore, formation of functional GJIC does not require binding of Cx43 with ZO-1. Regulation of Cx43 phosphorylation by ZO-1 was also suggested.[275] ZO-1 might regulate the assembly of Cx43 into gap junctional plaques.[167, 264] The transcription factor ZO-1-associated nucleic acid-binding protein (ZONAB) interacted with ZO-1, and colocalized at cell-cell junctions, which implicated a role of gene expression regulation.[247] This function was further solidified by the dependence of association of Cx43 with ZO-1 on cell cycle stages.[280] Cx43 bound to PDZ2 domain of ZO-2 in normal rat kidney epithelial cells or mouse heart tissues, and was cell cycle stage independent,

however.[248] Other connexins that interact with ZO-1 are Cx30,[221] Cx31.9,[222] Cx36,[223] Cx40,[258] Cx45,[275],[224, 225] Cx46,[226] Cx47,[221] and Cx50.[226]

Gap junctions and adherens junctions (formed by cadherin-mediated Ca^{2+}-dependent homophilic cell-cell adhesion) are closely related. Proteins found in adherens junctions may also interact with connexins. N-cadherin colocalized with Cx43 in NIH3T3 cells.[227] E-cadherin colocalized with Cx26 in hepatocytes.[228] The $p120^{ctn}$ catenin colocalized with Cx43 in neural crest cells.[229] Adherens junctions were required for the cell surface expression of Cx43 and gap junction formation studied by a siRNA gene knockdown method.[227] Treatment with antibody Fab fragments against N-CAM interfered with cell-cell communications.[139, 230] Gap junctions were perturbed in cultured cardiac myocytes isolated from N-cadherin-null mice.[231] Cardiac specific deletion of N-cadherin in adult mice significantly decreased Cx43 and Cx40.[232] Transient expression of α-catenin targeted both Cx43 and Cx32 to the cell surface and induced gap junction assembly.[233] Mutations in junctional protein plakoglobin and desmoplakin destabilized gap junctions.[234] N-cadherin cell surface expression and adherens junction formation also required Cx43 in cultured Novikoff hepatoma cells or NIH3T3 cells.[167, 266] However, Cx43 was not required for the organization of adhesion junctions at the intercalated disc in adult cardiac myocytes using a Cx43-knockout mouse model.[235] This discrepancy might be caused by the *in vitro* or *in vivo* methods or the different cell types used. It also seems reasonable that formation of mechanical connections (adherens junctions) does not require electrical connections (gap junctions). The adherens junction protein, β-catenin, is in the Wnt signaling pathway as a coactivator to stimulate the transcription of Wnt target genes. Wnt-1 regulated Cx43 gene expression in cultured neonatal rat cardiomyocytes.[268] However, the role of Wnt and β-catenin in

physiological gene expression of Cx43 is not clear. Signaling of Wnt pathway could also be β-catenin independent.[236]

Connexins may bind to cytoskeletal proteins. The Cx43 tail bound directly to the microtubule protein tubulin identified by pull-down experiments.[237] Spectrin might play a role in connecting connexins to actin microfilaments.[238] Another actin-binding protein drebrin interacted with Cx43 to stabilize Cx43 at junctional regions.[239] Annular gap junctions are the double-membrane, intracellular structure that is formed by connexin proteins.[151] Cytoskeletal elements were also involved in annular gap junction turnover.[240]

Cx43 colocalized and coimmunoprecipitated with caveolin-1, the marker protein of specialized lipid raft domains, caveolae, in NIH 3T3 cells.[241] Some other transfected connexins, Cx32, Cx36, and Cx46, were also targeted to lipid rafts. However, Cx26 and Cx50 were excluded from these membrane microdomains.[241] The functional roles of the association of connexins with caveolins have not been studied. Whether there is *in vivo* interaction of caveolin-1 with cardiovascular connexins is not known. Because lipid rafts provide structural microdomains for many signaling molecules,[242] this association may serve signaling roles. Interestingly, caveolin-1 regulated inter-endothelial cell permeability in lungs *in vivo.*[243]

CaM colocalized with Cx32 in Xenopus oocytes,[244] and bound neuronal gap junction proteins Cx35,Cx36 and Cx34.7.[245] One role of CaM is to control gap junctional gating in responding to alterations of pH.

Connective tissue growth factor CCN3 (NOV) bound Cx43 and inhibited the growth of C6 glioma cells.[296, 297] The C-terminus of Cx43 was required for this interaction, which was specific because Cx40 and Cx32 did not associate with NOV. Further studies are needed to investigate the *in vivo* interaction of Cx43 and NOV.

CIP85 (Cx43-interacting protein of 85-kDa) is a new member of the Cx43 binding proteins involved in the degradation of Cx43 through the lysosomal pathway.[246] CIP85 was ubiquitously expressed in mouse and human tissues, although the expression in vascular tissues has not been studied. CIP150 is another novel Cx43 interacting protein which regulates the Cx43 plasma membrane localization in rat cells.[247]

FAK coimmunoprecipitated with Cx26 in prostate cancer cells.[248] Inhibitors of gap junctions reduced invasion and migration. In view of the broad functions of FAK in regulating cell adhesion and other related processes,[249] and the connexin expression regulation by extracellular matrix components,[250] interactions between connexin proteins with FAK deserves to be studied further.

2.3.6 Roles of connexins independent of intercellular junctions

Connexins have been reported to inhibit the growth of cells independent of gap junctional activities.[136, 251-255] However, the mechanisms are poorly understood. Several lines of evidence suggested a role of connexins in gene regulation. Expression of Cx26 upregulated an anti-angiogenic protein thrombospondin-1, and downregulated another angiogenesis-related gene connective tissue growth factor.[256] Cx43 transfection reduced the expression of monocyte chemotactic protein-1 (MCP-1).[257] FAK is another candidate as mentioned before.[248] Enhanced Cx43 expression increased the protein level of the cyclin-dependent kinase (CDK) inhibitor p27,[258] through inhibiting the expression of Skp2.[259] Cx43CT was localized in nuclei of cardiomyocytes and HeLa cells, which might suggest a gene regulation role.[255] However, there is no report on nuclear localization of whole Cx43 molecules yet.

Cx43 has been found to be localized in mitochondria of HUVECs treated with homocysteine[260] and of rat, mouse, pig, and human hearts.[313, 314] However, the exact localization was reported to be either at the outer[261] or inner mitochondrial membrane.[262] Cx43 was transported into mitochondria through the regular mitochondrial protein import machinery.[262] Cx43 in mitochondria played roles in protecting hearts with ischemic preconditioning.[263]

2.3.7 Gap junction studies using transgenic animal models

Some connexin related transgenic animal models have been generated to study the possible functions of connexin *in vivo*.

Cx43-null mice died at birth with a failure in pulmonary gas exchange caused by a swelling and blockage of the right ventricular outflow tract,[264] with dysregulated coronary vasculogenesis.[317, 318] Altered innervation also might contribute to cardiac abnormalities in Cx43 null animals.[265, 266] The EC-specific loss of Cx43 allows studying Cx43 functions in ECs of live animals. The homozygous vascular EC Cx43 knockout mice survived to maturity. However, they were hypotensive and bradycardiac with a increased NO production (determined by measuring plasma nitrite and nitrate concentration), and elevated angiotensin I and II levels.[267] In contrast, no blood pressure alteration was observed using a similar technique.[268] Roles of Cx43 in regulating blood pressure were investigated by replacing Cx43 with Cx32 in the mouse line Cx43KI32 (KI32).[269] The renin expression in the kidneys of the homozygous mice was reduced compared with wide type and heterozygous littermates. Hypertension can be induced by clipping only one renal artery (the 2-kidney, 1-clip (2K1C) model). Interestingly, the 2K1C homozygous littermates remained normotensive and showed unchanged plasma renin activities.[269] The role of Cx43 in atherosclerosis and response to injuries was studied as well. The atherosclerotic lesions

of low-density lipoprotein (LDL) receptor-deficient mice were reduced in aortas of Cx43+/- mice compared with the Cx43+/+ controls.[10] Furthermore, the Cx43+/- mice had less neointima formation fallowing balloon distension injury.[270] However, mice with SMC-specific knockdown of Cx43 had more neointima formation responding to injuries induced by a wire.[271] The discrepancy may be because of the use of different models. There is only one half of the Cx43 gene left in all cells, including ECs, in Cx43+/- mice.[270] These LDL receptor-deficient mice were fed with high-fat diet as well. However, Cx43 gene was deleted from all SMCs.[271] The C57BL/6 mice with SMC-specific knockdown of Cx43 were fed with normal diet.

In contrast to Cx43, mice with the deletion of Cx40 or Cx37 can survive. However, Cx40-deficient mice showed impaired endothelium-dependent conduction of vasodilation along arterioles,[272] and were hypertensive.[273] Female mice lacking Cx37 were infertile.[274] However, mice with simultaneous deletion of Cx37 and Cx40 had severe vascular abnormalities and died perinatally, which demonstrated that Cx40 and Cx37 overlapped functionally.[275] The alteration of other types of connexin after ablation of one connexin is controversial. Mice deficient in Cx37 or Cx40 showed downregulation of non-ablated connexins in aortic endothelium, whereas, both Cx37 and Cx43 were increased in media in Cx40-/- aortas.[276] Interestingly, Cx40-deficient mice had renin-producing cells in the extraglomerular mesangium rather than in afferent arterioles.[277] This observation indicated that gap junctions are necessary for the correct juxtaglomerular positioning and recruitment of renin-producing cells. Furthermore, Cx40-dependent gap junctions are essential for the calcium-dependent negative control of renin secretion and synthesis induced by AngII and intrarenal pressure,[278] which may explain why the Cx40-deficient mice were hypertensive.[273]

Cx37 protected against atherosclerosis by regulating adhesion of monocytes to ECs in apolipoprotein E–deficient mice, which is one of the initial steps toward atherosclerosis.[279] Monocytes and macrophages express Cx37. Monocytes release ATP through Cx37 hemichannels to inhibit their adhesion to ECs. Therefore, more monocytes were adhered to ECs in the Cx37-deficient mice.

Embryos of Cx45-deficient mice had striking abnormalities in vascular development and died between embryonic day 9.5 and 10.5.[280] Vasculogenesis in these mice was normal, but transformation into mature vessels was blocked. TGF-β signaling was also defective.

2.3.8 Gap junction regulation by exogenous chemicals

Some chemicals that have cardiovascular implications have been applied to *in vitro* culture or animals to study the gap junction regulation.

TGF-β1. TGF-β1 treatment of cultured bovine aortic ECs upregulated Cx43 mRNA and protein with a intense vesicular staining, which colocalized with lysosomes.[281] TGF-β1 treatment reduced the Cx43 degradation through lysosomes. Neonatal rat ventricular myocytes also had more Cx43 protein upon TGF-β1 incubation.[282] Upregulation of Cx37 expression in confluent cells was suppressed by TGF-β1.[341, 343] However, the underlying mechanisms are unknown. One the other hand, Cx43 also mediated the functions of TGF-β1 through competing with Smad2/3 for binding to microtubules.[283] Of note, Smad2/3 are in the TGF-β1 signaling pathway. The binding of Cx43 to microtubules may induce the release of Smad2/3 from microtubules and lead to activations of the transcription of target genes induced by TGF-β stimulation.

TNF-α. TNF-α regulated Cx37, Cx40 and Cx43 in HUVECs differently.[284] Cx37 and Cx40 proteins were undetectable and the mRNA levels were reduced, whereas the Cx43 protein

level seemed to be unaltered otherwise with more perinuclear staining. The level of Cx43 mRNA remained unaltered although it was reported that Cx43 promoter activity was decreased by TNF-α in a rat myoblast cell line.[285] On the contrary, TNF-α increased the Cx43, but not Cx40 or Cx45, expression in neonatal rat cardiomyocytes.

NO. NO enhanced *de novo* formation of gap junctions between acutely coincubated HUVECs by increasing the incorporation of Cx40 into the plasma membrane, which was due to PKA activation.[286] The NO donor S-nitroso-N-acetylpenicillamine (SNAP) enhanced GJIC and the protein expression of Cx43 in mesangial cells by activating PKA as well.[287] Inhibition of NOS decreased the Cx43 mRNA and protein levels in rat aortas.[288] However, NO reduced the expression of Cx43 mRNA and protein in cultured human uterine myocytes.[289] SNAP also reduced transfer of carboxyfluorescein to adjacent confluent HUVECs.[342] The direct effect of NO on Cx43 in VSMCs has not been studied.

ET-1. The regulation of connexins by ET-1 is controversial. Short term ET-1 treatment led to a 50-75% inhibition in GJIC in human ovarian carcinoma cells through ET_A receptors. The inhibition was also regulated through Cx43 tyrosine phosphorylation by c-Src.[290] Treatment of cultured cortical astrocytes by ET-1 for 24 h inhibited Cx43 expression through ET_B receptors. However, ET-1 upregulated the Cx43 protein and mRNA expression and enhanced GJIC for long-term effects in rat hepatic stellate cells through ET_A and ET_B receptors.[291] ET-1 treatment of cultured neonatal rat ventricular myocytes for 24 h also increased Cx43 protein and communication through ET_A receptors and ERK1/2.[346] The effects of ET-1 on connexin expression of vascular cells have not been studied although ET-1 is important in the cardiovascular system.

AngII. Similar to ET-1, AngII increased the Cx43 protein level in cultured neonatal rat ventricular myocytes.[292, 293] AngII also increased both mRNA and protein of Cx43 in SMCs of human saphenous veins and internal mammary arteries.[294] These effects were through AT_1 receptors, ERK and p38 pathway. [292-294] AT_1 receptors also regulated cyclic stretch induced increase in Cx43 mRNA and protein in neonatal rat cardiomyocytes.[295] AngII level can be elevated by overexpressing angiotensin converting enzyme (ACE). However, both mRNA and protein of Cx43 were reduced in the hearts of cardiac-restricted ACE overexpression mice.[296] The AT_1 receptor antagonist candesartan also corrected increased Cx43, and decreased Cx40 and Cx37 protein levels in ECs of mesentery arteries in spontaneous hypertensive rats (SHR).[297] Inhibition of ACE in SHR restored the endothelial connexin expression in both aortas and caudal arteries, while ACE inhibition had no effects on medial connexin expression.[298] Therefore, the effects of AngII on connexin expression depend on cell types and specific experimental conditions.

VEGF. VEGF is an important signaling protein for both vasculogenesis (the *de novo* formation of the embryonic vascular system) and angiogenesis (the growth of blood vessels from pre-existing vasculature). VEGF is also a vasodilator and increases microvascular permeability. VEGF transiently disrupted communication among EA.hy926 ECs (a hybridoma of human aortic endothelium and adenocarcinoma) through the VEGFR-2, Src and ERK pathway.[299] The disruption involved ATP release, and the PI3K/Akt pathway as well in capillary ECs.[300] Upregulation of Cx43 by cyclic stretch in neonatal rat ventricular myocytes was mediated by VEGF,[282] in addition to AngII.[295] However, the relationship of VEGF and AngII in this process has not been studied.

FGF-2. FGF-2 is a member of the fibroblast growth factor family. It is also called basic fibroblast growth factor. FGF-2 decreased dye transfer between cardiomyocytes within 30 minutes of administration.[301] FGF-2 did not affect the Cx43 mRNA or protein level after 24 h. However, FGF-2 increased Cx43 phosphorylation. FGF-2 was further found to upregulate phosphorylation of the PKC target serines 262 and 368 of Cx43 in adult rat hearts.[302] In contrast, FGF-2 increased intercellular communication in cardiac fibroblasts at 6 h but not 30 minutes after bFGF treatment.[303] FGF-2 also increased Cx43 mRNA and protein at 6 h after addition. Similarly, FGF-2 increased dye transfer in a time-dependent manner in microvascular ECs.[304] Cx43 mRNA and protein were increased as well. FGF-2 also transiently increased gap junctional intercellular communication in VSMCs isolated from human umbilical cord arteries.[305] Intriguingly, FGF-2 inhibited gap junctions, while it stimulated ATP release via hemichannels in C6 glioma cells.[306]

Cholesterol. Cx37 and Cx40 were downregulated in aortas of mice fed with cholesterol-enriched diet. Cx40 remained depressed, but Cx37 recovered to 94% of the level found in non-cholesterol-fed mice after simvastatin treatment.[307] Hypercholesterolemia reduced Cx43 protein in medial SMCs at the rabbit aortoiliac bifurcation as compared with normal counterparts in control animals.[308]

Glucose. High glucose (22.2 mM) inhibited activities of gap junctions in bovine aortic ECs and SMCs compared to the normal glucose level (5.5 mM) through PKC.[367, 368] High glucose also elevated phosphorylated Cx43 rapidly in SMCs.[309] Regulation of gap junctions by glucose in microvascular ECs were also studied. High glucose (30 mM) reduced Cx43 mRNA and protein in rat microvascular ECs without affecting the Cx37 and Cx40 expression.[310] Furthermore, high glucose enhanced proteasome-dependent degradation of Cx43 in bovine

retinal ECs.[311] However, chronic effects of glucose on mRNA and protein of connexins in arterial vascular cells have not been studied.

Nicotine. Cx43 protein and communication function were reduced by nicotine, while Cx43 mRNA was upregulated in HUVECs. Statins reduced the effects of nicotine on connexins.[312]

Homocysteine (Hcy). Hcy is a homologue of the amino acid cysteine, differing in that its side chain contains an additional methylene group. A high level of blood serum homocysteine is a risk factor for cardiovascular diseases. Cx43 mRNA and protein were increased in Hcy-treated HUVECs. However, GJIC was not enhanced. Cx43 was also found to colocalize with mitochondria in Hcy-treated HUVECs[260] or in cardiomyocytes.[261-263]

Lipopolysaccharide (LPS). LPS is a major component of the outer membrane of Gram-negative bacteria, contributing largely to the structural integrity of the bacteria. LPS also protects the membrane from chemical attack. LPS is an endotoxin, inducing a strong immune response in animals. The LPS treatment of mice resulted in a reduction in endothelial Cx40 protein, while Cx37 was only changed slightly. The endothelial dye dye transfer was decreased by 49%.[313] LPS changed the Cx43 mRNA level dramatically and rapidly in rat hearts.[285]

Oxygen. Hypoxia/Reoxygenation regulated GJIC in HUVECs,[314] rat microvascular ECs,[374] rat thoracic aorta SMCs,[315] rat hearts,[316] cultured cardiomyocytes,[317] and rat astrocytes.[231] VSMCs cultured under a reduced oxygen partial pressure (15 mmHg) for 24 h showed increases in Cx43 mRNA, protein, and GJIC mediated through ROS.[315] However, hypoxia transiently disrupted GJIC and increased Cx43 dephosphorylation by PP2B,[231] or reduced the total Cx43 protein without affecting the unphosphorylated form of Cx43.[351] Hypoxia of rat hearts under Langendorff preparation dephosphorylated Cx43 and changed its localization to the entire

plasma membrane although ZO-1 localized at the intercalated disc normally.[316] Reoxygenation after hypoxia first disrupted GJIC followed by a return to normal.[314] Tyrosine and MAP kinases regulated the reduced GJIC in ECs.[318] Reversible dephosphorylation and rephosphorylation of Cx43 during hypoxia and reoxygenation were sensitive to the cellular ATP level.[319]

2.3.9 Gap junction regulation by mechanical factors

Studies have shown that gap junctions can be regulated by mechanical factors, such as flow or shear stress, pressure and stretch.

Flow (shear stress). *In situ* immunostaining revealed that endothelial Cx43 was mainly expressed at locations with disturbed flow, such as the downstream edge of the ostia of branching vessels and flow dividers, where exists spatial gradients in wall shear stress.[320] Consistent with this observation, shear stress spatial gradients in regions of disturbed flow created by a step in the flow chamber upregulated the expression of Cx43 in cultured bovine aortic ECs.[13] Connexin expression was further studied using two flow waveforms.[321] One was called athero-protective, which represented the flow in straight arteries. The other was called athero-prone, which exists in the regions of bifurcation and curvature. Again, Cx43 expression was upregulated by the athero-prone flow waveform after culturing for 24 h. However, the Cx43 mRNA level of ECs isolated from the region with disturbed flow in aortas of healthy adult pigs was downregulated in a microarray study, which was verified by quantitative real-time PCR.[322] Unfortunately, protein levels of Cx43 in these two regions were not detected. Because a higher mRNA level may not necessarily lead to a higher protein level, it is possible that there are more Cx43 proteins in the disturbed flow region of aortas of healthy adult pigs. Similarly, the mRNA levels of Cx43 were not measured in locations with disturbed flow.[320] Conducting these

"missing" experiments may give us a better understanding of the regulation of Cx43 by flow *in vivo*. A temporal gradient in shear stress upregulated Cx43 mRNA and protein in HUVECs as well.[323]

Cx40 and Cx37 are distributed more uniformly along the systemic arteries.[320] The Cx37 and Cx40 levels were elevated by the athero-protective flow waveform in HUVECs after culturing for 24 h.[321] However, athero-protective steady laminar flow downregulated Cx40 mRNA in cultured human aortic ECs.[324]

The regulation of the gap junctional dye transfer function of ECs by flow *in vitro* is still controversial. Dye spread was at a very low level in statically cultured human aortic ECs although there was a strong peripheral Cx43 and Cx40 staining.[325] Laminar flow for 24 h increased dye coupling 7.5-fold, which was attributed mainly to Cx40. Using the same cell type, laminar flow, however, reduced dye transfer between cells.[326]

Pressure (wall stress/strain). Vascular connexin expression correlated with *in vivo* blood pressure in different ways. Rats which were made hypertensive by clipping one renal artery (2K1C) or feeding deoxycorticosterone and salt (DOCA-salt model) had more Cx43 mRNA and protein in aortas (with ECs and SMCs).[358, 359] However, hypertensive rats induced by inhibiting NOS with N^G-nitro-L-arginine methyl ester (L-NAME model) had less Cx43 mRNA and protein in aortas although similar systemic blood pressure was obtained in these three models.[327] Cx43 protein in the media of aortas was also reduced in SHR.[298] In contrast, endothelial Cx43 in mesentery arteries was elevated in SHR. On the other hand, the antihypertensive drug carvedilol rectified the reduced expression of Cx43 and 37 in L-NAME model while only partially by atenolol although both drugs decreased blood pressure efficiently.[328] Similarly, the AT_1 receptor antagonist candesartan decreased endothelial Cx43 in

SHR while the combination of hydralazine and hydrochlorothiazide did not show the same effect although blood pressure was both decreased to normal.[297] The antihypertensive treatment by the inhibition of ACE also could not increase the reduced level of Cx43 in aortic SMCs.[298] Therefore, pressure does not regulate connexin expression independently *in vivo*. Other factors play roles as well, although these factors have yet to be identified.

A higher hydrostatic pressure (150 mmHg) did not increase Cx43 protein in bEnd.3 cells compared with the normal pressure (100 mmHg) at shear stress 0.3±0.1 or 6±3 dyne/cm^2.[12] Although pressure was pulsatile (pulse pressure 40 mmHg), there was no stretch in these experiments.

Stretch regulates gap junctions *in vitro*. Twenty percent static stretch of cultured VSMCs increased the Cx43 mRNA level by 2 h. The Cx43 protein level was increased by 4 h and remained elevated for 16 h.[14] Cyclic stretch (4%) for 4 h increased Cx43 protein in bEnd.3 cells with shear stress 6±3 dyne/cm^2.[12] Cyclic stretch also increased both mRNA and protein of Cx43 in cultured neonatal rat cardiomyocytes through AngII,[295] TGF-β1,[282] VEGF,[282] and was associated with the activation of Na-H exchangers.[329] The effects of stretch on Cx43 varied with extracellular matrix proteins.[330] Cyclic stretch increased the Cx43 protein level in cells grown on native collagen through β1 integrin; but there was no increase in cells grown on fibronectin or denatured collagen. Cyclic stretch may regulate Cx43 phosphorylation. For example, osteoblasts had more phosphorylated Cx43 under cyclic stretch although the steady state mRNA level did not change.[331]

2.4 OVERALL SUMMARY OF BACKGROUND

Previous studies have clearly demonstrated that mechanical factors regulate vascular structure and functions. Vascular cells have the capability of sensing and transducing mechanical factors through complex mechanisms. However, controversies still exist regarding to the effects of mechanical factors on vascular cells, and the underlying mechanisms. Part of the reason is because of the different methodologies utilized in different studies.

Vascular gap junctions are important for the homeostasis of the vasculature. There is association between vascular gap junctions and vascular diseases (e.g., hypertension). Previous studies have shown that vascular gap junctions are regulated by mechanical factors in addition to chemicals. However, it is still not clear how mechanical factors regulate vascular gap junctions, and the mechanisms are largely unknown. Using *ex vivo* culture of arteries, we investigated the regulation of Cx43 by the mean pressure level and pulsatility in intact arteries. Our results demonstrate that both the mean pressure level and pulsatility regulate Cx43.

3.0 MATERIALS AND METHODS

3.1 ISOLATION OF RABBIT DESCENDING THORACIC AORTAS

All procedures involving animals were approved by the Institutional Animal Care and Use Committee of the University of Pittsburgh, and conform with the guidelines of the National Institute of Health for the care and use of laboratory animals (NIH Publication No. 85-23, revised 1996).

The descending thoracic aortas of male New Zealand white rabbits weighing 2 to 3 kg were harvested using a procedure adopted from Bardy *et al*.[332] The diameter of the aorta is around 5 mm. The length of the DTA is about 9 cm. Therefore, the rabbit aorta is appropriate for *ex vivo* culture. Rabbits were first anesthetized by a mixture of ketamine (45 mg/kg, Kataject®, Phoenix Pharmaceutics) and xylazine (5 mg/kg, Xyla-Ject®, Phoenix Pharmaceutics) injected intramuscularly for preparing the skin and ear veins. A heating pad was applied underneath the rabbit to maintain the temperature of the rabbit. Intra-venous catheters (22 GA, BD Insyte™, BD Biosciences) were used to infuse ketamine and saline. Ketamine (80 mg/kg·h) was then continuously infused during the procedure using a syringe infusion pump (model 22, Harvard Apparatus). Saline (0.9% sodium chloride, Hospira) was continuously infused via another ear vein. Rabbits were mechanically ventilated through the trachea using a Harvard rodent ventilator (model 683, Harvard Apparatus). Betadine® solution (containing 5% povidone-iodine, Perdue

Products L.P.) was applied to disinfect the skin. Abdominal and pleural cavities were opened to expose the DTA. The chest was expanded by a rib spreader. Blunt dissection techniques were used to isolate branches. Intercostal arteries were ligated with 6-0 silk sutures (18020-60, Fine science Tools). The warm (37 °C) Tyrode's salts solution with heparin (1 USP units/ml, Baxter Healthcare), papaverine (100 mg/liter, Sigma) and antibiotics (100 U/ml of penicillin, 100 μg/ml of streptomycin (Gibco), and 5 μg/ml of amphotericin B (Sigma)) was applied frequently to the outside of the aorta in order to prevent drying and spasm. Heparin (1000 U) was injected through an ear vein before cannulation. Then both ends of the DTA were cannulated using vessel cannulae (DLP®30003, Medtronic). The cannula closer to the heart was capped. A bag of Tyrode's salts solution with heparin (1U/ml), papaverine (100 mg/liter) and antibiotics (100 U/ml of penicillin, 100 μg/ml of streptomycin, and 5 μg/ml of amphotericin B) was connected to the distal cannula in order to prevent collapse of the DTA. Two custom-designed vascular stabilizers (Appendix C) held the DTA at *in vivo* length. Then the DTA was cut into two segments and put into a tray with Tyrode's salts solution. Each aortic segment was held at *in vivo* length by one stabilizer. The other end of the DTA was cannulated and connected to an *ex vivo* culture system.

3.2 PERFUSION ORGAN CULTURE OF AORTAS AND EXPERIMENTAL PROTOCOL

Perfusion organ culture of aortas. The *ex vivo* culture system is shown in Figure 3-1. The mean and pulsatile components of a pulsatile pressure could be adjusted individually. A computer-compatible/programmable drive (VX-07550-30, Cole-Parmer) and a six-roller

cartridge pump head (EW-07519-10, Cole-Parmer) with multi-channel cartridges (EW-07519-75, Cole-Parmer) (1, Figure 3-1) generated desired mean flow under different pressures. A compliance chamber (SA-07596-20, Cole-Parmer) (2, Figure 3-1A) reduced the pulsation of pressure and flow. A manual valve (C-98002-00, Cole-Parmer) (2, Figure 3-1B) was used instead to adjust the pulse pressure for pulsatile perfusion. An ultrasonic flow rate sensor and flow meter (Transonic Systems) (3) measured flow rates. A pressure transducer (DTX^{TM} Plus, BD Biosciences) and amplifier (LDS Test and Measurement) (4) measured pressure. The DTA was cultured in a custom-made polycarbonate chamber (5) in its *in vivo* length and flow direction. The culture medium was Dulbecco's Modified Eagle Medium (DMEM, Cambrex) supplemented with 10% FBS (Mediatech), 25 mM HEPES (Sigma), 100 U/ml of penicillin, 100 μg/ml of streptomycin (Gibco), and 2.5 μg/ml of amphotericin B (Sigma). The level of the mean pressure was adjusted by a manual valve (C-98450-37, Cole-Parmer) (6) downstream of the DTA. The Precision PharMed ® tubing was used for the pump. The rest was Nalgene® 180 Clear PVC tubing (Cole-Parmer). The entire loop was put into a standard water-jacketed CO_2 incubator (3250, Forma Scientific) with 7.5% CO_2 to maintain the physiological pH and temperature. The partial pressures of CO_2 and O_2 (pCO_2, pO_2), and pH were measured by a blood gas analyzer (ABL5, Radiometer America). All components that contacted the culture medium were sterilized through autoclave or ethylene oxide. One LabVIEW program (National Instruments) was running to collect the flow and pressure data.

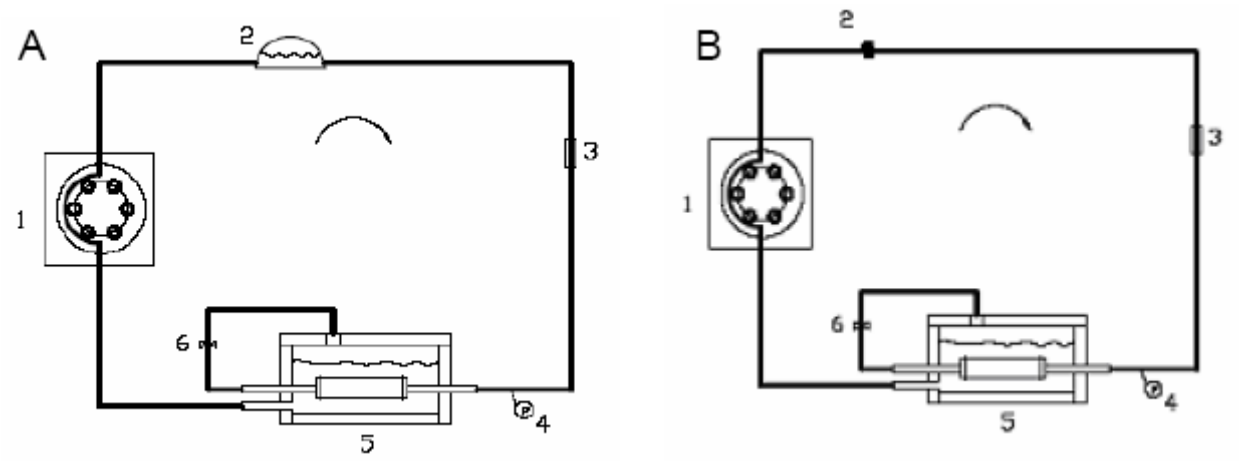

Figure 3-1 Schematic of the perfusion organ culture system.

The system shown in A generates steady pressure and flow. The system in B generates pulsatile pressure and flow. 1: MasterFlex pump, 2: compliance chamber in (A), or manual pinch valve in (B), 3: flow probe, 4: pressure probe, 5: culture chamber, 6: manual valve.

TUNEL apoptosis assay. Arterial sections were detected for apoptosis using the TUNEL (Transferase-mediated dUTP Nick End Labeling) assay (ApopDETEK Red Cell Death Assay, Enzo Life Sciences, NY) in order to test the *ex vivo* culture system. Broken DNA molecules are stained red in this assay. Nuclei are stained blue by DAPI (4'-6-Diamidino-2-phenylindole). The colocalization of red and blue represents apoptotic cells, which are magenta in merged images. Arteries were fixed in 4% paraformaldehyde for 3 h at room temperature, followed by preservation in 30% sucrose at 4 °C. Both fresh (Figure 3-2A, 10 μm section radially) and cultured DTAs (steady pressure 140 mmHg, 40 ml/min, 22 h, 5 μm-section longitudinally, Figure 3-2B) had very few positive apoptotic staining. The DNase I treated positive control section stained most nuclei positive (Figure 3-2C), while the section without the terminal deoxynucleotidyl transferase did not show specific apoptotic staining (Figure 3-2D).

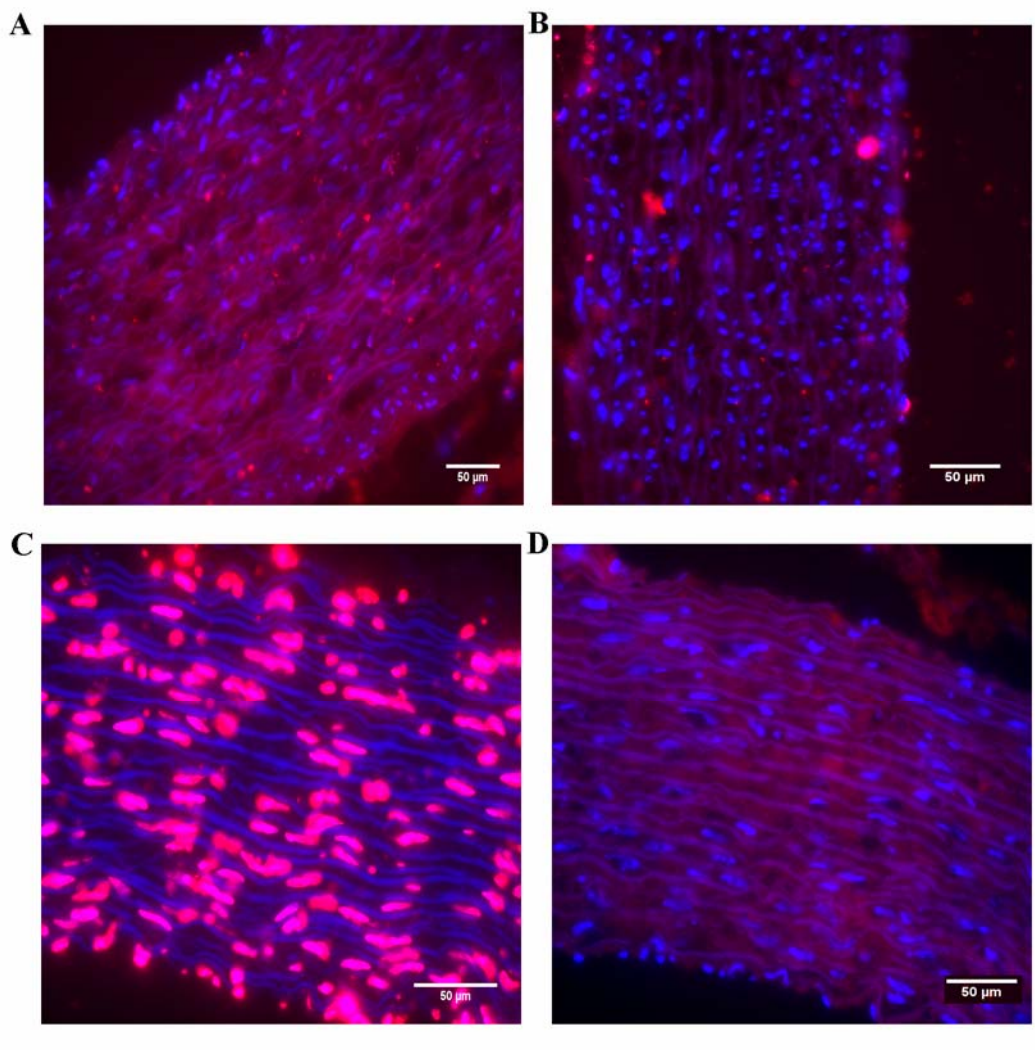

Figure 3-2 TUNEL apoptosis detection of aortic sections.

Colocalization (pink) of fragmented DNA (red) and nuclei (blue) signify apoptotic cells. The DTA cultured at 140 mmHg, 40 ml/min for 22 hours showed very few apoptotically positive staining (B) as the freshly isolated control sample (A). The DNase I treated section had strong staining (C). The section without the terminal deoxynucleotidyl transferase in the reaction solution had no specific apoptotic staining (D).

Vasocontraction test of cultured DTA. One DTA was cultured under steady pressure 210 mmHg and steady flow 200 ml/min for 24 h. Epinephrine-induced vasoconstriction was used to assess the contractility of the DTA after culturing for 24 h. This test was conducted at a distending pressure of 100 mmHg and epinephrine (Sigma) concentration of 1 mg/liter. The outer diameter of the DTA was measured using a Nikon SMZ645 stereomicroscope. Figure 3-3

shows the relative outer diameter after epinephrine was added. The DTA contracted rapidly and vigorously following addition of epinephrine, which demonstrated the viability and functionality of the cultured DTA.

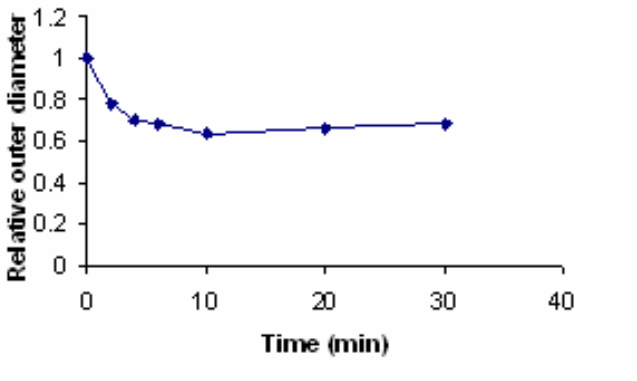

Figure 3-3 Vasocontraction test of cultured DTA.

The diameter change of DTA after culturing at 210 mmHg for 24 h was measured following addition of epinephrine to the culture medium at 1mg/liter at the end of culture (time zero in the figure). The DTA contracted quickly following epinephrine addition.

Experimental Protocols. Experiments were conducted in a pair-wise fashion. Each aorta was cut into two segments that were arbitrarily cultured under either an experimental or control condition. Some experiments were designed to study the effects of the mean pressure level. Therefore, aortas were cultured under either high steady pressure (150 mmHg, without pulsatility), or normal (low) steady pressure (80 mmHg) as the control for 6 h or 24 h. The duration of 6 h culture was thought to be a short-term, while the relatively long effect was studied by 24 h culture (long-term). The diameter of DTA under 80 mmHg was similar to the *in vivo* value.[87] The flow was 20 ml/min, which was lower than the physiological one (~200 ml/min).[87] Both segments were cultured under pulsatile conditions but with different mean pressure (80 versus. 150 mmHg, pulse pressure 30 mmHg for both, mean flow 25 ml/min, 192

cycles/min) in one set of experiments for 24 h. The diameter change under this pulsatile condition was not measured in this study. However, the pulsatile pressure 70~90 mmHg induced 10% cyclic stretch of the DTA.[87] To detect the effects of cylcic stretch compared with steady stretch, one vessel was cultured under pulsatile perfusion (mean pressure 80 mmHg, pulse pressure 30 mmHg, mean flow 25 ml/min); the other one was under steady pressure (80 mmHg) with the same flow. Because of the nonlinearity of the mechanical properties of aortas, the cyclic stretch is larger under the same pulse pressure (30 mmHg) if the mean pressure is 80 mmHg compared with 150 mmHg.[15] Therefore, one set of experiments was performed to clarify the effect of cyclic stretch versus cyclic stress by culturing one segment with pulsatile perfusion (mean pressure 150 mmHg, pulse 30 mmHg), the other one with steady high pressure (150 mmHg) for 24 h. The Src specific inhibitor PP1 (10 μM, BIOMOL, PA) was added to the media of steady high or low pressure at the onset of experiments to investigate the role of Src. PP1 is a a highly specific inhibitor of Src family kinases.[333] The concentration of PP1 (10 μM) has been used by most, if not all, studies using PP1.[31, 334, 335] Arteries cultured pulsatile had more superoxide,[87] which mainly come from NADPH oxidase.[336] The inhibitor of NADPH oxidase apocynin (0.4 mM, Sigma) was added to the media of pulsatile perfusion for 24 h to explore the role of ROS on mediating the Cx43 regulation by cyclic stretch. Apocynin (0.4 mM) was also added to the media of relaxed aortas (in a Petri dish) for 6 h. Apocynin is a methoxy-substituted catechol. It impedes the assembly of the $p47^{phox}$ with the membrane-bound NADPH oxidase complex.[337] Apocynin was used at 1 mM for mouse aortas,[338] 0.3 mM for rat femoral arteries.[111]

Superoxide measurement. Apocynin is a methoxy-substituted catechol, which exists in some plants. Apocynin impedes the assembly of the p47phox and p67phox subunits with the

membrane NADPH oxidase complex,[339] thus inhibits the full activation of NADPH oxidase. However, apocynin increased superoxide in aortic fibroblasts.[340] In order to test if apocynin actually inhibited NADPH oxidase, levels of superoxide were measured using the chemiluminescence dye L-012.[341] In three separate experiments, AngII (1.3 μM, Fisher Scientific), superoxide dismutase (SOD, 100 U/ml, Sigma), and apocynin (0.4 mM) was added to a vial with an aortic ring in a Krebs-HEPES buffer (pH 7.4; in mM: NaCl 99, KCl 4.69, $CaCl_2$ 1.87, $MgSO_4$ 1.2, NaHEPES 20, K_2HPO_4 1.03, $NaHCO_3$ 25, and D(+)Glucose 11.1),[341] respectively. The concentration of L-012 (Wako Pure Chemical Industries) was 100 μM. Photons were counted for two seconds in every minute using the Femtomaster FB14 luminometer (Zylux).

3.3 PROTEIN EXTRACTION, ELECTROPHORESIS AND WESTERN BLOT

Protein extraction. After culture, aortas were snap-frozen in liquid nitrogen. Frozen tissues were stored at -80 °C until use. Tissues of the same rabbit were processed together. Samples were maintained cold by putting on ice or in a cold room during protein extraction. Tissues in a lysis buffer were cut into small pieces, and homogenized. The lysis buffer contained: NaCl 150 mM, Tris 20 mM pH7.5, ethylenediamine-tetraacetic acid (EDTA, 1 mM), aprotinin 10 μg/ml, pepstatin A 11.4 μg/ml, leupeptin 15 μg/ml, phenylmethanesulfonyl fluoride (PMSF, 2 mM), activated sodium orthovanadate 2mM, sodium fluoride 50mM, and sodium dodecyl sulfate (SDS, 1%). After sonicating 3×10 seconds, samples were incubated for 45 minutes. Then, samples were centrifuged for 15 minutes at 13,000 rpm. Supernatants were aspirated and stored at -80 °C. Protein concentrations were measured by the BCA method (23227, Pierce), which was

more compatible with detergents (SDS here). The protein concentrations were around 2 μg/μl for most samples.

SDS-PAGE (polyacrylamide gel electrophoresis) and Western blot. Proteins can be separated according to their molecular weight using SDS-PAGE. Proteins are charged negatively by SDS. An electric current is used to drive protein molecules to the positive end across a polyacrylamide gel during electrophoresis. The polyacrylamide gel is a cross-linked matrix functioning as a sieve. Smaller proteins navigate faster. Protein samples from the same rabbit were analyzed in the same gel. Proteins in the sample buffer (1×, 3% SDS, 5% glycerol, 5% 2-mercaptoethanol, and bromophenol blue) were boiled for 5 minutes before loading. Protein concentrations were adjusted to the same by adding the lysis buffer. After centrifuging for 30 sec at a relative centrifugal force 10,000g, equal amounts of total proteins (15~40 μg) were carefully loaded into wells on 10% polyacrylamide gels. The BenchMark prestained protein ladder (Invitrogen) was also loaded to each gel to help determine the molecular weight. Proteins were then electrophoresed at 200 volts using a Bio-Rad Mini-Protean III apparatus.

Separated proteins were electrophoretically transferred to polyvinylidene difluoride membranes (PVDF, Millipore) at 320 mA for 80 minutes in a cold room. The transfer buffer had 25 mM Tris, 192 mM glycine, 0.3 g/liter SDS, and 20% methanol. Proteins were transferred out of the gel except at the top under this transfer condition (Figure 3-4). Membranes were blocked for 1 h at room temperature in order to reduce non-specific bindings. The blocking solution was 5% non-fat dried milk for most antibodies or 5% bovine serum albumin (BSA) for total Src and total Akt antibodies in 20 mM Tris buffered saline (TBS, pH 7.5) with 0.1% tween-20 (TBST). Membranes were then incubated with primary antibodies. The dilution and incubation were: rabbit polyclonal anti-Cx43 (immunogen is a synthetic peptide derived from the cytoplasmic

loop of rat Cx43, affinity purified, 71-0700, Zymed Laboratories), 1:250 (1 μg/ml), overnight (in the cold room otherwise specified); rabbit polyclonal anti-non-phospho-Src (Tyr-527, active Src, immunogen is a synthetic peptide (KLH-coupled) corresponding to residues surrounding Tyr527 of human Src, purified by protein A and peptide affinity chromatography, 2107, Cell Signaling Technology), 1:500, overnight; rabbit polyclonal anti-Src (total Src, immunogen is at the C-terminus of Fyn of human origin, affinity purified, sc-18, Santa Cruz Biotechnology), 1:2000 (0.1 μg/ml), overnight; mouse monoclonal anti-phospho-Akt (Ser473, active Akt, immunogen is a synthetic phospho-peptide (KLH-coupled) corresponding to residues around Ser473 of mouse Akt, 4051S, Cell Signaling Technology), 1:500, overnight; rabbit anti-Akt (total Akt, immunogen is a synthetic peptide (KLH-coupled) derived from the carboxy-terminal sequence of mouse Akt, purified by protein A and peptide affinity chromatography, 9272, Cell Signaling Technology), 1:1000, overnight; mouse monoclonal anti-p27kip (referred to as p27 hereafter) (immunogen is against mouse p27, IgG1, purified from tissue culture supernatant or ascites by affinity chromatography, 610241, BD Biosciences), 1:4000 (0.0625 μg/ml), overnight; mouse monoclonal anti-β-catenin (immunogen is amino acids 680-781 mapping at the C-terminus of β-catenin of human origin, IgG1, sc-7963, Santa Cruz Biotechnology), 1:1000 (0.2 μg/ml), overnight; and mouse monoclonal anti-β-actin (immunogen is slightly modified β-actin N-terminal peptide, Ac-Asp-Asp-Asp-Ile-Ala-Ala-Leu-Val-Ile-Asp-Asn-Gly-Ser-Gly-Lys, conjugated to KLH, IgG1, purified, A1978, Sigma) antibody, 1:1000, 45 minutes, room temperature. After washing 3×10 minutes in TBST, membranes were incubated with secondary antibodies for 1 h at room temperature. The new mouse monoclonal anti-rabbit IgG, light chain-specific antibody (211-032-171, Jackson ImmunoResearch Laboratories) was used to detect primary antibodies generated in rabbits at dilution 1:50,000. The goat anti-mouse antibody with

horseradish peroxidase (HRP) (554002, BD Pharmingen) was used to detect primary antibodies produced in mice. After washing 3×10 minutes in TBST, protein bands were detected by enhanced ECL reagents (ECL plus, GE Healthcare) for most proteins or regular ECL reagents (32106, Pierce) for β-actin. The Kodak Image Station 2000R (Eastman Kodak Company) was used to take images and do densitometric analysis of bands. Intensities of target protein bands were normalized to the corresponding bands of β-actin, which has been widely used as the control protein. Our results also demonstrated that protein levels of β-actin were not significantly changed in these culture conditions.

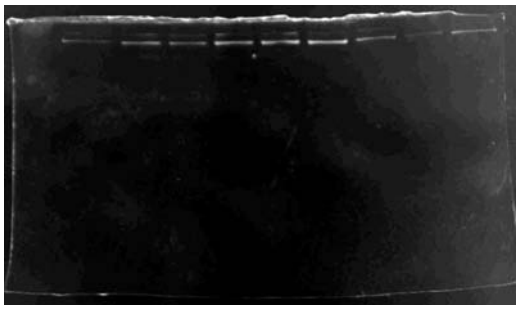

Figure 3-4 Coomassie blue staining of a transferred gel to test protein transfer efficiency.

Except at the top of the gel, proteins have been transferred out of the gel. The proteins at the top of the gel have very large molecular weights, which are out of the range of our interested proteins. Therefore, the transfer was efficient.

The specificity of the Cx43 bands was tested by omitting the primary antibody (secondary antibody only in Figure 3-5A) or incubating the immunogen peptide with the primary antibody. Proteins from a mouse heart (mH in Figure 3-5A) and a rabbit heart (rH) were loaded as the positive controls. There were no bands after omitting the primary antibody or with the immunogen peptide blocking (Figure 3-5A). Samples from the mouse and rabbit hearts, and

DTA had bands with a molecular weight around 43 kDa (Figure 3-5A). The corresponding positions of these membranes are shown in Figure 3-5B.

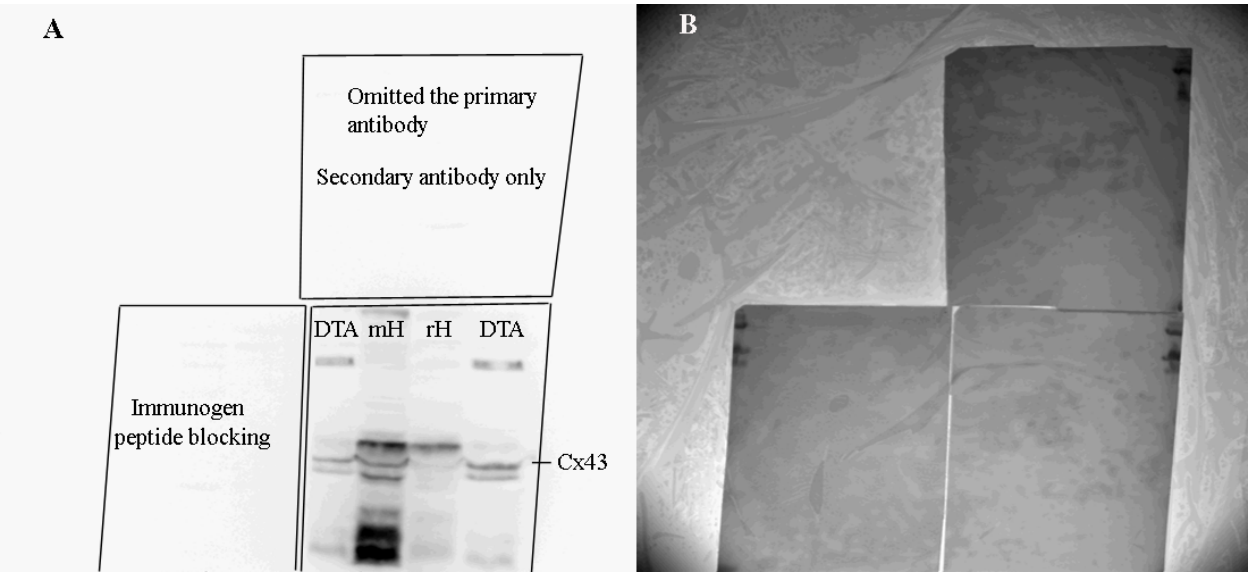

Figure 3-5 The Cx43 bands are specific to the Cx43 antibody.

The specificity of the Cx43 bands was tested by omitting the primary antibody (secondary antibody only in A) or incubating the immunogen peptide with the primary antibody. There were no bands after omitting the primary antibody or with the immunogen peptide blocking (A). Samples from the mouse and rabbit hearts, and DTA had bands with a molecular weight around 43 kDa (A). The corresponding positions of these membranes are shown in B and drawn in A.

Bands may reach saturation when too much protein is loaded. Possibility of Cx43 band saturation was tested by loading different amounts of total proteins (Figure 3-6). Bands of Cx43 and β-actin with 40 μg total proteins had an intensity which was approximately twice of that with 20 μg total proteins, respectively. Similarly, bands of Cx43 and β-actin with 20 μg total proteins had an intensity which was approximately twice of that with 10 μg total proteins, respectively Therefore, bands were not saturated for both Cx43 and β-actin when loading 40 μg total proteins.

Although we did not test the full range of linearality of Cx43 and β-actin, it was linear for the amount of total proteins loaded in this dissertation (15~40 μg).

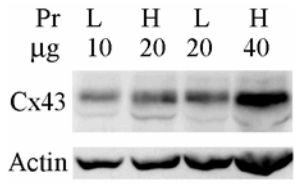

Figure 3-6 Saturation test of Cx43 bands.

Different amounts of total proteins from aortas cultured under high pressure (H, 150 mmHg) or low pressure (L, 80 mmHg) were loaded to test the linearality of Western blot for Cx43 and β-actin. It is approximately linear in the range of 10 to 40 μg total proteins, the amount that had been loaded in this study.

3.4 QUANTITATIVE MESSENGER RNA ANALYSIS

Real-time polymerase chain reaction (PCR) can be used to detect gene expression levels quantitatively. It is more sensitive and accurate than end-point PCR in which PCR products are detected after amplification by running gels. The TaqMan® PCR assay uses special probes and a fluorescent reporter dye to detect the cycle-by-cycle increase in the amount of PCR products in real time. Gene-specific primers and probes improve specificity of PCR results.

Total RNA extraction. After culture, aortas were snap-frozen in liquid nitrogen. Frozen tissues were stored at -80 °C until use. The RNeasy kit for fibrous tissues (Qiagen) was used to extract total RNA from aortas per manufacturer's protocol with modifications in order to increase the yield. Proteinase K was used to digest fibers. Genomic DNA molecules were degraded by the RNase-free DNase I treatment. RNA samples were diluted in 10 mM Tris pH7.0

buffer when measuring concentrations at A_{260} using a Spectronic Biomate spectrometer (Thermo Electron Corporation). The ratio of A_{260}/A_{280} is an estimate of the purity of RNA samples. A ratio of 1.9~2.0 indicates highly purified RNA. The integrity of RNA was checked using 1% agarose gel electrophoresis and ethidium bromide (EtBr) staining. The BioRad mini-sub cell GT system was used to cast gels and run electrophoresis. One example of EtBr staining was shown in Figure 3-7. The integrity of RNA sample was shown by the ratio of 28S to 18S ribosomal RNA, the most abundant RNA in mammalian cells. Undegraded total RNA samples have a ratio of 2, which was the case in Figure 3-6. RNA samples were stored at -80 °C until doing reverse transcription.

Figure 3-7 Integrity test of total RNA extracted from rabbit aortas.

Total RNA extracted from a rabbit descending thoracic aorta was separated by electrophoresis using an agarose gel. Bands were stained with ethidium bromide. The integrity of RNA sample was shown by the ratio of 28S (the upper band) to 18S (the lower band) ribosomal RNA. Two clear bands were detected. The 28S band was much stronger than the 18S band. Therefore, the RNA sample was not degraded.

Reverse transcription. mRNA molecules in total RNA samples were reverse transcribed to complimentary single-stranded DNA (cDNA), which was used in the subsequent PCR step. The High Capacity cDNA Archive Kit from Applied Biosystems was used. Random primers were used in this kit. The amount of total RNA that can be loaded in one reaction with volume 100 μl is 0.1~10 μg for this kit. Total RNA at the amount of 0.5 μg of total RNA was loaded into

a 0.2 ml thin wall PCR vial. The negative control for reverse transcription did not have the reverse transcriptase. Vials were kept at 25 °C for 15 minutes first. The reaction lasted for 2 h at 37 °C in a thermal cycler (TC-312, Techne) before vials were maintained at 4 °C. Samples were stored at -80 °C until doing PCR.

Real-time polymerase chain reaction. The TaqMan® gene expression assay was used to compare Cx43 mRNA levels using GAPDH as the reference, or Cx40 mRNA levels using VE-cadherin as the reference. The reason of choosing VE-cadherin as the reference is because both Cx40 and VE-cadherin are expressed in ECs only in rabbit descending thoracic aortas. The assay uses a single FAM™ dye-labeled TaqMan® probe with a DNA minor groove binder moiety and two unlabeled oligonucleotide primers. The TaqMan Universal PCR Master Mix (Applied Biosciences) contains necessary components for accurate amplification and detection of PCR products. These components are AmpliTaq Gold DNA polymerase, dNTPs with dUTP, passive internal reference ROX, optimized buffer components, and AmpErase Uracil N-glycosylase (UNG). The passive internal reference minimizes well-to-well variability that can result from a variety of causes, such as pipetting errors and sample evaporation. UNG eliminates products from previous PCR amplifications by excising uracil residues. Samples were loaded into a 96-well plate in triplicate. The reaction volume was 25 µl in each well. The plate was covered by an optical adhesive cover (Applied Biosciences). PCR was conducted in the TaqMan® core facility of the Genomics and Proteomics Core Laboratories of the University of Pittsburgh. Samples were kept at 50 °C for 2 minutes first. Temperature was increased to 95 °C and kept for 12 minutes before the amplification reaction. Forty cycles were repeated. Each cycle was held at 95 °C for 15 seconds and at 60 °C for 1 minute. The primers and probes for rabbit Cx43 gene (GI # 39981122, NCBI CoreNucleotide accession # AY382590), GAPDH gene (GI # 406106, NCBI

CoreNucleotide accession # L23961), Cx40 gene (GI # 81238392, NCBI CoreNucleotide accession # DQ242483), and VE-cadherin (Ensembl gene ID ENSOCUG00000016941) are as follows:

Cx43 forward primer 5'-AGTGCAGAACAAAACCGAATGG-3'

Cx43 reverse primer 5'-GCTGTGCATGGGAGTTGGA-3'

Cx43 probe 5'-CAGGCAGGAAGTACCATC-3'

GAPDH forward primer 5'-CGGATTTGGCCGCATTGG-3'

GAPDH reverse primer 5'-GGCGACAACATCCACTTTGC-3'

GAPDH probe 5'-CCAGGGCTGCTTTTAA-3'

Cx40 forward primer 5'-GGTGCTGCAGATCATCTTCGT-3'

Cx40 reverse primer 5'-TCTTGCGCTTCTCCTGCAT-3'

Cx40 probe 5'-CCTGGTGTACATGGGCCAC-3'

VE cadherin -forward primer 5'-TCCGTGCCCGAGATGTC-3'

VE cadherin -reverse primer 5'-CGCATCCACTGCTGTCACA-3'

VE cadherin -probe 5'-ACCGAGGTCCCCACAGAT-3'

Levels of mRNA were relatively quantified using the comparative Ct (ΔΔCt) method. The threshold cycle (Ct) is the PCR cycle at which there is a significant increase in reporter fluorescence signal above a baseline in a given well. ΔCt is the difference between the threshold cycle of a target gene and the threshold cycle of the corresponding reference gene in the same well. Therefore, ΔCt = Ct (target) – Ct (endogenous reference). ΔΔCt is the difference between the average ΔCt value of an experimental sample and the average ΔCt for the corresponding control sample. Thus, ΔΔCt = ΔCt (experimental sample) – ΔCt (control sample). The fold

change in mRNA is calculated by the equation: Expression fold value = $2^{-\Delta\Delta Ct}$. Ct values were obtained using the software SDS2.2 (Applied Biosciences).

A series of cDNA samples in triplicate was loaded in order to compare the amplification efficiency under different substrate concentrations using cDNA generated by reverse transcription from 100 ng, 25 ng, 5 ng, 1 ng, and 0.2 ng of total RNA. Figure 3-8 shows fluorescent signal changes over amplification cycles for Cx43 (right curves) and GAPDH (left curves) at 10 ng total RNA in triplicate. Cycles from 3 to 15 were used to calculate the baseline signal. The threshold value was 0.17. The Cx43 no-template negative control well had no amplification. The Cx43 no-reverse-transcription control well showed amplification. But the Ct value was 37.7, which was much larger than the Ct values of reverse transcribed samples (~21). The GAPDH no-template or no-reverse-transcription negative control well had amplification with Ct 35.89, 32.22 respectively, which were much larger than the Ct values of reverse transcribed samples (~17). Based on the Ct values under different concentrations of cDNA (or total RNA), the amplification efficiency of Cx43 and GAPDH was 94.6% and 96.9%, respectively (Efficiency = $(10^{-1/slope}-1)\times100\%$; For Cx43, Ct=-3.46log[RNA]+28.11. For GAPDH, Ct=-3.4log[RNA]+24.93. The slope was -3.46, -3.4, respectively). Therefore, both cDNA samples were amplified efficiently and had similar efficiency which was close to 100%. The ΔCt values ($Ct_{Cx43} - Ct_{GAPDH}$) at different cDNA concentrations were similar as well (ΔCt=-0.06log[RNA]+3.18. The very small slope (0.06) represents independence of ΔCt on RNA concentration). These analyses verified that $2^{-\Delta\Delta Ct}$ method could be used to compare gene expression levels of rabbit Cx43 in arterial tissues.

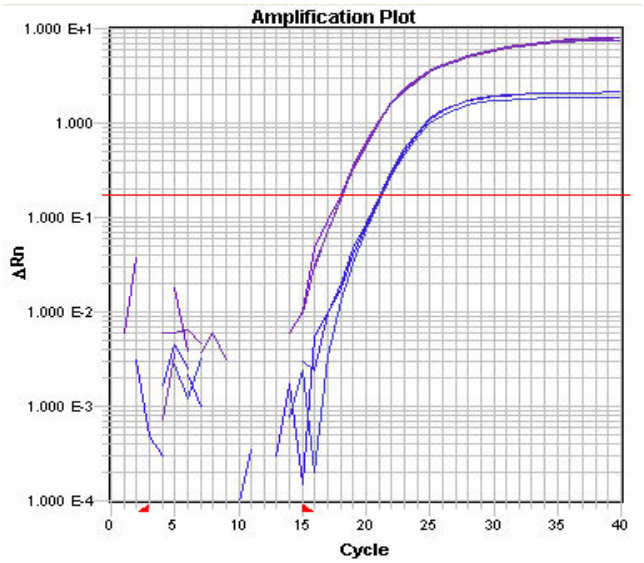

Figure 3-8 One example of the PCR amplification plot of Cx43 (right) and GAPDH (left) genes.

3.5 IMMUNOHISTOCHEMISTRY AND CONFOCAL MICROSCOPY

Expression of connexin proteins in rabbit DTAs has not been reported. Freshly harvested rabbit DTAs were stained either *en face* or after sectioning (8 μm) for Cx43, Cx40 and Cx37, the most common connexin proteins in large arteries. *E*n face staining of the endothelium used whole mounts of aortic rings (5 mm long). To prepare DTAs for section, DTAs were frozen in isopentane (Fisher Scientific) at -160 °C which was achieved using liquid nitrogen. DTAs were then embedded in Tissue-Tek® O.C.T. Compound (Fisher Scientific) which was frozen on dry ice. Cardiac ventricles have abundant Cx43 expression in intercalated discs. Therefore, rabbit left ventricles were processed similarly to DTAs to act as the positive control of Cx43 staining. Aortic rings and sections were fixed in -20 °C acetone (Sigma) for 10 minutes. After brief washing, samples were blocked in phosphate buffered saline (PBS, Sigma) with 10% normal goat serum (Sigma) and 1% BSA (Calbiochem) for 1 h at room temperature. Samples were then

incubated at 4 °C overnight with the rabbit polyclonal anti-Cx43 (71-0700, Zymed), 1:50 dilution (5 μg/ml); anti-Cx40 (immunogen is a peptide with 19 amino acids of mouse Cx40, affinity purified, IgG1, Cx40-A, Alpha Diagnostic Intl.), 1:100 (10 μg/ml); or anti-Cx37 (immunogen is a peptide with 16 amino acids of mouse Cx37, affinity purified, IgG1, Cx37A11-A, Alpha Diagnostic Intl.), 1:200 (5 μg/ml), primary antibody, respectively. Antibodies were diluted in PBS. After washing in PBS for 3×15 minutes, samples were incubated with the goat anti-rabbit IgG-Alexa Fluor 488 secondary antibody (Molecular Probes), 1:500 with PBS for 1 h at room temperature. After washing in PBS for 3×15 minutes, nuclei were stained with propidium iodide in the Vectashield mounting medium (Vector Laboratories). Secure-seal adhesive spacers (Molecular Probes) were used to mount the axially opened aortic tissues. Peripheries of coverslips were sealed using nail polish. Images were taken sequentially using the upright Leica TCS-SL laser scanning confocal microscope (Leica Microsystems GmbH, Germany). As a negative control, the slide with secondary antibody only was included such that no staining was visible for this slide under the same imaging settings. Images were projected and adjusted contrasts using NIH ImageJ.

3.6 STATISTICAL ANALYSIS

Data were expressed as means ± standard errors (SE). Differences between the experimental groups and the controls were compared using paired t-test in SigmaPlot (Systat Software). In case of non-normal distribution, non-parametric tests were performed. In most cases, three to five independent experiments were performed in each group. Differences were considered significant when $P < 0.05$.

4.0 RESULTS

4.1 CONNEXIN EXPRESSION IN RABBIT DESCENDING THORACIC AORTAS

Rabbit descending thoracic aortas were used to study regulation of gap junctions by mechanical factors. Therefore, it was necessary to know the connexin expression pattern in these aortas. Freshly isolated aortas were stained *en face* for ECs or sectioned for both ECs and SMCs. Connexin proteins were stained green. Nuclei were stained red by propidium iodide in the mounting medium. Images were taken using a scanning confocal microscope. Endothelial cells expressed Cx43 with a typical punctate staining pattern (Figure 4-1). Cx40 (Figure 4-2) and Cx37 (Figure 4-3) were also expressed in ECs with strong staining at cell peripheries. Cx43 was strongly expressed in SMCs as well (Figure 4-4). However, Cx40 was not expressed in SMCs (Figure 4-5). Similarly, Cx37 was not expressed in SMCs (Figure 4-6). The very few green staining in the media was most likely caused by incomplete washing and/or macrophages, which express Cx37. Cx43 was detected using a widely used antibody (71-0700, Zymed). It was known that cardiac ventricles express Cx43. As a positive control of this antibody, sections of rabbit left ventricles were stained with this rabbit polyclonal antibody (Figure 4-7A). Another mouse monoclonal antibody (MAB3067, Chemicon) gave a similar staining pattern of rabbit ventricles (Figure 4-7B, note the different scale from A).

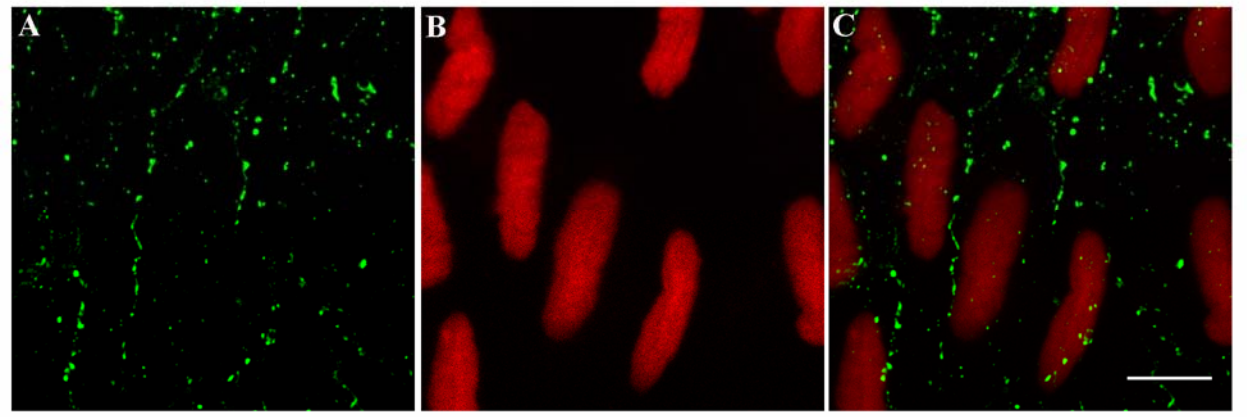

Figure 4-1 Cx43 is expressed in endothelial cells of rabbit descending thoracic aortas.

A fresh DTA was *En face* stained for Cx43 in ECs. The typical punctate staining pattern of connexin was visible (A). Nuclei were stained red (B). Most staining of Cx43 was peripheral (C, merge of A and B). The scale bar equals 10 μm.

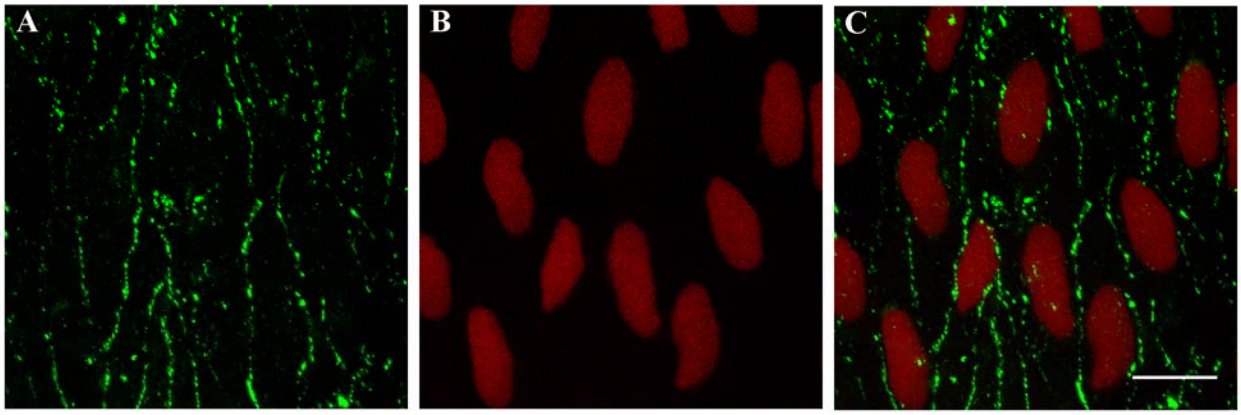

Figure 4-2 Cx40 is expressed in endothelial cells of rabbit descending thoracic aortas.

A fresh DTA was *En face* stained for Cx40 in ECs. The typical punctate staining pattern of connexin was visible (A). Nuclei were stained red (B). Most staining of Cx40 was peripheral (C, merge of A and B). The scale bar equals 10 μm.

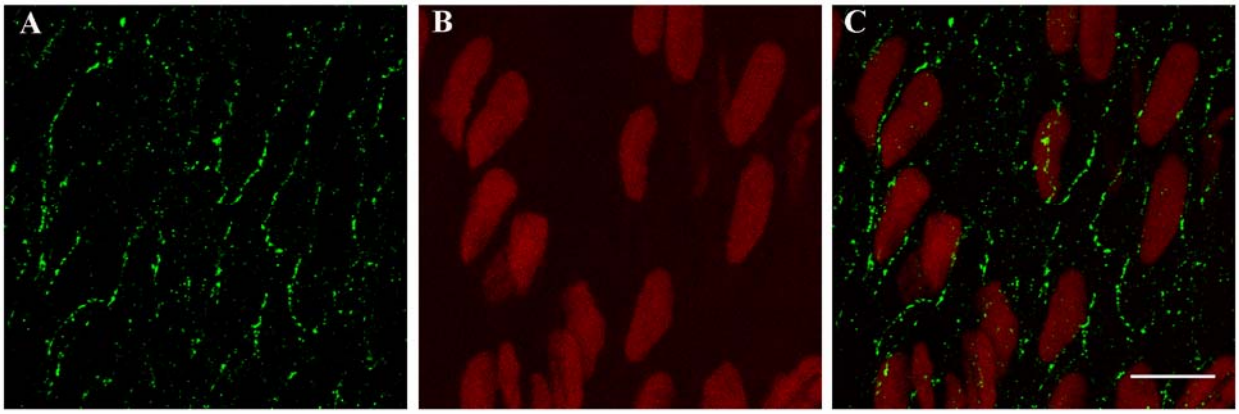

Figure 4-3 Cx37 is expressed in endothelial cells of rabbit descending thoracic aortas.

A fresh DTA was *En face* stained for Cx37 in ECs. The typical punctate staining pattern of connexin was visible (A). Nuclei were stained red (B). Most staining of Cx37 was peripheral (C, merge of A and B). The scale bar equals 10 μm.

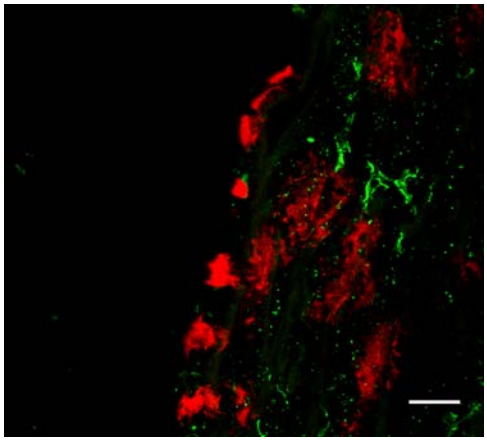

Figure 4-4 Cx43 is expressed in smooth muscle cells of rabbit descending thoracic aortas.

A fresh DTA was frozen and sectioned at 8 μm thickness. Cx43 was stained as green, while nuclei were stained as red. The scale bar equals 10 μm.

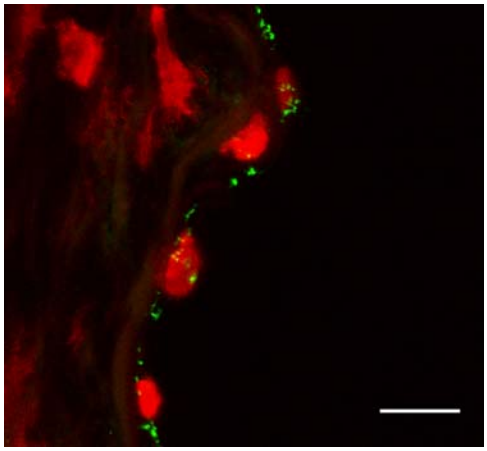

Figure 4-5 Cx40 is not expressed in smooth muscle cells of rabbit descending thoracic aortas.

A fresh DTA was frozen and sectioned at 8 μm thickness. Cx40 was stained as green, while nuclei were stained as red. The scale bar equals 10 μm.

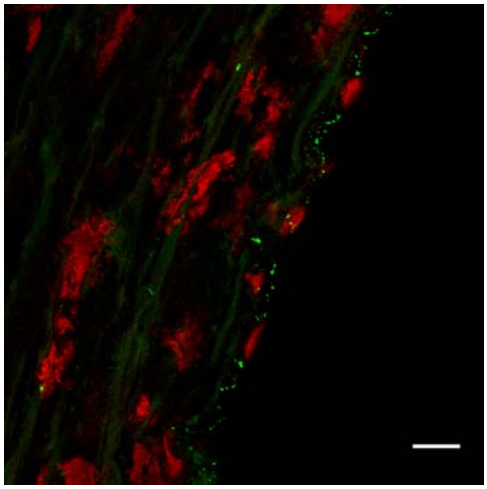

Figure 4-6 Cx37 is not expressed in smooth muscle cells of rabbit descending thoracic aortas.

A fresh DTA was frozen and sectioned at 8 μm thickness. Cx37 was stained as green, while nuclei were stained as red. The scale bar equals 10 μm.

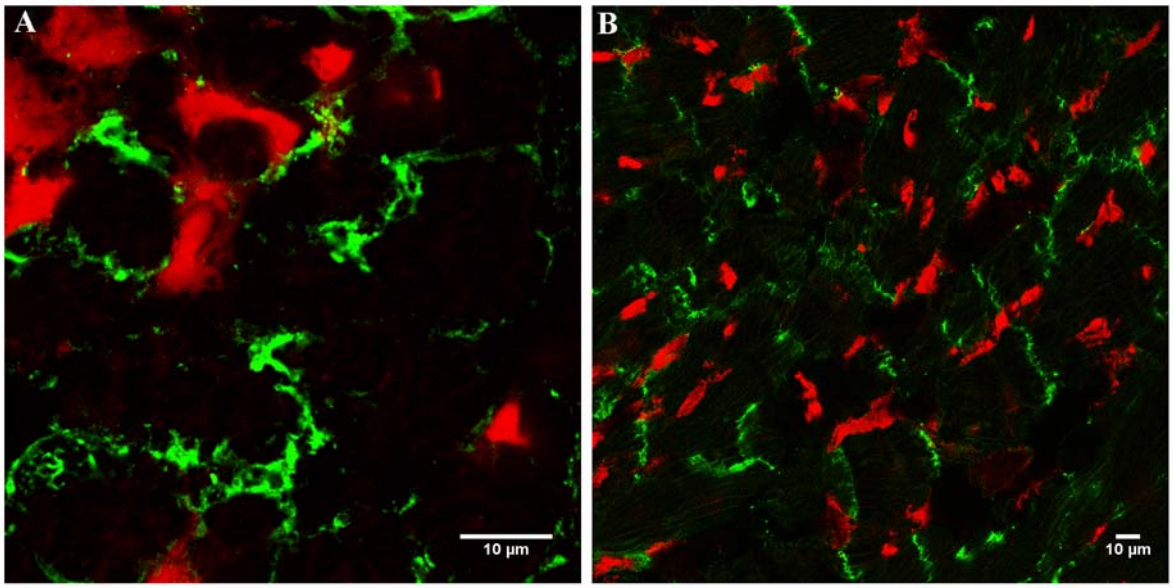

Figure 4-7 Rabbit left ventricle staining of Cx43.

The heart tissue was snap-frozen in liquid nitrogen, and cryosectioned at 6 µm thickness. Cx43 was stained as green using the antibody 71-0700, Zymed (A) or MAB3067, Chemicon (B), while nuclei were stained as red.

In summary, ECs in rabbit descending thoracic aortas express Cx43, Cx40 and Cx37, while VSMCs express Cx43 only. This expression pattern is consistent with that observed in large arteries.

4.2 REGULATION OF GAP JUNCTIONS BY THE MEAN PRESSURE LEVEL

4.2.1 Regulation of gap junction expression by the steady pressure level

Rabbit descending thoracic aortas were harvested, and cultured under steady high pressure (150 mmHg, HPr) or normal (low) pressure (80 mmHg, LPr) for short- (6 h) or long-term (24 h). The

flow was the same (20 ml/min). Proteins and RNA molecules were extracted and analyzed. Western blot was used to quantitatively detect the protein levels. The rabbit polyclonal anti-Cx43 antibody could detect a few bands of Cx43 because of the different phosphorylation states (Figure 4-8). The results were expressed as the ratio of HPr to LPr. To compare mRNA levels, the mRNA of GAPDH was used as the reference (control) gene. Short-term high pressure increased the Cx43 mRNA level significantly (1.93±0.18-fold, $P<0.01$, Figure 4-9). Furthermore, the Cx43 protein level was also increased by short-term high pressure (2.26±0.29-fold, $P<0.05$, Figure 4-9).

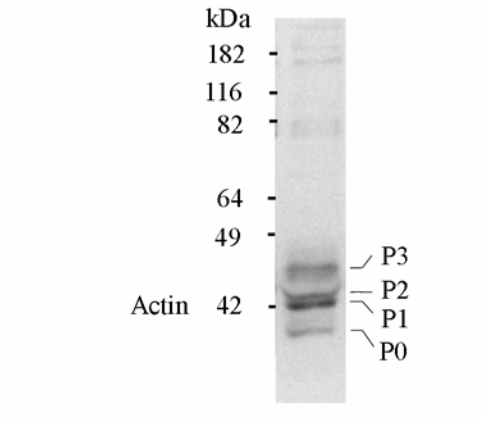

Figure 4-8 The Cx43 antibody (71-0700) can detect a few bands of the Cx43 protein because of phosphorylation.

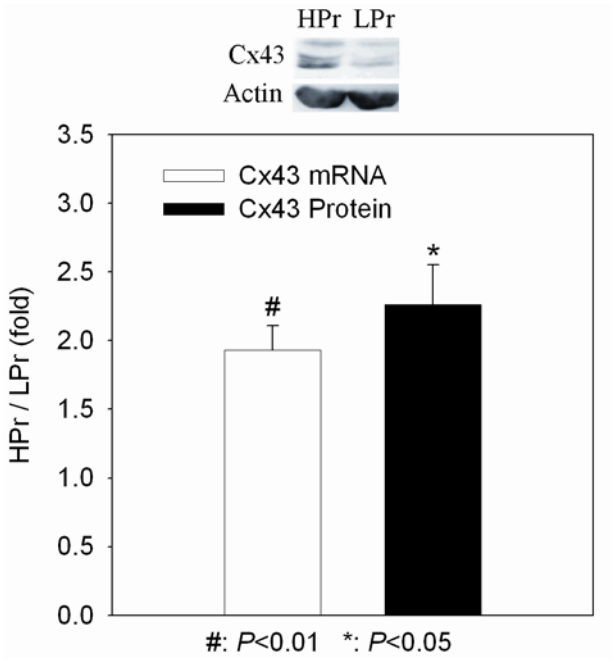

Figure 4-9 Short-term (6 h) regulation of Cx43 expression by steady pressure.

The rabbit descending thoracic aorta was cut into two segments. One segment was cultured under high steady pressure (HPr, 150 mmHg), while the other segment was under low steady pressure (LPr, 80 mmHg) for short-term (6 h). Flow was the same (20 ml/min). GAPDH was the reference gene for comparing the Cx43 mRNA levels. The Cx43 protein levels were normalized by the corresponding □-actin protein levels. Results were expressed as ratios of high to low steady pressure values. High steady pressure increased the Cx43 mRNA and total protein levels after 6 h. Error bars indicate SE of 5 independent experiments**.**

Cx43 can also be regulated in terms of different phosphorylation states. To quantify the different phosphorylation states, ratios of phosphorylated (the band P1, P2 and P3 in figure 4-8) to non-phosphorylated (the band P0 in figure 4-8) Cx43 were calculated. In cases where there were only three bands, the lowest one (i.e., the smallest molecular weight) was treated as P0. Short-term high steady pressure reduced the ratio of phosphorylated to non-phosphorylated Cx43 as compared with the low pressure controls (0.69±0.07-fold, $P<0.05$, Figure 4-10).

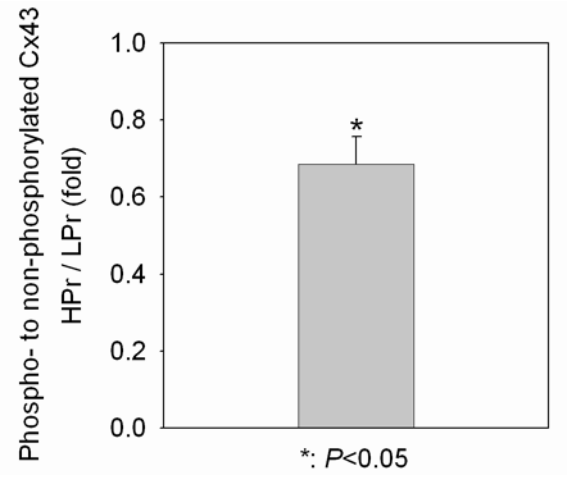

Figure 4-10 Short-term (6 h) regulation of Cx43 phosphorylation by steady pressure.

One segment of the DTA was cultured under high steady pressure (HPr, 150 mmHg), while the other segment was under low steady pressure (LPr, 80 mmHg) for short-term (6 h). Flow was the same (20 ml/min). High steady pressure decreased the level of phosphorylated to non-phosphorylated Cx43 protein after 6 h. The error bar indicates SE of 5 independent experiments**.**

In addition, the mRNA levels of Cx40 in aortas were detected. Of note, Cx40 is only expressed in ECs. However, the analyzed RNA samples came from VSMCs as well. Therefore, the reference gene is critical for the accurate comparison of Cx40 gene expression. Two genes were tried. One was again GAPDH, which is expressed in both ECs and SMCs. The Cx40 mRNA levels were similar between aortas cultured under short-term high and low steady pressure (1.21±0.26-flod, Figure 4-11). The other one was VE-cadherin, which is an EC-specific protein at adherens junctions. The Cx40 mRNA levels were also not significantly different (1.71±0.60-flod). The VE-cadherin mRNA levels were similar if using GAPDH as the reference gene (0.81±0.15-flod).

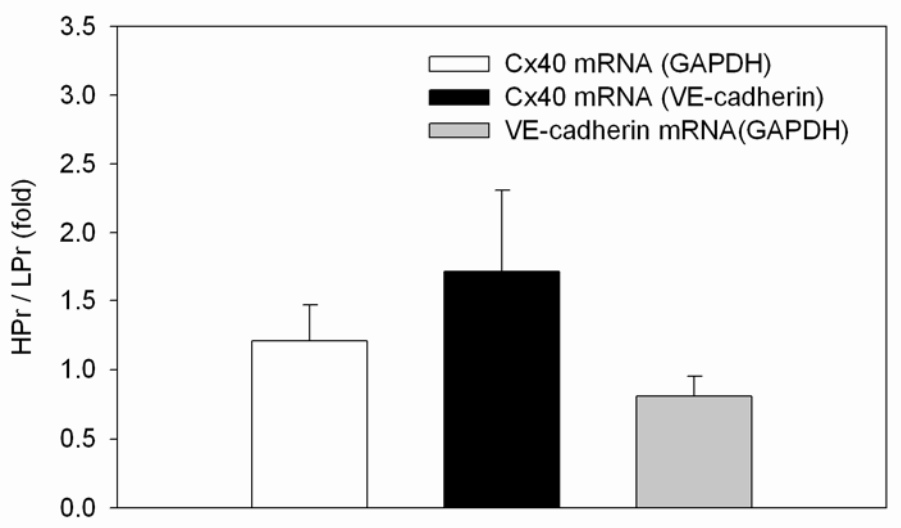

Figure 4-11 Short-term (6 h) regulation of Cx40 mRNA expression by steady pressure.

One segment of the DTA was cultured under high steady pressure (HPr, 150 mmHg), while the other segment was under low steady pressure (LPr, 80 mmHg) for short-term (6 h). Flow was the same (20 ml/min). GAPDH or VE-cadherin was the reference gene for comparing the Cx40 mRNA levels. GAPDH was the reference gene for comparing the VE-cadherin mRNA levels. High steady pressure did not significantly alter the Cx40 mRNA level using either GAPDH or VE-cadherin as the reference gene. High steady pressure also did not significantly alter the VE-cadherin mRNA level. Error bars indicate SE of 5 independent experiments**.**

Aortas were also cultured for 24 h to investigate the long-term effects of steady pressure on gap junctions. The Cx43 mRNA level was increased by high pressure after 24 h (3.13±0.38-fold, $P<0.01$, Figure 4-12). However, the protein levels were similar (1.18±0.10-fold).

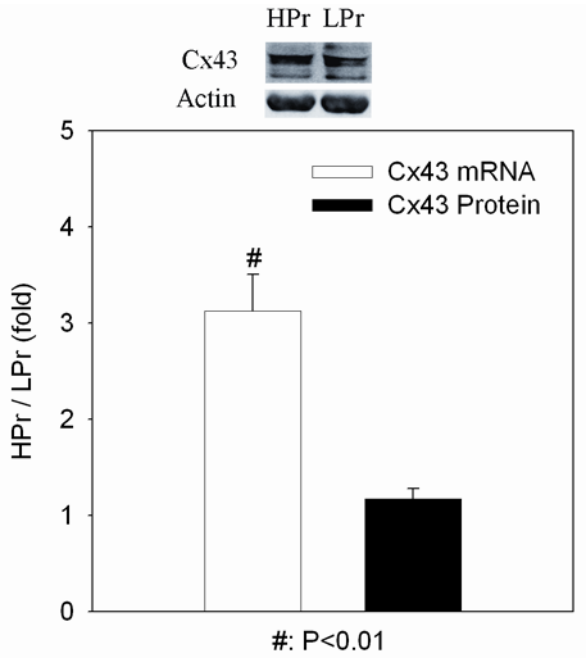

Figure 4-12 Long-term (24 h) regulation of Cx43 expression by steady pressure.

One segment of the DTA was cultured under high steady pressure (HPr, 150 mmHg), while the other segment was under low steady pressure (LPr, 80 mmHg) for long-term (24 h). Flow was the same (20 ml/min). High steady pressure increased the Cx43 mRNA levels. However, the Cx43 total protein levels were similar after 24 h. Error bars indicate SE of 5 independent experiments**.**

The ratios of phosphorylated to non-phosphorylated Cx43 were similar between aortas under high and low steady pressure for long-term (24 h) cultures (0.79±0.09-fold, Figure 4-13).

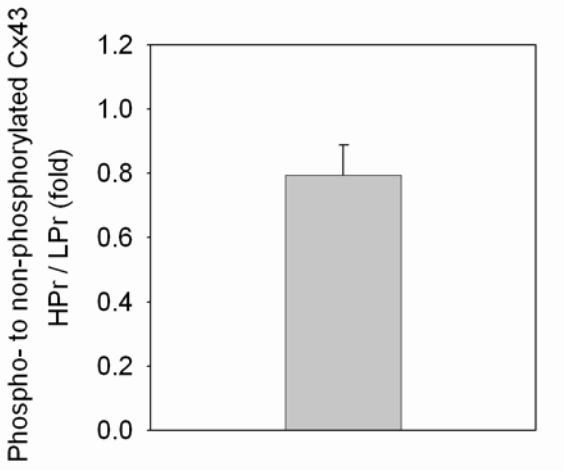

Figure 4-13 Long-term (24 h) regulation of Cx43 phosphorylation by steady pressure.

One segment of the DTA was cultured under high steady pressure (HPr, 150 mmHg), while the other segment was under low steady pressure (LPr, 80 mmHg) for long-term (24 h). Flow was the same (20 ml/min). The ratios of phosphorylated to non-phosphorylated Cx43 were similar between aortas under high and low steady pressure. The error bar indicates SE of 5 independent experiments.

The Cx40 mRNA levels were not different after culturing for long-term under high or low steady pressure using either GAPDH (1.03±0.37-flod, Figure 4-14) or VE-cadherin (0.90±0.33-flod) as the control. The VE-cadherin mRNA levels were also similar if using GAPDH as the control (1.69±0.97-flod).

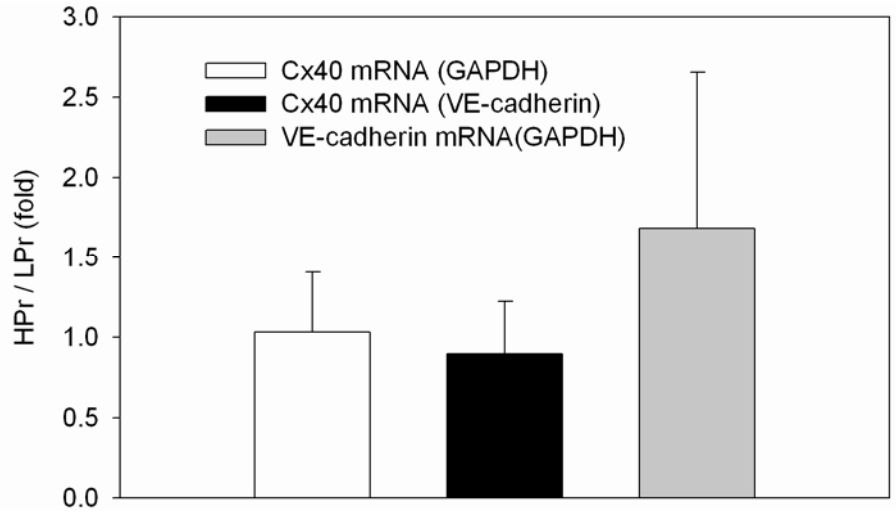

Figure 4-14 Long-term (24h) regulation of Cx40 mRNA expression by steady pressure.

One segment of the DTA was cultured under high steady pressure (HPr, 150 mmHg), while the other segment was under low steady pressure (LPr, 80 mmHg) for long-term (24 h). Flow was the same (20 ml/min). GAPDH or VE-cadherin was the reference gene for comparing the Cx40 mRNA levels. GAPDH was the reference gene for comparing the VE-cadherin mRNA levels. High steady pressure did not significantly alter the Cx40 mRNA level using either GAPDH or VE-cadherin as the reference gene after 24 h. High steady pressure also did not significantly alter the VE-cadherin mRNA level. Error bars indicate SE of 5 independent experiments**.**

To examine whether intraluminal perfusion rate affected the steady pressure-induced regulation of the Cx43 protein level, aortas were cultured under a higher flow (300 ml/min) for 24 h in one experiment. Again, the protein level of Cx43 was not increased by high steady pressure (Figure 4-15).

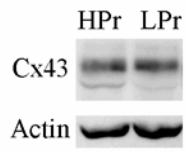

Figure 4-15 Long-term (24 h) regulation of the Cx43 protein level by steady pressure at high flow (300 ml/min).

In one experiment, one segment of the DTA was cultured under high steady pressure (HPr, 150 mmHg), while the other segment was under low steady pressure (LPr, 80 mmHg) for long-term (24 h). Flow was the same for these two segments (300 ml/min). The Cx43 total protein levels were similar.

To study the effects of culture duration on Cx43 protein levels, samples for 6 h and 24 h cultures under the same steady pressure level (low or high) were loaded onto the same gel. The Cx43 protein level was increased from 6 to 24 h in culture under low (Figure 4-16) or high (Figure 4-17) steady pressure.

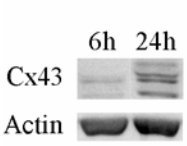

Figure 4-16 The Cx43 protein level is increased from 6 to 24 h under low steady pressure.

Protein samples from aortas cultured under low steady pressure (80 mmHg) for 6 or 24 h were detected the Cx43 protein levels using Western blot to study the culture duration effects. The bands shown are representative of 4 independent experiments.

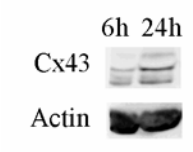

Figure 4-17 The Cx43 protein level is increased from 6 to 24 h under high steady pressure.

Protein samples from aortas cultured under high steady pressure (150 mmHg) for 6 or 24 h were detected the Cx43 protein levels using Western blot to study the culture duration effects. The bands shown are representative of 4 independent experiments.

4.2.2 Effects of pressure pulsatility on the mean pressure level-induced regulation of gap junction expression

High steady pressure did not upregulate the Cx43 protein level at 24 h. However, *in vivo* blood pressure has both mean and pulsatile components. It is possible that the presence of pressure pulsatility may alter the mean pressure-induced regulation of Cx43 expression. To examine this issue, experiments were repeated with the addition of the same pulse pressure (30 mmHg peak-to-peak amplitude, 192 cycles/min) to both high (150 mmHg) and low (80 mmHg) mean pressures. Data were collected after 24 h with intraluminal flow of 25 ml/min. High pressure increased Cx43 mRNA (3.09±1.03-fold, n=3, Figure 4-18) although it was not statistically significant. However, the Cx43 protein levels were again similar (0.86±0.25-fold). Thus, the presence of pressure pulsatility does not alter the mean pressure-induced regulation of Cx43 expression.

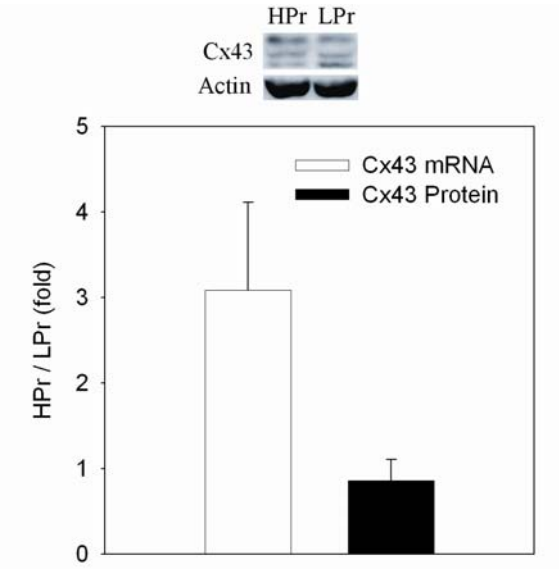

Figure 4-18 Long-term (24 h) regulation of Cx43 expression by mean pressure in the presence of pressure pulsatility.

One segment of the DTA was cultured under high pulsatile pressure (HPr, mean pressure 150 mmHg, pulse pressure 30 mmHg, 192 cycles/min), while the other segment was under low pulsatile pressure (LPr, mean pressure 80 mmHg, pulse pressure 30 mmHg, 192 cycles/min) for long-term (24 h). Mean flow was the same (25 ml/min). High pressure increased Cx43 mRNA although it was not statistically significant. The Cx43 protein levels were similar. Error bars indicate SE of 3 independent experiments.

Long-term high mean pressure in the presence of pressure pulsatility did not alter the ratio of phosphorylated to non-phosphorylated Cx43 (1.34±0.31-fold, Figure 4-19). Therefore, long-term (24 h) high pressure, either steady or pulsatile, does not alter the ratio of phosphorylated to non-phosphorylated Cx43.

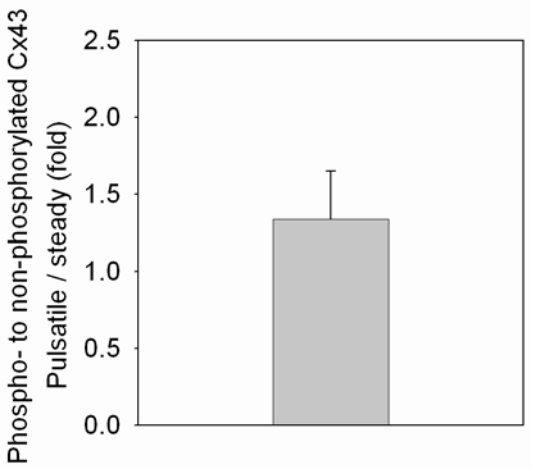

Figure 4-19 Long-term (24 h) regulation of Cx43 phosphorylation by mean pressure in the presence of pressure pulsatility.

One segment of the DTA was cultured under high pulsatile pressure (HPr, mean pressure 150 mmHg, pulse pressure 30 mmHg, 192 cycles/min), while the other segment was under low pulsatile pressure (LPr, mean pressure 80 mmHg, pulse pressure 30 mmHg, 192 cycles/min) for long-term (24 h). Mean flow was the same (25 ml/min). The ratios of phosphorylated to non-phosphorylated Cx43 were similar between aortas under high and low mean pressure. The error bar indicates SE of 3 independent experiments.

4.2.3 Potential mechanisms underlying regulation of Cx43 by the steady pressure level

Src regulation. Src is known to be involved in transducing shear stress[31] and pressure.[83] Therefore, levels of active (nonphospho-Y527) and total Src were quantified to study whether Src was involved in the steady pressure-induced regulation of Cx43 expression. For short-term (6 h) cultures, the active and total Src levels and the ratio of the two (active/total) were not different between the low and high pressure groups (Figure 4-20). In contrast, active Src was more for high steady pressure in long-term (24 h) cultures (1.95±0.23-fold, $P<0.05$, Figure 4-21). Total Src was also increased (1.56±0.24-fold), although it did not reach the statistically significant level ($P=0.067$). The ratios of active to total Src were again similar (1.17±0.10-fold).

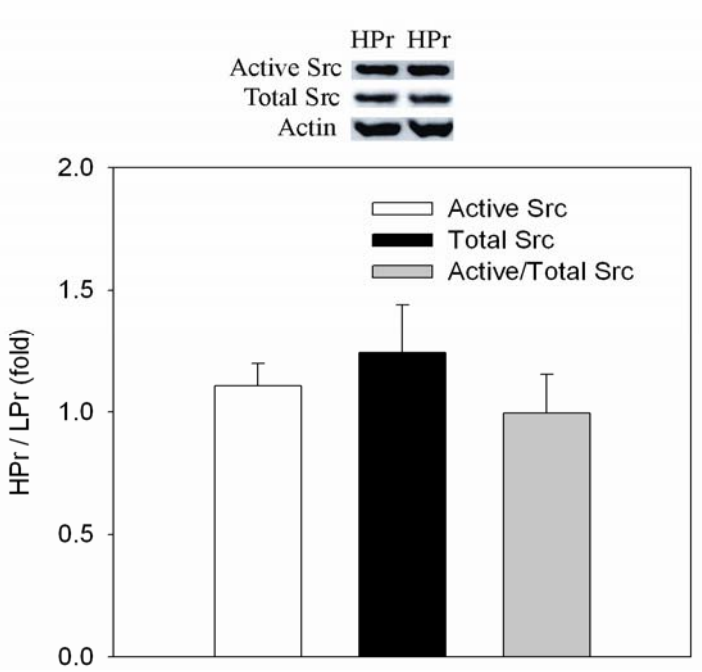

Figure 4-20 Short-term (6 h) regulation of Src by steady pressure.

One segment of the DTA was cultured under high steady pressure (HPr, 150 mmHg), while the other segment was under low steady pressure (LPr, 80 mmHg) for short-term (6 h). Flow was the same (20 ml/min). The levels of active and total Src, and the ratio of these two were similar between the low and high pressure groups. Error bars indicate SE of 5 independent experiments**.**

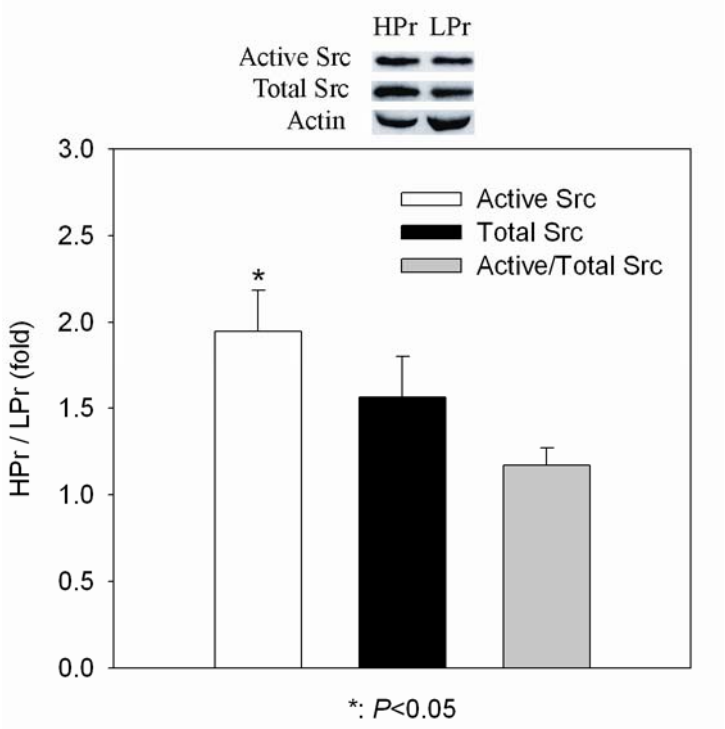

Figure 4-21 Long-term (24 h) regulation of Src by steady pressure.

One segment of the DTA was cultured under high steady pressure (HPr, 150 mmHg), while the other segment was under low steady pressure (LPr, 80 mmHg) for long-term (24 h). Flow was the same (20 ml/min). The levels of active Src were significantly increased by high pressure. The levels of total Src were also increased by high pressure, although it was not statistically significant. The ratios of these two were similar between the low and high pressure groups. Error bars indicate SE of 5 independent experiments.

We investigated whether the presence of pressure pulsatility affected different mean pressure levels-induced changes in Src regulation. Because we observed differential Src regulation by long-term (24 h) cultures only (*vide supra*), experiments in the presence of pressure pulsatility were conducted for this culture duration only. Active Src was still more for high mean pressure (1.43±0.10-fold, $P<0.05$, Figure 4-22). Total Src was not significantly different (1.38±0.15-fold, $P=0.13$). The ratios of active to total Src were again similar. Thus, the presence of pressure pulsatility does not alter the pattern of Src regulation by the mean pressure

level. Specifically, an increase in the mean pressure level elevates levels of total and active Src in long-term (24 h) cultures, without changing the percentage of active Src in total Src.

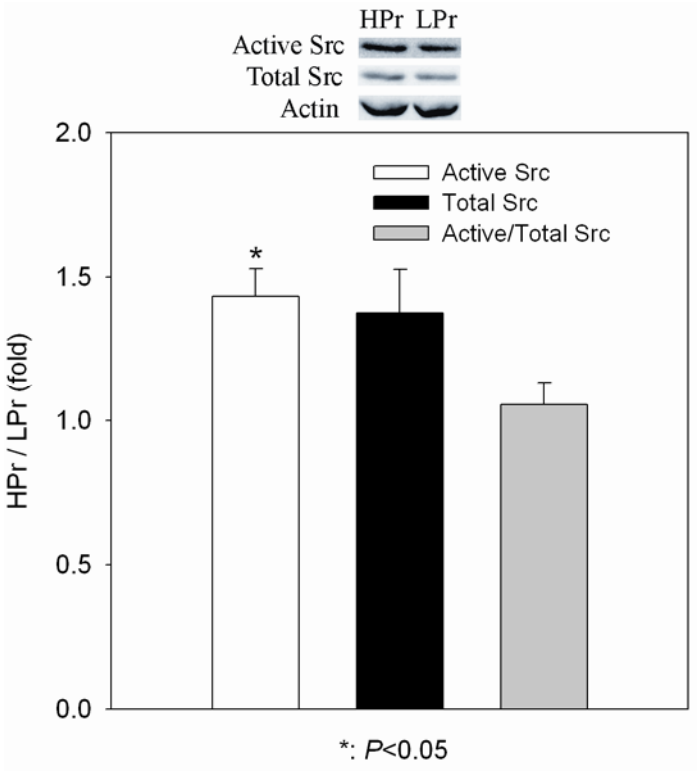

Figure 4-22 Long-term (24 h) regulation of Src by mean pressure in the presence of pressure pulsatility.

One segment of the DTA was cultured under high pulsatile pressure (HPr, mean pressure 150 mmHg, pulse pressure 30 mmHg, 192 cycles/min), while the other segment was under low pulsatile pressure (LPr, mean pressure 80 mmHg, pulse pressure 30 mmHg, 192 cycles/min) for long-term (24 h). Mean flow was the same (25 ml/min). The levels of active Src were significantly increased by high pressure. The levels of total Src were also increased by high pressure, although it was not statistically significant. Error bars indicate SE of 3 independent experiments.

Experiments with Src inhibition. The Src inhibitor PP1 is commonly used to explore the role of Src. Because we observed differential regulation of Cx43 mRNA and protein by high pressure for short-term (6 h) cultures only, PP1 (10 μM) was added to the media of high steady

pressure cultures for 6 h at the onset of culturing in one set of experiments. Both the mRNA and protein levels of Cx43 were similar after Src inhibition (Figure 4-23). Therefore, Src inhibition blocked the increase of both mRNA and protein of Cx43 by high steady pressure (Figure 4-9). Src may mediate upregulation of both mRNA and protein levels of Cx43 by short-term high pressure. The levels of active and total Src were similar between the two culture conditions. Consequently, the ratio of active to total Src was not different. Therefore, PP1 does not alter expression of Src for short-term cultures. It inhibits the activity of Src.

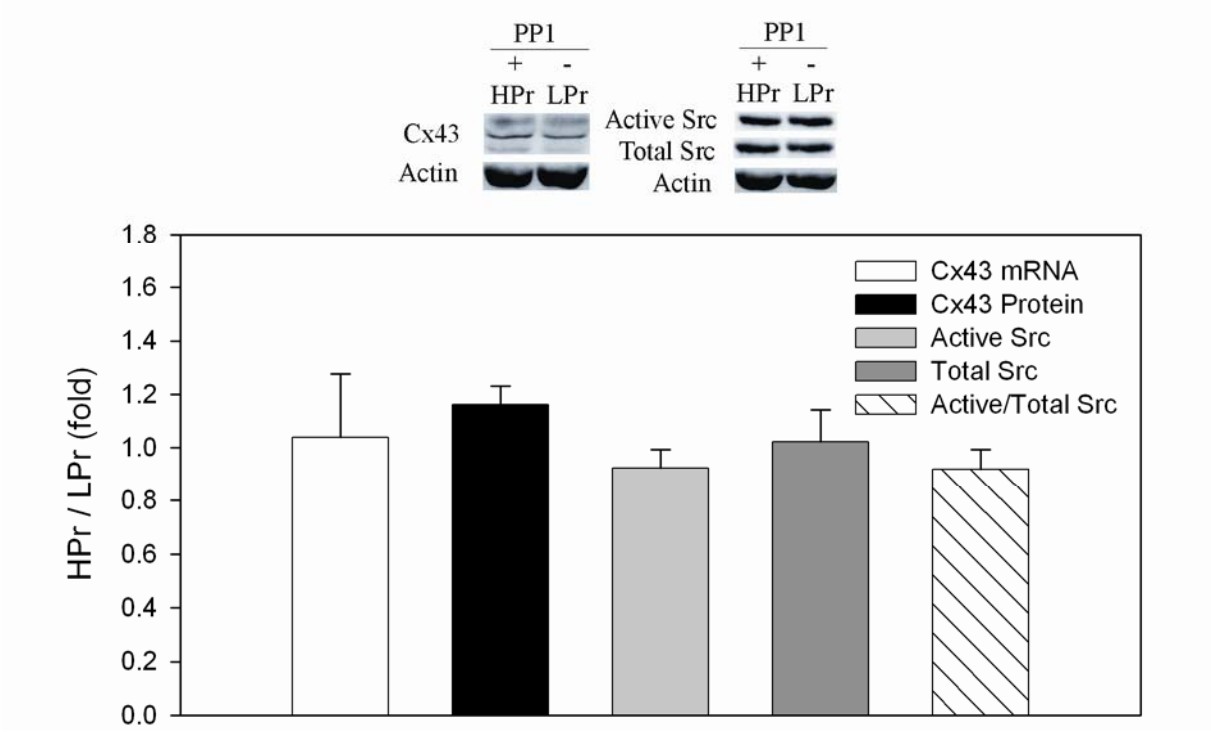

Figure 4-23 Src may mediate short-term (6 h) regulation of Cx43 expression by steady pressure.

One segment of the DTA was cultured under high steady pressure (HPr, 150 mmHg) with the Src inhibitor PP1 (10 μM), while the other segment was under low steady pressure (LPr, 80 mmHg) for short-term (6 h). Flow was the same (20 ml/min). The mRNA and protein levels of Cx43 were similar between the low and high pressure groups after Src inhibition, respectively. The levels of active and total Src, and the ratio of these two were also similar between the low and high pressure groups after Src inhibition. Error bars indicate SE of 4 independent experiments.

We observed that short-term high steady pressure reduced the ratio of phosphorylated to non-phosphorylated Cx43 as compared with the low steady pressure controls (Figure 4-10). However, the ratios were similar after Src inhibition (0.95±0.17-fold, Figure 4-24). Therefore, inhibition of Src eliminated the difference in the ratio of phosphorylated to non-phosphorylated Cx43. Src may mediate downregulation of Cx43 phosphorylation by short-term high steady pressure.

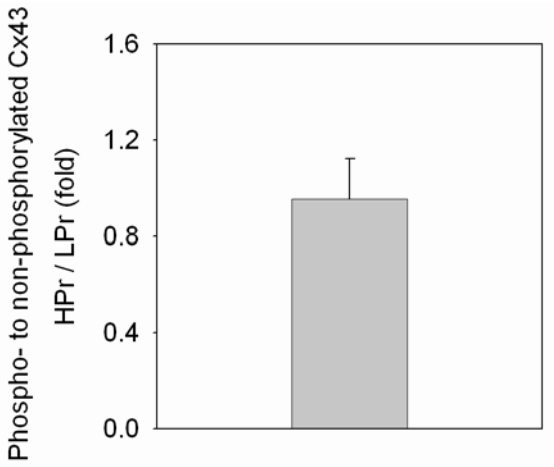

Figure 4-24 Src may mediate short-term (6 h) regulation of Cx43 phosphorylation by steady pressure.

One segment of the DTA was cultured under high steady pressure (HPr, 150 mmHg) with the Src inhibitor PP1 (10 μM), while the other segment was under low steady pressure (LPr, 80 mmHg) for short-term (6 h). Flow was the same (20 ml/min). The ratios of phosphorylated to non-phosphorylated Cx43 were similar between the low and high pressure groups after Src inhibition. The error bar indicates SE of 4 independent experiments.

Other molecules-p27. The phenotypes of cells, such as proliferation, may alter gap junction expression. The protein p27 is a cyclin-dependent kinase inhibitor, and inhibits cell proliferation. Its level is reduced when cells are proliferating. In order to see whether cells had entered or had the tendency of entering cell cycles under high pressure for 6 h, levels of p27

were quantified using Western blot. There was no significant difference between these two pressure levels at 6 h (0.80±0.11-fold, Figure 4-25). Therefore, the protein level of p27 is not affected by the pressure level in short-term culture. The p27 protein levels were still similar after inhibition of Src in aortas cultured under high pressure for 6 h (1.05±0.09-fold, Figure 4-26). Thus, Src does not affect the relative protein levels of p27 between these two pressure levels for short-term cultures.

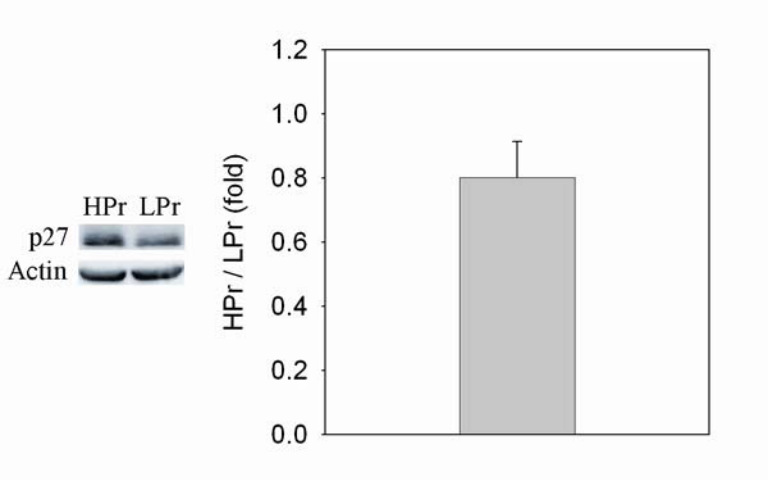

Figure 4-25 Short-term (6 h) regulation of the p27 protein level by steady pressure.

One segment of the DTA was cultured under high steady pressure (HPr, 150 mmHg), while the other segment was under low steady pressure (LPr, 80 mmHg) for short-term (6 h). Flow was the same (20 ml/min). The p27 protein levels were similar between the low and high pressure groups. The error bar indicates SE of 5 independent experiments.

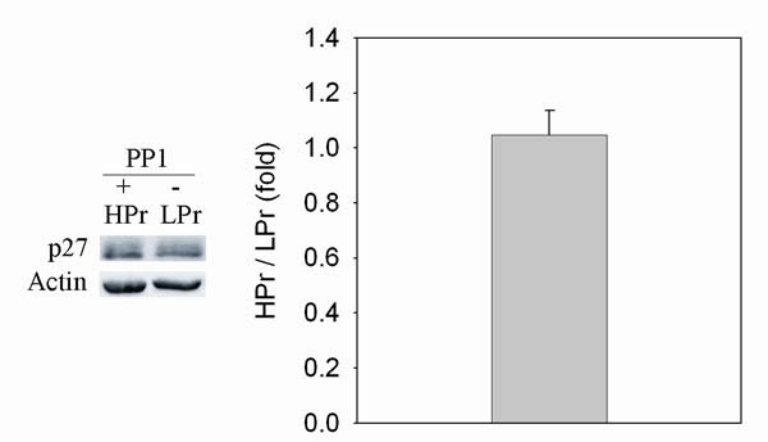

Figure 4-26 Short-term (6 h) Src inhibition using PP1 in the media of high pressure cultures does not affect regulation of the p27 protein level by steady pressure.

One segment of the DTA was cultured under high steady pressure (HPr, 150 mmHg) with the Src inhibitor PP1 (10 μM), while the other segment was under low steady pressure (LPr, 80 mmHg) for short-term (6 h). Flow was the same (20 ml/min). The p27 protein levels were similar between the low and high pressure groups. The error bar indicates SE of 4 independent experiments**.**

However, long-term (24 h) high steady pressure significantly reduced the p27 protein level (0.49±0.13-flod, $P<0.05$, Figure 4-27). Similarly, long-term (24 h) high mean pressure with pulsatility reduced the protein level of p27 (0.56±0.11-fold, n=3, $P=0.056$, Figure 4-28). Therefore, long-term (24 h) high pressure downregulates the protein level of p27. This regulation pattern is not altered by pressure pulsatility. It is thus expected that cells cultured under high pressure for 24 h have a stronger tendency of proliferating compared with those under low pressure.

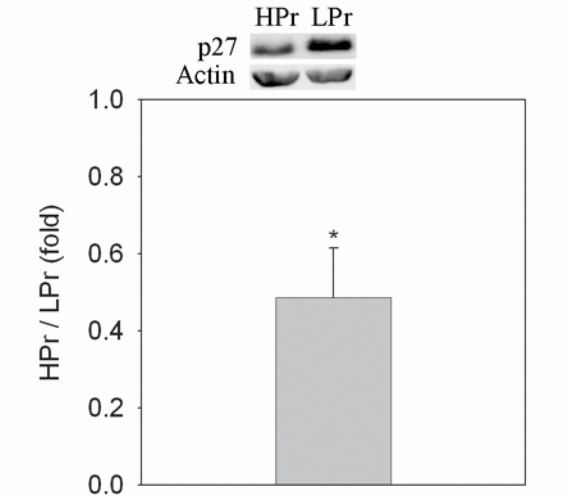

Figure 4-27 Long-term (24 h) regulation of the p27 protein level by steady pressure.

One segment of the DTA was cultured under high steady pressure (HPr, 150 mmHg), while the other segment was under low steady pressure (LPr, 80 mmHg) for long-term (24 h). Flow was the same (20 ml/min). The protein levels of p27 were significantly decreased by long-term high pressure. Error bars indicate SE of 5 independent experiments.

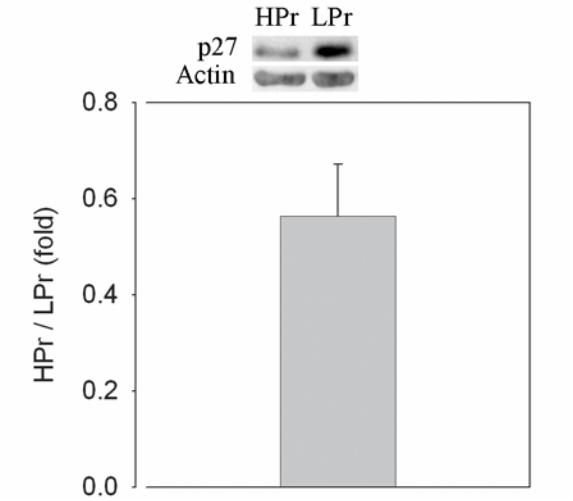

Figure 4-28 Long-term (24 h) regulation of the p27 protein level by mean pressure in the presence of pressure pulsatility.

One segment of the DTA was cultured under high pulsatile pressure (HPr, mean pressure 150 mmHg, pulse pressure 30 mmHg, 192 cycles/min), while the other segment was under low pulsatile pressure (LPr, mean pressure 80 mmHg, pulse pressure 30 mmHg, 192 cycles/min) for long-term (24 h). Mean flow was the same (25 ml/min). The protein levels of p27 were decreased by long-term high pressure although it was not statistically significant. Error bars indicate SE of 3 independent experiments.

Other molecules-beta-catenin. Wnt proteins are a large family of secreted polypeptides that regulate cell-cell interactions both during embryogenesis and in adults. Beta-catenin is an important protein in the Wnt signaling pathway. Beta-catenin was involved in upregulation of Cx43 by Wnt in cardiac myocytes.[342] Tyrosine phosphorylation of beta-catenin was increased by integrin, one of the sensors for mechanical forces.[334] Therefore, the protein level of beta-catenin was quantified by Western blot to explore whether beta-catenin protein levels were altered by mechanical factors. The protein levels of beta-catenin were similar between these two pressure levels for short-term cultures (1.1±0.18-fold, Figure 4-29). Therefore, the protein level of beta-catenin is not regulated by the short-term (6 h) pressure level.

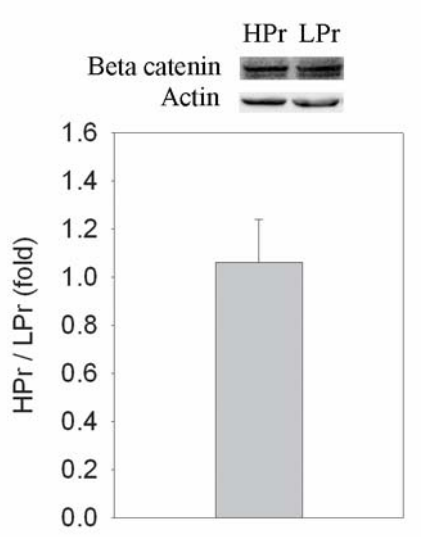

Figure 4-29 Short-term (6 h) regulation of the beta-catenin protein level by steady pressure.

One segment of the DTA was cultured under high steady pressure (HPr, 150 mmHg), while the other segment was under low steady pressure (LPr, 80 mmHg) for short-term (6 h). Flow was the same (20 ml/min). The beta-catenin protein levels were similar between the low and high pressure groups. The error bar indicates SE of 5 independent experiments.

Other molecules-CD31. The glycoprotein CD31 (or PECAM-1) mediates intercellular junctions between ECs. CD31 was also a mechanosensor.[343] The level of CD31 may indicate the

integrity of the endothelium as well. The CD31 protein levels were not different between these two steady pressure levels at 24 h (Figure 4-30). Therefore, the protein level of CD31 is not differentially regulated by the long-term (24 h) steady pressure level.

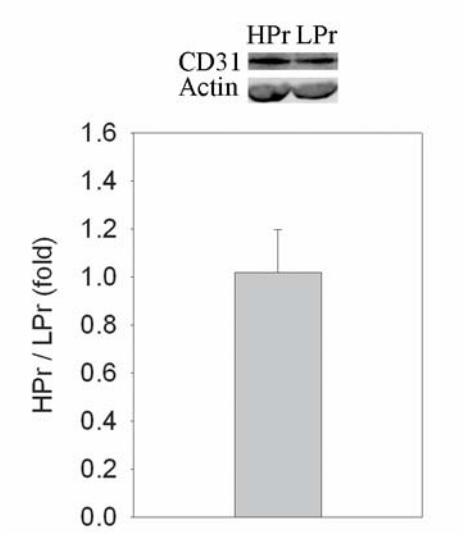

Figure 4-30 Long-term (24 h) regulation of the CD31 protein level by steady pressure.

One segment of the DTA was cultured under high steady pressure (HPr, 150 mmHg), while the other segment was under low steady pressure (LPr, 80 mmHg) for long-term (24 h). Flow was the same (20 ml/min). The CD31 protein levels were similar between the low and high pressure groups. The error bar indicates SE of 5 independent experiments.

Other molecules-Akt. Protein kinase B (PKB) or Akt can be activated by static stretch in VSMCs *in vitro*.[344] In an effort of identifying signaling molecules transducing mechanical forces in intact aortas, protein levels of active (phosphor-Ser473) and total Akt were quantified using Western blot. Akt was strongly activated by long-term (24 h) high mean pressure compared with low mean pressure (3.74±0.58-fold, n=3, $P<0.05$, Figure 4-31). However, the total Akt protein levels were similar between these two groups (0.97±0.14-fold). Moreover, the ratio of active to total Akt was significantly increased by high mean pressure (3.87±0.21-fold, $P<0.01$). Therefore,

high pressure regulates Akt through increasing the activation of Akt without affecting the total protein level of Akt.

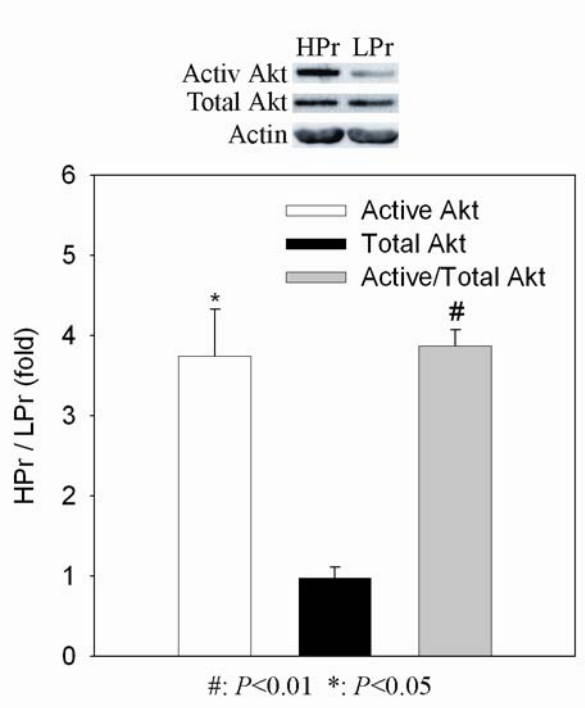

Figure 4-31 Long-term (24 h) regulation of Akt by mean pressure in the presence of pressure pulsatility.

One segment of the DTA was cultured under high pulsatile pressure (HPr, mean pressure 150 mmHg, pulse pressure 30 mmHg, 192 cycles/min), while the other segment was under low pulsatile pressure (LPr, mean pressure 80 mmHg, pulse pressure 30 mmHg, 192 cycles/min) for long-term (24 h). Mean flow was the same (25 ml/min). The levels of active Akt were increased by long-term high pressure, although the levels of total Akt were similar. The ratios of active to total Akt were also increased by long-term high pressure. Error bars indicate SE of 3 independent experiments.

In summary, both short- (6 h) and long-term (24 h) high steady pressures upregulate the mRNA level of Cx43. The protein level of Cx43 is also elevated by short-term high steady pressure. Src may regulate the increases in both mRNA and protein of Cx43 by short-term high steady pressure. Long-term high steady pressure does not increase the protein level of Cx43. This regulation pattern is the same in the presence of pressure pulsatility. Intraluminal flow also does

not alter this pattern. The mRNA level of Cx40 is not differentially regulated by steady pressure levels. Cells have a stronger tendency of proliferation after 24 h high pressure cultures. More Akt is activated by high pressure.

4.3 REGULATION OF GAP JUNCTIONS BY CYCLIC STRETCH INDUCED BY PULSATILE PRESSURE

4.3.1 Regulation of gap junction expression by pulsatile pressure

Arteries are cyclically stretched by pulsatile pressure. The level of stretch depends on the compliance of a blood vessel, the mean blood pressure, and pulse pressure. The compliance of a blood vessel can be altered by hypertension, aging, etc. Cyclic stretch is important to vascular structure and function. However, the mechanisms of transducing cyclic stretch into biochemical signals by vascular cells are not well understood. Aortic segments from the same rabbit were cultured under pulsatile (pulse pressure 30 mmHg, mean pressure 80 mmHg, mean flow 25 ml/min, 192 cycles/min) or steady (80 mmHg) pressure to study regulation of gap junctions by pulsatile pressure.

Aortas under pulsatile pressure (Pul) had similar Cx43 mRNA levels to those under steady pressure (Ste) (0.74±0.15-fold, P=0.183, Figure 4-32) at 6 h. However, pulsatile pressure unexpectedly decreased the Cx43 total protein level at 6 h (0.63±0.05-fold, P<0.01). Aortas under pulsatile pressure had a larger ratio of phosphorylated to non-phosphorylated Cx43 (2.03±0.43-fold, P<0.05, Figure 4-33).

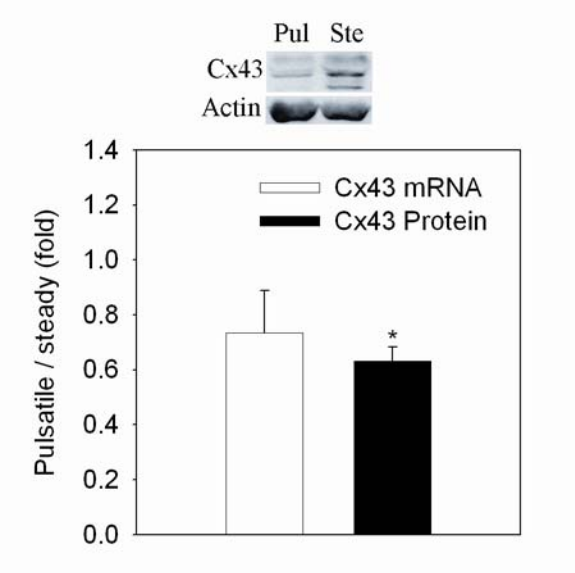

Figure 4-32 Short-term (6 h) regulation of Cx43 expression by pulsatile pressure.

One segment of the DTA was cultured under pulsatile pressure (Pul, mean pressure 80 mmHg, pulse pressure 30 mmHg, 192 cycles/min), while the other segment was under steady pressure (Ste, mean pressure 80 mmHg, pulse pressure 0 mmHg) for short-term (6 h). Mean flow was the same (25 ml/min). The Cx43 mRNA levels were not significantly altered by short-term pulsatile pressure. However, the Cx43 protein levels were significantly decreased by short-term pulsatile pressure. Error bars indicate SE of 5 independent experiments.

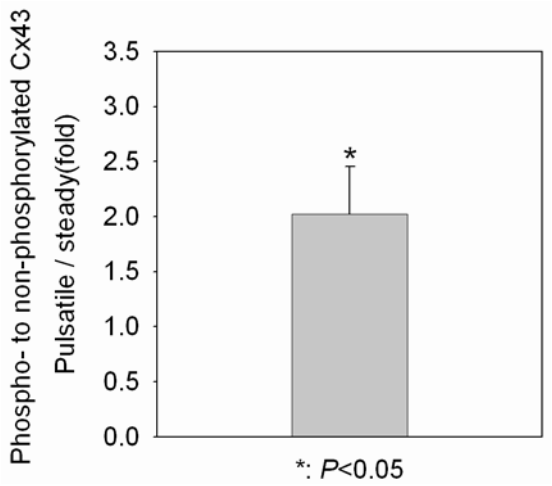

Figure 4-33 Short-term (6 h) regulation of Cx43 phosphorylation by pulsatile pressure.

One segment of the DTA was cultured under pulsatile pressure (Pul, mean pressure 80 mmHg, pulse pressure 30 mmHg, 192 cycles/min), while the other segment was under steady pressure (Ste, mean pressure 80 mmHg, pulse pressure 0 mmHg) for short-term (6 h). Mean flow was the same (25 ml/min). The ratios of phosphorylated to non-phosphorylated Cx43 were significantly increased by short-term pulsatile pressure. The error bar indicates SE of 5 independent experiments.

Aortas were cultured for 24 h under the same conditions. Although the level of mRNA was increased slightly by pulsatile pressure at 24 h (1.63±0.45-fold, Figure 4-34), pulsatile pressure decreased the Cx43 protein level (0.49±0.09-fold, $P<0.01$). There were no significant differences in the ratios of phosphorylated to non-phosphorylated Cx43 protein (1.20±0.41-fold, Figure 4-35). Therefore, pulsatile pressure reduces the Cx43 protein level for both short- and long-term cultures. The decreased Cx43 protein level is not because of the decreased Cx43 mRNA level. The relative level of phosphorylated to non-phosphorylated Cx43 is differentially regulated by short- and long-term pulsatile pressures.

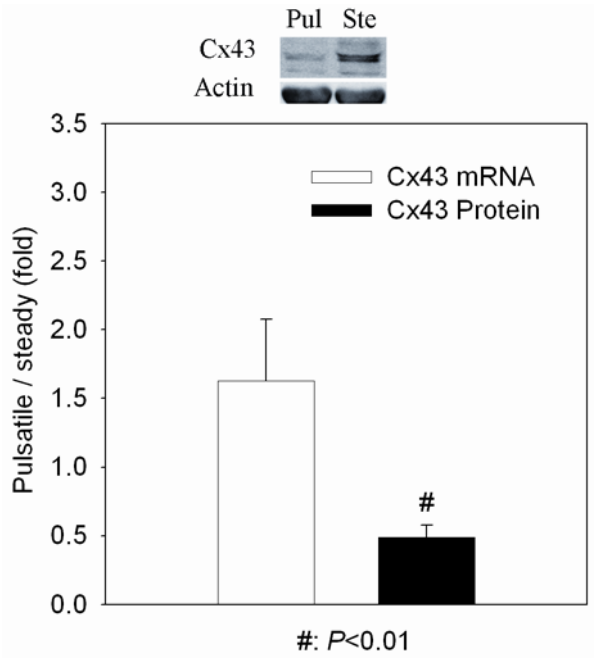

Figure 4-34 Long-term (24 h) regulation of Cx43 expression by pulsatile pressure.

One segment of the DTA was cultured under pulsatile pressure (Pul, mean pressure 80 mmHg, pulse pressure 30 mmHg, 192 cycles/min), while the other segment was under steady pressure (Ste, mean pressure 80 mmHg, pulse pressure 0 mmHg) for long-term (24 h). Mean flow was the same (25 ml/min). The Cx43 mRNA levels were not significantly altered by long-term pulsatile pressure. However, the Cx43 protein levels were significantly decreased by long-term pulsatile pressure. Error bars indicate SE of 5 independent experiments.

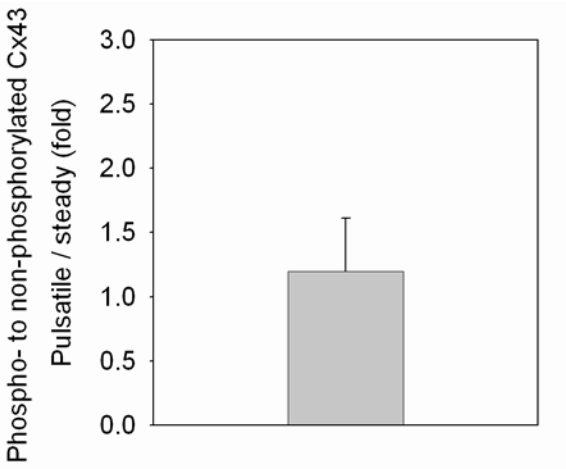

Figure 4-35 Long-term (24 h) regulation of Cx43 phosphorylation by pulsatile pressure.

One segment of the DTA was cultured under pulsatile pressure (Pul, mean pressure 80 mmHg, pulse pressure 30 mmHg, 192 cycles/min), while the other segment was under steady pressure (Ste, mean pressure 80 mmHg, pulse pressure 0 mmHg) for long-term (24 h). Mean flow was the same (25 ml/min). The ratios of phosphorylated to non-phosphorylated Cx43 were not significantly altered by long-term pulsatile pressure. The error bar indicates SE of 5 independent experiments.

4.3.2 Regulation of Cx43 expression by long-term pulsatile pressure with a higher mean pressure – cyclic stretch regulates Cx43 expression

The wall stress of arteries is changing cyclically under pulsatile pressure as well. To differentiate the effect of cyclic deformation in diameter (cyclic stretch) from cyclic change in wall stress (cyclic stress), both aortas from the same rabbit were cultured under a higher mean pressure (150 versus 80 mmHg) for 24 h. The pulse pressure was the same (30 mmHg). Aortas had less cyclic stretch under a higher mean pressure (150) because of the nonlinear mechanical property of arteries.[15] The Cx43 mRNA and protein levels were similar between pulsatile and steady perfusion conditions, respectively (Figure 4-36). Therefore, it was the cyclic stretch, instead of cyclic stress, that decreased the Cx43 protein level (Figure 4-34). The relative levels of phosphorylated to non-phosphorylated Cx43 were not significantly different (1.39±0.27-fold,

Figure 4-37). Thus, long-term (24 h) pulsatile pressure does not differentially regulate the ratio of phosphorylated to non-phosphorylated Cx43 compared with steady pressure (stretch).

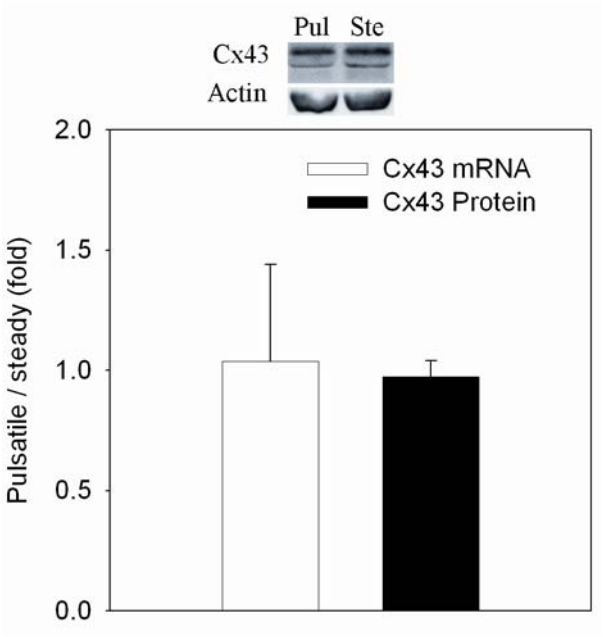

Figure 4-36 Long-term (24 h) regulation of Cx43 expression by pulsatile pressure under a higher mean pressure (150 mmHg).

One segment of the DTA was cultured under pulsatile pressure (Pul, mean pressure 150 mmHg, pulse pressure 30 mmHg, 192 cycles/min), while the other segment was under steady pressure (Ste, the same mean pressure 150 mmHg, pulse pressure 0 mmHg) for long-term (24 h). Mean flow was the same (25 ml/min). The Cx43 mRNA and protein levels were not significantly different between these two culture conditions. Error bars indicate SE of 3 independent experiments.

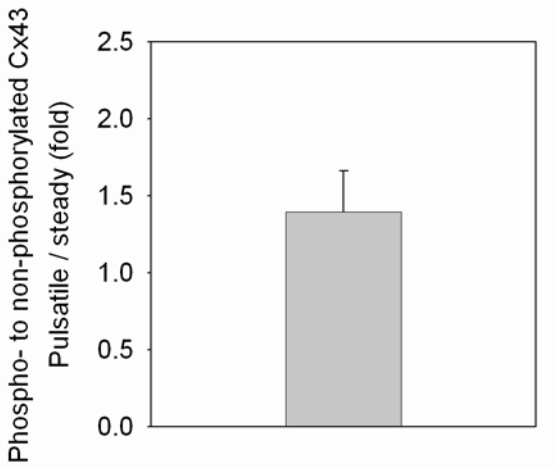

Figure 4-37 Long-term (24 h) regulation of Cx43 phosphorylation by pulsatile pressure under a higher mean pressure (150 mmHg).

One segment of the DTA was cultured under pulsatile pressure (Pul, mean pressure 150 mmHg, pulse pressure 30 mmHg, 192 cycles/min), while the other segment was under steady pressure (Ste, the same mean pressure 150 mmHg, pulse pressure 0 mmHg) for long-term (24 h). Mean flow was the same (25 ml/min). The ratios of phosphorylated to non-phosphorylated Cx43 protein were not significantly different between these two culture conditions. The error bar indicates SE of 3 independent experiments.

4.3.3 Potential mechanisms underlying the regulation of Cx43 by cyclic stretch

Src regulation. Levels of active and total Src were quantified using Western blot to study whether Src was regulated differentially by pulsatile pressure compared to steady pressure. For short-term (6 h) cultures, active (1.11±0.21-fold) and total (1.03±0.08-fold) Src levels and the ratio of the two (active/total) were not different between the pulsatile and steady pressure groups (Figure 4-38). Therefore, Src is not differentially regulated by steady pressure (Figure 4-20) or pulsatile pressure for the short-term (6 h) culture duration. In contrast, active Src was less for pulsatile pressure (0.65±0.06-fold, $P<0.01$, Figure 4-39) in long-term (24 h) cultures. Total Src was also decreased (0.70±0.07-fold, $P<0.05$). The ratios of active to total Src were similar. Therefore, pulsatile pressure regulates Src by reducing the active and total Src without changing

the ratio of these two. However, active and total Src, and the ratios of these two were not significantly different between aortas cultured under the pulsatile pressure with a higher mean pressure (150 mmHg) and the same level of steady pressure (Figure 4-40). Hence, it is the cyclic stretch, instead of cyclic stress, that decreases the active and total protein levels of Src at 24 h (Figure 4-39).

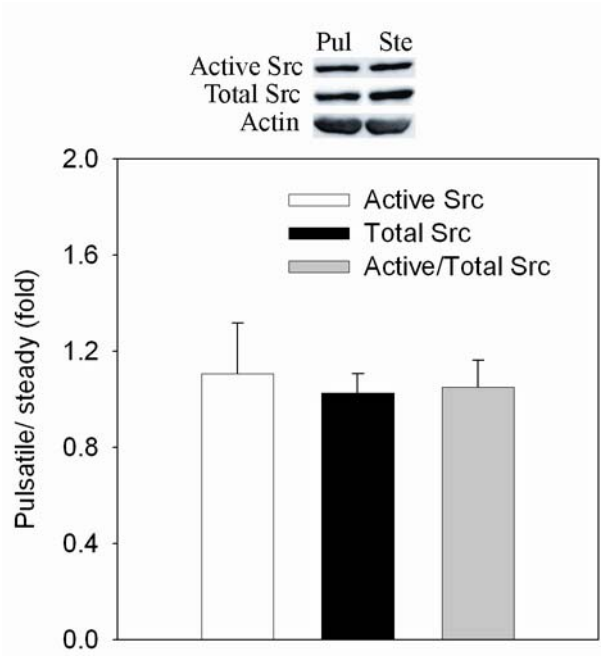

Figure 4-38 Short-term (6 h) regulation of Src by pulsatile pressure.

One segment of the DTA was cultured under pulsatile pressure (Pul, mean pressure 80 mmHg, pulse pressure 30 mmHg, 192 cycles/min), while the other segment was under steady pressure (Ste, mean pressure 80 mmHg, pulse pressure 0 mmHg) for short-term (6 h). Mean flow was the same (25 ml/min). The levels of active and total Src, and the ratios of these two were not different between these two culture conditions. Error bars indicate SE of 5 independent experiments.

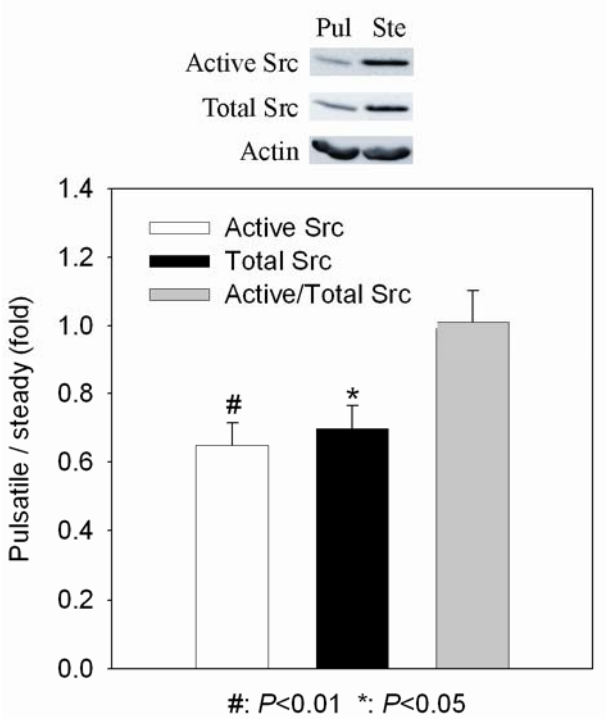

Figure 4-39 Long-term (24 h) regulation of Src by pulsatile pressure.

One segment of the DTA was cultured under pulsatile pressure (Pul, mean pressure 80 mmHg, pulse pressure 30 mmHg, 192 cycles/min), while the other segment was under steady pressure (Ste, mean pressure 80 mmHg, pulse pressure 0 mmHg) for long-term (24 h). Mean flow was the same (25 ml/min). The levels of active and total Src were significantly reduced by pulsatile pressure. However, the ratios of these two were not different between these two culture conditions. Error bars indicate SE of 5 independent experiments.

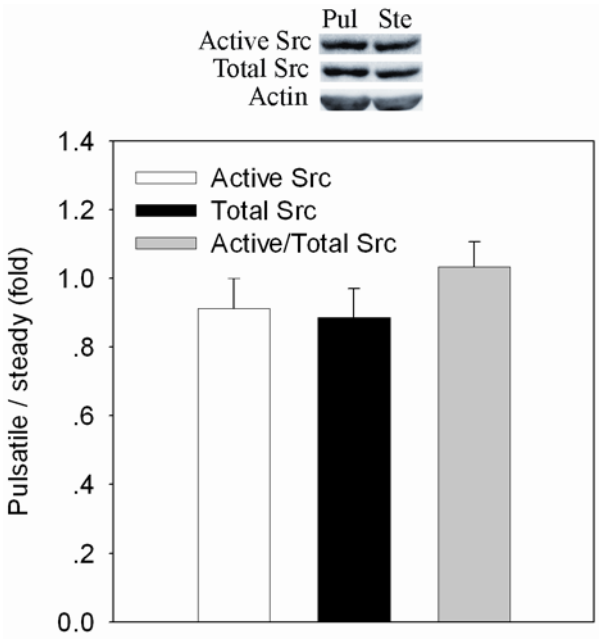

Figure 4-40 Long-term (24 h) regulation of Src by pulsatile pressure under a higher mean pressure (150 mmHg).

One segment of the DTA was cultured under pulsatile pressure (Pul, mean pressure 150 mmHg, pulse pressure 30 mmHg, 192 cycles/min), while the other segment was under steady pressure (Ste, the same mean pressure 150 mmHg, pulse pressure 0 mmHg) for long-term (24 h). Mean flow was the same (25 ml/min). The levels of active and total Src, and the ratios of these two were not different between these two culture conditions. Error bars indicate SE of 3 independent experiments.

Experiments with Src inhibition. We observed differential regulation Cx43 and Src by long-term (24 h) cyclic stretch. Because there was more active Src in aortas cultured under steady pressure (80 mmHg), the Src kinase inhibitor PP1 (10 μM) was added to the culture media of steady pressure cultures for 24 h at the onset of culturing to study the role of Src in mediating the regulation of Cx43 by cyclic stretch. There was more Cx43 mRNA (2.82±0.56-flod, $P<0.05$, Figure 4-41) in aortas cultured under cyclic stretch after Src inhibition. However, Cx43 protein was no longer significantly less after Src inhibition (0.72±0.14-fold, $P=0.135$). Thus, Src may mediate downregulation of Cx43 protein by cyclic stretch. Active Src was still less under cyclic stretch after Src inhibition (0.68±0.08-flod, $P<0.05$). Total Src was less as well (0.74±0.08-flod,

P=0.05). The ratios of active to total Src were similar. Therefore, long-term (24 h) inhibition of Src using PP1 does not alter the levels of active and total Src. It inhibits the function of Src. The ratios of phosphorylated to non-phosphorylated Cx43 were still similar after Src inhibition (Figure 4-42). Therefore, Src does not regulate the relative ratio of phosphorylated to non-phosphorylated Cx43 between long-term (24 h) pulsatile and steady pressure cultures.

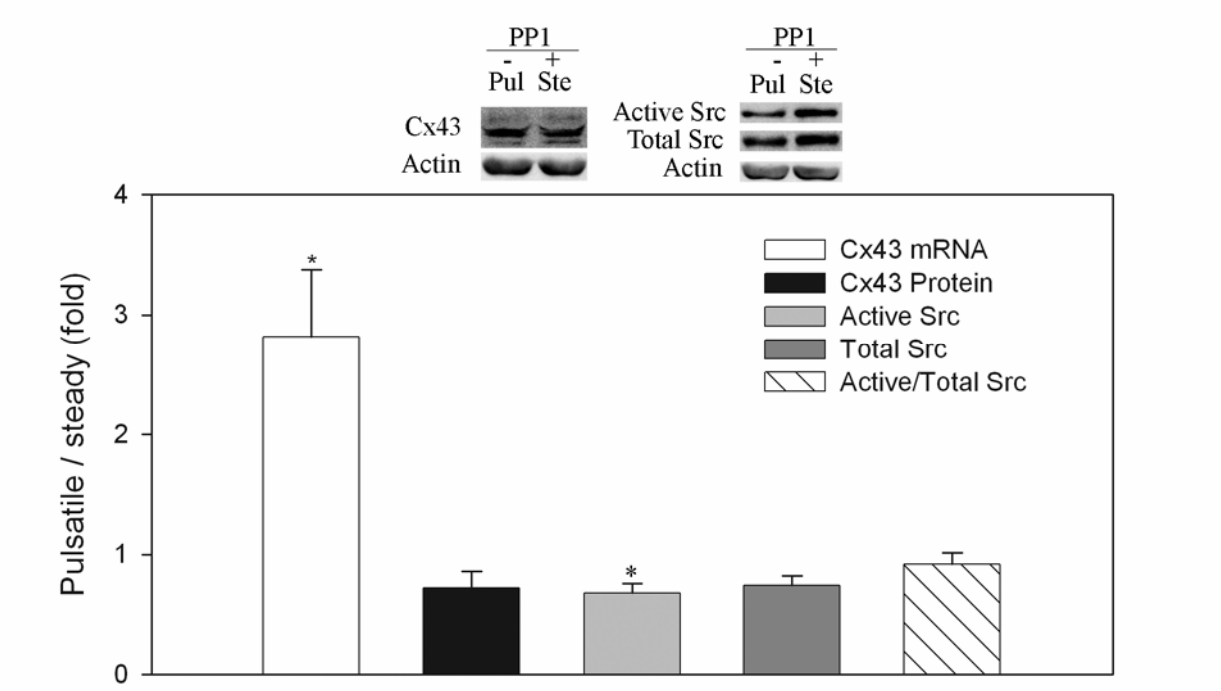

Figure 4-41 Src may regulate downregulation of the Cx43 protein level by cyclic stretch.

One segment of the DTA was cultured under pulsatile pressure (Pul, mean pressure 80 mmHg, pulse pressure 30 mmHg, 192 cycles/min), while the other segment was under steady pressure (Ste, mean pressure 80 mmHg, pulse pressure 0 mmHg) with the Src inhibitor PP1 (10 μM) for long-term (24 h). Mean flow was the same (25 ml/min). The Cx43 mRNA levels were higher in aortas under cyclic stretch after Src inhibition. However, the Cx43 protein levels were similar. The active Src was still less in aortas under cyclic stretch after Src inhibition. The total Src was less as well. Error bars indicate SE of 4 independent experiments.

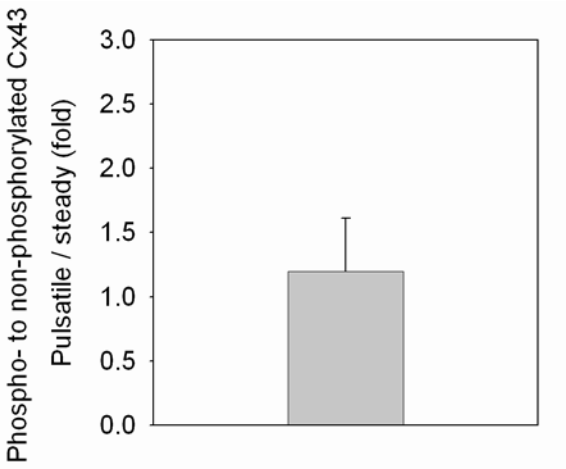

Figure 4-42 Long-term (24 h) regulation of Cx43 phosphorylation by cyclic stretch after inhibition of Src in aortas cultured under steady pressure.

One segment of the DTA was cultured under pulsatile pressure (Pul, mean pressure 80 mmHg, pulse pressure 30 mmHg, 192 cycles/min), while the other segment was under steady pressure (Ste, mean pressure 80 mmHg, pulse pressure 0 mmHg) with the Src inhibitor PP1 (10 μM) for long-term (24 h). Mean flow was the same (25 ml/min).The ratios of phosphorylated to non-phosphorylated Cx43 were similar. Error bars indicate SE of 4 independent experiments.

Experiments with Reactive oxygen species inhibition. ROS mediated the regulation of Cx43 by static stretch in VSMCs.[315] Aortas cultured under pulsatile perfusion had more ROS compared to those under steady perfusion.[87] Therefore, ROS may mediate the differential regulation of Cx43 protein by cyclic and steady stretch. NADPH oxidase is the major enzyme that generates ROS in arteries. The NADPH oxidase inhibitor apocynin was planned to be used in this study. However, apocynin has been reported to have actually increased ROS in vascular fibroblasts.[340] Levels of superoxide in rabbit aortic rings were thus measured using an L-012 enhanced chemiluminescence method to test whether apocynin had the same effect on whole blood vessels. AngII has been known to increase superoxide production. The counts were increased following AngII addition to the buffer (Figure 4-43A). SOD can reduce the superoxide level, which was verified in a segment of rabbit aorta (Figure 4-43B). Therefore, we could

successfully measure ROS using our protocol. Apocynin (0.4 mM) immediately reduced the superoxide production (Figure 4-43C). This effect lasted for the measurement duration (75 minutes). Therefore, apocynin is indeed an inhibitor of ROS. Apocynin (0.4 mM) was then added to the media of pulsatile perfusion at the onset of culturing for 24 h to elucidate the role of ROS in mediating the regulation of Cx43 by stretch. The Cx43 mRNA levels were not significantly different after inhibition (0.70±0.22-fold, Figure 4-44). The levels of Cx43 protein were also similar to the controls after ROS inhibition (0.90±0.2-fold). Thus, inhibition of ROS using apocynin increased the Cx43 protein level in aortas with cyclic stretch. Downregulation of the Cx43 protein level by long-term cyclic stretch may be mediated by ROS. Furthermore, inhibition of ROS elevated the ratio of phosphorylated to non-phosphorylated Cx43 in aortas with cyclic stretch (1.57±0.12-flod, $P<0.05$, Figure 4-45). Thus, a certain level of ROS is needed to maintain a similar level of phosphorylated Cx43 (Figure 4-35). Active Src was also increased in aortas under cyclic stretch by apocynin at 24 h, leading to a similar level of active Src (Figure 4-44). The levels of total Src were similar as well. Again, there were no significant differences in the ratios of active to total Src (1.45±0.41-fold). Therefore, we observed interactions between ROS and Src. The elevated level of ROS in aortas under cyclic stretch may decrease the levels of active and total Src compared with aortas under steady stretch.

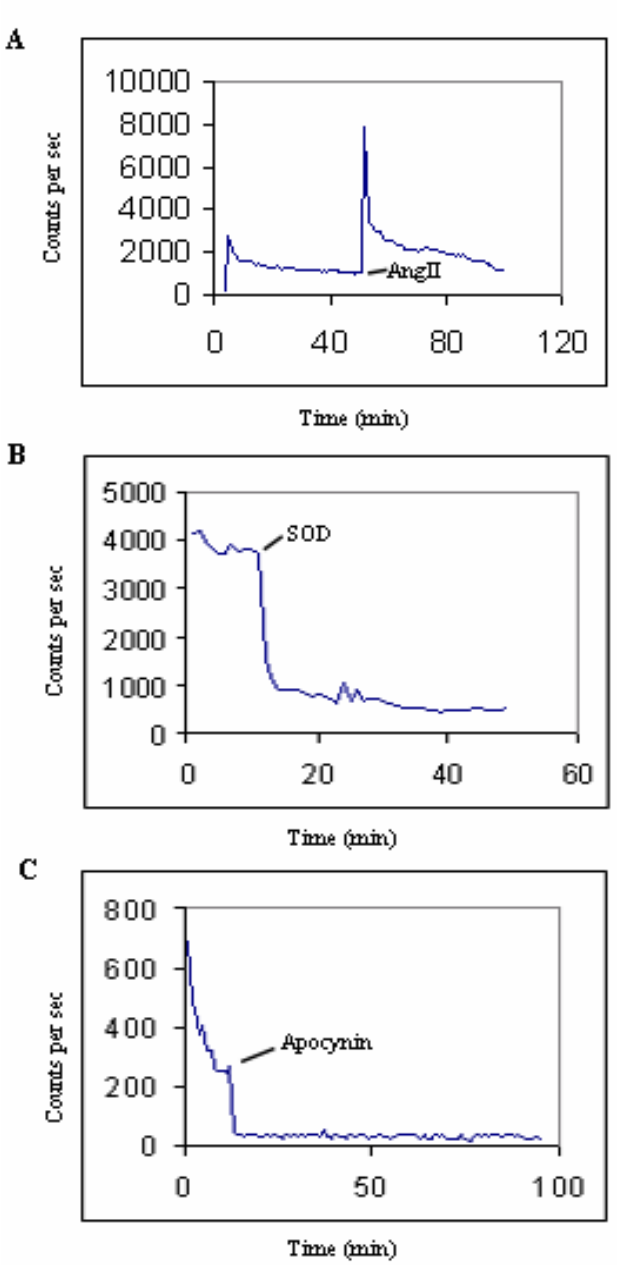

Figure 4-43 Superoxide measurement using L-012 in aortic rings.

The production of superoxide in aortas was increased after addition of AngII, decreased after addition of SOD. Apocynin (0.4 mM) also suppressed production of superoxide.

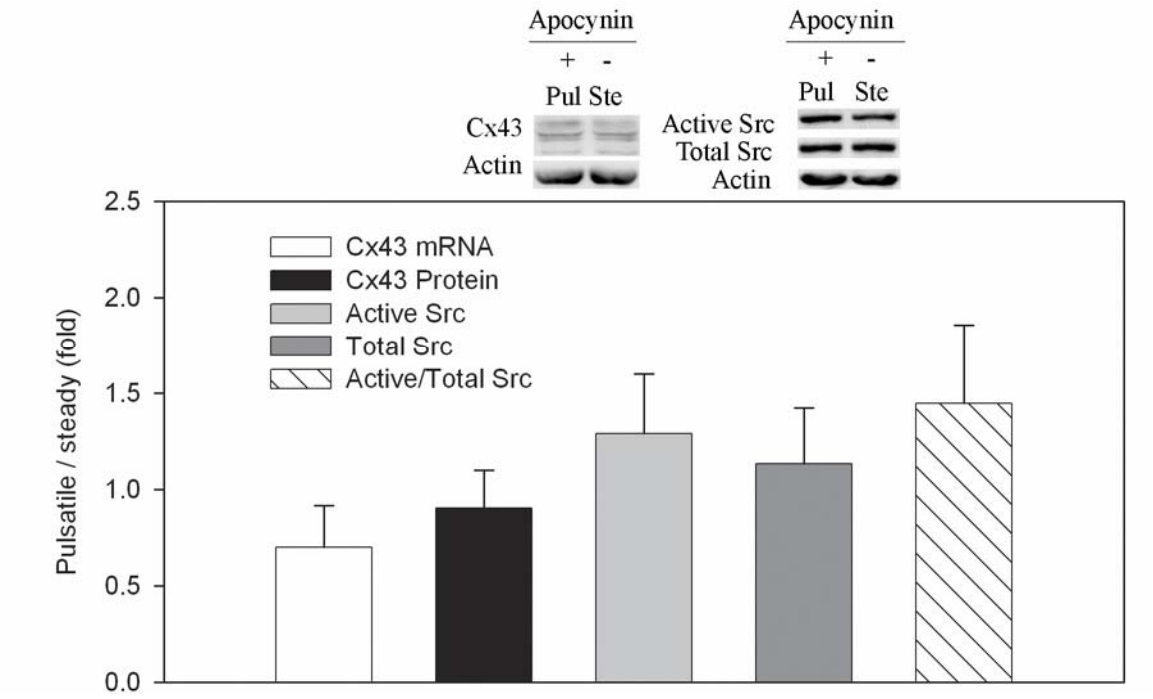

Figure 4-44 Reactive oxygen species may mediate regulation of Cx43 by long-term (24 h) cyclic stretch.

One segment of the DTA was cultured under pulsatile pressure (Pul, mean pressure 80 mmHg, pulse pressure 30 mmHg, 192 cycles/min) with the ROS inhibitor apocynin (0.4 mM), while the other segment was under steady pressure (Ste, mean pressure 80 mmHg, pulse pressure 0 mmHg) for long-term (24 h). Mean flow was the same (25 ml/min).The mRNA and protein levels of Cx43 were not significantly different. The levels of active and total Src, and the ratio of these two were similar as well after ROS inhibition. Error bars indicate SE of 4 independent experiments.

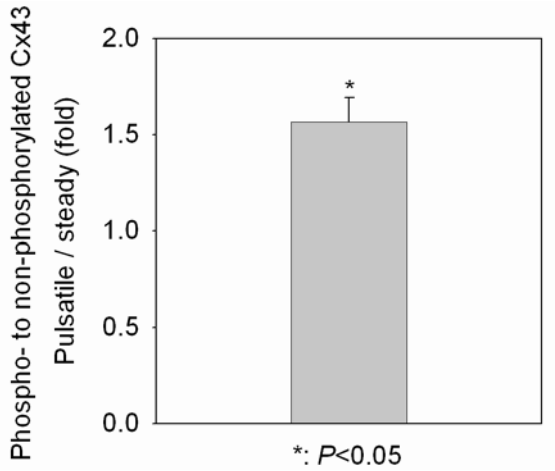

Figure 4-45 Reactive oxygen species may mediate regulation of Cx43 phosphorylation by long-term (24 h) cyclic stretch.

One segment of the DTA was cultured under pulsatile pressure (Pul, mean pressure 80 mmHg, pulse pressure 30 mmHg, 192 cycles/min) with the ROS inhibitor apocynin (0.4 mM), while the other segment was under steady pressure (Ste, mean pressure 80 mmHg, pulse pressure 0 mmHg) for long-term (24 h). Mean flow was the same (25 ml/min). The ratios of phosphorylated to non-phosphorylated Cx43 were increased in aortas under cyclic stretch and ROS inhibition. The error bar indicates SE of 4 independent experiments.

The effect of increasing the Cx43 protein level by apocynin was further studied by adding apocynin (0.4 mM) to aortas cultured in a relaxed state (without intraluminal pressure and flow) for 6 h. Apocycin significantly increased the Cx43 protein level (1.88±0.16-flod, $P<0.05$, Figure 4-46). Active and total Src, and the ratio of these two were not different for this short duration, which was the same as short-term (6 h) steady pressure (Figure 4-20) and pulsatile pressure (Figure 4-38) cultures.

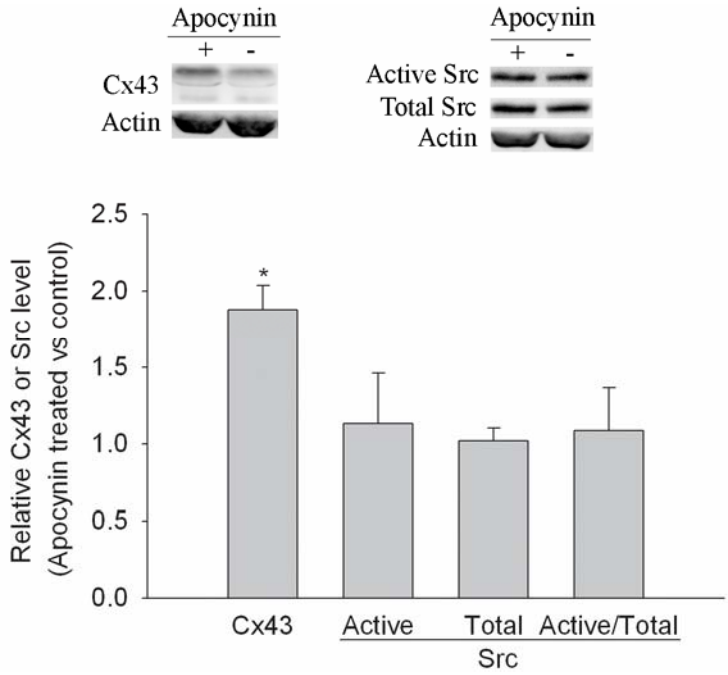

Figure 4-46 Apocynin increases the Cx43 protein level in relaxed aortas at 6 h.

Apocynin (0.4 mM) was added to aortas cultured in a relaxed state for 6 h. Apocycin significantly increased the Cx43 protein level. Active and total Src, and the ratio of these two were not different. Error bars indicate SE of 3 independent experiments.

Other molecules-p27. The protein levels of p27 were quantified using Western blot to study whether there was a difference in proliferation between aortas cultured under pulsatile and steady stretch. There were no differences in the p27 protein levels between aortas under cyclic and steady stretch for short-term (6 h) (1.04±0.13-fold, Figure 4-47) or long-term (24 h) (1.08±0.11-fold, Figure 4-48) cultures. Inhibition of Src using PP1 in the media for aortas with steady stretch for 24 h did not alter the relative level of p27 protein (0.92±0.11-flod, Figure 4-49) as well. Therefore, the p27 protein level is not differentially regulated by any of these culture conditions. The proliferation status does not account for the difference in Cx43 protein expression between aortas cultured under pulsatile and steady stretch for up to 24 h.

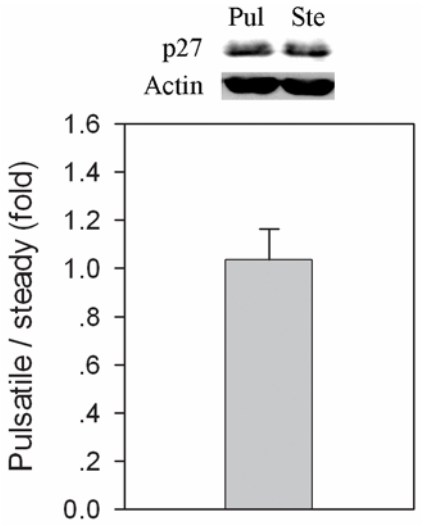

Figure 4-47 Short-term (6 h) regulation of the p27 protein level by cyclic stretch.

One segment of the DTA was cultured under pulsatile pressure (Pul, mean pressure 80 mmHg, pulse pressure 30 mmHg, 192 cycles/min), while the other segment was under steady pressure (Ste, mean pressure 80 mmHg, pulse pressure 0 mmHg) for short-term (6 h). Mean flow was the same (25 ml/min). The p27 protein levels were similar. The error bar indicates SE of 5 independent experiments.

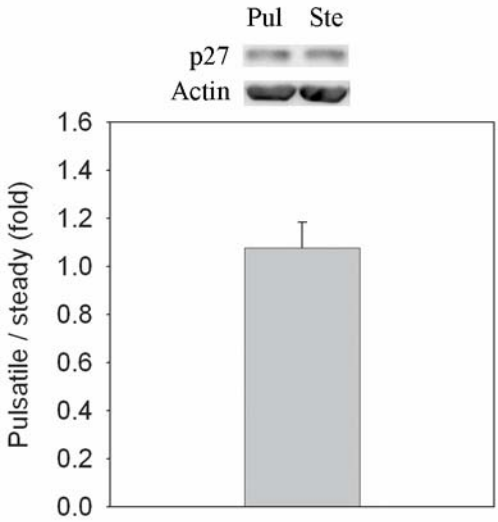

Figure 4-48 Long-term (24 h) regulation of the p27 protein level by cyclic stretch.

One segment of the DTA was cultured under pulsatile pressure (Pul, mean pressure 80 mmHg, pulse pressure 30 mmHg, 192 cycles/min), while the other segment was under steady pressure (Ste, mean pressure 80 mmHg, pulse pressure 0 mmHg) for long-term (24 h). Mean flow was the same (25 ml/min). The p27 protein levels were similar. The error bar indicates SE of 5 independent experiments.

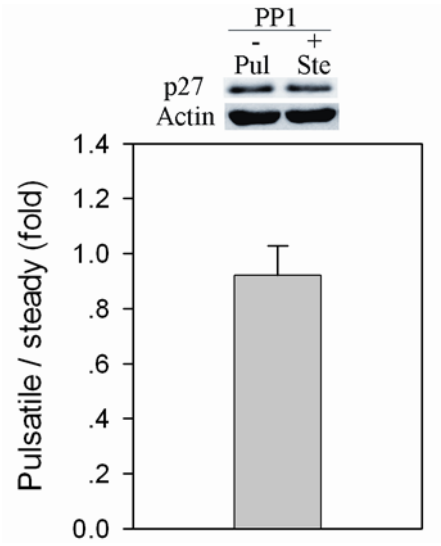

Figure 4-49 Inhibition of Src in aortas under steady stretch for 24 h does not alter the relative level of p27 protein.

One segment of the DTA was cultured under pulsatile pressure (Pul, mean pressure 80 mmHg, pulse pressure 30 mmHg, 192 cycles/min), while the other segment was under steady pressure (Ste, mean pressure 80 mmHg, pulse pressure 0 mmHg) with the Src inhibitor PP1 (10 μM) for long-term (24 h). Mean flow was the same (25 ml/min). The p27 protein levels were similar. The error bar indicates SE of 4 independent experiments.

Other molecules-beta-catenin. The protein levels of beta-catenin were quantified using Western blot to study whether beta-catenin was differentially regulated by cyclic and steady stretch at the total protein level. There were no differences in the beta-catenin protein levels between aortas under cyclic and steady stretch for short-term (6 h) (1.09±0.18-fold, Figure 4-50) or long-term (24 h) (1.06±0.07-fold, Figure 4-51) cultures. Inhibition of Src using PP1 in the media for aortas with steady stretch for 24 h did not alter the relative levels of beta-catenin (0.97±0.07-flod, Figure 4-52) as well. Therefore, the relative levels of beta-catenin protein are not differentially regulated by any of these culture conditions.

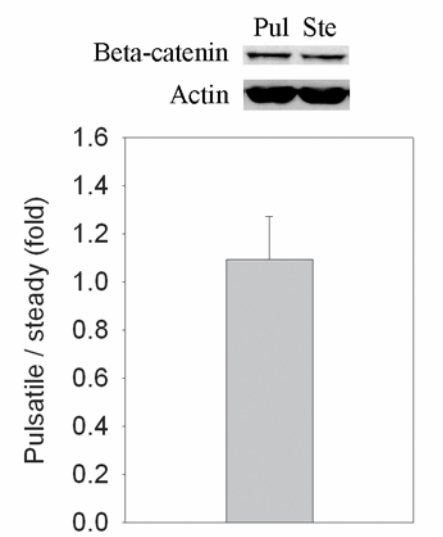

Figure 4-50 Short-term (6 h) regulation of the beta-catenin protein level by cyclic stretch.

One segment of the DTA was cultured under pulsatile pressure (Pul, mean pressure 80 mmHg, pulse pressure 30 mmHg, 192 cycles/min), while the other segment was under steady pressure (Ste, mean pressure 80 mmHg, pulse pressure 0 mmHg) for short-term (6 h). Mean flow was the same (25 ml/min). The beta-catenin protein levels were similar. The error bar indicates SE of 5 independent experiments.

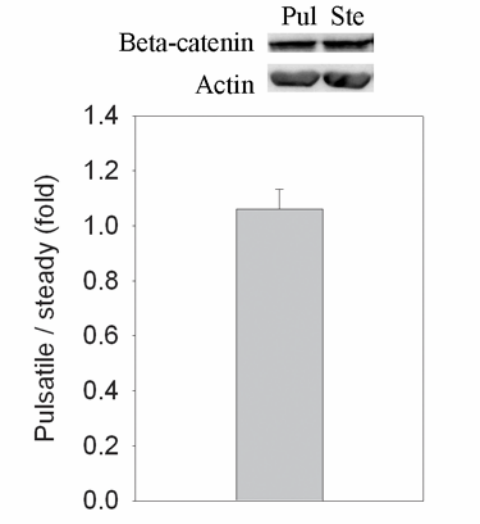

Figure 4-51 Long-term (24 h) regulation of the beta-catenin protein level by cyclic stretch.

One segment of the DTA was cultured under pulsatile pressure (Pul, mean pressure 80 mmHg, pulse pressure 30 mmHg, 192 cycles/min), while the other segment was under steady pressure (Ste, mean pressure 80 mmHg, pulse pressure 0 mmHg) for long-term (24 h). Mean flow was the same (25 ml/min). The beta-catenin protein levels were similar. The error bar indicates SE of 5 independent experiments.

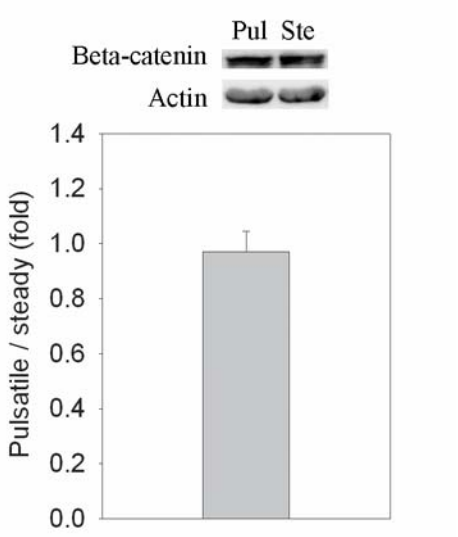

Figure 4-52 Inhibition of Src in aortas under steady stretch for 24 h does not alter the relative level of beta-catenin protein.

One segment of the DTA was cultured under pulsatile pressure (Pul, mean pressure 80 mmHg, pulse pressure 30 mmHg, 192 cycles/min), while the other segment was under steady pressure (Ste, mean pressure 80 mmHg, pulse pressure 0 mmHg) with the Src inhibitor PP1 (10 μM) for long-term (24 h). Mean flow was the same (25 ml/min). The beta-catenin protein levels were similar. The error bar indicates SE of 4 independent experiments.

Other molecules-Akt. Differential regulation of Akt by pulsatile and steady pressure in intact arteries has not been reported. Levels of active and total Akt were quantified by Western blot. Pulsatile pressure (mean 80 mmHg) for 6 h decreased the level of active Akt (0.47±0.14-fold, $P<0.05$, Figure 4-53). However, the levels of total Akt were not different (0.91±0.13-fold). Therefore, short–term (6 h) pulsatile pressure decreased the ratio of active Akt to total Akt (0.33±0.11-fold, $P<0.01$). Similarly, pulsatile pressure for long-term (24 h) cultures decreased active Akt (0.52±0.06-fold, $P<0.01$, Figure 4-54). Again, the levels of total Akt were not different (1.10±0.11-fold). Long-term pulsatile pressure thus decreased the ratio of active Akt to total Akt (0.44±0.03-fold, $P<0.001$). However, the levels of active Akt and the ratios of active to total Akt were no longer different when aortas were cultured for 24 h under a higher mean

pressure (150 mmHg) (Figure 4-55). As discussed before, aortas were cyclically stretched much less at this high mean pressure level by the same pulse pressure (30 mmHg). Therefore, it was cyclic stretch, instead of cyclic stress, that decreases Akt activation compared to steady stretch.

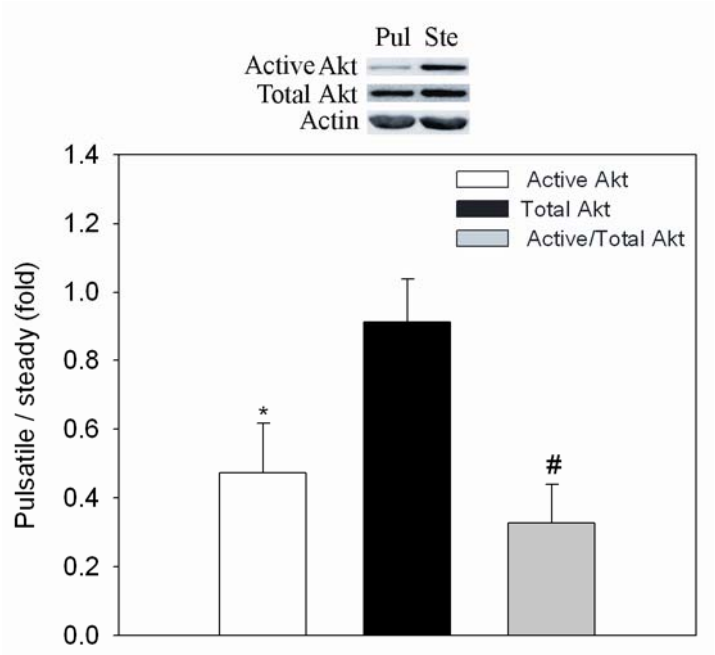

Figure 4-53 Short-term (6 h) regulation of Akt by cyclic stretch.

One segment of the DTA was cultured under pulsatile pressure (Pul, mean pressure 80 mmHg, pulse pressure 30 mmHg, 192 cycles/min), while the other segment was under steady pressure (Ste, mean pressure 80 mmHg, pulse pressure 0 mmHg) for short-term (6 h). Mean flow was the same (25 ml/min). The levels of active Akt were reduced by cyclic stretch. However, the levels of total Akt were similar. Thus, the ratios of active to total Akt were reduced by cyclic stretch. Error bars indicate SE of 5 independent experiments.

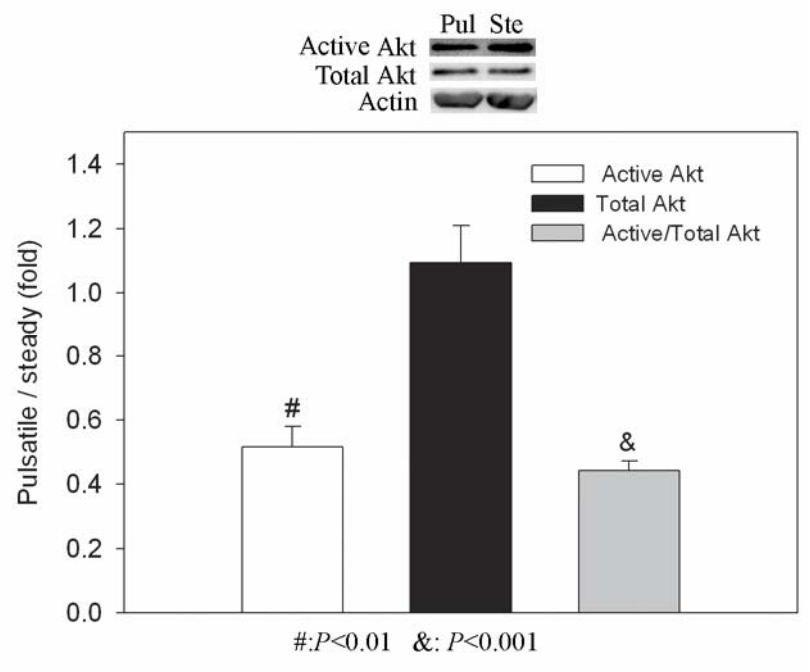

Figure 4-54 Long-term (24 h) regulation of Akt by cyclic stretch.

One segment of the DTA was cultured under pulsatile pressure (Pul, mean pressure 80 mmHg, pulse pressure 30 mmHg, 192 cycles/min), while the other segment was under steady pressure (Ste, mean pressure 80 mmHg, pulse pressure 0 mmHg) for long-term (24 h). Mean flow was the same (25 ml/min). The levels of active Akt were reduced cyclic stretch. However, the levels of total Akt were similar. Thus, the ratios of active to total Akt were reduced by cyclic stretch. Error bars indicate SE of 5 independent experiments.

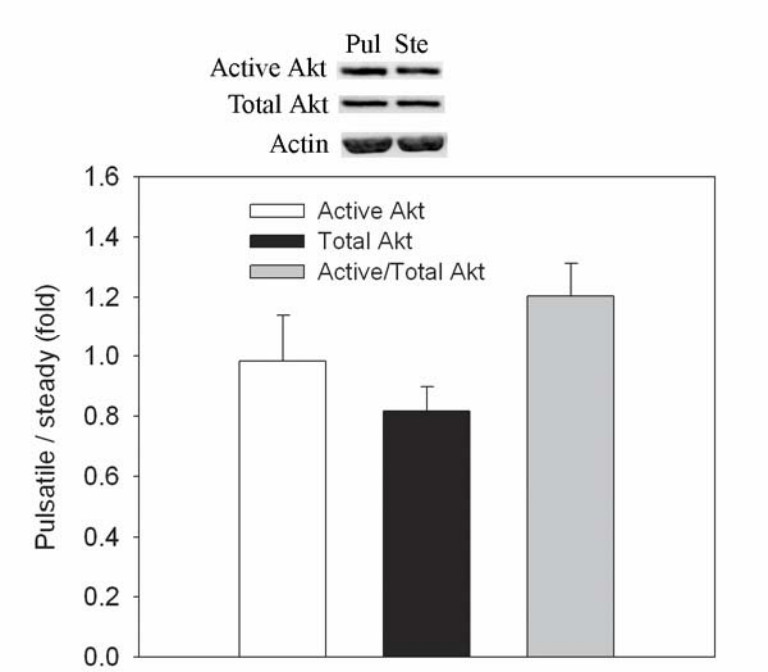

Figure 4-55 Long-term regulation of Akt by pulsatile pressure with a higher mean pressure (150 mmHg).

One segment of the DTA was cultured under pulsatile pressure (Pul, mean pressure 150 mmHg, pulse pressure 30 mmHg, 192 cycles/min), while the other segment was under steady pressure (Ste, the same mean pressure 150 mmHg, pulse pressure 0 mmHg) for long-term (24 h). Mean flow was the same (25 ml/min). The levels of active and total Akt, and the ratios of these two were not different between these two culture conditions. Error bars indicate SE of 3 independent experiments.

There was more active Akt in aortas under cyclic stretch (Figure 4-54). Interestingly, inhibition of Src decreased the level of active Akt in aortas under steady stretch for 24 h, because there was more active Akt in aortas under cyclic stretch after Src inhibition (1.85±0.21-flod, $P<0.05$, Figure 4-56). However, the level of total Akt was not increased (0.69±0.15-flod, $P=0.126$). The ratio of active to total Akt was also higher in aortas under cyclic stretch after Src inhibition (3.05±0.66-flod, $P=0.054$).

The effects of ROS inhibition by apocynin on Akt activation were studied. The level of active Akt was still less in aortas under cyclic stretch with apocynin for 24 h (0.63±0.13-fold, $P<0.05$, Figure 4-57). The levels of total Akt were not different (0.92±0.10-fold). The ratio of

active to total Akt was less in aortas under cyclic stretch (0.68±0.12-fold, $P<0.05$). Therefore, the level of ROS does not alter the regulatory pattern of Akt by long-term cyclic stretch.

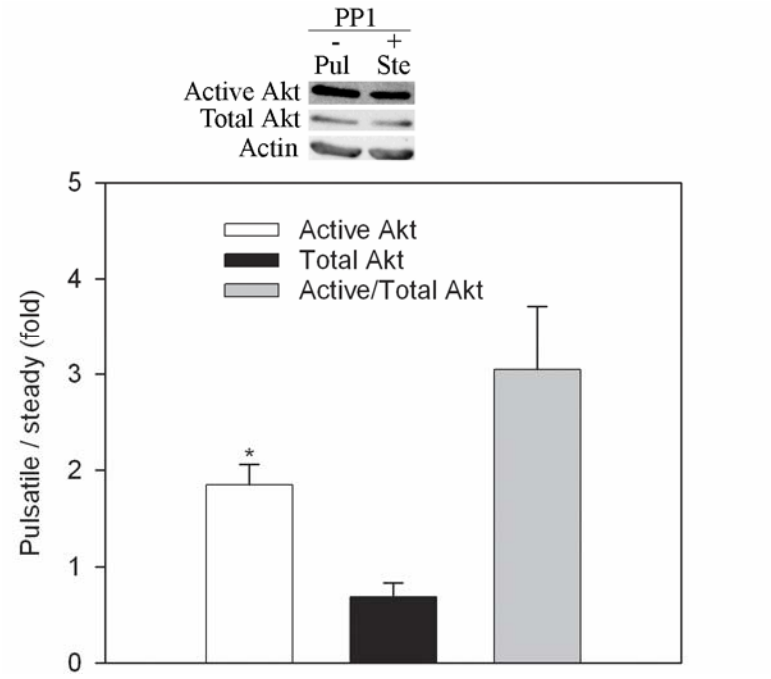

Figure 4-56 Src may regulate Akt activation by long-term (24 h) steady stretch.

One segment of the DTA was cultured under pulsatile pressure (Pul, mean pressure 80 mmHg, pulse pressure 30 mmHg, 192 cycles/min), while the other segment was under steady pressure (Ste, mean pressure 80 mmHg, pulse pressure 0 mmHg) with the Src inhibitor PP1 (10 μM) for long-term (24 h). Mean flow was the same (25 ml/min). The levels of active Akt were more in aortas under cyclic stretch after Src inhibition. There were no differences in the levels of total Akt.The ratio of active to total Akt was larger in aortas under cyclic stretch after Src inhibition. The error bar indicates SE of 4 independent experiments.

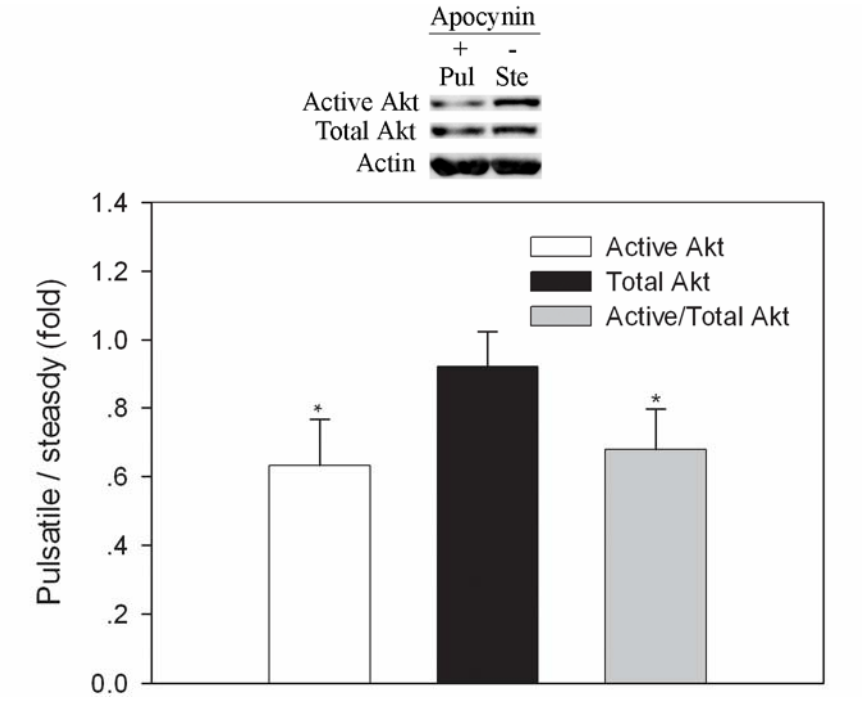

Figure 4-57 Inhibition of reactive oxygen species using apocynin does not alter the long-term (24 h) regulation pattern of Akt by cyclic stretch.

One segment of the DTA was cultured under pulsatile pressure (Pul, mean pressure 80 mmHg, pulse pressure 30 mmHg, 192 cycles/min) with the ROS inhibitor apocynin (0.4 mM), while the other segment was under steady pressure (Ste, mean pressure 80 mmHg, pulse pressure 0 mmHg) for long-term (24 h). Mean flow was the same (25 ml/min). The levels of active Akt were less in aortas under cyclic stretch. There were no differences in the levels of total Akt.The ratio of active to total Akt was smaller in aortas under cyclic stretch after ROS inhibition. Error bars indicate SE of 4 independent experiments.

In summary, short- (6 h) or long-term (24 h) cyclic stretch downregulates the Cx43 protein level compared to steady stretch. However, the mRNA level is not differentially regulated by cyclic and steady stretch for these two culture durations. Therefore, cyclic stretch regulates Cx43 protein, but not mRNA. There are no differences in cell proliferation between cyclic and steady stretch for these two culture durations, respectively. Thus, the differential regulation of the Cx43 protein level by cyclic stretch can not be explained by alterations in proliferation. There are no differences in the levels of active and total Src, and the ratios of these two for short-term cultures. However, there is less active Src in aortas under cyclic stretch for 24

h. The experiments using a Src specific inhibitor reveal Src as the possible mediator of the regulation of the Cx43 protein level by cyclic stretch. Another such potential mediator is ROS.

Akt is also differentially regulated by cyclic stretch. Akt activation is reduced by both short- (6 h) and long-term (24 h) cyclic stretch compared to steady stretch, while the total protein level of Akt is not affected. Src inhibition in aortas under steady stretch reverses the relative level of active Akt, without affecting the total protein level of Akt. Therefore, activation of Akt is very sensitive to the activity of Src. In contrast, inhibition of ROS does not alter the relative level of active Akt between aortas under cyclic and steady stretch, demonstrating differential regulation of Cx43 and Akt by ROS.

4.4 OTHER CONTROL EXPERIMENTS

Proteins from fresh rabbit aortas that were frozen immediately after harvesting were extracted in some experiments. These fresh aortas represented the *in vivo* controls. Cx43 protein levels from these fresh aortas were quantified using Western blot along with protein samples from *ex vivo* cultured aortas. The Cx43 protein level was increased after culturing for 6 h under low steady pressure compared with the fresh aortas (4.27±0.61-fold, $P<0.05$, Figure 4-58). The Cx43 protein level in the aorta under cyclic stretch for 6 h relative to the fresh aorta was studied in one experiment. The *ex vivo* cultured aorta with cyclic stretch had more Cx43 protein (Figure 4-59).

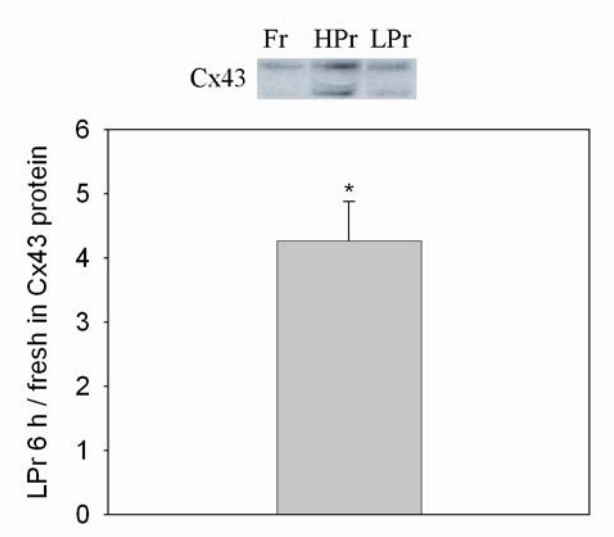

Figure 4-58 The Cx43 protein level is increased after 6 h under low steady pressure (80 mmHg) compared with fresh aortas (Fr).

The Cx43 protein levels in aortas cultured under low steady pressure (LPr, 80 mmHg) for short-term (6 h) were compared with those in aortas just harvested from rabbits (fresh). The Cx43 protein level was increased after culture. The error bar indicates SE of 5 independent experiments.

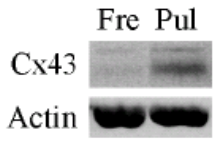

Figure 4-59 The Cx43protein level is increased after 6 h under cyclic stretch compared with the fresh aorta (Fre).

The Cx43 protein level in one aorta cultured under cyclic stretch for short-term (6 h) was compared with that in a fresh aorta. The Cx43 protein level was increased after culture.

Rabbit aortas were also cultured in a relaxed state for 1 day (1D), 4 days and 7 days in order to see the effects of loss in mechanical factors. The Cx43 protein level was increased after 1 day in a relaxed state as compared with the fresh aortas (Figure 4-60). The increase was more prominent after 4 days in a relaxed state. There was no further increase after 7 days. The protein

p27 followed a similar pattern (Figure 4-60). Therefore, proliferation of aortic cells in a relaxed state is inhibited.

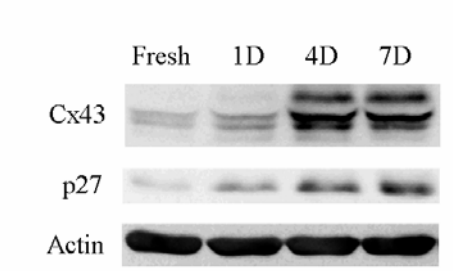

Figure 4-60 The protein levels of Cx43 and p27 are increased in aortas cultured in a relaxed state for up to 7 days (7D) as compared with fresh aortas. One typical example of three independent experiments is shown.

The levels of active Src were not altered significantly compared to fresh aortas (1.10±0.28-fold for 1D, 0.66±0.14-fold for 4D, 0.82±0.21-fold for 7D in Figure 4-61). Similarly, the levels of total Src were close to that in fresh aortas (1.32±0.16-fold for 1D, 0.78±0.23-fold for 4D, 1.07±0.25-fold for 7D in Figure 4-61). The ratios of active to total Src were significantly different only after 7 days (0.80±0.11-fold for 1D, 0.91±0.13-fold for 4D, 0.72±0.03-fold for 7D in Figure 4-61). Therefore, less Src is activated after 7 days in a relaxed state.

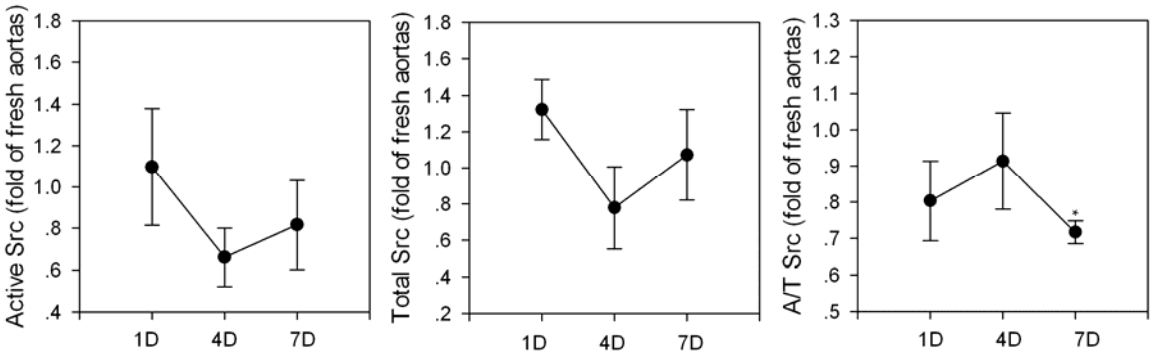

Figure 4-61 The Src levels in aortas cultured in a relaxed state for up to seven days.

The active Akt level was significantly less than that in fresh aortas after 1 day in a relaxed state (0.21±0.04-fold, P=0.002, Figure 4-62). However, the active Akt levels were similar after 4 days (0.96±0.55-fold). Active Akt was slightly reduced after 7 days although the difference was not statistically significant (0.64±0.12-fold, P=0.089). The mean level of total Akt was elevated similarly for all three time points (around 1.5-fold), however, it was not statistically significant because of large variations. The ratio of active to total Akt was less after 1 day, although it was not statistically significant (0.28±0.19-fold, P=0.066). The reduced ratio was significant after 4 days (0.65±0.05-fold, P<0.05). It was not significantly different after 7 days (0.82±0.32-fold). Therefore, active Akt and the ratio of active to total Akt are dynamically regulated in aortas cultured under a relaxed state.

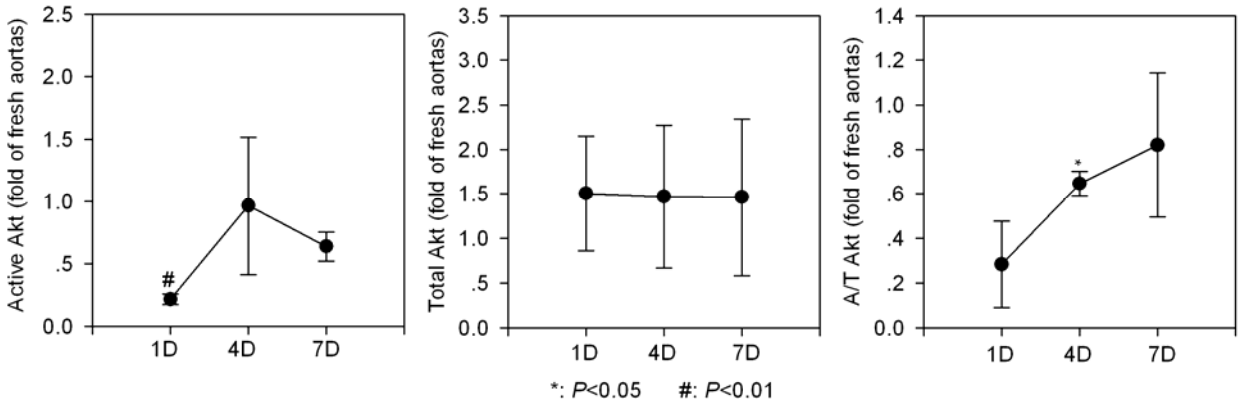

Figure 4-62 The Akt levels in aortas cultured in a relaxed state for up to seven days.

Levels of active and total Akt, and the ratios of these two were compared with those in fresh aortas. The active Akt level was significantly less than that in fresh aortas after 1 day in a relaxed state. However, it was similar after 4 days. Active Akt was slightly reduced after 7 days. The mean level of total Akt was non-significantly increased similarly for all three time points. The ratio of active to total Akt was less after 1 day, although it was not statistically significant. The reduced ratio was significant after 4 days. It was not significantly different after 7 days.

5.0 DISCUSSION

5.1 SUMMARY AND DISCUSSION OF RESULTS

Using an *ex vivo* preparation, we have shown that Cx43 in arteries is regulated by the mean pressure level and this regulation is time-dependent. Short-term (6 h) high pressure upregulated both mRNA and protein of Cx43. However, only the mRNA level of Cx43 was increased by high pressure under a relatively longer (24 h) culture duration. The Cx43 protein level was similar between two culture conditions at 24 h. This regulatory pattern in Cx43 protein level was not affected by flow levels. It was also not affected by the presence of pressure pulsatility. Src may mediate upregulation of both mRNA and protein of Cx43 by short-term high pressure.

We have also shown that Cx43 in arteries is regulated by pressure pulsatility and this regulation is time-independent. The Cx43protein level was downregulated by pulsatile pressure-induced cyclic stretch as compared with steady stretch induced by steady intraluminal pressure for both 6 and 24 h in culture, although the mRNA level of Cx43 was not significantly different for either culture duration. Cyclic stretch for 24 h also reduced levels of active and total Src as compared to the steady stretch. Results from the inhibition experiments (inhibition of Src in cultures with steady stretch and inhibition of ROS in cultures with cyclic stretch) suggest a role of Src in mediating the upregulation of Cx43 protein by steady stretch and a role of ROS in mediating the downregulation of Cx43 protein by cyclic stretch.

5.1.1 Effects of mean pressure level on arterial gap junctions

Hypertension is one of the most common cardiovascular diseases. Although changes in gap junction expression have been observed *in vivo* in various forms of hypertension,[345] there is a great deal of variability in the patterns of responses. In addition, whether connexin expression is involved in the genesis and/or maintenance of hypertension is still an open question. Both upregulation and downregulation of Cx43 mRNA and protein levels in aortas have been reported.[345] It appears that alteration of Cx43 expression depends on the specific hypertension model, where many factors may be differentially altered. Thus, use of *in vivo* hypertensive animal models can not establish a direct relation between blood pressure and gap junctions. In addition, both the mean blood pressure and pulse pressure are elevated in hypertensive subjects, making it difficult to identify individual effects. The *ex vivo* culture system used in the present study enables us to control mean and pulse pressures independently. We first studied the direct effects of the mean pressure level on gap junctions in arteries.

Cx43. We found that the Cx43 mRNA level was upregulated by both short- (6 h) and long-term (24 h) high steady pressure cultures (Figures 4-9 and 4-12). However, the Cx43 protein level was upregulated by short-term (6 h) high steady pressure only (Figure 4-9). The presence of pressure pulsatility did not alter this mean pressure-induced regulation pattern (Figure 4-18). Therefore, the mean pressure level *per se* does regulate Cx43 expression and this regulation appears to be time-dependent.

There are two well-recognized phenotypes in VSMCs: contractile and synthetic. Connexin expression may be altered as cells change phenotypes. For example, the Cx43 protein level was upregulated as *in vitro* cultured VSMCs changed from a contractile to synthetic phenotype.[346] Cx43 mRNA and protein were increased in human saphenous veins that were

cultured at a relaxed state for up to 14 days.[347] Similarly, our results showed that aortas cultured in a relaxed state for 7 days had more Cx43 protein compared to fresh aortas (Figure 4-60). High pressure may promote growth, proliferation, and synthetic activity of VSMCs. Thus, high pressure was expected to increase the Cx43 protein level. However, such an increase was observed only for the 6 h culture; aortas cultured under high pressure for 24 h did not have more Cx43 protein compared to the low-pressure culture at the same time point. We wanted to examine whether the cell phenotype had been changed in these *ex vivo* cultured aortas. The protein p27 blocks activity of cyclin-dependent protein kinase2 (CDK2) /cyclin A and CDK2/cyclin E, which are complexes required for cell-cycle progression and cell proliferation. Therefore, levels of p27 were quantified to study the status of VSMCs cultured under high or low pressure. For 6 h cultures, the p27 protein level was not significantly different (Figure 4-25), which demonstrated that increases in Cx43 mRNA and protein by high steady pressure at 6 h were not because of a difference in cell proliferation. For 24 h cultures, the p27 protein level was less in aortas under high pressure (Figures 4-27 and 4-28), indicating that these cells under high pressure were moving towards proliferation although more studies are needed in order to test proliferation. The observation that the Cx43 prtein level was not affected by high pressure at 24 h indicates longer cuture durations may be necessary to see the effect of decreased p27 on Cx43 protein level. This conjecture is supported by a previous study wherein DNA synthesis, a hallmark of cell proliferation, was similar between aortas cultured under high and low pressure levels for 3 days.[332] Finally, there was more Cx43 mRNA in aortas under high pressure for 24 h. This observation, together with the known effect of high pressure on phenotypes of VSMCs, it is expected that chronic (i.e., many days) high pressure will upregulate the Cx43 protein level.

As mentioned before, aortas from L-NAME hypertensive rats have lower levels of Cx43 mRNA and protein.[327] This may be attributable to NO because the NO donor S-nitroso-N-acetylpenicillamine increased Cx43 protein expression in mesangial cells.[287]

Cx40. Cx40 mRNA levels were also quantified in aortas cultured under steady pressure for either 6 or 24 h (Figures 4-11 and 4-14). Either GAPDH or VE-cadherin was used as the reference gene. The Cx40 mRNA levels were not significantly different in any case. Therefore, Cx40 mRNA is not differentially regulated by the pressure level. The VE-cadherin mRNA level was not significantly different as well, which verified the validity of using VE-cadherin as the reference gene for Cx40.

5.1.2 Effects of pulsatile pressure on arterial gap junctions

Effects of pulsatile pressure on gap junctions of intact blood vessels have not been studied. Pulsatile pressure stretches a blood vessel cyclically. The level of stretch depends on the compliance of the blood vessel in addition to the level of pulse pressure, which has been recognized as a risk factor for cardiovascular diseases. Generally, a higher pulse pressure is related to the reduction in vascular compliance. However, the molecular mechanisms underlying effects of compliance and the associated cyclic stretch on remodeling of intact vascular tissues are poorly understood. We found cyclic stretch of intact aortas decreased the Cx43 protein level for both short- (6 h) and long-term (24 h) cultures, compared to the steady stretch controls. This result was unexpected because several cell culture studies have shown increased Cx43 protein by cyclic stretch as compared with static controls in ECs,[12] neonatal rat cardiomyocytes,[330] and osteoblasts.[331] Nevertheless, there are several fundamental differences between *ex vivo* and *in vitro* studies. First, *in vitro* studies typically use relaxed or unstretched condition as the reference

state; all changes due to a test condition are compared with respect to this state. This may be problematic because blood vessels are constantly stretched due to the mean pressure, and therefore, one needs to use this steady-stretch condition as the reference state, not the relaxed or unstretched state when comparing the differential effects of cyclic and steady stretch. This is what we did in our *ex vivo* studies. Second, the intrinsic delicate three dimensional structural and compositional aspects of a blood vessel are maintained in an *ex vivo* culture. It has been shown that the components of extracellular matrix affect regulation of Cx43 protein by cyclic stretch in cardiac myocytes.[330] Third, cells cultured in two dimensions (i.e., on a flat surface) may have altered phenotypes, which can affect responses to mechanical factors. Thus, results using whole-vessels are more likely to reveal the *in vivo* situation.

5.1.3 Possible role of Src in mediating the regulation of arterial Cx43 expression by pressure

Src and Src-family proteins are non-receptor protein-tyrosine kinases playing prominent roles in cell proliferation, differentiation, growth, and migration.[348] There are nine members in the Src kinase family.[349] Among these members, Src, Fyn, Yes, and Yrk are ubiquitously expressed. Expression of other members (Blk, Fgr, Hck, Lck, and Lyn) is more restricted. However, it is not known how many members and at what levels these proteins are expressed in ECs and VSMCs. Although these members are functionally redundant, each member may also have specific roles. For example, all three members, Src, Yes and Fyn, were required for VEGF-induced growth of human retinal microvascular ECs studied using the small interference RNA gene knockdown technique.[350] Interestingly, cell migration induced by VEGF was significantly increased in Fyn-deficient cells; however, it was decreased in Yes-deficient cells. Furthermore, reduction in Fyn,

but not Src or Yes, impaired VEGF-induced tube formation. However, the specific roles of these members in arterial ECs and VSMCs are not known.

Src can be activated, as quantified by the ratio of active to total Src, by stretch or shear stress, in addition to growth factors.[351] Src was found to be involved in steady pressure-induced FAK phosphorylation using a Src-family kinase inhibitor PP2 for 24 h.[83] The levels of active Src (Tyr-418) were measured using Western blot in rat mesentery arteries.[352] Src was transiently (lasted for less than 5 minutes) activated by high steady pressure.[352] However, activation of Src by steady or pulsatile pressure in elastic arteries has not been detected using Western blot. We found that there were no differences in the levels of Src activation at 6 h or 24 h between aortas under high and low steady pressure cultures (Figures 4-20 and 4-21), or cyclic and steady stretch cultures (Figures 4-38 and 4-39). Thus, it appears that the pressure-induced Src activation is short-lived (less than 5 minutes). Such transient Src activation has also been observed in ECs subjected to shear stress.[353] Here, Src activation peaked after exposure to flow for 10 minutes.

A recent finding may explain why the initial activation of Src by high pressure was transient. The Src family kinase Lyn was activated by erythropoietin in red blood cells.[354] Lyn was found to interact with an adaptor protein Cbp (C-terminal Src kinase-binding protein), which recruited the negative regulator of Lyn, the complex of C-terminal Src kinase (Csk) and Csk-like protein-tyrosine kinase (Ctk). Activated Lyn phosphorylated Cbp on Tyr314, which recruited Csk/Ctk to suppress Lyn kinase activity.

A diffent temporal pattern was observed for pressure-induced changes in total Src. While there were no pressure-induced changes in total Src at 6 h, it was altered at 24 h: high mean pressure had more total Src compared to low mean pressure (Figure 4-21), and steady stretch had more total Src compared to cyclic stretch with the same mean stretch (Figure 4-39). The increase

in total Src at 24 h may come from new synthesis of Src, which may explain why there was no difference at 6 h. This pattern of total Src regulation in aortic cells is different from that in pulmonary epithelial cells, in which cyclic stretch for 24 h did not increase total Src as compared to static control cells.[355]

Although Western blot failed to detect the difference of active Src, the extensively used Src inhibitor PP1 eliminated the increase in both mRNA and protein of Cx43 by high pressure at 6 h (Figure 4-23). The reason of this discrepancy may be that PP1 inhibited some members of the Src-family kinases (Fyn, Hck and Lck[333, 349, 356]) which could not be detected by the Src antibody, and these members played roles in transducing mechanical forces and deformation. The antibody for total Src (sc-18, Santa Cruz Biotechnology) can detect Src p60, Yes p62, Fyn p59 and c-Fgr p55 based on the product sheet from the company. However, there was only one single band around 60 kDa in our results. Thus, c-Fgr p55 was not detected because its molecular weight is far from 60 kDa. For the same reason, Yes p62 was most likely not detected. However, it is possible that Fyn p59 was also detected because its molecular weight was very close to 60 kDa. We tried the antibody for Yes (sc-14, Santa Cruz Biotechnology) and Fyn (sc-434, Santa Cruz Biotechnology). Unfortunately, they did not work for rabbit aortic tissues. The antibody for active Src (nonphospho-Tyr-527, 2107, Cell Signaling Technology) may react with Yes p62 and Fyn p59 in addition to Src. Again, there was only one single band around 60 kDa in our results. Therefore, Yes p62 may not be detected. However, it is possible that Fyn p59 was also detected. Obviously, more studies are needed in order to explain definitely the discrepancy.

To explore the role of Src in mediating differential activation of ERK1/2 by steady and cyclic stretch, PP2 was added to the culture media for aortas under cyclic stretch.[83] Based on our results, it is not surprising that PP2 did not block differential activation of ERK1/2 because

aortas with steady stretch actually had more active Src. In our study, PP1 reduced the Cx43 protein level in aortas under steady stretch, resulting in similar levels between cyclic and steady stretch cultures (Figure 4-41). PP1 also downregulated Cx43 mRNA, leading to more mRNA in aortas with cyclic stretch. Thus, a certain level of Src activity is necessary for maintaining Cx43 mRNA. There were more Cx43 mRNA (Figure 4-12) and Src (Figure 4-21) in aortas under high pressure for 24 h. It is possible that Src was involved in upregulating Cx43 mRNA by high pressure. This role of Src may be revealed using the Src inhibitor PP1 in aortas under high pressure.

Inhibition of Src using PP1 did not alter activation of Src by high pressure or cyclic stretch at 6 or 24 h. However, PP1 inhibited the rapid autophosphorylation and activation of Src by high pressure.[352] Therefore, the mechanism of short-term inhibition of Src by PP1 is different from that of longer-term inhibition. It is known that PP1 binds to the ATP pocket of Hck and Lck, two other members of the Src-family kinases.[356] Src has the same ATP binding domain as that of Hck. However, PP1 did not compete with ATP for the inhibition of Src because increasing the concentration of ATP did not affect the IC_{50} value of PP1 for Src inhibition.[356] It is not known why the mechanism of short-term inhibition of Src by PP1 is different from that of long-term inhibition.

5.1.4 Possible role of reactive oxygen species in mediating the regulation of Cx43 expression by pressure

In a previous study, ROS mediated upregulation of Cx43 mRNA and protein by static stretch (20%) in VSMCs.[315] Arteries under higher steady pressure produced more superoxide.[111] Therefore, superoxide may have mediated increases of both Cx43 mRNA (6 and 24 h) and

protein (6 h) by high steady pressure in our study, which is analogous to the static stretch in the previous study.[315] Experiments using inhibitors of ROS may reveal the role of ROS in mediating regulation of Cx43 by the mean pressure level.

Rabbit aortas under cyclic stretch had more superoxide compared to steady stretch.[87] However, we found that there was less Cx43 protein in aortas under cyclic stretch. Inhibition of NADPH oxidase using apocynin elevated the Cx43 protein level in aortas under cyclic stretch. Furthermore, apocynin increased the Cx43 protein level in aortas cultured relaxed in Petri dishes (Figure 4-46). Thus, ROS may also reduce the Cx43 protein level. Taken together, ROS may play different roles in mediating mean pressure-induced and cyclic stretch-induced regulation of Cx43 expression, suggesting that factors other than ROS may be involved in this regulation.

5.1.5 Interactions between Src and reactive oxygen species

It is interesting to note that active and total Src were elevated by inhibition of ROS in aortas under cyclic stretch (Figure 4-44). It has been known that there are two-way interactions between Src and ROS. Src was required for the tyrosine phosphorylation of caveolin 1 in arterial ECs induced by H_2O_2.[357] On the other hand, Src mediated ROS production induced by platelet-derived growth factor (PDGF).[358] Our data demonstrated, for the first time, that long-term (24 h) inhibition of ROS in aortas under cyclic stretch increased the protein level of Src. Considering the essential roles of ROS in the vasculature, this may be one compensatory response to inhibition of ROS. However, the role of Src in the increase of Cx43 protein by NADPH oxidase inhibition needs further investigation. Dual inhibition of ROS and Src may be able to reveal the consequences without effective compensation of Src.

5.1.6 Different regulatory patterns of Cx43 expression by the mean pressure level and cyclic stretch

The regulatory patterns of Cx43 mRNA expression by the mean pressure level and cyclic stretch were different. The Cx43 mRNA level was increased by high steady pressure for both short- (6 h) and long-term (24 h) cultures. However, the Cx43 mRNA levels were similar between aortas under cyclic and steady stretch cultures for these two durations. The differential regulatory patterns of Cx43 mRNA expression by the mean pressure level and cyclic stretch may be because of the different roles of Src. Src mediated the elevated Cx43 mRNA level by short-term high steady pressure because the Cx43 mRNA levels were similar after Src inhibition (Figure 4-23). However, the elevated active Src level in aortas under steady stretch did not result in more Cx43 mRNA although Src is important for maintaining a certain level of Cx43 mRNA because inhibition of Src decreased Cx43 mRNA, leading to more Cx43 mRNA in aortas under cyclic stretch (Figure 4-41).

The regulatory patterns of Cx43 protein expression by the mean pressure level and cyclic stretch were also different. The Cx43 protein level was increased by high steady pressure for short-term cultures (Figure 4-9). However, the Cx43 protein levels were similar after long-term (24 h) culture using the same culture conditions (Figure 4-12). Therefore, regulation of the Cx43 protein level by the mean pressure level is culture duration dependent. In contrast, there was less Cx43 protein in aortas under cyclic stretch for both short- (6 h) and long-term (24 h) cultures. Hence, regulation of the Cx43 protein level by cyclic stretch is not culture duration dependent.

5.1.7 Dissociation of the Cx43 protein level from the mRNA level

Our results showed that more Cx43 mRNA might not be associated with more Cx43 protein (Figures 4-12, 4-18 and 4-41). For example, although the Cx43 protein levels were similar, there was more mRNA at 24 h in aortas under high steady pressure (Figure 4-12) or aortas with cyclic stretch and Src inhibition (Figure 4-41). Protein levels depend on rates of protein synthesis and degradation. The rate of protein synthesis depends on the amount of the mRNA and the translational efficiency from mRNA to protein. The rate of protein degradation may not be related to the mRNA level at all. Hence, it is possible to observe a dissoacition between mRNA and protein levels. Cx43 protein is degraded rapidly.[359] Therefore, it is necessary to study both the mRNA and protein levels of Cx43 in order to have a better understanding of Cx43 regulation.[345] Further studies are needed to clarify the exact mechanisms of this discrepancy. Inhibitors of protein synthesis and/or degradation can be used for this purpose.

5.1.8 Cx43 phosphorylation

Cx43 phosphorylation affects the trafficking, assembly, internalization, degradation and gating of Cx43 gap junction channels.[160] Therefore, regulation of Cx43 is likely to include phosphorylation in addition to the mRNA and total protein levels. Ratios of phosphorylated (P1+P2+P3 in Figure 4-8) to non-phosphorylated (P0) Cx43 have been used to compare the status of phosphorylation of cardiac Cx43.[296] Using this approach, we observed examples of both statistically significant changes (Figures 4-10 and 4-33) and no changes (Figures 4-13) in Cx43 phosphorylation status. However, there are some concerns regarding the calculation of this ratio. Based on our Western blots, it is clear that most Cx43 proteins in aortic tissues were

phosphorylated; the amount of Cx43 protein in the P0 state (i.e., non-phosphorylated) was very small. Thus, there may be large errors in the calculation of the ratio which has the level of P0 (a small number) in the denominator. This issue needs further investigation.

As introduced in Section 2.3.3, many amino acids of the Cx43 protein can be phosphorylated. The ratios mentioned above do not take into account the specifically phosphorylated amino acids. To fully understand regulation of Cx43 by mechanical forces, it is necessary to know the differential phosphorylation of these amino acids by mechanical factors, in addition to the regulation at the total protein level. For instance, long-term high pressure did not increase the total Cx43 protein level. However, there was more active Src in aortas with high pressure. Src has been reported to phosphorylate Tyr-247 and Tyr-265 of Cx43.[170] Hence, it is possible that high pressure increases phosphorylation of these two sites, even in the absence of an increae in the total protein level. Antibodies for these specific amino acids are needed for this purpose. We have tried a few commercially available phospho-Cx43 antibodies. Unfortunately, none of them worked for rabbit aortic tissues.

5.1.9 Regulation of Cx40 and Cx37 by pressure

The mRNA levels of Cx40 were not significantly altered by different levels of steady pressure for both short- (Figure 4-11) and long-term (Figure 4-14) cultures. The Cx40 protein level may be regulated by pressure. However, the Cx40 antibodies we have tried did not have a sufficient affinity to the Cx40 protein. Therefore, Cx40 protein levels could not be measured using Western blot. *En face* immunostaining could also detect Cx40 protein expression in ECs. Unfortunately, the Cx40 staining of cultured aortas was much weaker compared with fresh aortas, which prevented us from doing quantitative comparison of the Cx40 protein levels in aortas cultured

under different conditions. The sequence of the rabbit Cx37 gene is known (Ensembl gene ID: ENSOCUG00000000325). Unfortunately, the Cx37 mRNA levels could not be detected using the TaqMan® gene expression assay (the following primers and probe were tried: forward 5'-TGCCGCTGCCTCAGT-3', reverse 5'-GTCGGCAGAAGGGTCTGA-3'; probe 5'-CCCTGGCCCTGCCGTG-3'). The protein levels of Cx37 could not be quantitatively analyzed for the same reasons as those for Cx40.

5.1.10 Effects of flow on pressure-induced regulation of arterial gap junctions

As discussed in Section 2.3.9, flow or fluid shear stress also regulates gap junctions. The flow rate used in this study was lower than the physiological value, just as in other *ex vivo* studies using rabbit aortas.[83, 87, 332, 360] Low flow did not alter the integrity of ECs for 24 h cultures.[360] The major effects of flow have been assumed to be on ECs. However, the mRNA and protein of Cx43 analyzed in this study mostly came from VSMCs. Thus, we observed mainly the effects of pressure on gap junctions of VSMCs. Moreover, the same flow level was used for both aortic segments which were cultured under different mean pressure levels or pulse pressures. Therefore, the results of regulation of gap junctions by the mean pressure level or pulse pressures obtained under a flow level are expected to the same if another flow level is used. For example, regulation of the Cx43 protein level by long-term high steady pressure under low flow (Figure 4-12) was not altered at high flow (Figure 4-15).

5.2 CLINICAL IMPLICATIONS

We studied regulation of arterial Cx43 by pressure. Cx43 has been associated with cardiovascular diseases and cancer. However, interpretation of gap junctional studies in a clinical sense has been difficult. The possible causative roles of Cx43 in some diseases are under investigation (as revealed by searching CRISP, Computer Retrieval of Information on Scientific Projects). Because Cx43 is not the major connexin protein in arterial ECs, the possible role of endothelial Cx43 in vascular diseases may not be attributable to the chemical transfer function of gap junctions. Even though arterial VSMCs may express Cx43 as the only connexin protein, Cx43 is not absolutely required for VSMCs because mice with SMC-specific deletion of the Cx43 gene had normal blood pressure and heart rate.[271]

The role of vascular Cx43 may be more prominent in pathological conditions, such as injuries. However, Cx43 may be both beneficial and detrimental. For example, the Cx43+/- mice had less neointima formation following balloon distension injuries as compared with Cx43+/+ controls.[270] Moreover, there were smaller cardiac infarcts in Cx43+/- mice than wild-type controls following coronary ligation.[361] In contrast, mice with SMC-specific knockout of Cx43 had more neointima formation responding to injury induced by a wire.[271] Loss of Cx43 blocked the protective effect of ischemia preconditioning on myocardial ischemia-reperfusion injury.[362] Furthermore, Cx43 was upregulated in rat carotid arteries following balloon catheter injuries.[363] However, the *in vivo* study of gap junctions has been hindered by the lack of specific inhibitors. Nevertheless, it is reasonable to think that a certain level of Cx43 is needed in VSMCs.

Cx43 expression is altered in several animal models of hypertension. However, it is not known whether Cx43 expression is also altered in hypertensive humans. Even in the animal

models, it is not known whether Cx43 actively contributes to hypertension. The use of transgenic animals may help answer this question.

Stiffer vasculature is considered to be a risk factor for cardiovascular diseases, although the molecular mechanisms are poorly understood. Increased vascular stiffness has been reported in several physiological (e.g., normal aging) and pathological (e.g., chronic hypertension, atherosclerosis, accelerated aging) conditions. The level of cyclic stretch of a stiffer blood vessel is less under the same pulse pressure. Our results showed that cyclic stretch reduced Cx43 protein as compared with the steady stretch controls. Thus, it is speculated that stiffer vessels *in vivo* will have more Cx43 protein. Elevated Cx43 protein may play a role in mediating responses to injuries, inflammation, and other risk factors through its junctional and non-junctional functions. However, definitive data regarding this do not exist.

5.3 ADVANTAGES OF METHODOLOGY

Using the *ex vivo* culture method, we studied the effects of the mean pressure level and pulsatility on arterial gap junctions. The intrinsic delicate structure of arteries was maintained in our study. As the importance of extracellular matrix in regulating cellular processes is increasingly recognized, our method is advantageous over *in vitro* cell culture studies. We studied mainly the effects of stretch on VSMCs, which do not exist as a monolayer *in vivo*. Even though three dimensional cultures of VSMCs have been used to study vascular biology and engineering, the delicate structure of native blood vessels has not been recreated. The chemical components of native blood vessels are also different from those engineered constructs. We compared the effects of cyclic stretch versus steady stretch, which can be studied *in vitro* using

two dimensional culture of VSMCs as well. However, VSMCs that exist as a monolayer may respond to stretch differently from VSMCs in blood vessels. Moreover, there is intraluminal flow in our system. Therefore, we can also study the interaction of ECs with SMCs in arteries.

Blood pressure and pulsatility can not be readily manipulated *in vivo*. It is not possible to just alter one single hemodynamic parameter *in vivo* without changing others. For example, the mean pressure proximal to a binding cast could be increased *in vivo*, however, the pulse pressure was also increased.[364] Although casts can be placed around arteries to reduce cyclic stretch, wall stress may be altered as well. Moreover, this approach may interfere with arterial function and other organ systems, leading to responses to injuries. We were able to adjust mean and pulse pressures independently using the *ex vivo* method. Flow can also be independently adjusted.

5.4 DISADVANTAGES OF METHODOLOGY

We could investigate the effect of just one mechanical factor on intact arteries using the *ex vivo* method. However, *ex vivo*-cultured blood vessels are in an environment different from the *in vivo* situation. Although culture media have been optimized for cell culture, the medium is different from blood in many ways. For example, blood cells and many other chemicals are not in the culture medium. Using whole blood would be an alternative in this aspect. However, thrombosis will be rapidly formed in the perfusion system, and it is hard to clean the perfusion components. Anticoagulating reagents may reduce thrombosis. Nevertheless, these reagents may interfere with vascular responses to mechanical factors.

One challenge relating to *ex vivo* culture of intact arteries is to maintain the integrity of the endothelium. Endothelial cells can be easily lost by any manipulation of arteries. We were

very careful in protecting ECs from loss. Aortic spasm could happen during harvesting aortas, which may damage ECs. Papaverine was applied frequently to the adventitia of aortas. However, it was not possible to completely prevent spasm when the chest was open during the procedure. Aortas contract after isolation, which may also damage ECs. The *in vivo* length was maintained using clamps. Aortas were prevented from collapse after isolation using a bag with Tyrode's salts solution that was put at a higher position than that of aortas. These methods helped protect ECs. However, as the primary antigen presenting cells of the body, primary ECs are very sensitive to their environment. It is thus possible that *ex vivo* cultured ECs may behave differently after they are taken out of the body. In contrast, there are many layers of VSMCs in rabbit aortas. These cells are embedded between thick fibers, thus protected against injuries. Therefore, the *ex vivo* perfusion method is more suitable for studying effects of mechanical forces on VSMCs.

Biological assays may be difficult to be performed on aortas. Most assays have been developed for *in vitro* cell culture studies. For example, measuring the dye transfer function of gap junctions in aortas was very difficult, as discussed in detail in Appendix A. Cultured HUVECs had good recovery after photobleaching. However, most bleaches did not have good recovery in ECs of aortas. It is also more difficult to do Western blot and PCR. As for studying the molecular mechanisms, there are fewer options when using tissues. Genes in cultured cells can be readily manipulated. The small interference RNA method has been widely used to knockdown specific genes in cells. However, using chemical inhibitors is the only option in most cases if using tissues. Moreover, most these commercially available chemicals target molecules that have been well studied, which means it is very difficult to study novel molecules in tissues. The volume of culture medium is also much larger than that of a typical culture dish, which

makes it expensive to use some chemicals. *Ex vivo* culture of blood vessels is also restricted by suitable animal models. Mice and rats have small blood vessels that are not the first choice for *ex vivo* culture. Larger animals are better for *ex vivo* culture. However, the genomes of large animals are either unknown or inferior in quality, which makes molecular analysis and manipulation of cultured tissues difficult.

5.5 RECOMMENDATIONS FOR FUTURE WORK

Regulation of arterial gap junctions by mechanical factors can be further studied in the future. We studied the effect of mean pressure on Cx43 for up to 24 h. Longer culture duration may be able to reveal the effects of high pressure, which induces hypertrophy and hyperplasia of vascular cells *in vivo*. For this chronic culture, it is better to culture both vessels under pulsatile conditions but with different mean pressure in order to avoid rapid adaptation of VSMCs to steady stretch. The exact duration will be determined by the days that are needed for VSMCs to synthesize significantly more proteins and/or DNA molecules.

Cyclic stretch decreased the Cx43 protein levels, while the mRNA levels were not decreased. Studies can be done to investigate Cx43 translation and degradation to know the reasons of this regulatory pattern. Chemicals that inhibit protein translation and/or degradation can be added to the culture medium. Cx43 proteins are mainly degraded in lysosomes. Therefore, inhibitors of lysosomes can be used to study Cx43 degradation.

We found that Src and ROS might mediate cyclic stretch-induced Cx43 protein reduction. More studies are needed to investigate the exact roles of Src and ROS in regulation of Cx43 by the pressure level and stretch. Src is related to integrins at focal adhesions. Therefore, Src is at

the upstream of the signaling pathway. The downstream signaling proteins need to be identified. Because there is very few information about the differentially regulated genes and proteins by cyclic versus steady stretch, high throughput gene and protein arrays may help identify those potential targets. Some growth factors and their receptors, such as EGF, FGF, and PDGF, may be involved in transducing mechanical forces. Since NADPH oxidase is the major source of ROS in blood vessels, NADPH oxidase may be regulated by cyclic stretch. More ROS in aortas under cyclic stretch may accelerate Cx43 protein degradation, which needs to be tested in the future.

Cx43 protein is highly phosphorylated at many amino acids. Knowing the regulation in total protein level is just a small part of the story. More and better antibodies for the phosphorylated amino acids are needed for this task. Furthermore, the functions of these phosphorylation events need to be explored, which requires using multiple advanced techniques. The functional consequences of reduced Cx43 protein level by cyclic stretch need to be explored. One direction is to study the intracellular signaling role of Cx43, in addition to material transfer.

6.0 CONCLUSIONS

One of the main findings of this dissertation is that arterial Cx43 is regulated by the mean pressure *ex vivo*. Short-term (6 h) high pressure upregulates both mRNA and protein of Cx43. However, a relatively longer (24 h) culture under high pressure only increases the mRNA level of Cx43. The protein level of Cx43 is not elevated by high pressure for 24 h under both low and high flow levels. This result is not affected when both segments are cultured under pulsatile pressure but with different mean pressure levels. Since chronic high pressure will promote hypertrophy and hyperplasia of VSMCs, and the Cx43 protein level is upregulated in VSMCs with a synthetic phenotype, chronic high pressure is expected to increase the Cx43 protein level in arteries. Src may mediate upregulation of both mRNA and protein of Cx43 by short-term high pressure. The mRNA level of Cx40 is not significantly altered by high pressure.

Another finding is that arterial Cx43 is regulated by pressure pulsatility *ex vivo*. The protein level of Cx43 is downregulated by cyclic stretch as compared with steady stretch induced by a steady intraluminal pressure for both 6 and 24 h in culture, although the mRNA level of Cx43 is not significantly different at either duration. Levels of active and total Src are reduced in aortas under cyclic stretch for 24 h. Src may mediate downregulation of Cx43 protein by cyclic stretch. A certain level of active Src in aortas under steady stretch is required to maintain a comparable level of Cx43 mRNA to that in aortas under cyclic stretch. Downregulation of Cx43 protein by cyclic stretch may be mediated by ROS. However, the mRNA level of Cx43 in aortas

under cyclic stretch is not affected by the level of ROS. There are interactions between Src and ROS. Inhibition of ROS in aortas under cyclic stretch increases the levels of active and total Src.

Short-term (6 h) high pressure (150 mmHg) does not affect the cell cycle entry (the p27 protein level). However, cells have a stronger tendency of entering the cell cycle after 24 h under high pressure. There is no significant difference in the tendency of entering the cell cycle between aortas cultured under steady and cyclic stretch for both short- (6 h) and long-term (24 h).

Pressure regulates activation of Akt. More Akt is activated in aortas under high pressure for 24 h. Both short- (6 h) and long-term (24 h) cyclic stretch reduce activation of Akt compare to steady stretch. Src, but not ROS, mediates differential activation of Akt by cyclic and steady stretch. The total protein level of Akt is not regulated by any of these conditions. Therefore, Src and Akt have different regulatory patterns by pressure.

APPENDIX A

ENDEAVORS TO CHARACTERIZE ARTERIAL GAP JUNCTION FUNCTION

The basic function of gap junctions is to provide a pathway for material transfer between adjacent cells. We tried several techniques to quantify this function in our aortic samples. Unfortunately, we could not acquire good dada for the quantitative comparison of the function of gap junctions in cultured aortas due to technical problems.

A.1 SCRAPE LOADING/DYE TRANSFER ASSAY

Scrape loading/dye transfer is the fastest and simplest method to evaluate gap junctional intercellular communication.[365] It can simultaneously measure dye transfer in coupled cells. The fluorescent dye Lucifer Yellow (molecular weight 457 Da) is used most commonly in this technique. It can be easily transferred through gap junction channels. Lucifer Yellow can be visualized under a microscope using a UV light source (absorbance 428 nm, emission 536 nm). However, Lucifer Yellow can not enter cells through intact cell membranes. Scrape is thus used to break cell membranes and load Lucifer Yellow. Another fluorescent dye that is larger than the gap junction channel exclusion limit is used simultaneously as a control to show the scraped

position. Rhodamine–dextran conjugates (molecular weight 10,000 Da, absorbance 555 nm, emission 580 nm) are most commonly used for this purpose. The rate of dye transfer depends on the number of gap junctions and the conductance of individual channels.

One aortic ring was cut open longitudinally. It was then put into the PBS solution with 0.5 mg/ml Lucifer Yellow (L1177, Molecular Probes) and 1 mg/ml rhodamine–dextran conjugate (D1824, Molecular Probes). A surgical blade was used to gently scrape the luminal side of the aorta. After incubating for 3 minutes in dark, the aorta was washed in PBS and fixed in 4% paraformaldehyde PBS solution for 5 minutes. Images were taken under an Olympus wide field epifluorescence microscope. Unfortunately, Lucifer Yellow was everywhere along the surface of the aorta. The scrape line could not be identified.

Scrape loading has been commonly used to study gap junctions of cultured cells on coverslips. It is very difficult to maintain the integrity of the endothelium of an elastic aorta during this procedure.

A.2 CUT-END LOADING/DYE TRANSFER ASSAY

One variation of scrape loading is cut-end loading of tissues. Aortic rings that were just cut from longer aortas were incubated in PBS with Lucifer Yellow (5 mg/ml) and rhodamine–dextran (3 mg/ml) for 5 or 10 minutes. Aortas were quickly washed three times in PBS before fixation in 4% paraformaldehyde PBS solution overnight. After washing, aortas were frozen in isopentane which had been cooled in liquid nitrogen. Aortas were embedded in OCT and sectioned. Images were taken using a confocal microscope. The elastic fibers were strongly stained by Lucifer

Yellow (Figure A-1). However, VSMCs did not have much staining even at the edges. This assay is thus not good for studying aortic gap junctions.

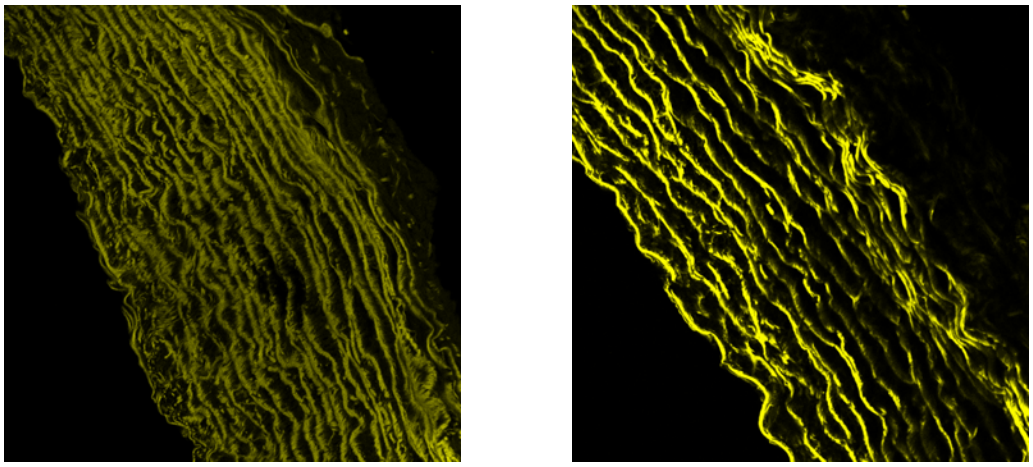

Figure A-1 Cut-end loading of Lucifer Yellow into aortas for 5 (left) or 10 (right) minutes.

A.3 FLUORESCENCE RECOVERY AFTER PHOTOBLEACHING (FRAP)

FRAP is a more advanced technique to study the dye transfer function of gap junctions. The principle of FRAP is to observe the rate of recovery of fluorescence by diffusion of a fluorescent marker into an area which contains the same marker but has been rendered non-fluorescent via an intense pulse of photobleaching laser light.[366] A rate constant of recovery can be obtained from the recorded recovery curve. Therefore, functions of gap junctions in different cells can be quantitatively compared. Calcein AM (Invitrogen) was commonly used as the fluorescent marker. Calcein AM is membrane-permeable and thus can be introduced into cells via incubation. Calcein AM is then hydrolyzed by endogenous esterases in live cells into the

negatively charged green fluorescent calcein, which is membrane-impermeable and retained in the cytoplasm.

HUVECs cultured on a coverslip were used to test the FRAP technique. HUVECs were loaded with 6.25 μM calcein AM for 30 minutes at 37 °C and then washed 3 times with PBS. The DMEM medium and HUVECs were maintained at 37 °C using an incubated open chamber (Harvard Apparatus, MA). FRAP was performed on an inverted Olympus Fluoview 1000 confocal microscope using a 40x oil, 1.3 NA objective. After initial imaging with a 488 nm laser line (0.4% laser output), an oval region was bleached for 2 seconds using a 405 nm laser line at its 100% intensity. Sequential images were taken every 30 seconds for 7 minutes. The control for photobleaching associated with imaging can be assessed by determining average intensity over time in regions far from the bleached region. Cells were successfully loaded with calcein (Figure A-2A). One area was just bleached (Figure A-2B). It was rapidly recovered a few minutes later (Figure A-2C). The time series of average intensity was shown in Figure A-2D. The control area had a stable intensity. Therefore, FRAP can be used to assess gap junctions in cultured HUVECs.

FRAP was then used to detect the dye transfer function of endothelial cells in aortas. Aortic rings were opened longitudinally to lay flat in DMEM medium and loaded with 6.25 μM calcein AM for 30 minutes at 37 °C. Aortas were then washed 3 times with PBS. Aortas were held against the coverslip of a single-chamber Lab-Tek chamber slide system (Nalge Nunc International, NY) using a custom made plastic insert on the adventitia side of the aorta. Therefore, ECs could be visualized by an inverted Olympus Fluoview 1000 confocal microscope with a 40x oil, 1.3 NA objective (Figure A-3A). DMEM media and aortas were maintained at 37 °C. After initial imaging with a 488 nm laser line (0.4% laser output), an oval region was bleached for 2 seconds using a 405 nm laser line at its 100% intensity. Sequential images were

taken every 30 seconds for 7 minutes. One example is shown in Figure A-4. Unlike HUVECs, the bleached area was not recovered well.

Endothelial cells may not have a good environment when they are against a coverslip (Figure A-3A). A gap can be left between the coverslip and endothelial cells (Figure A-3B). A 10X air objective was needed in this case in order to be focused. However, the image quality was much worse. A higher concentration of calcein may increase signal intensity. Unfortunately, high concentration of calcein is toxic to cells, and results in non-uniform loading in cells.

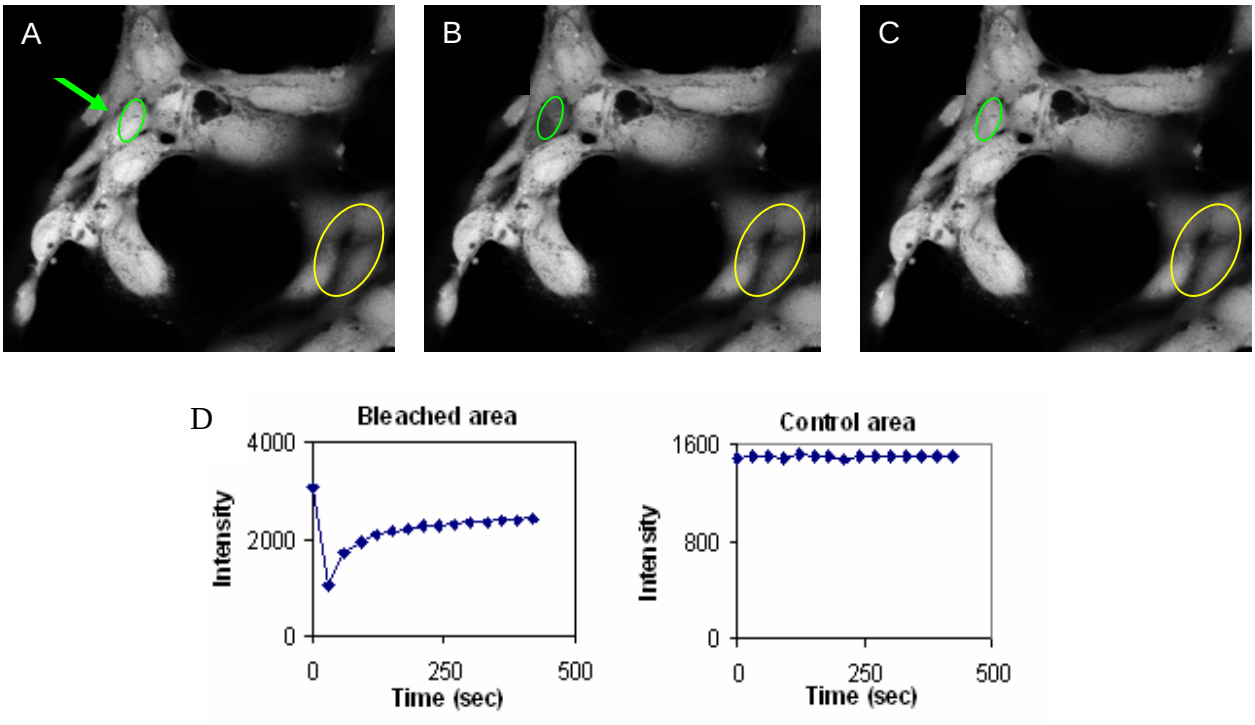

Figure A-2 FRAP of HUVECs cultured on a coverslip.

The arrow points to the bleaching area.

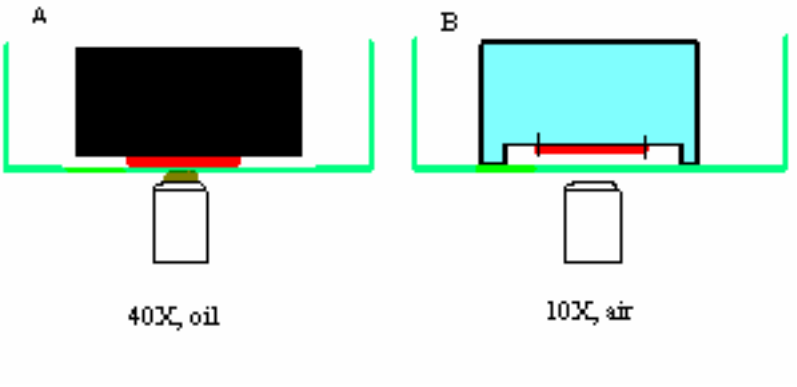

Figure A-3 Two setups of FRAP on aortas.

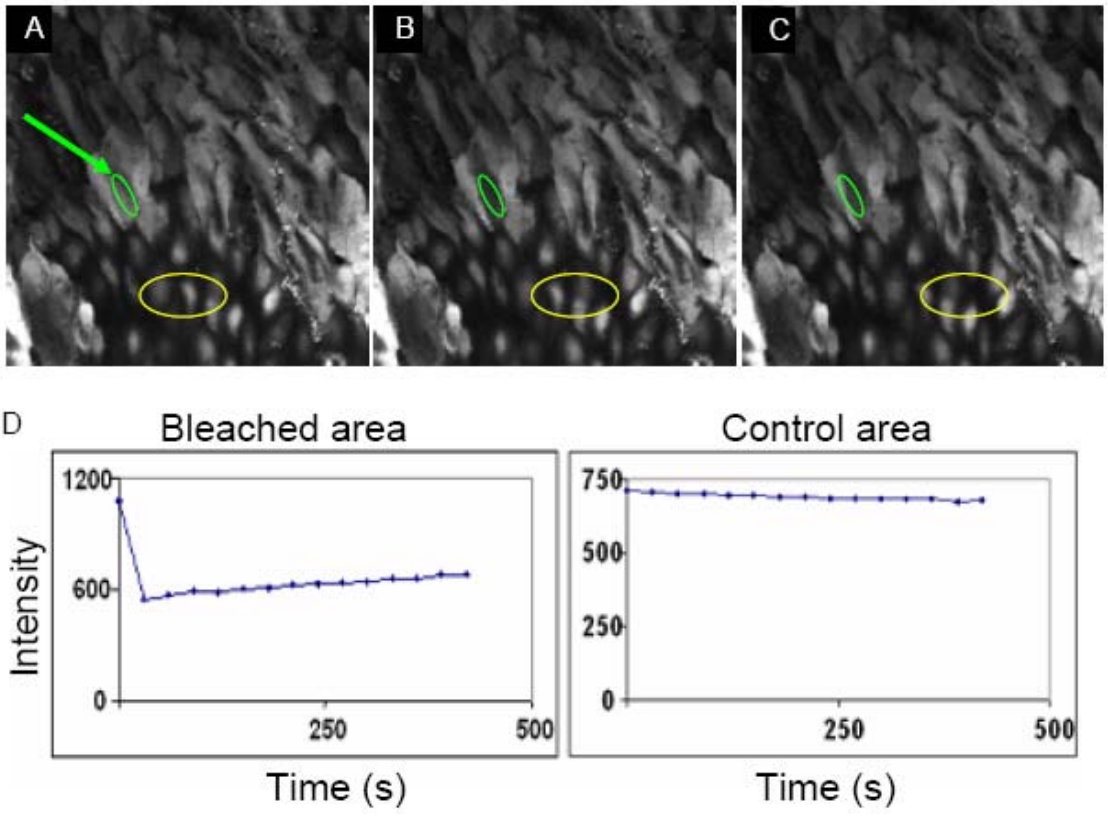

Figure A-4 FRAP of rabbit aortas.

There is another challenge of doing FRAP on aortas. There are many layers of SMCs in rabbit aortas. Therefore, an aorta may vigorously contract and relax, which leads to an alteration

in field of view, and loss of focus. The intensity in the designated area is thus altered by the movement. The parachute assay may overcome this limitation.[367] It is a noninvasive technique to detect the diffusion of fluorescent dyes through gap junctions from pre-loaded cells to unlabelled cells. Some endothelial cells were loaded with calcein. Rabbit aortas were opened longitudinally and incubated with these preloaded cells. However, there was not much staining in rabbit endothelial cells after 1 h incubation.

Gap junction channels are dynamically gated. Any perturbation, either mechanical or chemical, can thus alter the conductance of these channels. The assays that have been tested used aortas in a relaxed state. The properties of gap junctions in these cells may be different from those in aortas with physiological mechanical conditions. The best assay should use perfused aortas, which presents tremendous challenges.

APPENDIX B

IN VITRO CONTROL OF PULSATILE PRESSURE AND FLOW

The Vascular system is subjected to mechanical forces, such as blood shear stress and pressure. An *in vitro* system that has the capability of precisely manipulating these mechanical forces is an important supplement to *in vivo* and *in vitro* cell culture studies in which mechanical forces are not controlled. Specifically, we wanted to have a system wherein pressure and flow could be controlled independelty, both in terms of their magnitude and waveform morphology. Although we devoted a great deal of effort to this part of the project, we were only partially successful. Our efforts are described below; hopefully, this will be helpful for future attempts to fully implement the envisioned system. We will first discuss a model-based analysis that outlines the control strategy and also demonstrate its feasibility.

B.1 MATHEMATICAL MODELING OF SIMULTANEOUSLY CONTROLLING PULSATILE PRESSURE AND FLOW

Control strategy. There are two variables (pulsatile pressure and flow) that need to be dynamically controlled. For each of these two variables, there are two components. One is the

mean. The other is the pulse. The mean flow and pressure can be easily controlled. For example, the mean flow can be obtained using the combination of a Masterflex peristaltic pump and a dampener. The mean pressure can be achieved by adjusting a valve at the downstream of the blood vessel. Because the mean flow and pressure are constant, they do not need to be dynamically controlled. However, the pulse components of pressure and flow need to be dynamically controlled. One syringe pump at the upstream of the blood vessel can be used to mainly control the pulse flow. Another syringe pump at the downstream of the blood vessel can be used to mainly control the pulse pressure. Therefore, this is a multiple input-multiple output (MIMO) control problem. These two pumps can be controlled in real-time using PID (**P**roportional, **I**ntegral and **D**ifferential) controllers based on the difference between the desired and measured variables.

The Model. A model was constructed using Simulink, one of the toolboxes in Matlab (Mathworks Inc.) using analogies between mechanical (pressure, flow, inertia and compliance) and electrical (voltage, current, conductance and capacitance) systems (Figure B-1). A limiter and a low pass filter were applied to the output of the upstream PID controller to take into account the fact that the pump is physically restrained (e.g., the maximal speed of the movement).

Modeling results. The steady flow pump is always running for these simulations. The terminal load is also pre-adjusted to maintain the mean pressure. If both upstream and downstream pulsatile pumps do not work, only the mean pressure and flow are achieved (Figure B-2). However, when the upstream pulsatile pump is also working, the pulse flow is well controlled (Figure B-3). But the pressure waveform is different from the desired one. The pump runs smoothly. In contrast, when only the downstream pulsatile pump is working, the pressure is

well controlled (Figure B-4). However, the flow waveform is not desired. Both pulse flow and pressure are well controlled when both pulsatile pumps are running (Figure B-5). Therefore, it is possible to control both pressure and flow waveforms simultaneously using one upstream and one downstream pulsatile pump.

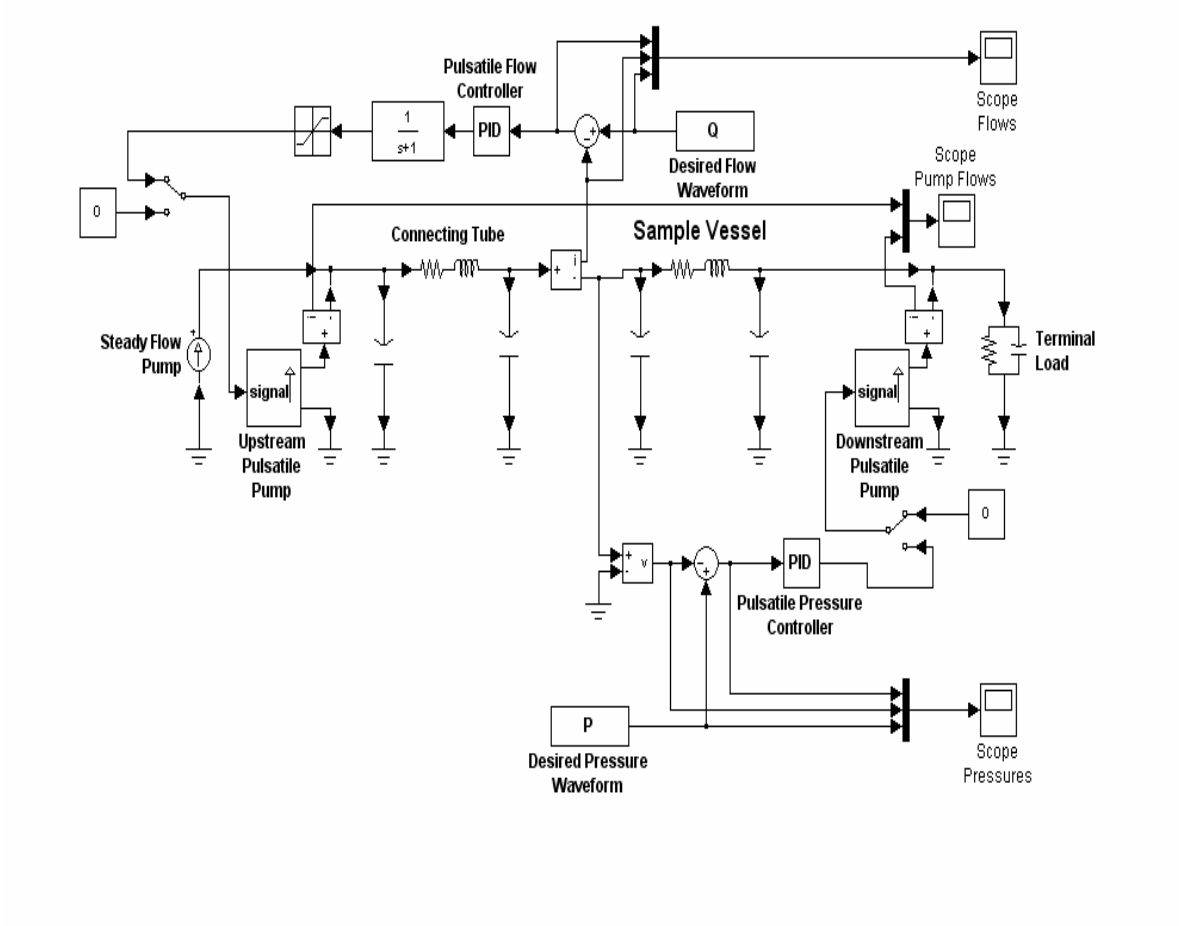

Figure B-1 Diagram of the simulink model for pulsatile pressure and flow control.

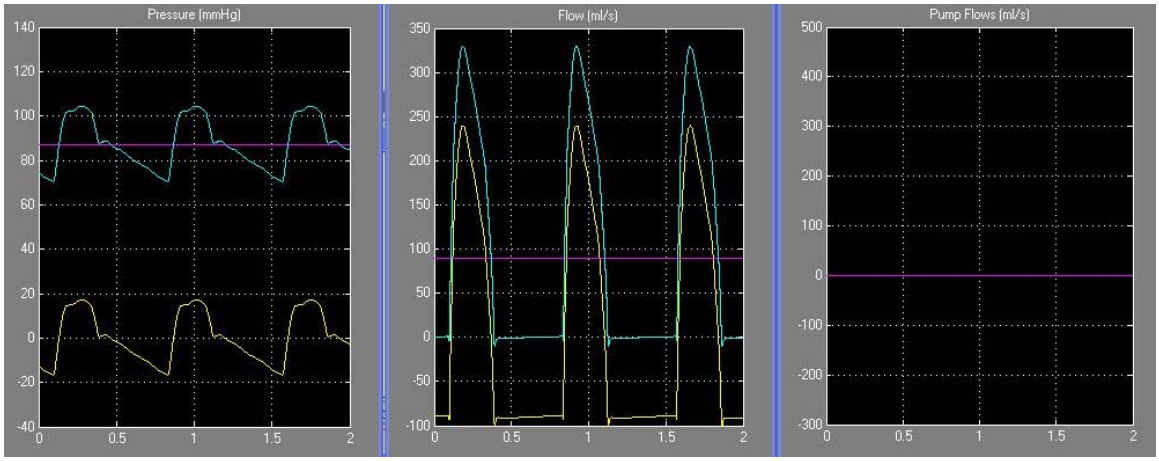

Figure B-2 Mathematical simulation when both pulsatile pumps are not working.

For both pressure and flow, only the mean is achieved. Cyan - the desired waveforms. Magenta - the achieved values. Yellow - the error (the desired value – the achieved value).

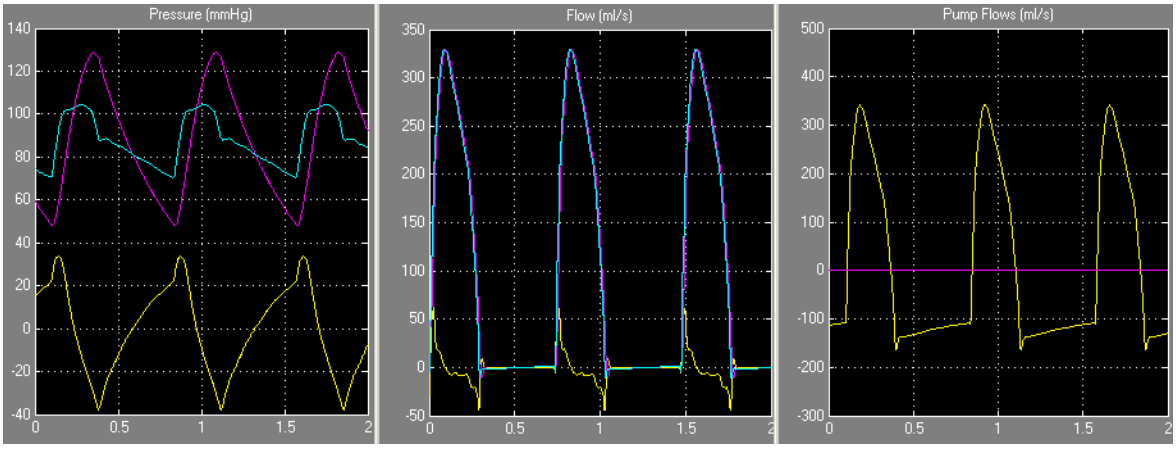

Figure B-3 Mathematical simulation when only the upstream pulsatile pump is working. Pressure is not controlled. Its shape is different from the desired one. Flow is achieved. Cyan - the desired waveforms. Magenta - the achieved values. Yellow - the error or the pulsatile pump flow.

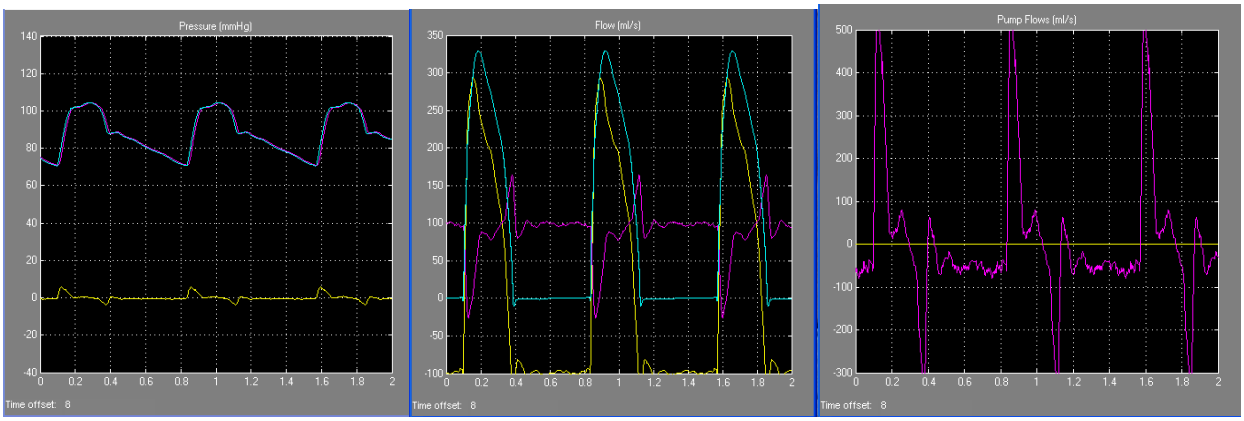

Figure B-4 Mathematical simulation when only the downstream pulsatile pump is working.

Pressure is well controlled. Flow is not controlled. Its shape is different from the desired one. Cyan - the desired waveforms. Magenta - the achieved values. Yellow - the error or the pulatile pump flow.

Figure B-5 Mathematical simulation when both pulsatile pumps are working.

Pressure is well controlled. Flow is also well controlled. Therefore, this system maintains mean pressure, mean flow, pulse flow, and pulse pressure. Cyan - the desired waveforms in A and B. Magenta - the achieved values in A and B, the output of the downstream pulsatile pump in C. Yellow - the error in A and B, the output of the upstream pulsatile pump in C.

B.2 MODEL PREDICTIVE CONTROL OF PULSATILE FLOW IN AN *IN VITRO* SYSTEM

In the idealized model (Figure B-1), parameters of the system are known. The pumps can also move very rapidly. However, these are not the case in reality. Therefore, we wanted to construct a model of the real system. Then, some control strategies were applied to control these variables. Model predictive control (MPC) has been used in chemical process control problems. Therefore, MPC was used to recreate the required flow waveform.

Methods

Perfusion system. A pulsatile flow has two components. One is the mean flow. The other is the pulsatile part. The current setup was aimed at the rabbit aortic flow waveform, which had negative flow. The mean flow was generated through a MasterFlex peristaltic pump (A in Figure B-6, Cole-Parmer) with a dampener (B, Cole-Parmer) filled with air in the upper part. A syringe pump (D) was used to generate the pulsatile part of the flow. This syringe pump was driven by a linear voice coil motor (LA25-42-000A, BEI Kimco Magnetics), which was controlled in real-time. A sensor was connected to the shaft of the motor to provide position information (DS16 displacement sensor, Equipment Solutions Inc.). A one-way valve (C, Cole-Parmer) was used to prevent backflow. The in-line flow rate sensor (E) and pressure transducer (F) were connected upstream of the vessel culture chamber (G). The mean pressure was adjusted with a valve (H). The medium entered into a reservoir (I). Data acquisition was through the Quanser DAQ board (Quanser Inc., Canada).

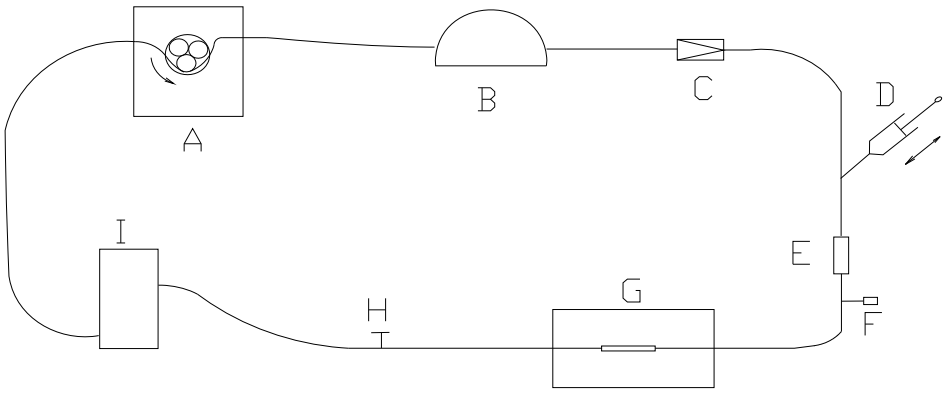

Figure B-6 Schematic of the pulsatile perfusion system.

A: MasterFlex peristaltic pump; B: dampener; C: one-way valve; D: syringe pump driven by a linear motor; E: in-line flow rate sensor; F: pressure transducer; G: culture chamber; H: manual valve; I: reservoir.

Control strategy. MPC does not designate a specific control strategy but a very ample range of control methods which make an explicit use of a model of the process to obtain the control signal by minimizing an objective function. The model is used to predict the process output at future time instants. One specific algorithm, Dynamic Matrix Control (DMC), was used to control the movement of the linear motor in this project. DMC uses the step response model:

$$y(t) = \sum_{i=1}^{\infty} g_i \Delta u(t-i)$$

Where, g_i is the coefficient of the step response, u is the input to the system, y is the output.

The linear motion of the motor changes the measured flow. The position change of the motor is the input to the system; flow is the output. Because it was not practical to have a perfect step change in the motor position, a ramp change of position was applied to derive the step response coefficients g_i. The position control was through the Quanser system, which provided a real-time control platform. The Quanser system was based on Simulink. A PID loop was used to

control the position. The total position change was divided into W segments; the number of step response coefficients was M. The formula to calculate the step response coefficients matrix G is

$$G=(UTU)^{-1}U^{T}Y,$$

Where, U is the input (position) matrix, Y is the output (flow) matrix. An example of the step response model is shown in Figure B-7.

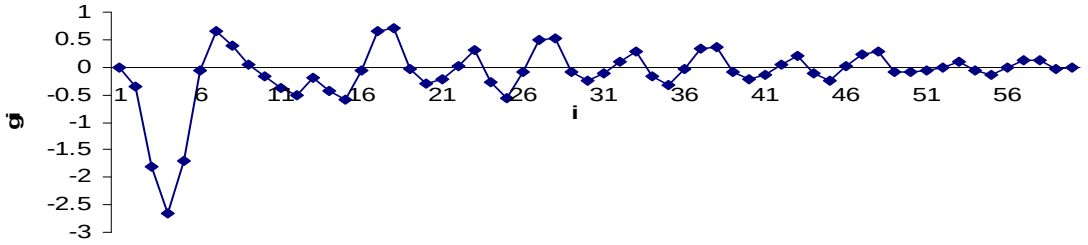

Figure B-7 One example of the step response.

DMC used the concepts of free and forced responses, which express the control sequence as the addition of the two signals:

$$u(t) = u_f(t) + u_c(t)$$

Where, $u_f(t)$ corresponds to the past inputs; $u_c(t)$ is the control move in the future.

The objective of a DMC controller is to control the output as close to the setpoint as possible in the lease-square sense with the possibility of the inclusion of a penalty term on the input moves. The objective function is

$$J = \sum_{j=1}^{p}[\hat{y}(t+j|t) - w(t+j)]^2 + \sum_{j=1}^{m}\lambda[\Delta u(t+j-1)]^2$$

Where, $\hat{y}$ is the predicted output, w is the output reference (desired flow rate), p is the prediction horizon, m is the control horizon, λ is the input penalty factor.

If there are no constraints, the solution by minimizing J is

$$u=(G^TG+\lambda I)^{-1}G^T(w-f)$$

Where, G is the system's dynamic matrix, which has the step response coefficients as its elements, I is the unit matrix, f is the free response including disturbance terms. In this algorithm, m and λ can be adjusted. It should be mentioned that only the first element of u was actually sent to the controller as the input. The position input u was then used as the command in the inner PID position control loop. The output signal from the real-time program was input to a brush type PWM servo amplifier (MSA-12-80, Galil Motion Control) first before it reached the motor.

Results

Using one quarter of the measured rabbit aortic flow waveform as the command, the actual flow rate is shown in Figure B-8. These two waveforms matched pretty well.

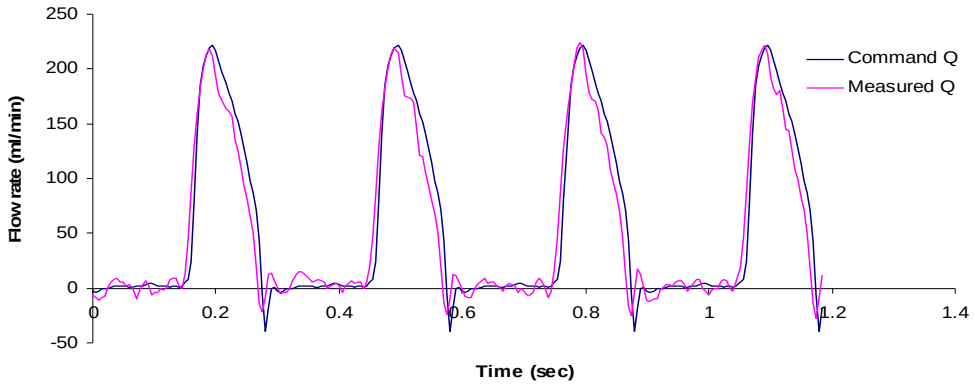

Figure B-8 The command and actual flow rates generated using the DMC control.

However, as simulated in B-3, the pressure waveform was not desired. Further efforts had been devoted to control the pressure waveform simultaneously. One method was to use a PID

controller to control the downstream pump. However, the movement of this downstream pump also changed the flow generated by the upstream pump. Therefore, there were interactions between these two pumps. The model (Figure B-7) generated when only the upstream pump was running was no longer valid. It was necessary to construct a model when both pumps were running. However, the quality of the model was very poor for this two inputs-two outputs problem, especially for the pressure model. Without good models of flow and pressure for each of these two pumps, it is not possible to recreate pressure and flow waveforms which are very dynamic (steep slope, high frequency (3 Hz for rabbits)).

A feasible method is to control flow dynamically using an upstream pump while manipulating the properties of the loop to match the impedance of the system, thus a reasonable good pressure waveform can be realized. One simulation example of changing the compliance of the downstream tubing is shown in Figure B-9. The pressure waveforms match well after increasing the compliance.

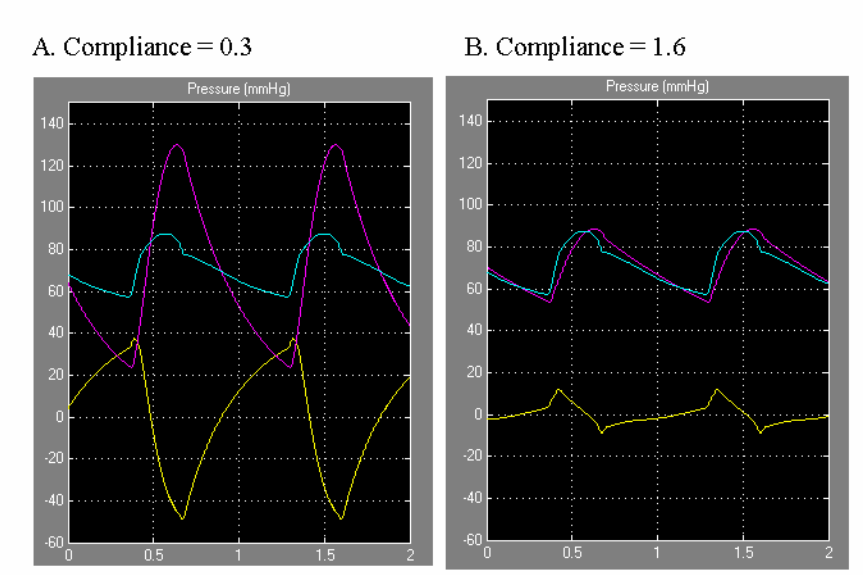

Figure B-9 Mathematical simulation of the effects of changing the compliance of the downstream tubing when only the upstream pulsatile pump is working.

Pressure is not actively controlled. Its shape is much different from the desired one when the compliance is low. However, the achieved pressure waveform is very close to the desired one by increasing the compliance from 0.3 to 1.6. Flow control is achieved in both cases. Cyan - the desired waveforms. Magenta - the achieved values. Yellow - the error.

APPENDIX C

DRAWINGS OF THE VASCULAR STABILIZER

Vascular stabilizers were cumtom-designed and manufactured to maintain the in vivo length of a rabbit aorta after havesting. A stabilizer has two parts: a clamp bar and a slider. The pictures and drawings were generaged in SolidWorks (SolidWorks Corp.) and are shown here.

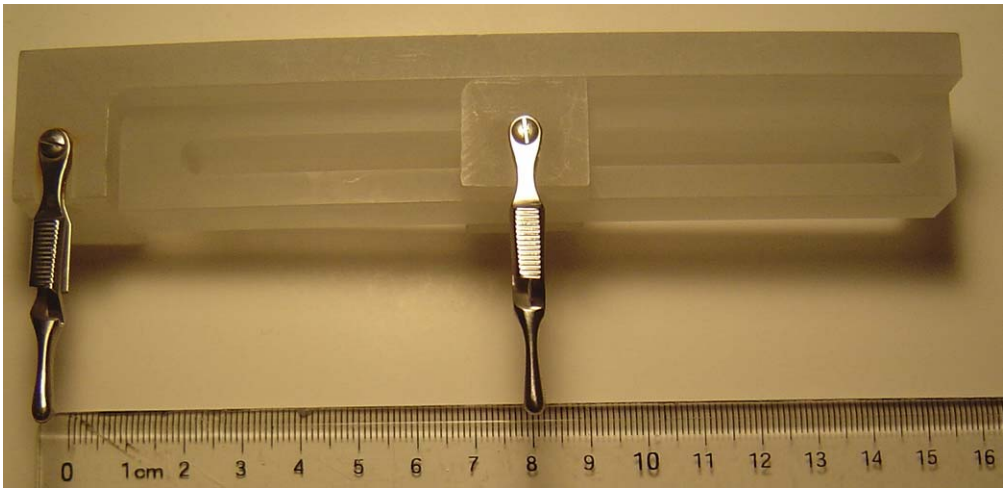

Figure C-1 The stabilzer.

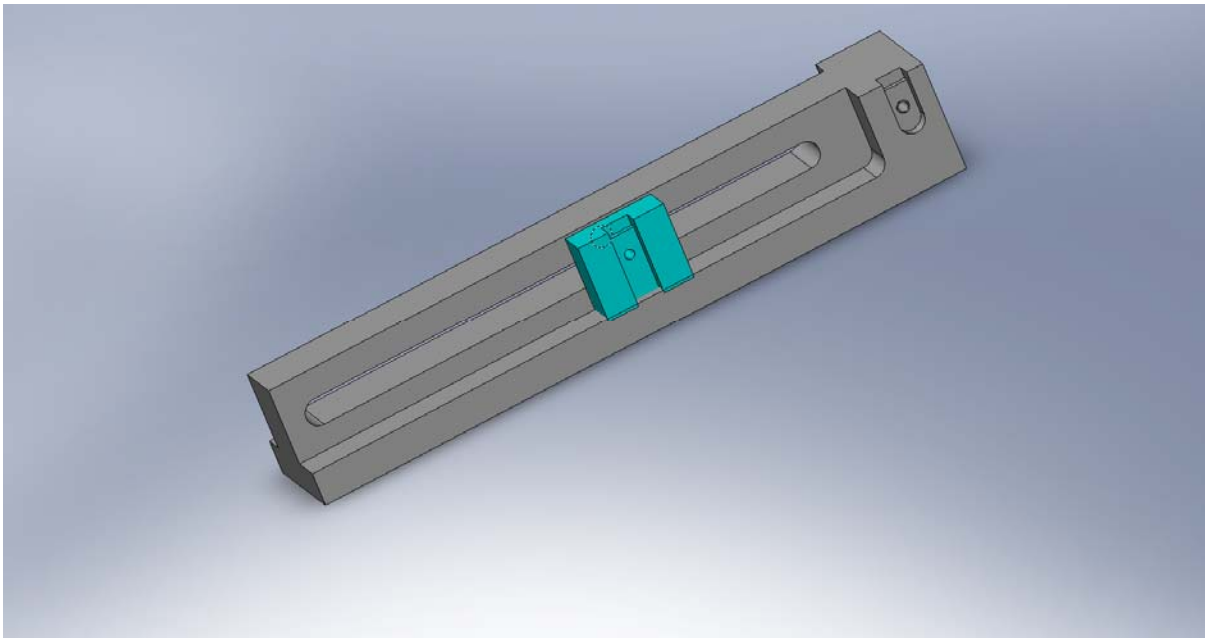

Figure C-2 The three dimentional view of a vascular stabilizer showing the clamp bar and slider.

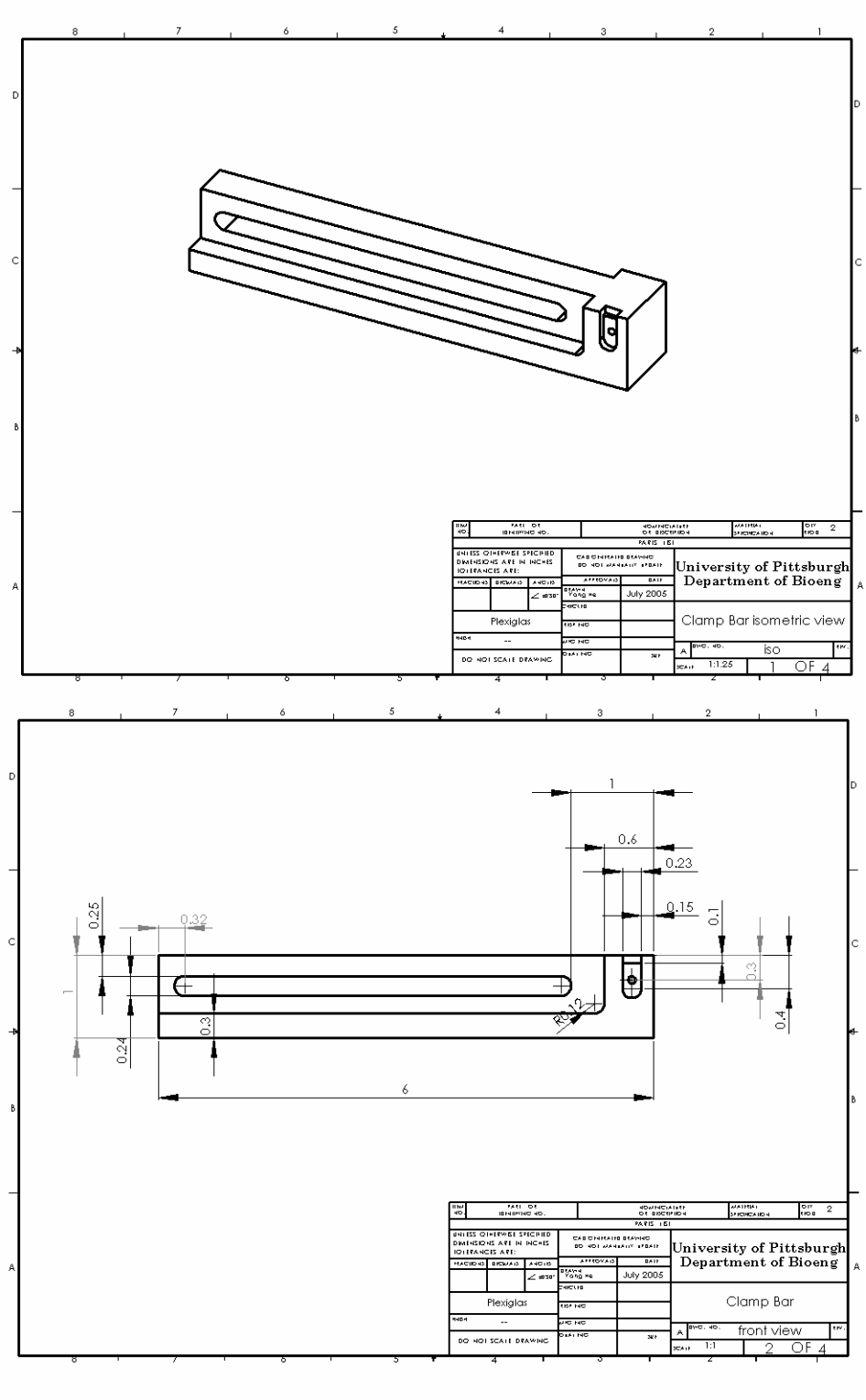

Figure C-3 The isometric and front views of the clamp bar.

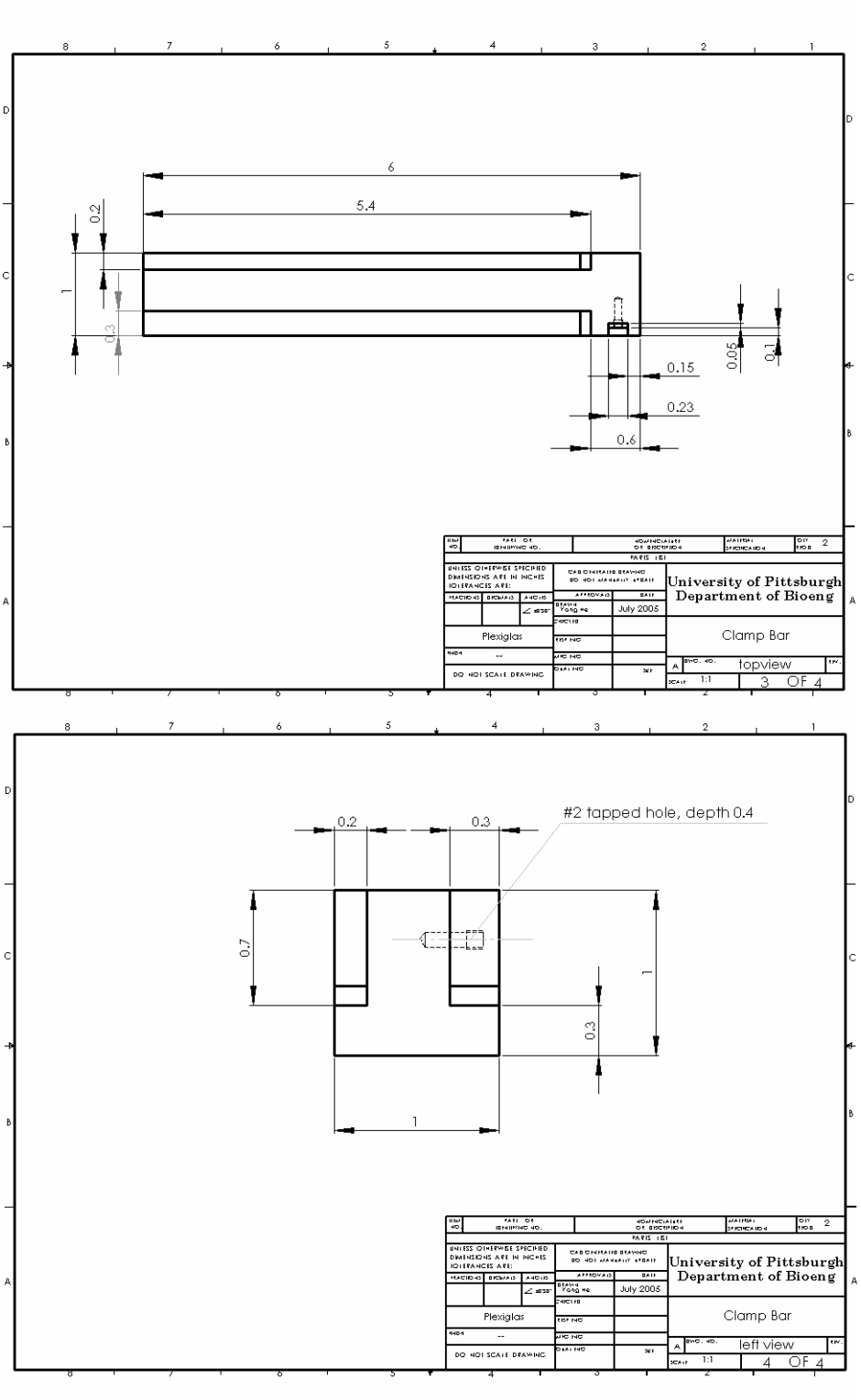

Figure C-4 The top and left views of the clamp bar.

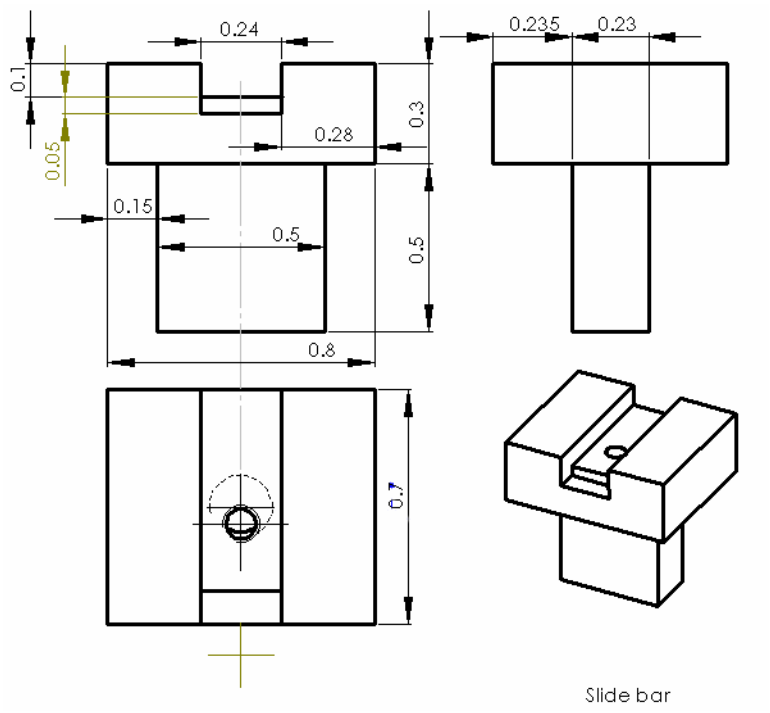

Figure C-5 The slider.

BIBLIOGRAPHY

1. Harrison D, Griendling KK, Landmesser U, Hornig B, Drexler H. Role of oxidative stress in atherosclerosis. *The American Journal of Cardiology.* 2003;91(3, Supplement 1):7-11.

2. VanderLaan PA, Reardon CA, Getz GS. Site Specificity of Atherosclerosis: Site-Selective Responses to Atherosclerotic Modulators. *Arterioscler Thromb Vasc Biol.* 2004;24(1):12-22.

3. Ku DN, Giddens DP, Zarins CK, Glagov S. Pulsatile flow and atherosclerosis in the human carotid bifurcation. Positive correlation between plaque location and low oscillating shear stress. *Arteriosclerosis.* 1985;5(3):293-302.

4. Davies PF. Flow-Mediated Endothelial Mechanotransduction. *PHYSIOLOGICAL REVIEWS.* 1995;75(3):591-560.

5. Malek AM, Alper SL, Izumo S. Hemodynamic shear stress and its role in atherosclerosis. *Jama.* 1999;282(21):2035-2042.

6. Garin G, Berk BC. Flow-mediated signaling modulates endothelial cell phenotype. *Endothelium.* 2006;13(6):375-384.

7. Moore J, Berry J. Fluid and solid mechanical implications of vascular stenting. *Ann Biomed Eng.* 2002;30(4):498-508.

8. Kumar NM, Gilula NB. The Gap Junction Communication Channel. *Cell.* 1996;84(3):381-388.

9. Haefliger JA, Nicod P, Meda P. Contribution of connexins to the function of the vascular wall. *Cardiovascular Research.* 2004;62(2):345-356.

10. Kwak BR, Veillard N, Pelli G, Mulhaupt F, James RW, Chanson M, Mach F. Reduced connexin43 expression inhibits atherosclerotic lesion formation in low-density lipoprotein receptor-deficient mice. *Circulation.* 2003;107(7):1033-1039.

11. Liao Y, Regan CP, Manabe I, Owens GK, Day KH, Damon DN, Duling BR. Smooth Muscle-Targeted Knockout of Connexin43 Enhances Neointimal Formation in Response to Vascular Injury. *Arterioscler Thromb Vasc Biol.* 2007.

12. Kwak B, Silacci P, Stergiopulos N, Hayoz D, Meda P. Shear stress and cyclic circumferential stretch, but not pressure, alter connexin43 expression in endothelial cells. *Cell Communication & Adhesion.* 2005;12(5 - 6):261-270.

13. DePaola N, Davies PF, Pritchard WF, Jr., Florez L, Harbeck N, Polacek DC. Spatial and temporal regulation of gap junction connexin43 in vascular endothelial cells exposed to controlled disturbed flows in vitro. *Proc Natl Acad Sci U S A.* 1999;96(6):3154-3159.

14. Cowan DB, Lye SJ, Langille BL. Regulation of vascular connexin43 gene expression by mechanical loads. *Circ Res.* 1998;82(7):786-793.

15. Wolinsky H, Glagov S. Structural basis for the static mechanical properties of the aortic media. *Circ Res.* 1964;14:400-413.

16. Ku DN. BLOOD FLOW IN ARTERIES. *Annu. Rev. Fluid Mech.* 1997;29(1):399-434.

17. Chen K-D, Li Y-S, Kim M, Li S, Yuan S, Chien S, Shyy JY-J. Mechanotransduction in Response to Shear Stress. ROLES OF RECEPTOR TYROSINE KINASES, INTEGRINS, AND Shc. *J. Biol. Chem.* 1999;274(26):18393-18400.

18. Jalali S, del Pozo MA, Chen K-D, Miao H, Li Y-S, Schwartz MA, Shyy JY-J, Chien S. Integrin-mediated mechanotransduction requires its dynamic interaction with specific extracellular matrix (ECM) ligands. *PNAS.* 2001;98(3):1042-1046.

19. Kuchan M, H J, JA F. Role of G proteins in shear stress-mediated nitric oxide production by endothelial cells. *Am J Physiol.* 1994;267:C753-C758.

20. Tzima E, Irani-Tehrani M, Kiosses WB, Dejana E, Schultz DA, Engelhardt B, Cao G, DeLisser H, Schwartz MA. A mechanosensory complex that mediates the endothelial cell response to fluid shear stress. *Nature.* 2005;437(7057):426-431.

21. Weinbaum S, Zhang X, Han Y, Vink H, Cowin SC. Mechanotransduction and flow across the endothelial glycocalyx. *PNAS.* 2003;100(13):7988-7995.

22. Flaherty JT, Pierce JE, Ferrans VJ, Patel DJ, Tucker WK, Fry DL. Endothelial nuclear patterns in the canine arterial tree with particular reference to hemodynamic events. *Circ Res.* 1972;30(1):23-33.

23. Helmlinger G, Geiger RV, Schreck S, Nerem RM. Effects of pulsatile flow on cultured vascular endothelial cell morphology. *J Biomech Eng.* 1991;113(2):123-131.

24. Langille BL, O'Donnell F. Reductions in arterial diameter produced by chronic decreases in blood flow are endothelium-dependent. *Science.* 1986;231(4736):405-407.

25. Yu J, Bergaya S, Murata T, Alp IF, Bauer MP, Lin MI, Drab M, Kurzchalia TV, Stan RV, Sessa WC. Direct evidence for the role of caveolin-1 and caveolae in mechanotransduction and remodeling of blood vessels. *J Clin Invest.* 2006;116(5):1284-1291.

26. Yamamoto K, Sokabe T, Matsumoto T, Yoshimura K, Shibata M, Ohura N, Fukuda T, Sato T, Sekine K, Kato S, Isshiki M, Fujita T, Kobayashi M, Kawamura K, Masuda H, Kamiya A, Ando J. Impaired flow-dependent control of vascular tone and remodeling in P2X4-deficient mice. *Nat Med.* 2006;12(1):133-137.

27. Castier Y, Brandes RP, Leseche G, Tedgui A, Lehoux S. p47phox-Dependent NADPH Oxidase Regulates Flow-Induced Vascular Remodeling. *Circ Res.* 2005;97(6):533-540.

28. Radel C, Carlile-Klusacek M, Rizzo V. Participation of caveolae in beta1 integrin-mediated mechanotransduction. *Biochemical and Biophysical Research Communications.* 2007;358(2):626-631.

29. Nadaud S, Philippe M, Arnal J-F, Michel J-B, Soubrier F. Sustained Increase in Aortic Endothelial Nitric Oxide Synthase Expression In Vivo in a Model of Chronic High Blood Flow. *Circ Res.* 1996;79(4):857-863.

30. Uematsu M, Y O, JP N, K N, TJ M, RW A, RM N, DG H. Regulation of endothelial cell nitric oxide synthase mRNA expression by shear stress. *Am J Physiol.* 1995;269:C1371-C1378.

31. Davis ME, Cai H, Drummond GR, Harrison DG. Shear Stress Regulates Endothelial Nitric Oxide Synthase Expression Through c-Src by Divergent Signaling Pathways. *Circ Res.* 2001;89(11):1073-1080.

32. Weber M, Hagedorn CH, Harrison DG, Searles CD. Laminar Shear Stress and 3' Polyadenylation of eNOS mRNA. *Circ Res.* 2005;96(11):1161-1168.

33. Boo YC, Sorescu G, Boyd N, Shiojima I, Walsh K, Du J, Jo H. Shear Stress Stimulates Phosphorylation of Endothelial Nitric-oxide Synthase at Ser1179 by Akt-independent Mechanisms. ROLE OF PROTEIN KINASE A. *J. Biol. Chem.* 2002;277(5):3388-3396.

34. Zhang Y, Lee T-S, Kolb EM, Sun K, Lu X, Sladek FM, Kassab GS, Garland T, Jr, Shyy JY-J. AMP-Activated Protein Kinase Is Involved in Endothelial NO Synthase Activation in Response to Shear Stress. *Arterioscler Thromb Vasc Biol.* 2006;26(6):1281-1287.

35. Garcia-Cardena G, Fan R, Shah V, Sorrentino R, Cirino G, Papapetropoulos A, Sessa W. Dynamic activation of endothelial nitric oxide synthase by Hsp90. *Nature.* 1998;392(6678):821-824.

36. Dekker RJ, van Thienen JV, Rohlena J, de Jager SC, Elderkamp YW, Seppen J, de Vries CJM, Biessen EAL, van Berkel TJC, Pannekoek H, Horrevoets AJG. Endothelial KLF2 Links Local Arterial Shear Stress Levels to the Expression of Vascular Tone-Regulating Genes. *Am J Pathol.* 2005;167(2):609-618.

37. Atkins GB, Jain MK. Role of Kruppel-Like Transcription Factors in Endothelial Biology. *Circ Res.* 2007;100(12):1686-1695.

38. Parmar KM, Larman HB, Dai G, Zhang Y, Wang ET, Moorthy SN, Kratz JR, Lin Z, Jain MK, Gimbrone MA, Jr., Garcia-Cardena G. Integration of flow-dependent endothelial phenotypes by Kruppel-like factor 2. *J. Clin. Invest.* 2006;116(1):49-58.

39. Wang N, Miao H, Li YS, Zhang P, Haga JH, Hu Y, Young A, Yuan S, Nguyen P, Wu CC, Chien S. Shear stress regulation of Kruppel-like factor 2 expression is flow pattern-specific. *Biochem Biophys Res Commun.* 2006;341(4):1244-1251.

40. Sen-Banerjee S, Mir S, Lin Z, Hamik A, Atkins GB, Das H, Banerjee P, Kumar A, Jain MK. Kruppel-Like Factor 2 as a Novel Mediator of Statin Effects in Endothelial Cells. *Circulation.* 2005;112(5):720-726.

41. Lin Z, Kumar A, SenBanerjee S, Staniszewski K, Parmar K, Vaughan DE, Gimbrone MA, Jr, Balasubramanian V, Garcia-Cardena G, Jain MK. Kruppel-Like Factor 2 (KLF2) Regulates Endothelial Thrombotic Function. *Circ Res.* 2005;96(5):e48-57.

42. Lin Z, Hamik A, Jain R, Kumar A, Jain MK. Kruppel-Like Factor 2 Inhibits Protease Activated Receptor-1 Expression and Thrombin-Mediated Endothelial Activation. *Arterioscler Thromb Vasc Biol.* 2006;26(5):1185-.

43. Boon RA, Fledderus JO, Volger OL, van Wanrooij EJA, Pardali E, Weesie F, Kuiper J, Pannekoek H, ten Dijke P, Horrevoets AJG. KLF2 Suppresses TGF-{beta} Signaling in Endothelium Through Induction of Smad7 and Inhibition of AP-1. *Arterioscler Thromb Vasc Biol.* 2007;27(3):532-539.

44. Magid R, Davies PF. Endothelial protein kinase C isoform identity and differential activity of PKCzeta in an athero-susceptible region of porcine aorta. *Circ Res.* 2005;97(5):443-449.

45. Hwang J, Ing MH, Salazar A, Lassegue B, Griendling K, Navab M, Sevanian A, Hsiai TK. Pulsatile Versus Oscillatory Shear Stress Regulates NADPH Oxidase Subunit Expression: Implication for Native LDL Oxidation. *Circ Res.* 2003;93(12):1225-1232.

46. Sorescu GP, Sykes M, Weiss D, Platt MO, Saha A, Hwang J, Boyd N, Boo YC, Vega JD, Taylor WR, Jo H. Bone Morphogenic Protein 4 Produced in Endothelial Cells by Oscillatory Shear Stress Stimulates an Inflammatory Response. *J. Biol. Chem.* 2003;278(33):31128-31135.

47. Csiszar A, Labinskyy N, Smith KE, Rivera A, Bakker ENTP, Jo H, Gardner J, Orosz Z, Ungvari Z. Downregulation of Bone Morphogenetic Protein 4 Expression in Coronary Arterial Endothelial Cells: Role of Shear Stress and the cAMP/Protein Kinase A Pathway. *Arterioscler Thromb Vasc Biol.* 2007;27(4):776-782.

48. Acevedo A, Bowser S, Gerritsen M, Bizios R. Morphological and proliferative responses of endothelial cells to hydrostatic pressure: role of fibroblast growth factor. *J Cell Physiol.* 1993;157(3):603-614.

49. Schwartz EA, Bizios R, Medow MS, Gerritsen ME. Exposure of Human Vascular Endothelial Cells to Sustained Hydrostatic Pressure Stimulates Proliferation : Involvement of the {alpha}V Integrins. *Circ Res.* 1999;84(3):315-322.

50. Tokunaga O, Watanabe T. Properties of endothelial cell and smooth muscle cell cultured in ambient pressure. *In Vitro Cell Dev Biol.* 1987;23(8):528-534.

51. Shin H, Gerritsen M, Bizios R. Regulation of endothelial cell proliferation and apoptosis by cyclic pressure. *Annals of biomedical engineering.* 2002;30(3):297-304.

52. Hishikawa K, Nakaki T, Marumo T, Suzuki H, Kato R, Saruta T. Pressure Enhances Endothelin-1 Release From Cultured Human Endothelial Cells. *Hypertension.* 1995;25(3):449-452.

53. Tokunaga O, Fan J, Watanabe T. Atherosclerosis and endothelium. Part II. Properties of aortic endothelial and smooth muscle cells cultured at various ambient pressures. *Acta Pathol Jpn.* 1989;39(6):356-362.

54. Sasamoto A, Nagino M, Kobayashi S, Naruse K, Nimura Y, Sokabe M. Mechanotransduction by integrin is essential for IL-6 secretion from endothelial cells in response to uniaxial continuous stretch. *Am J Physiol Cell Physiol.* 2005;288(5):C1012-1022.

55. Shin H, Bizios R, Gerritsen M. Cyclic pressure modulates endothelial barrier function. *Endothelium.* 2003;10(3):179-187.

56. Dixit M, Loot AE, Mohamed A, Fisslthaler B, Boulanger CM, Ceacareanu B, Hassid A, Busse R, Fleming I. Gab1, SHP2, and Protein Kinase A Are Crucial for the Activation of the Endothelial NO Synthase by Fluid Shear Stress. *Circ Res.* 2005;97(12):1236-1244.

57. Zhao S, Suciu A, Ziegler T, Moore JE, Jr, Burki E, Meister J-J, Brunner HR. Synergistic Effects of Fluid Shear Stress and Cyclic Circumferential Stretch on Vascular Endothelial Cell Morphology and Cytoskeleton. *Arterioscler Thromb Vasc Biol.* 1995;15(10):1781-1786.

58. Kaunas R, Nguyen P, Usami S, Chien S. Cooperative effects of Rho and mechanical stretch on stress fiber organization. *Proc Natl Acad Sci U S A.* 2005;102(44):15895-15900.

59. Naruse K, Yamada T, Sai X, Hamaguchi M, Sokabe M. Pp125FAK is required for stretch dependent morphological response of endothelial cells. *Oncogene.* 1998;17(4):455-463.

60. Kaunas R, Usami S, Chien S. Regulation of stretch-induced JNK activation by stress fiber orientation. *Cell Signal.* 2006.

61. Shin HY, Smith ML, Toy KJ, Williams PM, Bizios R, Gerritsen ME. VEGF-C mediates cyclic pressure-induced endothelial cell proliferation. *Physiol. Genomics.* 2002;11(3):245-251.

62. Cevallos M, Riha GM, Wang X, Yang H, Yan S, Li M, Chai H, Yao Q, Chen C. Cyclic strain induces expression of specific smooth muscle cell markers in human endothelial cells. *Differentiation.* 2006;74(9-10):552-561.

63. Morrow D, Cullen JP, Cahill PA, Redmond EM. Cyclic Strain Regulates the Notch/CBF-1 Signaling Pathway in Endothelial Cells: Role in Angiogenic Activity. *Arterioscler Thromb Vasc Biol.* 2007;27(6):1289-1296.

64. Takeda H, Komori K, Nishikimi N, Nimura Y, Sokabe M, Naruse K. Bi-phasic activation of eNOS in response to uni-axial cyclic stretch is mediated by differential mechanisms in BAECs. *Life Sci.* 2006;79(3):233-239.

65. Li M, Chiou K-R, Bugayenko A, Irani K, Kass DA. Reduced Wall Compliance Suppresses Akt-Dependent Apoptosis Protection Stimulated by Pulse Perfusion. *Circ Res.* 2005;97(6):587-595.

66. Hishikawa K, Luscher TF. Pulsatile stretch stimulates superoxide production in human aortic endothelial cells. *Circulation.* 1997;96(10):3610-3616.

67. Wang DM, Tarbell JM. Modeling interstitial flow in an artery wall allows estimation of wall shear stress on smooth muscle cells. *J Biomech Eng.* 1995;117(3):358-363.

68. Sharma R, Yellowley CE, Civelek M, Ainslie K, Hodgson L, Tarbell JM, Donahue HJ. Intracellular calcium changes in rat aortic smooth muscle cells in response to fluid flow. *Annals of biomedical engineering.* 2002;30(3):371-378.

69. Civelek M, Ainslie K, Garanich JS, Tarbell JM. Smooth muscle cells contract in response to fluid flow via a Ca2+-independent signaling mechanism. *J Appl Physiol.* 2002;93(6):1907-1917.

70. Oancea E, Wolfe JT, Clapham DE. Functional TRPM7 Channels Accumulate at the Plasma Membrane in Response to Fluid Flow. *Circ Res.* 2006;98(2):245-253.

71. Papadaki M, Tilton RG, Eskin SG, McIntire LV. Nitric oxide production by cultured human aortic smooth muscle cells: stimulation by fluid flow. *Am J Physiol.* 1998;274(2 Pt 2):H616-626.

72. Garanich JS, Pahakis M, Tarbell JM. Shear stress inhibits smooth muscle cell migration via nitric oxide-mediated downregulation of matrix metalloproteinase-2 activity. *Am J Physiol Heart Circ Physiol.* 2005;288(5):H2244-2252.

73. Wang H, Yan S, Chai H, Riha GM, Li M, Yao Q, Chen C. Shear stress induces endothelial transdifferentiation from mouse smooth muscle cells. *Biochemical and Biophysical Research Communications.* 2006;346(3):860-865.

74. Birukov KG, Bardy N, Lehoux S, Merval R, Shirinsky VP, Tedgui A. Intraluminal Pressure Is Essential for the Maintenance of Smooth Muscle Caldesmon and Filamin Content in Aortic Organ Culture. *Arterioscler Thromb Vasc Biol.* 1998;18(6):922-927.

75. Albinsson S, Nordstrom I, Hellstrand P. Stretch of the vascular wall induces smooth muscle differentiation by promoting actin polymerization. *The Journal of biological chemistry.* 2004;279(33):34849-34855.

76. Morrow D, Scheller A, Birney YA, Sweeney C, Guha S, Cummins PM, Murphy R, Walls D, Redmond EM, Cahill PA. Notch-mediated CBF-1/RBP-J{kappa}-dependent regulation of human vascular smooth muscle cell phenotype in vitro. *Am J Physiol Cell Physiol.* 2005;289(5):C1188-1196.

77. Tsuda Y, Okazaki M, Uezono Y, Osajima A, Kato H, Okuda H, Oishi Y, Yashiro A, Nakashima Y. Activation of extracellular signal-regulated kinases is essential for pressure-induced proliferation of vascular smooth muscle cells. *European Journal of Pharmacology.* 2002;446(1-3):15-24.

78. MAYR M, LI C, ZOU Y, HUEMER U, HU Y, XU Q. Biomechanical stress-induced apoptosis in vein grafts involves p38 mitogen-activated protein kinases. *FASEB J.* 2000;14(2):261-270.

79. Wernig F, Mayr M, Xu Q. Mechanical stretch-induced apoptosis in smooth muscle cells is mediated by beta1-integrin signaling pathways. *Hypertension.* 2003;41(4):903-911.

80. Zampetaki A, Zhang Z, Hu Y, Xu Q. Biomechanical stress induces IL-6 expression in smooth muscle cells via Ras/Rac1-p38 MAPK-NF-kappaB signaling pathways. *Am J Physiol Heart Circ Physiol.* 2005;288(6):H2946-2954.

81. Morrow D, Sweeney C, Birney YA, Guha S, Collins N, Cummins PM, Murphy R, Walls D, Redmond EM, Cahill PA. Biomechanical regulation of hedgehog signaling in vascular smooth muscle cells in vitro and in vivo. *Am J Physiol Cell Physiol.* 2007;292(1):C488-496.

82. Romer LH, Birukov KG, Garcia JG. Focal adhesions: paradigm for a signaling nexus. *Circ Res.* 2006;98(5):606-616.

83. Lehoux S, Esposito B, Merval R, Tedgui A. Differential regulation of vascular focal adhesion kinase by steady stretch and pulsatility. *Circulation.* 2005;111(5):643-649.

84. Reusch HP, Chan G, Ives HE, Nemenoff RA. Activation of JNK/SAPK and ERK by Mechanical Strain in Vascular Smooth Muscle Cells Depends on Extracellular Matrix Composition. *Biochemical and Biophysical Research Communications.* 1997;237(2):239-244.

85. Xu Q, Liu Y, Gorospe M, Udelsman R, Holbrook NJ. Acute hypertension activates mitogen-activated protein kinases in arterial wall. *J Clin Invest.* 1996;97(2):508-514.

86. Birukov KG, Lehoux S, Birukova AA, Merval R, Tkachuk VA, Tedgui A. Increased Pressure Induces Sustained Protein Kinase C–Independent Herbimycin A–Sensitive Activation of Extracellular Signal–Related Kinase 1/2 in the Rabbit Aorta in Organ Culture *Circ Res.* 1997;81(6):895-903.

87. Lehoux S, Esposito B, Merval R, Loufrani L, Tedgui A. Pulsatile stretch-induced extracellular signal-regulated kinase 1/2 activation in organ culture of rabbit aorta involves reactive oxygen species. *Arterioscler Thromb Vasc Biol.* 2000;20(11):2366-2372.

88. Hishikawa K, Oemar BS, Yang Z, Luscher TF. Pulsatile Stretch Stimulates Superoxide Production and Activates Nuclear Factor-{kappa}B in Human Coronary Smooth Muscle. *Circ Res.* 1997;81(5):797-803.

89. Lemarie CA, Esposito B, Tedgui A, Lehoux S. Pressure-Induced Vascular Activation of Nuclear Factor-{kappa}B: Role in Cell Survival. *Circ Res.* 2003;93(3):207-212.

90. Lemarie CA, Tharaux P-L, Esposito B, Tedgui A, Lehoux S. Transforming Growth Factor-{alpha} Mediates Nuclear Factor {kappa}B Activation in Strained Arteries. *Circ Res.* 2006;99(4):434-441.

91. Newby AC. Matrix metalloproteinases regulate migration, proliferation, and death of vascular smooth muscle cells by degrading matrix and non-matrix substrates. *Cardiovasc Res.* 2006;69(3):614-624.

92. Asanuma K, Magid R, Johnson C, Nerem RM, Galis ZS. Uniaxial strain upregulates matrix-degrading enzymes produced by human vascular smooth muscle cells. *Am J Physiol Heart Circ Physiol.* 2003;284(5):H1778-1784.

93. Grote K, Flach I, Luchtefeld M, Akin E, Holland SM, Drexler H, Schieffer B. Mechanical Stretch Enhances mRNA Expression and Proenzyme Release of Matrix Metalloproteinase-2 (MMP-2) via NAD(P)H Oxidase-Derived Reactive Oxygen Species. *Circ Res.* 2003;92(11):80e-86.

94. Mavromatis K, Fukai T, Tate M, Chesler N, Ku DN, Galis ZS. Early Effects of Arterial Hemodynamic Conditions on Human Saphenous Veins Perfused Ex Vivo. *Arterioscler Thromb Vasc Biol.* 2000;20(8):1889-1895.

95. Sharony R, Pintucci G, Saunders PC, Grossi EA, Baumann FG, Galloway AC, Mignatti P. Matrix metalloproteinase expression in vein grafts: role of inflammatory mediators and

extracellular signal-regulated kinases-1 and -2. *Am J Physiol Heart Circ Physiol.* 2006;290(4):H1651-1659.

96. Meng X, Mavromatis K, Galis ZS. Mechanical stretching of human saphenous vein grafts induces expression and activation of matrix-degrading enzymes associated with vascular tissue injury and repair. *Exp Mol Pathol.* 1999;66(3):227-237.

97. Brooks PC, Stromblad S, Sanders LC, von Schalscha TL, Aimes RT, Stetler-Stevenson WG, Quigley JP, Cheresh DA. Localization of matrix metalloproteinase MMP-2 to the surface of invasive cells by interaction with integrin alpha v beta 3. *Cell.* 1996;85(5):683-693.

98. Chesler NC, Ku DN, Galis ZS. Transmural pressure induces matrix-degrading activity in porcine arteries ex vivo. *Am J Physiol Heart Circ Physiol.* 1999;277(5):H2002-2009.

99. Lehoux S, Lemarie CA, Esposito B, Lijnen HR, Tedgui A. Pressure-induced matrix metalloproteinase-9 contributes to early hypertensive remodeling. *Circulation.* 2004;109(8):1041-1047.

100. Galis ZS, Johnson C, Godin D, Magid R, Shipley JM, Senior RM, Ivan E. Targeted Disruption of the Matrix Metalloproteinase-9 Gene Impairs Smooth Muscle Cell Migration and Geometrical Arterial Remodeling. *Circ Res.* 2002;91(9):852-859.

101. Watts SW, Rondelli C, Thakali K, Li X, Uhal B, Pervaiz MH, Watson RE, Fink GD. Morphological and biochemical characterization of remodeling in aorta and vena cava of DOCA-salt hypertensive rats. *Am J Physiol Heart Circ Physiol.* 2007;292(5):H2438-2448.

102. Vorp D, Peters D, Webster M. Gene expression is altered in perfused arterial segments exposed to cyclic flexure ex vivo. *Annals of biomedical engineering.* 1999;27(3):366-371.

103. Cummins PM, von Offenberg Sweeney N, Killeen MT, Birney YA, Redmond EM, Cahill PA. Cyclic strain-mediated matrix metalloproteinase regulation within the vascular endothelium: a force to be reckoned with. *Am J Physiol Heart Circ Physiol.* 2007;292(1):H28-42.

104. von Offenberg Sweeney N, Cummins PM, Birney YA, Cullen JP, Redmond EM, Cahill PA. Cyclic strain-mediated regulation of endothelial matrix metalloproteinase-2 expression and activity. *Cardiovascular Research.* 2004;63(4):625-634.

105. Wang B-W, Chang H, Lin S, Kuan P, Shyu K-G. Induction of matrix metalloproteinases-14 and -2 by cyclical mechanical stretch is mediated by tumor necrosis factor-[alpha] in cultured human umbilical vein endothelial cells. *Cardiovascular Research.* 2003;59(2):460-469.

106. Malgorzata Milkiewicz FMEIEGTLH. Static strain stimulates expression of matrix metalloproteinase-2 and VEGF in microvascular endothelium via JNK- and ERK-dependent pathways. *Journal of cellular biochemistry.* 2007;100(3):750-761.

107. Yamaguchi S, Yamaguchi M, Yatsuyanagi E, Yun SS, Nakajima N, Madri JA, Sumpio BE. Cyclic strain stimulates early growth response gene product 1-mediated expression

of membrane type 1 matrix metalloproteinase in endothelium. *Lab Invest.* 2002;82(7):949-956.

108. Bedard K, Krause KH. The NOX family of ROS-generating NADPH oxidases: physiology and pathophysiology. *Physiol Rev.* 2007;87(1):245-313.

109. Sung H-J, Yee A, Eskin SG, McIntire LV. Cyclic strain and motion control produce opposite oxidative responses in two human endothelial cell types. *Am J Physiol Cell Physiol.* 2007;293(1):C87-94.

110. Oeckler RA, Kaminski PM, Wolin MS. Stretch enhances contraction of bovine coronary arteries via an NAD(P)H oxidase-mediated activation of the extracellular signal-regulated kinase mitogen-activated protein kinase cascade. *Circ Res.* 2003;92(1):23-31.

111. Ungvari Z, Csiszar A, Huang A, Kaminski PM, Wolin MS, Koller A. High Pressure Induces Superoxide Production in Isolated Arteries Via Protein Kinase C-Dependent Activation of NAD(P)H Oxidase. *Circulation.* 2003;108(10):1253-1258.

112. Schmelter M, Ateghang B, Helmig S, Wartenberg M, Sauer H. Embryonic stem cells utilize reactive oxygen species as transducers of mechanical strain-induced cardiovascular differentiation. *FASEB J.* 2006;20(8):1182-1184.

113. Valiunas V, Polosina YY, Miller H, Potapova IA, Valiuniene L, Doronin S, Mathias RT, Robinson RB, Rosen MR, Cohen IS, Brink PR. Connexin-specific cell-to-cell transfer of short interfering RNA by gap junctions. *J Physiol (Lond).* 2005;568(2):459-468.

114. Musil LS, Le A-CN, VanSlyke JK, Roberts LM. Regulation of connexin degradation as a mechanism to increase gap junction assembly and function. *Journal of Biological Chemistry.* 2000;275(33):25207-25215.

115. Darrow BJ, Laing JG, Lampe PD, Saffitz JE, Beyer EC. Expression of multiple connexins in cultured neonatal rat ventricular myocytes. *Circulation Research.* 1995;76(3):381-387.

116. Segretain D, Falk MM. Regulation of connexin biosynthesis, assembly, gap junction formation, and removal. *Biochimica et Biophysica Acta (BBA) - Biomembranes.* 2004;1662(1-2):3-21.

117. Sohl G, Willecke K. Gap junctions and the connexin protein family. *Cardiovascular Research.* 2004;62(2):228-232.

118. Beyer EC, Paul DL, Goodenough DA. Connexin43: a protein from rat heart homologous to a gap junction protein from liver. *J Cell Biol.* 1987;105(6 Pt 1):2621-2629.

119. Pfeifer I, Anderson C, Werner R, Oltra E. Redefining the structure of the mouse connexin43 gene: selective promoter usage and alternative splicing mechanisms yield transcripts with different translational efficiencies. *Nucleic Acids Res.* 2004;32(15):4550-4562.

120. Teunissen BEJ, Jansen AT, Mutsaers NAM, Vuerhard MJ, Vos MA, Bierhuizen MFA. Primary structure, organization, and expression of the rat connexin45 gene. *DNA and Cell Biology.* 2007;26(2):108-115.

121. Bennett MV, Zheng X, Sogin ML. The connexins and their family tree. *Soc Gen Physiol Ser.* 1994;49:223-233.

122. Falk MM, Gilula NB. Connexin Membrane Protein Biosynthesis Is Influenced by Polypeptide Positioning within the Translocon and Signal Peptidase Access. *J. Biol. Chem.* 1998;273(14):7856-7864.

123. Giepmans BNG. Gap junctions and connexin-interacting proteins. *Cardiovascular Research.* 2004;62(2):233-245.

124. Das Sarma J, Wang F, Koval M. Targeted gap junction protein constructs reveal connexin-specific differences in oligomerization. *Journal of Biological Chemistry.* 2002;277(23):20911-20918.

125. Maza J, Sarma JD, Koval M. Defining a Minimal Motif Required to Prevent Connexin Oligomerization in the Endoplasmic Reticulum. *J. Biol. Chem.* 2005;280(22):21115-21121.

126. He DS, Jiang JX, Taffet SM, Burt JM. Formation of heteromeric gap junction channels by connexins 40 and 43 in vascular smooth muscle cells. *PNAS.* 1999;96(11):6495-6500.

127. Brink PR, Cronin K, Banach K, Peterson E, Westphale EM, Seul KH, Ramanan SV, Beyer EC. Evidence for heteromeric gap junction channels formed from rat connexin43 and human connexin37. *Am J Physiol.* 1997;273(4 Pt 1):C1386-1396.

128. Elfgang C, Eckert R, Lichtenberg-Frate H, Butterweck A, Traub O, Klein R, Hulser D, Willecke K. Specific permeability and selective formation of gap junction channels in connexin-transfected HeLa cells. *J. Cell Biol.* 1995;129(3):805-817.

129. Gemel J, Valiunas V, Brink PR, Beyer EC. Connexin43 and connexin26 form gap junctions, but not heteromeric channels in co-expressing cells. *J Cell Sci.* 2004;117(Pt 12):2469-2480.

130. Falk MM. Cell-Free Synthesis for Analyzing the Membrane Integration, Oligomerization, and Assembly Characteristics of Gap Junction Connexins. *Methods.* 2000;20(2):165-179.

131. Lauf U, Giepmans BNG, Lopez P, Braconnot S, Chen S-C, Falk MM. Dynamic trafficking and delivery of connexons to the plasma membrane and accretion to gap junctions in living cells. *PNAS.* 2002;99(16):10446-10451.

132. Gaietta G, Deerinck TJ, Adams SR, Bouwer J, Tour O, Laird DW, Sosinsky GE, Tsien RY, Ellisman MH. Multicolor and electron microscopic imaging of connexin trafficking. *Science.* 2002;296(5567):503-507.

133. Rothman JE, Wieland FT. Protein sorting by transport vesicles. *Science.* 1996;272(5259):227-234.

134. Thomas T, Jordan K, Simek J, Shao Q, Jedeszko C, Walton P, Laird DW. Mechanisms of Cx43 and Cx26 transport to the plasma membrane and gap junction regeneration. *J Cell Sci.* 2005;118(19):4451-4462.

135. Musil LS, Goodenough DA. Biochemical analysis of connexin43 intracellular transport, phosphorylation, and assembly into gap junctional plaques. *J Cell Biol.* 1991;115(5):1357-1374.

136. Olbina G, Eckhart W. Mutations in the second extracellular region of connexin 43 prevent localization to the plasma membrane, but do not affect its ability to suppress cell growth. *Mol Cancer Res.* 2003;1(9):690-700.

137. Laing JG, Chou BC, Steinberg TH. ZO-1 alters the plasma membrane localization and function of Cx43 in osteoblastic cells. *J Cell Sci.* 2005;118(10):2167-2176.

138. Jongen W, Fitzgerald D, Asamoto M, Piccoli C, Slaga T, Gros D, Takeichi M, Yamasaki H. Regulation of connexin 43-mediated gap junctional intercellular communication by Ca2+ in mouse epidermal cells is controlled by E- cadherin. *J. Cell Biol.* 1991;114(3):545-555.

139. Meyer R, Laird D, Revel J, Johnson R. Inhibition of gap junction and adherens junction assembly by connexin and A-CAM antibodies. *J. Cell Biol.* 1992;119(1):179-189.

140. Fujimoto K, Nagafuchi A, Tsukita S, Kuraoka A, Ohokuma A, Shibata Y. Dynamics of connexins, E-cadherin and alpha-catenin on cell membranes during gap junction formation. *J Cell Sci.* 1997;110 (Pt 3):311-322.

141. Perkins GA, Goodenough DA, Sosinsky GE. Formation of the gap junction intercellular channel requires a 30[deg] rotation for interdigitating two apposing connexons. *Journal of Molecular Biology.* 1998;277(2):171-177.

142. Bao X, Chen Y, Reuss L, Altenberg GA. Functional Expression in Xenopus Oocytes of Gap-junctional Hemichannels Formed by a Cysteine-less Connexin 43. *J. Biol. Chem.* 2004;279(11):9689-9692.

143. Cottrell GT, Burt JM. Functional consequences of heterogeneous gap junction channel formation and its influence in health and disease. *Biochimica et Biophysica Acta (BBA) - Biomembranes.* 2005;1711(2):126-141.

144. Desplantez T, Halliday D, Dupont E, Weingart R. Cardiac connexins Cx43 and Cx45: Formation of diverse gap junction channels with diverse electrical properties. *Pflugers Archiv European Journal of Physiology.* 2004;448(4):363-375.

145. Bruzzone R, Haefliger J, Gimlich R, Paul D. Connexin40, a component of gap junctions in vascular endothelium, is restricted in its ability to interact with other connexins. *Mol. Biol. Cell.* 1993;4(1):7-20.

146. Yeh HI, Rothery S, Dupont E, Coppen SR, Severs NJ. Individual gap junction plaques contain multiple connexins in arterial endothelium. *Circ Res.* 1998;83(12):1248-1263.

147. Jordan K, Solan JL, Dominguez M, Sia M, Hand A, Lampe PD, Laird DW. Trafficking, Assembly, and Function of a Connexin43-Green Fluorescent Protein Chimera in Live Mammalian Cells. *Mol. Biol. Cell.* 1999;10(6):2033-2050.

148. BJORKMAN N. A study of the ultrastructure of the granulosa cells of the rat ovary. *Acta Anatomica.* 1962;51:125-147.

149. Naus CCG, Hearn S, Zhu D, Nicholson BJ, Shivers RR. Ultrastructural Analysis of Gap Junctions in C6 Glioma Cells Transfected with Connexin43 cDNA. *Experimental Cell Research.* 1993;206(1):72-84.

150. Windoffer R, Beile B, Leibold A, Thomas S, Wilhelm U, Leube RE. Visualization of gap junction mobility in living cells. *Cell Tissue Res.* 2000;299(3):347-362.

151. Larsen W, Tung H, Murray S, Swenson C. Evidence for the participation of actin microfilaments and bristle coats in the internalization of gap junction membrane. *J. Cell Biol.* 1979;83(3):576-587.

152. Leithe E, Rivedal E. Epidermal growth factor regulates ubiquitination, internalization and proteasome-dependent degradation of connexin43. *J Cell Sci.* 2004;117(7):1211-1220.

153. Thomas MA, Zosso N, Scerri I, Demaurex N, Chanson M, Staub O. A tyrosine-based sorting signal is involved in connexin43 stability and gap junction turnover. *J Cell Sci.* 2003;116(Pt 11):2213-2222.

154. Berthoud VM, Minogue PJ, Laing JG, Beyer EC. Pathways for degradation of connexins and gap junctions. *Cardiovasc Res.* 2004;62(2):256-267.

155. Hicke L, Dunn R. Regulation of membrane protein transport by ubiquitin and ubiquitin-binding proteins. *Annu Rev Cell Dev Biol.* 2003;19:141-172.

156. Leithe E, Rivedal E. Ubiquitination and Down-regulation of Gap Junction Protein Connexin-43 in Response to 12-O-Tetradecanoylphorbol 13-Acetate Treatment. *J. Biol. Chem.* 2004;279(48):50089-50096.

157. Leykauf K, Salek M, Bomke J, Frech M, Lehmann W-D, Durst M, Alonso A. Ubiquitin protein ligase Nedd4 binds to connexin43 by a phosphorylation-modulated process. *J Cell Sci.* 2006;119(17):3634-3642.

158. Thomas T, Telford D, Laird DW. Functional domain mapping and selective trans-dominant effects exhibited by Cx26 disease-causing mutations. *The Journal Of Biological Chemistry.* 2004;279(18):19157-19168.

159. Laird DW. Connexin phosphorylation as a regulatory event linked to gap junction internalization and degradation. *Biochimica et Biophysica Acta (BBA) - Biomembranes.* 2005;1711(2):172-182.

160. Lampe PD, Lau AF. The effects of connexin phosphorylation on gap junctional communication. *Int J Biochem Cell Biol.* 2004;36(7):1171-1186.

161. Diestel S, Eckert R, Hulser D, Traub O. Exchange of serine residues 263 and 266 reduces the function of mouse gap junction protein connexin31 and exhibits a dominant-negative effect on the wild-type protein in HeLa cells. *Exp Cell Res.* 2004;294(2):446-457.

162. Diez JA, Elvira M, Villalobo A. The epidermal growth factor receptor tyrosine kinase phosphorylates connexin32. *Mol Cell Biochem.* 1998;187(1-2):201-210.

163. Traub O, Hertlein B, Kasper M, Eckert R, Krisciukaitis A, Hulser D, Willecke K. Characterization of the gap junction protein connexin37 in murine endothelium, respiratory epithelium, and after transfection in human HeLa cells. *Eur J Cell Biol.* 1998;77(4):313-322.

164. Musil L, Cunningham B, Edelman G, Goodenough D. Differential phosphorylation of the gap junction protein connexin43 in junctional communication-competent and -deficient cell lines. *J. Cell Biol.* 1990;111(5):2077-2088.

165. van Veen TA, van Rijen HV, Jongsma HJ. Electrical conductance of mouse connexin45 gap junction channels is modulated by phosphorylation. *Cardiovasc Res.* 2000;46(3):496-510.

166. Jiang JX, Paul DL, Goodenough DA. Posttranslational phosphorylation of lens fiber connexin46: a slow occurrence. *Invest Ophthalmol Vis Sci.* 1993;34(13):3558-3565.

167. Arneson ML, Cheng HL, Louis CF. Characterization of the ovine-lens plasma-membrane protein-kinase substrates. *Eur J Biochem.* 1995;234(2):670-679.

168. Berthoud VM, Montegna EA, Atal N, Aithal NH, Brink PR, Beyer EC. Heteromeric connexons formed by the lens connexins, connexin43 and connexin56. *European Journal of Cell Biology.* 2001;80(1):11-19.

169. Traub O, Look J, Dermietzel R, Brummer F, Hulser D, Willecke K. Comparative characterization of the 21-kD and 26-kD gap junction proteins in murine liver and cultured hepatocytes. *J Cell Biol.* 1989;108(3):1039-1051.

170. Lin R, Warn-Cramer BJ, Kurata WE, Lau AF. v-Src phosphorylation of connexin 43 on Tyr247 and Tyr265 disrupts gap junctional communication. *J. Cell Biol.* 2001;154(4):815-828.

171. Cooper CD, Lampe PD. Casein kinase 1 regulates connexin-43 gap junction assembly. *Journal of Biological Chemistry.* 2002;277(47):44962-44968.

172. Yogo K, Ogawa T, Akiyama M, Ishida N, Takeya T. Identification and functional analysis of novel phosphorylation sites in Cx43 in rat primary granulosa cells. *FEBS Lett.* 2002;531(2):132-136.

173. Lampe PD, TenBroek EM, Burt JM, Kurata WE, Johnson RG, Lau AF. Phosphorylation of connexin43 on serine368 by protein kinase C regulates gap junctional communication. *J Cell Biol.* 2000;149(7):1503-1512.

174. Richards TS, Dunn CA, Carter WG, Usui ML, Olerud JE, Lampe PD. Protein kinase C spatially and temporally regulates gap junctional communication during human wound repair via phosphorylation of connexin43 on serine368. *J. Cell Biol.* 2004;167(3):555-562.

175. Solan JL, Fry MD, TenBroek EM, Lampe PD. Connexin43 phosphorylation at S368 is acute during S and G2/M and in response to protein kinase C activation. *J Cell Sci.* 2003;116(Pt 11):2203-2211.

176. Saez JC, Nairn AC, Czernik AJ, Fishman GI, Spray DC, Hertzberg EL. Phosphorylation of connexin43 and the regulation of neonatal rat cardiac myocyte gap junctions. *J Mol Cell Cardiol.* 1997;29(8):2131-2145.

177. TenBroek EM, Lampe PD, Solan JL, Reynhout JK, Johnson RG. Ser364 of connexin43 and the upregulation of gap junction assembly by cAMP. *J. Cell Biol.* 2001;155(7):1307-1318.

178. Darrow BJ, Fast VG, Kleber AG, Beyer EC, Saffitz JE. Functional and structural assessment of intercellular communication. Increased conduction velocity and enhanced connexin expression in dibutyryl cAMP-treated cultured cardiac myocytes. *Circ Res.* 1996;79(2):174-183.

179. Paulson AF, Lampe PD, Meyer RA, TenBroek E, Atkinson MM, Walseth TF, Johnson RG. Cyclic AMP and LDL trigger a rapid enchancement in gap junction assembly through a stimulation of connexin trafficking. *Journal of Cell Science.* 2000;113(17):3037-3049.

180. Somekawa S, Fukuhara S, Nakaoka Y, Fujita H, Saito Y, Mochizuki N. Enhanced Functional Gap Junction Neoformation by Protein Kinase A-Dependent and Epac-Dependent Signals Downstream of cAMP in Cardiac Myocytes. *Circ Res.* 2005;97(7):655-662.

181. Britz-Cunningham SH, Shah MM, Zuppan CW, Fletcher WH. Mutations of the Connexin43 gap-junction gene in patients with heart malformations and defects of laterality. *New England Journal of Medicine.* 1995;332(20):1323-1329.

182. Ek-Vitorin JF, Calero G, Morley GE, Coombs W, Taffet SM, Delmar M. pH regulation of connexin43: Molecular analysis of the gating particle. *Biophysical Journal.* 1996;71(3):1273-1284.

183. Levin M, Mercola M. Gap Junctions Are Involved in the Early Generation of Left-Right Asymmetry. *Developmental Biology.* 1998;203(1):90-105.

184. Lin D, Takemoto DJ. Oxidative Activation of Protein Kinase C{gamma} through the C1 Domain: EFFECTS ON GAP JUNCTIONS. *J. Biol. Chem.* 2005;280(14):13682-13693.

185. Doble BW, Ping P, Kardami E. The [epsi] subtype of protein kinase C is required for cardiomyocyte connexin-43 phosphorylation. *Circulation Research.* 2000;86(3):293-301.

186. Bao X, Altenberg GA, Reuss L. Mechanism of regulation of the gap junction protein connexin 43 by protein kinase C-mediated phosphorylation. *Am J Physiol Cell Physiol.* 2004;286(3):C647-654.

187. Doble BW, Dang X, Ping P, Fandrich RR, Nickel BE, Jin Y, Cattini PA, Kardami E. Phosphorylation of serine 262 in the gap junction protein connexin-43 regulates DNA synthesis in cell-cell contact forming cardiomyocytes. *J Cell Sci.* 2004;117(Pt 3):507-514.

188. Lampe PD, Kurata WE, Warn-Cramer BJ, Lau AF. Formation of a distinct connexin43 phosphoisoform in mitotic cells is dependent upon p34cdc2 kinase. *J Cell Sci.* 1998;111 (Pt 6):833-841.

189. Cheng H-L, Louis CF. Functional effects of casein kinase I-catalyzed phosphorylation on lens cell-to-cell coupling. *Journal of Membrane Biology.* 2001;181(1):21-30.

190. Yin X, Jedrzejewski PT, Jiang JX. Casein Kinase II Phosphorylates Lens Connexin 45.6 and Is Involved in Its Degradation. *J. Biol. Chem.* 2000;275(10):6850-6856.

191. Cottrell GT, Lin R, Warn-Cramer BJ, Lau AF, Burt JM. Mechanism of v-Src- and mitogen-activated protein kinase-induced reduction of gap junction communication. *American Journal of Physiology - Cell Physiology.* 2003;284(2 53-2):C511-C520.

192. Lidington D, Tyml K, Ouellette Y. Lipopolysaccharide-induced reductions in cellular coupling correlate with tyrosine phosphorylation of connexin 43. *Journal of Cellular Physiology.* 2002;193(3):373-379.

193. Guan X, Wilson S, Schlender KK, Ruch RJ. Gap-junction disassembly and connexin 43 dephosphorylation induced by 18 beta-glycyrrhetinic acid. *Mol Carcinog.* 1996;16(3):157-164.

194. Xie H, Laird DW, Chang TH, Hu VW. A mitosis-specific phosphorylation of the gap junction protein connexin43 in human vascular cells: biochemical characterization and localization. *J Cell Biol.* 1997;137(1):203-210.

195. Cruciani V, Kaalhus O, Mikalsen S-O. Phosphatases Involved in Modulation of Gap Junctional Intercellular Communication and Dephosphorylation of Connexin43 in Hamster Fibroblasts: 2B or Not 2B? *Experimental Cell Research.* 1999;252(2):449-463.

196. Chu G, Carr AN, Young KB, Lester JW, Yatani A, Sanbe A, Colbert MC, Schwartz SM, Frank KF, Lampe PD. Enhanced myocyte contractility and Ca2+ handling in a calcineurin transgenic model of heart failure. *Cardiovascular Research.* 2002;54(1):105-116.

197. Giepmans BN, Feiken E, Gebbink MF, Moolenaar WH. Association of connexin43 with a receptor protein tyrosine phosphatase. *Cell Commun Adhes.* 2003;10(4-6):201-205.

198. Schroeder MJ, Webb DJ, Shabanowitz J, Horwitz AF, Hunt DF. Methods for the detection of paxillin post-translational modifications and interacting proteins by mass spectrometry. *J Proteome Res.* 2005;4(5):1832-1841.

199. Grigera PR, Jeffery ED, Martin KH, Shabanowitz J, Hunt DF, Parsons JT. FAK phosphorylation sites mapped by mass spectrometry. *J Cell Sci.* 2005;118(Pt 21):4931-4935.

200. Naitoh K, Ichikawa Y, Miura T, Nakamura Y, Miki T, Ikeda Y, Kobayashi H, Nishihara M, Ohori K, Shimamoto K. MitoK(ATP) channel activation suppresses gap junction permeability in the ischemic myocardium by an ERK-dependent mechanism. *Cardiovasc Res.* 2006.

201. Rose B, Loewenstein WR. Permeability of cell junction depends on local cytoplasmic calcium activity. *Nature.* 1975;254(5497):250-252.

202. Turin L, Warner A. Carbon dioxide reversibly abolishes ionic communication between cells of early amphibian embryo. *Nature.* 1977;270(5632):56-57.

203. Peracchia C. Communicating junctions and calmodulin: inhibition of electrical uncoupling in Xenopus embryo by calmidazolium. *J Membr Biol.* 1984;81(1):49-58.

204. Peracchia C, Sotkis A, Wang XG, Peracchia LL, Persechini A. Calmodulin Directly Gates Gap Junction Channels. *J. Biol. Chem.* 2000;275(34):26220-26224.

205. Van Eldik LJ, Hertzberg Elliot L., Berdan RC, Gilula NB. Interaction of calmodulin and other calcium-modulated proteins with mammalian and arthropod junctional membrane proteins. *Biochemical and Biophysical Research Communications.* 1985;126(2):825-832.

206. Bukauskas FF, Bukauskiene A, Bennett MVL, Verselis VK. Gating properties of gap junction channels assembled from connexin43 and connexin43 fused with green fluorescent protein. *Biophysical Journal.* 2001;81(1):137-152.

207. Li H, Liu TF, Lazrak A, Peracchia C, Goldberg GS, Lampe PD, Johnson RG. Properties and regulation of gap junctional hemichannels in the plasma membranes of cultured cells. *J Cell Biol.* 1996;134(4):1019-1030.

208. Thimm J, Mechler A, Lin H, Rhee S, Lal R. Calcium-dependent open/closed conformations and interfacial energy maps of reconstituted hemichannels. *J Biol Chem.* 2005;280(11):10646-10654.

209. Stout CE, Costantin JL, Naus CCG, Charles AC. Intercellular Calcium Signaling in Astrocytes via ATP Release through Connexin Hemichannels. *J. Biol. Chem.* 2002;277(12):10482-10488.

210. Braet K, Vandamme W, Martin PEM, Evans WH, Leybaert L. Photoliberating inositol-1,4,5-trisphosphate triggers ATP release that is blocked by the connexin mimetic peptide gap 26. *Cell Calcium.* 2003;33(1):37-48.

211. Ye Z-C, Wyeth MS, Baltan-Tekkok S, Ransom BR. Functional hemichannels in astrocytes: A novel mechanism of glutamate release. *Journal of Neuroscience.* 2003;23(9):3588-3596.

212. Bruzzone S, Guida L, Zocchi E, Franco L, De Flora A. Connexin 43 hemi channels mediate Ca2+-regulated transmembrane NAD+ fluxes in intact cells. *Faseb J.* 2001;15(1):10-12.

213. Weissman TA, Riquelme PA, Ivic L, Flint AC, Kriegstein AR. Calcium Waves Propagate through Radial Glial Cells and Modulate Proliferation in the Developing Neocortex. *Neuron.* 2004;43(5):647-661.

214. Giepmans BNG, Moolenaar WH. The gap junction protein connexin43 interacts with the second PDZ domain of the zona occludens-1 protein. *Current Biology.* 1998;8(16):931-934.

215. Sorgen PL, Duffy HS, Sahoo P, Coombs W, Delmar M, Spray DC. Structural Changes in the Carboxyl Terminus of the Gap Junction Protein Connexin43 Indicates Signaling between Binding Domains for c-Src and Zonula Occludens-1. *J. Biol. Chem.* 2004;279(52):54695-54701.

216. Hunter AW, Barker RJ, Zhu C, Gourdie RG. Zonula Occludens-1 Alters Connexin43 Gap Junction Size and Organization by Influencing Channel Accretion. *Mol. Biol. Cell.* 2005;16(12):5686-5698.

217. Duffy HS, Ashton AW, O'Donnell P, Coombs W, Taffet SM, Delmar M, Spray DC. Regulation of connexin43 protein complexes by intracellular acidification. *Circ Res.* 2004;94(2):215-222.

218. Toyofuku T, Akamatsu Y, Zhang H, Kuzuya T, Tada M, Hori M. c-Src regulates the interaction between connexin-43 and ZO-1 in cardiac myocytes. *J Biol Chem.* 2001;276(3):1780-1788.

219. Barker RJ, Price RL, Gourdie RG. Increased Association of ZO-1 With Connexin43 During Remodeling of Cardiac Gap Junctions. *Circ Res.* 2002;90(3):317-324.

220. Segretain D, Fiorini C, Decrouy X, Defamie N, Prat JR, Pointis G. A proposed role for ZO-1 in targeting connexin 43 gap junctions to the endocytic pathway. *Biochimie.* 2004;86(4-5):241-244.

221. Penes MC, Li X, Nagy JI. Expression of zonula occludens-1 (ZO-1) and the transcription factor ZO-1-associated nucleic acid-binding protein (ZONAB)-MsY3 in glial cells and colocalization at oligodendrocyte and astrocyte gap junctions in mouse brain. *Eur J Neurosci.* 2005;22(2):404-418.

222. Nielsen PA, Beahm DL, Giepmans BNG, Baruch A, Hall JE, Kumar NM. Molecular cloning, functional expression, and tissue distribution of a novel human Gap junction-forming protein, connexin-31.9: Interaction with zona occludens protein-1. *Journal of Biological Chemistry.* 2002;277(41):38272-38283.

223. Li X, Olson C, Lu S, Kamasawa N, Yasumura T, Rash JE, Nagy JI. Neuronal connexin36 association with zonula occludens-1 protein (ZO-1) in mouse brain and interaction with the first PDZ domain of ZO-1. *Eur J Neurosci.* 2004;19(8):2132-2146.

224. Kausalya PJ, Reichert M, Hunziker W. Connexin45 directly binds to ZO-1 and localizes to the tight junction region in epithelial MDCK cells. *FEBS Letters.* 2001;505(1):92-96.

225. Laing JG, Manley-Markowski RN, Civitelli R, Steinberg TH, Koval M. Connexin45 Interacts with Zonula Occludens-1 and Connexin43 in Osteoblastic Cells. *Journal of Biological Chemistry.* 2001;276(25):23051-23055.

226. Nielsen PA, Baruch A, Shestopalov VI, Giepmans BNG, Dunia I, Benedetti EL, Kumar NM. Lens connexins Cx46 and Cx50 interact with zonula occludens protein-1 (ZO-1). *Molecular Biology of the Cell.* 2003;14(6):2470-2481.

227. Wei C-J, Francis R, Xu X, Lo CW. Connexin43 Associated with an N-cadherin-containing Multiprotein Complex Is Required for Gap Junction Formation in NIH3T3 Cells. *J. Biol. Chem.* 2005;280(20):19925-19936.

228. Fujimoto K, Nagafuchi A, Tsukita S, Kuraoka A, Ohokuma A, Shibata Y. Dynamics of connexins, E-cadherin and ?-catenin on cell membranes during gap junction formation. *Journal of Cell Science.* 1997;110(3):311-322.

229. Xu X, Li WE, Huang GY, Meyer R, Chen T, Luo Y, Thomas MP, Radice GL, Lo CW. Modulation of mouse neural crest cell motility by N-cadherin and connexin 43 gap junctions. *J Cell Biol.* 2001;154(1):217-230.

230. Keane R, Mehta P, Rose B, Honig L, Loewenstein W, Rutishauser U. Neural differentiation, NCAM-mediated adhesion, and gap junctional communication in neuroectoderm. A study in vitro. *J. Cell Biol.* 1988;106(4):1307-1319.

231. Luo Y, Radice GL. Cadherin-mediated adhesion is essential for myofibril continuity across the plasma membrane but not for assembly of the contractile apparatus. *J Cell Sci.* 2003;116(8):1471-1479.

232. Li J, Patel VV, Kostetskii I, Xiong Y, Chu AF, Jacobson JT, Yu C, Morley GE, Molkentin JD, Radice GL. Cardiac-specific loss of N-cadherin leads to alteration in connexins with conduction slowing and arrhythmogenesis. *Circ Res.* 2005;97(5):474-481.

233. Govindarajan R, Zhao S, Song X-H, Guo R-J, Wheelock M, Johnson KR, Mehta PP. Impaired Trafficking of Connexins in Androgen-independent Human Prostate Cancer Cell Lines and Its Mitigation by alpha -Catenin. *J. Biol. Chem.* 2002;277(51):50087-50097.

234. SAFFITZ JE. Dependence of Electrical Coupling on Mechanical Coupling in Cardiac Myocytes: Insights Gained from Cardiomyopathies Caused by Defects in Cell-Cell Connections. *Ann NY Acad Sci.* 2005;1047(1):336-344.

235. Gutstein DE, Liu F-y, Meyers MB, Choo A, Fishman GI. The organization of adherens junctions and desmosomes at the cardiac intercalated disc is independent of gap junctions. *J Cell Sci.* 2003;116(5):875-885.

236. Almeida M, Han L, Bellido T, Manolagas SC, Kousteni S. Wnt Proteins Prevent Apoptosis of Both Uncommitted Osteoblast Progenitors and Differentiated Osteoblasts by {beta}-Catenin-dependent and -independent Signaling Cascades Involving Src/ERK and Phosphatidylinositol 3-Kinase/AKT. *J. Biol. Chem.* 2005;280(50):41342-41351.

237. Giepmans BNG, Verlaan I, Hengeveld T, Janssen H, Calafat J, Falk MM, Moolenaar WH. Gap junction protein connexin-43 interacts directly with microtubules. *Current Biology.* 2001;11(17):1364-1368.

238. Toyofuku T, Yabuki M, Otsu K, Kuzuya T, Hori M, Tada M. Direct Association of the Gap Junction Protein Connexin-43 with ZO-1 in Cardiac Myocytes. *J. Biol. Chem.* 1998;273(21):12725-12731.

239. Butkevich E, Hulsmann S, Wenzel D, Shirao T, Duden R, Majoul I. Drebrin Is a Novel Connexin-43 Binding Partner that Links Gap Junctions to the Submembrane Cytoskeleton. *Current Biology.* 2004;14(8):650-658.

240. Murray SA, Williams SY, Dillard CY, Narayanan SK, McCauley J. Relationship of cytoskeletal filaments to annular gap junction expression in human adrenal cortical tumor cells in culture. *Exp Cell Res.* 1997;234(2):398-404.

241. Schubert AL, Schubert W, Spray DC, Lisanti MP. Connexin family members target to lipid raft domains and interact with caveolin-1. *Biochemistry.* 2002;41(18):5754-5764.

242. Krajewska WM, Maslowska I. Caveolins: structure and function in signal transduction. *Cell Mol Biol Lett.* 2004;9(2):195-220.

243. Miyawaki-Shimizu K, Predescu D, Shimizu J, Broman M, Predescu S, Malik AB. siRNA-Induced Caveolin-1 Knock-Down in Mice Increases Lung Vascular Permeability via the Junctional Pathway. *Am J Physiol Lung Cell Mol Physiol.* 2005.

244. Sotkis A, Wang XG, Yasumura T, Peracchia LL, Persechini A, Rash JE, Peracchia C. Calmodulin colocalizes with connexins and plays a direct role in gap junction channel gating. *Cell Communication & Adhesion.* 2001;8(4-6):277-281.

245. Burr GS, Mitchell CK, Keflemariam YJ, Heidelberger R, O'Brien J. Calcium-dependent binding of calmodulin to neuronal gap junction proteins. *Biochemical and Biophysical Research Communications.* 2005;335(4):1191-1198.

246. Lan Z, Kurata WE, Martyn KD, Jin C, Lau AF. Novel rab GAP-like protein, CIP85, interacts with connexin43 and induces its degradation. *Biochemistry.* 2005;44(7):2385-2396.

247. Akiyama M, Ishida N, Ogawa T, Yogo K, Takeya T. Molecular cloning and functional analysis of a novel Cx43 partner protein CIP150. *Biochem Biophys Res Commun.* 2005.

248. Tate AW, Lung T, Radhakrishnan A, Lim SD, Lin X, Edlund M. Changes in gap junctional connexin isoforms during prostate cancer progression. *Prostate.* 2006;66(1):19-31.

249. Cohen LA, Guan JL. Mechanisms of focal adhesion kinase regulation. *Curr Cancer Drug Targets.* 2005;5(8):629-643.

250. Lampe PD, Nguyen BP, Gil S, Usui M, Olerud J, Takada Y, Carter WG. Cellular Interaction of Integrin alpha 3beta 1 with Laminin 5 promotes Gap Junctional Communication. *J. Cell Biol.* 1998;143(6):1735-1747.

251. Huang RP, Fan Y, Hossain MZ, Peng A, Zeng ZL, Boynton AL. Reversion of the neoplastic phenotype of human glioblastoma cells by connexin 43 (cx43). *Cancer Research.* 1998;58(22):5089-5096.

252. Qin H, Shao Q, Curtis H, Galipeau J, Belliveau DJ, Wang T, Alaoui-Jamali MA, Laird DW. Retroviral Delivery of Connexin Genes to Human Breast Tumor Cells Inhibits in Vivo Tumor Growth by a Mechanism That Is Independent of Significant Gap Junctional Intercellular Communication. *J. Biol. Chem.* 2002;277(32):29132-29138.

253. Krutovskikh VA, Troyanovsky SM, Piccoli C, Tsuda H, Asamoto M, Yamasaki H. Differential effect of subcellular localization of communication impairing gap junction protein connexin43 on tumor cell growth in vivo. *Oncogene.* 2000;19(4):505-513.

254. Moorby C, Patel M. Dual Functions for Connexins: Cx43 Regulates Growth Independently of Gap Junction Formation. *Experimental Cell Research.* 2001;271(2):238-248.

255. Lin JH-C, Yang J, Liu S, Takano T, Wang X, Gao Q, Willecke K, Nedergaard M. Connexin mediates gap junction-independent resistance to cellular injury. *Journal of Neuroscience.* 2003;23(2):430-441.

256. Qin H, Shao Q, Thomas T, Kalra J, Alaoui-Jamali MA, Laird DW. Connexin26 regulates the expression of angiogenesis-related genes in human breast tumor cells by both GJIC-dependent and -independent mechanisms. *Cell Commun Adhes.* 2003;10(4-6):387-393.

257. Huang R, Lin Y, Wang CC, Gano J, Lin B, Shi Q, Boynton A, Burke J, Huang R-P. Connexin 43 Suppresses Human Glioblastoma Cell Growth by Down-Regulation of Monocyte Chemotactic Protein 1, as Discovered Using Protein Array Technology. *Cancer Res.* 2002;62(10):2806-2812.

258. Zhang YW, Morita I, Ikeda M, Ma KW, Murota S. Connexin43 suppresses proliferation of osteosarcoma U2OS cells through post-transcriptional regulation of p27. *Oncogene.* 2001;20(31):4138-4149.

259. Zhang YW, Nakayama K, Morita I. A novel route for connexin 43 to inhibit cell proliferation: negative regulation of S-phase kinase-associated protein (Skp 2). *Cancer Res.* 2003;63(7):1623-1630.

260. Li H, Brodsky S, Kumari S, Valiunas V, Brink P, Kaide J, Nasjletti A, Goligorsky MS. Paradoxical overexpression and translocation of connexin43 in homocysteine-treated endothelial cells. *Am J Physiol Heart Circ Physiol.* 2002;282(6):H2124-2133.

261. Goubaeva F, Mikami M, Giardina S, Ding B, Abe J, Yang J. Cardiac mitochondrial connexin 43 regulates apoptosis. *Biochem Biophys Res Commun.* 2007;352(1):97-103.

262. Rodriguez-Sinovas A, Boengler K, Cabestrero A, Gres P, Morente M, Ruiz-Meana M, Konietzka I, Miro E, Totzeck A, Heusch G, Schulz R, Garcia-Dorado D. Translocation of Connexin 43 to the Inner Mitochondrial Membrane of Cardiomyocytes Through the Heat Shock Protein 90-Dependent TOM Pathway and Its Importance for Cardioprotection. *Circ Res.* 2006.

263. Boengler K, Dodoni G, Rodriguez-Sinovas A, Cabestrero A, Ruiz-Meana M, Gres P, Konietzka I, Lopez-Iglesias C, Garcia-Dorado D, Di Lisa F. Connexin 43 in cardiomyocyte mitochondria and its increase by ischemic preconditioning. *Cardiovascular Research.* 2005;67(2):234-244.

264. Reaume AG, De Sousa PA, Kulkarni S, Langille BL, Zhu D, Davies TC, Juneja SC, Kidder GM, Rossant J. Cardiac malformation in neonatal mice lacking connexin43. *Science.* 1995;267(5205):1831-1834.

265. Iacobas DA, Iacobas S, Li WEI, Zoidl G, Dermietzel R, Spray DC. Genes controlling multiple functional pathways are transcriptionally regulated in connexin43 null mouse heart. *Physiol. Genomics.* 2005;20(3):211-223.

266. Huang GY, Cooper ES, Waldo K, Kirby ML, Gilula NB, Lo CW. Gap Junction-mediated Cell-Cell Communication Modulates Mouse Neural Crest Migration. *J. Cell Biol.* 1998;143(6):1725-1734.

267. Liao Y, Day KH, Damon DN, Duling BR. Endothelial cell-specific knockout of connexin 43 causes hypotension and bradycardia in mice. *PNAS.* 2001;98(17):9989-9994.

268. Theis M, de Wit C, Schlaeger TM, Eckardt D, Kruger O, Doring B, Risau W, Deutsch U, Pohl U, Willecke K. Endothelium-specific replacement of the connexin43 coding region by a lacZ reporter gene. *Genesis.* 2001;29(1):1-13.

269. Haefliger JA, Krattinger N, Martin D, Pedrazzini T, Capponi A, Doring B, Plum A, Charollais A, Willecke K, Meda P. Connexin43-dependent mechanism modulates renin secretion and hypertension. *J Clin Invest.* 2006;116(2):405-413.

270. Chadjichristos CE, Matter CM, Roth I, Sutter E, Pelli G, Luscher TF, Chanson M, Kwak BR. Reduced Connexin43 Expression Limits Neointima Formation After Balloon Distension Injury in Hypercholesterolemic Mice. *Circulation.* 2006;113(24):2835-2843.

271. Liao Y, Regan CP, Manabe I, Owens GK, Day KH, Damon DN, Duling BR. Smooth muscle-targeted knockout of connexin43 enhances neointimal formation in response to vascular injury. *Arterioscler Thromb Vasc Biol.* 2007;27(5):1037-1042.

272. de Wit C, Roos F, Bolz S-S, Kirchhoff S, Kruger O, Willecke K, Pohl U. Impaired Conduction of Vasodilation Along Arterioles in Connexin40-Deficient Mice. *Circ. Res.* 2000;86(6):649-655.

273. de Wit C, Roos F, Bolz S-S, Pohl U. Lack of vascular connexin 40 is associated with hypertension and irregular arteriolar vasomotion. *Physiological Genomics.* 2003;13(2):169-177.

274. Simon AM, Goodenough DA, Li E, Paul DL. Female infertility in mice lacking connexin 37. *Nature.* 1997;385(6616):525-529.

275. Simon AM, McWhorter AR. Vascular Abnormalities in Mice Lacking the Endothelial Gap Junction Proteins connexin37 and connexin40. *Developmental Biology.* 2002;251(2):206-220.

276. Simon AM, McWhorter AR. Decreased intercellular dye-transfer and downregulation of non-ablated connexins in aortic endothelium deficient in connexin37 or connexin40. *J Cell Sci.* 2003;116(Pt 11):2223-2236.

277. Kurtz L, Schweda F, de Wit C, Kriz W, Witzgall R, Warth R, Sauter A, Kurtz A, Wagner C. Lack of Connexin 40 Causes Displacement of Renin-Producing Cells from Afferent Arterioles to the Extraglomerular Mesangium. *J Am Soc Nephrol.* 2007.

278. Wagner C, de Wit C, Kurtz L, Grunberger C, Kurtz A, Schweda F. Connexin40 is Essential for the Pressure Control of Renin Synthesis and Secretion. *Circ Res.* 2007.

279. Wong CW, Christen T, Roth I, Chadjichristos CE, Derouette JP, Foglia BF, Chanson M, Goodenough DA, Kwak BR. Connexin37 protects against atherosclerosis by regulating monocyte adhesion. *Nat Med.* 2006.

280. Kruger O, Plum A, Kim J, Winterhager E, Maxeiner S, Hallas G, Kirchhoff S, Traub O, Lamers W, Willecke K. Defective vascular development in connexin 45-deficient mice. *Development.* 2000;127(19):4179-4193.

281. Larson DM, Christensen TG, Sagar GD, Beyer EC. TGF-beta1 induces an accumulation of connexin43 in a lysosomal compartment in endothelial cells. *Endothelium.* 2001;8(4):255-260.

282. Pimentel RC, Yamada KA, Kleber AG, Saffitz JE. Autocrine regulation of myocyte Cx43 expression by VEGF. *Circulation Research.* 2002;90(6):671-677.

283. Dai P, Nakagami T, Tanaka H, Hitomi T, Takamatsu T. Cx43 Mediates TGF-beta Signaling through Competitive Smads Binding to Microtubules. *Mol. Biol. Cell.* 2007;18(6):2264-2273.

284. van Rijen HV, van Kempen MJ, Postma S, Jongsma HJ. Tumour necrosis factor alpha alters the expression of connexin43, connexin40, and connexin37 in human umbilical vein endothelial cells. *Cytokine.* 1998;10(4):258-264.

285. Fernandez-Cobo M, Gingalewski C, Drujan D, De Maio A. DOWNREGULATION OF CONNEXIN 43 GENE EXPRESSION IN RAT HEART DURING INFLAMMATION. THE ROLE OF TUMOUR NECROSIS FACTOR. *Cytokine.* 1999;11(3):216-224.

286. Hoffmann A, Gloe T, Pohl U, Zahler S. Nitric oxide enhances de novo formation of endothelial gap junctions. *Cardiovascular Research.* 2003;60(2):421-430.

287. Yao J, Hiramatsu N, Zhu Y, Morioka T, Takeda M, Oite T, Kitamura M. Nitric oxide-mediated regulation of connexin43 expression and gap junctional intercellular communication in mesangial cells. *J Am Soc Nephrol.* 2005;16(1):58-67.

288. Haefliger JA, Meda P, Formenton A, Wiesel P, Zanchi A, Brunner HR, Nicod P, Hayoz D. Aortic connexin43 is decreased during hypertension induced by inhibition of nitric oxide synthase. *Arterioscler. Thromb. Vasc. Biol.* 1999;19(7):1615-1622.

289. Roh C-R, Heo J-H, Yang S-H, Bae D-S. Regulation of connexin 43 by nitric oxide in primary uterine myocytes from term pregnant women. *American Journal of Obstetrics and Gynecology.* 2002;187(2):434-440.

290. Spinella F, Rosano L, Di Castro V, Nicotra MR, Natali PG, Bagnato A. Endothelin-1 decreases gap junctional intercellular communication by inducing phosphorylation of connexin 43 in human ovarian carcinoma cells. *The Journal Of Biological Chemistry.* 2003;278(42):41294-41301.

291. Fischer R, Reinehr R, Lu TP, Schonicke A, Warskulat U, Dienes HP, Haussinger D. Intercellular communication via gap junctions in activated rat hepatic stellate cells. *Gastroenterology.* 2005;128(2):433-448.

292. Dodge SM, Beardslee MA, Darrow BJ, Green KG, Beyer EC, Saffitz JE. Effects of angiotensin II on expression of the gap junction channel protein connexin43 in neonatal rat ventricular myocytes. *J Am Coll Cardiol.* 1998;32(3):800-807.

293. Polontchouk L, Ebelt B, Jackels M, Dhein S. Chronic effects of endothelin 1 and angiotensin II on gap junctions and intercellular communication in cardiac cells. *Faseb J.* 2002;16(1):87-89.

294. Jia G, Mitra AK, Cheng G, Gangahar DM, Agrawal DK. Angiotensin II and IGF-1 Regulate Connexin43 Expression Via ERK and p38 Signaling Pathways in Vascular Smooth Muscle Cells of Coronary Artery Bypass Conduits. *J Surg Res.* 2007.

295. Shyu KG, Chen CC, Wang BW, Kuan P. Angiotensin II receptor antagonist blocks the expression of connexin43 induced by cyclical mechanical stretch in cultured neonatal rat cardiac myocytes. *J Mol Cell Cardiol.* 2001;33(4):691-698.

296. Kasi VS, Xiao HD, Shang LL, Iravanian S, Langberg J, Witham EA, Jiao Z, Gallego CJ, Bernstein KE, Dudley SC. Cardiac restricted angiotensin converting enzyme overexpression causes conduction defects and connexin dysregulation. *Am J Physiol Heart Circ Physiol.* 2007.

297. Kansui Y, Fujii K, Nakamura K, Goto K, Oniki H, Abe I, Shibata Y, Iida M. Angiotensin II receptor blockade corrects altered expression of gap junctions in vascular endothelial cells from hypertensive rats. *Am J Physiol Heart Circ Physiol.* 2004;287(1):H216-224.

298. Rummery NM, Grayson TH, Hill CE. Angiotensin-converting enzyme inhibition restores endothelial but not medial connexin expression in hypertensive rats. *Journal of Hypertension.* 2005;23(2):317-328.

299. Suarez S, Ballmer-Hofer K. VEGF transiently disrupts gap junctional communication in endothelial cells. *Journal of Cell Science.* 2001;114(6):1229-1235.

300. Thuringer D. The Vascular Endothelial Growth Factor-Induced Disruption of Gap Junctions Is Relayed by an Autocrine Communication via ATP Release in Coronary Capillary Endothelium. *Ann NY Acad Sci.* 2004;1030(1):14-27.

301. Doble BW, Chen Y, Bosc DG, Litchfield DW, Kardami E. Fibroblast Growth Factor-2 Decreases Metabolic Coupling and Stimulates Phosphorylation as Well as Masking of Connexin43 Epitopes in Cardiac Myocytes. *Circ Res.* 1996;79(4):647-658.

302. Srisakuldee W, Nickel BE, Fandrich RR, Jiang ZS, Kardami E. Administration of fgf-2 to the heart stimulates connexin-43 phosphorylation at protein kinase C target sites. *Cell Commun Adhes.* 2006;13(1):13-19.

303. Doble BW, Kardami E. Basic fibroblast growth factor stimulates connexin-43 expression and intercellular communication of cardiac fibroblasts. *Mol Cell Biochem.* 1995;143(1):81-87.

304. Pepper MS, Meda P. Basic fibroblast growth factor increases junctional communication and connexin 43 expression in microvascular endothelial cells. *J Cell Physiol.* 1992;153(1):196-205.

305. Mensink A, Brouwer A, Van den Burg EH, Geurts S, Jongen WM, Lakemond CM, Meijerman I, Van der Wijk T. Modulation of intercellular communication between smooth muscle cells by growth factors and cytokines. *Eur J Pharmacol.* 1996;310(1):73-81.

306. De Vuyst E, Decrock E, De Bock M, Yamasaki H, Naus CC, Evans WH, Leybaert L. Connexin Hemichannels and Gap Junction Channels Are Differentially Influenced by Lipopolysaccharide and Basic Fibroblast Growth Factor. *Mol Biol Cell.* 2007;18(1):34-46.

307. Yeh HI, Lu CS, Wu YJ, Chen CC, Hong RC, Ko YS, Shiao MS, Severs NJ, Tsai CH. Reduced expression of endothelial connexin37 and connexin40 in hyperlipidemic mice: recovery of connexin37 after 7-day simvastatin treatment. *Arterioscler Thromb Vasc Biol.* 2003;23(8):1391-1397.

308. Polacek D, Bech F, McKinsey JF, Davies PF. Connexin43 gene expression in the rabbit arterial wall: effects of hypercholesterolemia, balloon injury and their combination. *J Vasc Res.* 1997;34(1):19-30.

309. Kuroki T, Inoguchi T, Umeda F, Ueda F, Nawata H. High glucose induces alteration of gap junction permeability and phosphorylation of connexin-43 in cultured aortic smooth muscle cells. *Diabetes.* 1998;47(6):931-936.

310. Sato T, Haimovici R, Kao R, Li A-F, Roy S. Downregulation of Connexin 43 Expression by High Glucose Reduces Gap Junction Activity in Microvascular Endothelial Cells *Diabetes.* 2002;51(5):1565-1571.

311. Fernandes R, Girao H, Pereira P. High Glucose Down-regulates Intercellular Communication in Retinal Endothelial Cells by Enhancing Degradation of Connexin 43 by a Proteasome-dependent Mechanism. *J. Biol. Chem.* 2004;279(26):27219-27224.

312. Tsai CH, Yeh HI, Tian TY, Lee YN, Lu CS, Ko YS. Down-regulating effect of nicotine on connexin43 gap junctions in human umbilical vein endothelial cells is attenuated by statins. *Eur J Cell Biol.* 2004;82(12):589-595.

313. Simon AM, McWhorter AR, Chen H, Jackson CL, Ouellette Y. Decreased intercellular communication and connexin expression in mouse aortic endothelium during lipopolysaccharide-induced inflammation. *J Vasc Res.* 2004;41(4):323-333.

314. Zhang YW, Morita I, Nishida M, Murota SI. Involvement of tyrosine kinase in the hypoxia/reoxygenation-induced gap junctional intercellular communication abnormality in cultured human umbilical vein endothelial cells. *Journal Of Cellular Physiology.* 1999;180(3):305-313.

315. Cowan DB, Jones M, Garcia LM, Noria S, del Nido PJ, McGowan FX, Jr. Hypoxia and stretch regulate intercellular communication in vascular smooth muscle cells through reactive oxygen species formation. *Arterioscler Thromb Vasc Biol.* 2003;23(10):1754-1760.

316. Matsushita S, Kurihara H, Watanabe M, Okada T, Sakai T, Amano A. Alterations of Phosphorylation State of Connexin 43 during Hypoxia and Reoxygenation are Associated with Cardiac Function. *J Histochem Cytochem.* 2005.

317. Zeevi-Levin N, Barac YD, Reisner Y, Reiter I, Yaniv G, Meiry G, Abassi Z, Kostin S, Schaper J, Rosen MR, Resnick N, Binah O. Gap junctional remodeling by hypoxia in cultured neonatal rat ventricular myocytes. *Cardiovasc Res.* 2005;66(1):64-73.

318. Rose K, Ouellette Y, Bolon M, Tyml K. Hypoxia/reoxygenation reduces microvascular endothelial cell coupling by a tyrosine and MAP kinase dependent pathway. *J Cell Physiol.* 2005;204(1):131-138.

319. Turner MS, Haywood GA, Andreka P, You L, Martin PE, Evans WH, Webster KA, Bishopric NH. Reversible connexin 43 dephosphorylation during hypoxia and reoxygenation is linked to cellular ATP levels. *Circ Res.* 2004;95(7):726-733.

320. Gabriels JE, Paul DL. Connexin43 Is highly localized to sites of disturbed flow in rat aortic endothelium but connexin37 and connexin40 are more uniformly distributed. *Circ Res.* 1998;83(6):636-643.

321. Dai G, Kaazempur-Mofrad MR, Natarajan S, Zhang Y, Vaughn S, Blackman BR, Kamm RD, Garcia-Cardena G, Gimbrone MA, Jr. Distinct endothelial phenotypes evoked by arterial waveforms derived from atherosclerosis-susceptible and -resistant regions of human vasculature. *PNAS.* 2004;101(41):14871-14876.

322. Passerini AG, Polacek DC, Shi C, Francesco NM, Manduchi E, Grant GR, Pritchard WF, Powell S, Chang GY, Stoeckert CJ, Jr., Davies PF. Coexisting proinflammatory and antioxidative endothelial transcription profiles in a disturbed flow region of the adult porcine aorta. *Proc Natl Acad Sci U S A.* 2004;101(8):2482-2487.

323. Bao X, Clark CB, Frangos JA. Temporal gradient in shear-induced signaling pathway: involvement of MAP kinase, c-fos, and connexin43. *Am J Physiol Heart Circ Physiol.* 2000;278(5):H1598-1605.

324. Brooks AR, Lelkes PI, Rubanyi GM. Gene expression profiling of human aortic endothelial cells exposed to disturbed flow and steady laminar flow. *Physiol.Genomics.* 2002;9(1):27-41.

325. Ebong EE, Kim S, Depaola N. Flow regulates intercellular communication in HAEC by assembling functional Cx40 and Cx37 gap junctional channels. *Am J Physiol Heart Circ Physiol.* 2006;290(5):H2015-2023.

326. Johnson TL, Nerem RM. Endothelial connexin 37, connexin 40, and connexin 43 respond uniquely to substrate and shear stress. *Endothelium.* 2007;14(4):215-226.

327. Haefliger JA, Meda P. Chronic hypertension alters the expression of Cx43 in cardiovascular muscle cells. *Braz J Med Biol Res.* 2000;33(4):431-438.

328. Yeh HI, Lee PY, Su CH, Tian TY, Ko YS, Tsai CH. Reduced expression of endothelial connexins 43 and 37 in hypertensive rats is rectified after 7-day carvedilol treatment. *Am J Hypertens.* 2006;19(2):129-135.

329. Wang T-L, Tseng Y-Z, Chang H. Regulation of Connexin 43 Gene Expression by Cyclical Mechanical Stretch in Neonatal Rat Cardiomyocytes. *Biochemical and Biophysical Research Communications.* 2000;267(2):551-557.

330. Shanker AJ, Yamada K, Green KG, Yamada KA, Saffitz JE. Matrix protein-specific regulation of Cx43 expression in cardiac myocytes subjected to mechanical load. *Circ Res.* 2005;96(5):558-566.

331. Ziambaras K, Lecanda F, Steinberg TH, Civitelli R. Cyclic stretch enhances gap junctional communication between osteoblastic cells. *J Bone Miner Res.* 1998;13(2):218-228.

332. Bardy N, Karillon GJ, Merval R, Samuel JL, Tedgui A. Differential effects of pressure and flow on DNA and protein synthesis and on fibronectin expression by arteries in a novel organ culture system. *Circ Res.* 1995;77(4):684-694.

333. Hanke JH, Gardner JP, Dow RL, Changelian PS, Brissette WH, Weringer EJ, Pollok BA, Connelly PA. Discovery of a novel, potent, and Src family-selective tyrosine kinase inhibitor. Study of Lck- and FynT-dependent T cell activation. *J Biol Chem.* 1996;271(2):695-701.

334. Wang Y, Jin G, Miao H, Li JY, Usami S, Chien S. Integrins regulate VE-cadherin and catenins: dependence of this regulation on Src, but not on Ras. *Proc Natl Acad Sci U S A.* 2006;103(6):1774-1779.

335. Watcharasit P, Tucholski J, Jope RS. Src family kinase involvement in muscarinic receptor-induced tyrosine phosphorylation in differentiated SH-SY5Y cells. *Neurochem Res.* 2001;26(7):809-816.

336. Brandes RP, Kreuzer J. Vascular NADPH oxidases: molecular mechanisms of activation. *Cardiovascular Research.* 2005;65(1):16-27.

337. Meyer JW, Holland JA, Ziegler LM, Chang MM, Beebe G, Schmitt ME. Identification of a functional leukocyte-type NADPH oxidase in human endothelial cells: A potential atherogenic source of reactive oxygen species. *Endothelium: Journal of Endothelial Cell Research.* 1999;7(1):11-22.

338. Oelze M, Warnholtz A, Faulhaber J, Wenzel P, Kleschyov AL, Coldewey M, Hink U, Pongs O, Fleming I, Wassmann S, Meinertz T, Ehmke H, Daiber A, Munzel T. NADPH oxidase accounts for enhanced superoxide production and impaired endothelium-dependent smooth muscle relaxation in BKbeta1-/- mice. *Arteriosclerosis, thrombosis, and vascular biology.* 2006;26(8):1753-1759.

339. Meyer JW, Schmitt ME. A central role for the endothelial NADPH oxidase in atherosclerosis. *FEBS Letters.* 2000;472(1):1-4.

340. Vejrazka M, Micek R, Stipek S. Apocynin inhibits NADPH oxidase in phagocytes but stimulates ROS production in non-phagocytic cells. *Biochim Biophys Acta.* 2005;1722(2):143-147.

341. Wassmann S, Stumpf M, Strehlow K, Schmid A, Schieffer B, Bohm M, Nickenig G. Interleukin-6 induces oxidative stress and endothelial dysfunction by overexpression of the angiotensin II type 1 receptor. *Circ Res.* 2004;94(4):534-541.

342. Ai Z, Fischer A, Spray DC, Brown AM, Fishman GI. Wnt-1 regulation of connexin43 in cardiac myocytes. *J Clin Invest.* 2000;105(2):161-171.

343. Tai L-k, Zheng Q, Pan S, Jin Z-G, Berk BC. Flow Activates ERK1/2 and Endothelial Nitric Oxide Synthase via a Pathway Involving PECAM1, SHP2, and Tie2. *J. Biol. Chem.* 2005;280(33):29620-29624.

344. Zhou R-H, Lee T-S, Tsou T-C, Rannou F, Li Y-S, Chien S, Shyy JY-J. Stent Implantation Activates Akt in the Vessel Wall: Role of Mechanical Stretch in Vascular Smooth Muscle Cells. *Arterioscler Thromb Vasc Biol.* 2003;23(11):2015-2020.

345. Figueroa XF, Isakson BE, Duling BR. Vascular gap junctions in hypertension. *Hypertension.* 2006;48(5):804-811.

346. Ko YS, Yeh HI, Haw M, Dupont E, Kaba R, Plenz G, Robenek H, Severs NJ. Differential expression of connexin43 and desmin defines two subpopulations of medial smooth muscle cells in the human internal mammary artery. *Arterioscler Thromb Vasc Biol.* 1999;19(7):1669-1680.

347. Deglise S, Martin D, Probst H, Saucy F, Hayoz D, Waeber G, Nicod P, Ris H-B, Corpataux J-M, Haefliger J-A. Increased connexin43 expression in human saphenous veins in culture is associated with intimal hyperplasia. *Journal of Vascular Surgery.* 2005;41(6):1043-1052.

348. Roskoski R, Jr. Src kinase regulation by phosphorylation and dephosphorylation. *Biochem Biophys Res Commun.* 2005;331(1):1-14.

349. Okutani D, Lodyga M, Han B, Liu M. Src protein tyrosine kinase family and acute inflammatory responses. *Am J Physiol Lung Cell Mol Physiol.* 2006;291(2):L129-141.

350. Werdich XQ, Penn JS. Src, Fyn and Yes play differential roles in VEGF-mediated endothelial cell events. *Angiogenesis.* 2005;8(4):315-326.

351. Lehoux S, CASTIER Y, TEDGUI A. Molecular mechanisms of the vascular responses to haemodynamic forces. *Journal of Internal Medicine.* 2006;259(4):381-392.

352. Rice DC, Dobrian AD, Schriver SD, Prewitt RL. Src Autophosphorylation is an Early Event in Pressure-Mediated Signaling Pathways in Isolated Resistance Arteries. *Hypertension.* 2002;39(2):502-507.

353. Jalali S, Li Y-S, Sotoudeh M, Yuan S, Li S, Chien S, Shyy JY-J. Shear Stress Activates p60src-Ras-MAPK Signaling Pathways in Vascular Endothelial Cells. *Arterioscler Thromb Vasc Biol.* 1998;18(2):227-234.

354. Ingley E, Schneider JR, Payne CJ, McCarthy DJ, Harder KW, Hibbs ML, Klinken SP. Csk-binding Protein Mediates Sequential Enzymatic Down-regulation and Degradation of Lyn in Erythropoietin-stimulated Cells. *J. Biol. Chem.* 2006;281(42):31920-31929.

355. Chaturvedi LS, Marsh HM, Basson MD. Src and focal adhesion kinase mediate mechanical strain-induced proliferation and ERK1/2 phosphorylation in human H441 pulmonary epithelial cells. *Am J Physiol Cell Physiol.* 2007;292(5):C1701-1713.

356. Karni R, Mizrachi S, Reiss-Sklan E, Gazit A, Livnah O, Levitzki A. The pp60c-Src inhibitor PP1 is non-competitive against ATP. *FEBS Lett.* 2003;537(1-3):47-52.

357. Chen Db, Li Sm, Qian XX, Moon C, Zheng J. Tyrosine Phosphorylation of Caveolin 1 by Oxidative Stress Is Reversible and Dependent on the c-src Tyrosine Kinase but Not Mitogen-Activated Protein Kinase Pathways in Placental Artery Endothelial Cells. *Biol Reprod.* 2005;73(4):761-772.

358. Catarzi S, Biagioni C, Giannoni E, Favilli F, Marcucci T, Iantomasi T, Vincenzini MT. Redox regulation of platelet-derived-growth-factor-receptor: role of NADPH-oxidase and c-Src tyrosine kinase. *Biochim Biophys Acta.* 2005;1745(2):166-175.

359. Beardslee MA, Laing JG, Beyer EC, Saffitz JE. Rapid turnover of connexin43 in the adult rat heart. *Circ Res.* 1998;83(6):629-635.

360. Yamawaki H, Lehoux S, Berk BC. Chronic physiological shear stress inhibits tumor necrosis factor-induced proinflammatory responses in rabbit aorta perfused ex vivo. *Circulation.* 2003;108(13):1619-1625.

361. Kanno S, Kovacs A, Yamada KA, Saffitz JE. Connexin43 as a determinant of myocardial infarct size following coronary occlusion in mice. *J Am Coll Cardiol.* 2003;41(4):681-686.

362. Ruiz-Meana M, Rodriguez-Sinovas A, Cabestrero A, Boengler K, Heusch G, Garcia-Dorado D. Mitochondrial connexin43 as a new player in the pathophysiology of myocardial ischemia-reperfusion injury. A viewpoint. *Cardiovasc Res.* 2007.

363. Yeh HI, Lupu F, Dupont E, Severs NJ. Upregulation of connexin43 gap junctions between smooth muscle cells after balloon catheter injury in the rat carotid artery. *Arterioscler. Thromb. Vasc. Biol.* 1997;17(11):3174-3184.

364. Tropea BI, Schwarzacher SP, Chang A, Asvar C, Huie P, Sibley RK, Zarins CK. Reduction of Aortic Wall Motion Inhibits Hypertension-Mediated Experimental Atherosclerosis. *Arterioscler Thromb Vasc Biol.* 2000;20(9):2127-2133.

365. el-Fouly MH, Trosko JE, Chang CC. Scrape-loading and dye transfer. A rapid and simple technique to study gap junctional intercellular communication. *Exp Cell Res.* 1987;168(2):422-430.

366. Wade MH, Trosko JE, Schindler M. A fluorescence photobleaching assay of gap junction-mediated communication between human cells. *Science.* 1986;232(4749):525-528.

367. Goldberg GS, Bechberger JF, Naus CCG. A pre-loading method of evaluating gap junctional communication by fluorescent dye transfer. *BioTechniques.* 1995;18(3):490-497.